THE ROLE OF TYPE 2 CANNABINOID RECEPTOR IN BONE METABOLISM

Antonia Sophocleous (BSc)

A thesis submitted for the degree of Doctor of Philosophy

University of Edinburgh

2009

To my family

DECLARATION

I hereby declare that this thesis has been composed by myself and the work described within, except where specifically acknowledged, is my own and that it has not been accepted in any previous application for a degree. The information obtained from sources other than this study is acknowledged in the text or included in the references.

Antonia Sophocleous

CONTENTS

CHAPTER ONE

CHAPTER TWO

CHAPTER FIVE

CHAPTER SIX

ACKNOWLEDGEMENTS

PUBLICATIONS FROM THESIS

Papers

Idris, A.I., **Sophocleous, A.**, Landao-Bassonga, E., van't Hof, R.J. & Ralston, S.H. (2008). Regulation of bone mass, osteoclast function, and ovariectomy-induced bone loss by the type 2 cannabinoid receptor. *Endocrinology*. **149**, 5619-5626.

Idris, A.I., **Sophocleous, A.**, Landao-Bassonga, E., Canals, M., Milligan, G.I., Baker, D., van't Hof, R.J. & Ralston, S.H. Cannabinoid receptor type 1 protects against age-related bone loss by regulating osteoblast and adipocyte differentiation in marrow stromal cells. *Cell metabolism.***10**, 139-147.

Sophocleous, A., Landao-Bassonga, E., van't Hof R.J., Ralston, S.H. & Idris, A.I. Regulation of osteoblast function and age-related bone loss by the type 2 cannabinoid receptor. ***(In preparation)***

Abstracts, Oral Presentations & Awards

Sophocleous, A., Landao-Bassonga.E., van't Hof, R.J., Ralston, S.H. & Idris, A.I. (2009). The type 2 cannabinoid receptor (CB2) protects against age-related osteoporosis by affecting bone formation and CB2 agonists exhibit anabolic activity *in vivo*.
-Presented at the 36th European Symposium on Calcified Tissues, Vienna, Austria, May 2009. **Received NEW INVESTIGATOR AWARD.**

Sophocleous, A., Landao-Bassonga, E., van't Hof, R.J., Ralston, S.H. & Idris, A.I. (2008). Cannabinoid receptor antagonists inhibit osteoclast formation *in vitro* and ovariectomy-induced bone loss *in vivo* through the CB1 and CB2 receptors. *Calcified Tissue International*, **82** (Suppl 1), S31.
-Presented at the 35th European Symposium on Calcified Tissues, Barcelona, Spain, May 2008. **Received NEW INVESTIGATOR AWARD.**

Sophocleous, A., Landao-Bassonga, E., van't Hof, R.J., Idris, A.I. & Ralston, S.H. (2008). Cannabinoid receptor 2 selective agonists stimulate osteoclast formation *in vitro* but act as anabolic agents *in vivo* by stimulating bone formation. *Bone*, **42** (Suppl 1), S31.
-Presented at the International Bone and Mineral Society workshop, Davos, Switzerland (March 2008). **Received TRAVEL AWARD.**

Sophocleous, A., Landao-Bassonga, E., van't Hof, R.J., Idris, A.I. and Ralston, S.H. (2007). Cannabinoid receptor agonists are potential bone anabolic agents which stimulate bone formation *in vitro* and increase bone mass *in vivo*. *Calcified Tissue International*, **80** (Suppl 1), S32.
-Presented at the 34th European Symposium on Calcified Tissues, Copenhagen, Denmark, May 2007. **Received TRAVEL AWARD.**

ABBREVIATIONS

1,25-(OH)$_2$ vitamin D$_3$	1,25-dihydroxyvitamin D$_3$
2-AG	2-arachidonyl glycerol
aa	Amino acid
AC	Adenylate cylase
Adrb2	β2-adrenergic receptors
AEA	Anandamide
ALP	Alkaline Phosphatase
αMEM	Alpha-Minimum Essential Medium
ANOVA	Analysis of variance
AP-1	Activator protein-1
BCA	Bicinchoninic acid
BFR	Bone formation rate
β-GP	Beta-glyderol phosphate
BM	Bone Marrow
BMD	Bone mineral density
BMP	Bone morphogenetic protein
BMPR	Bone morphogenetic protein receptor
BMU	Basic multicellular unit
bp	Base pair
BSP	Bone sialoprotein
BV/TV	Trabecular bone volume to total volume
C57BL/6	An inbred mouse strain
CA II	Cytosolic carbonic anhydrase II
Ca^{2+}	Calcium ions
cAMP	Cyclic AMP
Cbfα1	Core-binding factor α1
CDS	Coding sequence
c-Fms	Receptor of M-CSF
CFU-GM	Colony forming unit granulocyte-macrophage
CGRP	Calcitonin gene-related peptides
Cl$^-$	Chloride ions
CNR1	Type 1 Cannabinoid Receptor
CNR2	Type 2 Cannabinoid Receptor
CNR1$^{-/-}$	CNR1 knockout
CNR2$^{-/-}$	CNR2 knockout
CNS	Central nervous system
COLIA1	Type I collagen
CREB	cAMP response element-binding protein
Ct.Ar	Cross-sectional cortical area
Ct.BV	Cortical volume
Ct.Dm	Cortical diameter
Ct.Th	Cortical thickness
C-terminus	Carboxyl-terminus
CT (R)	Calcitonin (receptor)
CTX	C-terminal telopeptides of type I collagen

DAG	Diacylglycerol
DEPC	Diethyl Pyrocarbonate
dH$_2$O	Distilled water
Dkk1	Dickkopf 1
DMSO	Dimethyl sulfoxide
Dvl	Disheveled
EC$_{50}$	Half maximal effective concentration
ECM	Extracellular matrix
EDTA	Ethylenediaminetetraacetic acid
EP2	PGE2 receptor
ER	Oestrogen receptor
ERK	Extracellular regulated kinase
ET1	Endothelin-1
FAAH	Fatty acid amide hydrolase
FCS	Fetal Calf Serum
FGF	Fibroblast growth factors
FSH	Follicle stimulating hormone
FSHR	Follicle stimulating hormone receptor
Fz	Frizzled
G	Gauge
g, mg, μg, ng	Gram, milligram, microgram, nanogram
GC-MS	Gas chromatography – mass spectrometry
GM-CSF	Granulocyte-macrophage colony stimulating factor
GPCR	G protein-coupled receptor
Grb2	Growth factor receptor bound protein 2
GSK3	Glycogen synthase kinase 3
H$^+$	Hydrogen ions
HBSS	Hank's balanced salt solution
HCO$_3^-$	Bicarbonate ions
HRP	Horseradish peroxidase
HRT	Hormone-related therapy
IC$_{50}$	Half maximal inhibitory concentration
ID	Identification number
IFNγ	Interferon gamma
IGF	Insulin growth factor
IκB	Inhibitor of NFκB
IKK	IκB kinase
IL (R)	Interleukin (receptor)
JNK	c-Jun N-terminal kinase
K$^+$	Potassium ions
kb	Kilobase
kg	Kilogram
KLF	Krüppel-like factors
kV	Kilovolt
l, ml, μl	Litre, millilitre, microlitre
LD linkage	Linkage disequilibrium
LEF	Lymphoid-enhancer binding factor

LRP	LDL receptor-related protein
M, mM, μM, nM	Molar, millimolar, micromolar, nanomolar
m/sM-CSF	Membrane-bound/soluble M-CSF
m/sRANKL	Membrane-bound/Soluble RANKL
mA,	Milliampere
MAPK	Mitogen activated protein kinase
MAR	Mineral apposition rate
M-CSF	Macrophage colony stimulating factor
μCT	Micro computed tomography
MEA	2-Methoxyethyl acetate
Med.Cav.Dm	Medullary cavity diameter
MEK	MAPK kinase/ERK kinase
MΦ	Macrophages
MGL	Monoacylglycerol lipase
Mm, nm	Millimetre, nanometre
MMA	Methyl methacrylate
MMP	metalloproteinase
MSC	Mesenchymal stem cells
Na$^+$	Sodium ions
NAPE-PLD	N-acyl phosphatidylethanolamine phospholipase D
NEO	Neomycin
NFATc1	Nuclear factor of activated T cells 1
NF-κB	Nuclear factor κB
nNOS	Neuronal isoform of nitric oxide synthase
NO	Nitric oxide
NOS	Nitric oxide synthase
NPY	Neuropeptide Y
N-terminus	Amino-terminus
OA	Osteoarthritis
OB	Osteoblast
Ob.N/BS	Osteoblast number per bone surface
ObR	Leptin receptor
OC	Osteoclast
Oc.N/BS	Osteoclast umber per Bone Surface
Oc.S/BS	Active resorption area per bone surface
OCN	osteocalcin
ONJ	Osteonecrosis of the jaw
OPG	Osteoprotegerin
OPN	Osteopontin
OSN	Osteonectin
Osx	Osterix
p	Probability
PBS	Phosphate buffered saline
PDB	Paget's disease of bone
PDGF	Platelet-derived growth factors
PGE2	Prostaglandin E2
PI$_3$	Inositol triphosphate

PI3K	Phosphatidylinositol-3-Kinase
PINP	N-terminal propeptide of type I procollagen
PIP2	Phosphatidylinositol bisphosphate
PKA/B/C	Protein kinase A/B/C
PLC	Phospholipase C
PPARγ2	Peroxisome proliferator-activated receptor γ2
PTH	Parathyroid hormone
PTHR1	Type 1 PTH/PTHrP receptor
qPCR	Real time quantitative PCR
RANK	Receptor activator of NF-κB
RANKL	Receptor activator of NF-κB ligand
RGD	Arg-Gly-Asp tripeptide
RNA	Ribonucleic Acid
ROI	Region of interest
RPM	Revolutions per minute
Runx2	Runt-related transcription factor
sd	Standard deviation
sem/SEM	Standard error of mean
SERMs	Selective oestrogen-receptor modulators
SNP	Single nucleotide polymorphism
SOST	Sclerostin
Sox	DNA-binding SRY box
Tb.N	Trabecular number
Tb.Pf	Trabecular pattern factor
Tb.Sp	Trabecular separation
Tb.Th	Trabecular thickness
TBI	Traumatic brain injury
TE	Tris EDTA
TGF-β	Transforming growth factor-β
TM	Transmembrane
TMB	tetramethylbenzidine
TNF (R)	Tumour necrosis factor (receptor)
TRAcP	Tartrate-resistant acid phosphatase
TRAF	TNF receptor-associated factor
Trizol®	Total RNA Isolation reagent
TSH	Thyroid stimulating hormone
TSHR	Thyroid stimulating hormone receptor
UPL	Universal Probe Library
UTR	Untranslated region
UV	Ultraviolet
v/v	Volume to volume
VDR	Vitamin D receptor
VEGF	Vascular endothelial growth factor
w/v	Weight to volume

LIST OF FIGURES

LIST OF TABLES

The Role of Type 2 Cannabinoid Receptor in Bone Metabolism

Antonia Sophocleous
School of Molecular and Clinical Medicine
University of Edinburgh

ABSTRACT

Cannabinoid receptors play an important role in regulating bone mass and bone turnover. Studies in our laboratories have shown that young mice lacking type 1 cannabinoid receptor ($CNR1^{-/-}$) had increased bone mass and were resistant to ovariectomy-induced bone loss. Other workers have reported that type 2 cannabinoid receptor knockout mice ($CNR2^{-/-}$) develop age-related osteoporosis. The aim of this PhD thesis was to further investigate the role of CNR2 in bone metabolism *in vitro* and *in vivo*, using genetic and pharmacological approaches.

This study showed that $CNR2^{-/-}$ mice had normal bone mass and bone turnover at 3 months of age, but following ovariectomy, $CNR2^{-/-}$ mice were partially protected from bone loss, because of a mild defect in osteoclast formation and bone resorption. In keeping with this, studies *in vitro* showed that RANKL-stimulated bone marrow cultures from $CNR2^{-/-}$ mice had fewer osteoclasts than cultures from wild type littermates. The CNR2-selective antagonist/inverse agonist AM630, inhibited osteoclast formation in wild type bone marrow cultures *in vitro* and prevented ovariectomy-induced bone loss in wild type mice *in vivo*. In contrast, osteoclast cultures from $CNR2^{-/-}$ mice were resistant to the inhibitory effects of AM630 at low concentrations and $CNR2^{-/-}$ ovariectomised mice did not respond to its protective effects at low doses, consistent with a CNR2-mediated effect. These results indicate that CNR2 regulates bone loss under conditions of increased bone turnover, such as ovariectomy, by affecting osteoclast differentiation and function.

CNR2-deficient mice developed accelerated age-related osteoporosis and by 12 months of age they had a significant reduction in osteoblast numbers and bone formation,

whereas osteoclast numbers remained comparable to wild type littermates. In agreement with this, osteoblasts derived from bone marrow of *CNR2*$^{-/-}$ mice had reduced PTH-stimulated alkaline phosphatase activity and ability to form bone nodules, when compared with wild type cultures. The CNR2-selective agonist, HU308, stimulated bone nodule formation in wild type calvarial osteoblast cultures *in vitro* and reversed ovariectomy-induced bone loss in wild type mice *in vivo*. HU308 had blunted effects on bone nodule formation in cultures from *CNR2*$^{-/-}$ mice and no significant effects on ovariectomy-induced bone loss in *CNR2*$^{-/-}$ mice, indicating a CNR2-mediated effect. These studies demonstrate that CNR2 protects against age-related bone loss by mainly enhancing osteoblast differentiation and bone formation.

In conclusion, type 2 cannabinoid receptors protect from bone loss by maintaining bone remodelling at balance. In addition, type 2 cannabinoid receptor agonists show evidence of anabolic activity, whereas antagonists/inverse agonists show evidence of anti-osteoclastic activity *in vitro* and *in vivo*.

CHAPTER ONE
INTRODUCTION

1   INTRODUCTION

1.1   BONE

Bone is a dynamic, and specialized connective tissue that together with joint tissues such as cartilage and synovium, makes up the skeleton. In conjunction with muscles, bone supports body structures, protects internal organs, functions as a reservoir for calcium/phosphate ions and facilitates movement (Murray J.Favus [Editor], 2006).

Two types of bone are recognised according to the mechanism of development. Long bones such as tibia, femur, radius and humerus, are derived from endochondral ossification, whereas flat bones such as clavicle, mandible and skull bones are derived from intramembranous ossification. The main difference between these two processes of bone development is the presence of a cartilaginous phase in the former (Murray J.Favus [Editor], 2006).

Long bones have a cylindrical structure with a central medullary cavity hosting the main haemopoietic organ, the bone marrow (Figure 1.1). The bony tube is the diaphysis and is attached to wider edges, the epiphyses. The zone between the diaphysis and the epiphyses is called the metaphysis. During growth, there is strict separation between the metaphyseal and epiphyseal part of the bone by a layer of hyaline cartilage, known as the growth plate and is the growing portion of long bones. At the end of the growing period the growth plate is replaced by mineralised bone, leaving behind just the epiphyseal line. Flat bones are composed of two thin layers of bone enclosing a flattened medullary cavity with bone marrow (Murray J.Favus [Editor], 2006).

According to its structure, bone is classified into two types: cortical or compact bone and trabecular or cancellous bone (Figure 1.1).
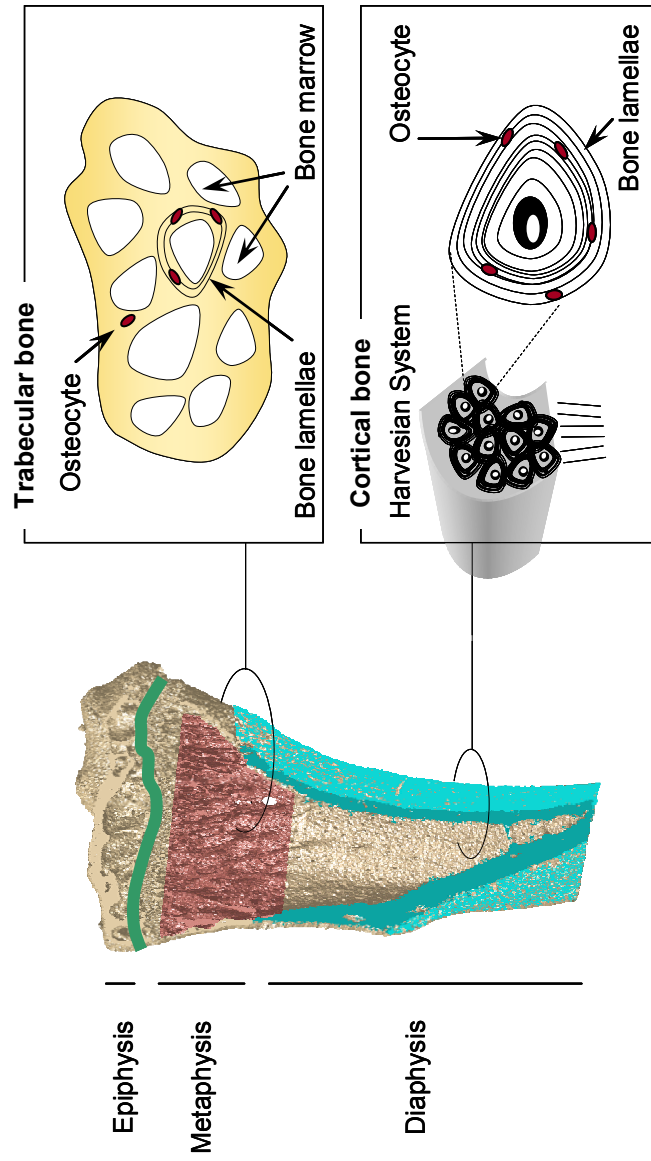
Figure 1.1: Types of bone. Trabecular bone is in brown and cortical bone in blue. The green line traces the growth plate. See text for descriptions.

Cortical bone is dense with a low remodelling rate per unit volume (Murray J.Favus [Editor], 2006). It constitutes 85% of the skeleton and is found in the diaphysis of long bones and the outer layer of flat bones (Murray J.Favus [Editor], 2006). In large mammals, the cortical bone is composed of repeating patterns of collagen fibres, organised into concentric lamellae which in turn are organised into cylindrical structures, collectively known as osteons or Haversian systems. In the centre of such systems are the Haversian canals that carry blood vessels and nerve fibres (Figure 1.1).

Trabecular bone has a spongy appearance and consists of interconnected trabeculae filled with bone marrow, which makes it metabolically more active than cortical bone (Murray J.Favus [Editor], 2006). Trabecular bone makes up the remaining 15% of the skeleton and is present mainly in flat bones and the ends of long bones (Murray J.Favus [Editor], 2006). Trabecular bone is also composed of Haversian systems with lamellar organisation of collagen fibres, but here the lamellae run parallel to each other (Figure 1.1).

Bone matrix comprises organic and inorganic parts. The most prominent organic element is type I collagen fibres which constitute 90% of the total protein of bone matrix (Murray J.Favus [Editor], 2006). The remaining 10% of bone matrix proteins include non-collagenous proteins, such as osteopontin (OPN), osteocalcin (OCN), osteonectin (OSN), bone sialoprotein (BSP) and proteoglycans, all thought to play a role in ossification and osteoblast adhesion to the matrix (Murray J.Favus [Editor], 2006). Mineralised matrix, is composed of type I collagen fibres and crystals of hydroxyapatite $[3Ca_3(PO_4)_2(OH)_2]$, the main inorganic component of bone.

1.2   CELLS IN THE BONE MICROENVIRONMENT

The main cells of bone are osteoblasts (the bone-forming cells), osteoclasts (the bone-resorbing cells), lining cells and osteocytes. All four types of cells play an important role in the bone remodelling cycle, the process that continuously renews existing bone in a sequence of resorptions, reversals, bone formations and quiescence states (Murray J.Favus [Editor], 2006).

1.2.1   Osteoblasts

Osteoblasts are mononucleated cells responsible for bone formation. At a microscopic level, mature osteoblasts have a cuboidal shape, a round nucleus, an elaborate endoplasmic reticulum and a large Golgi complex reflecting their high biosynthetic and secretory activity for the production of matrix constituents (Murray J.Favus [Editor], 2006).

Osteoblasts are derived from pluripotent progenitor cells, called mesenchymal stem cells (MSCs) found in the bone marrow. MSCs can differentiate into several cell types including osteoblasts, chondrocytes, adipocytes and myocytes (Katagiri and Takahashi, 2002). The lineage determination of MSCs is controlled by a combination of transcription factors, hormones and growth factors (Figure 1.2).

Runt-related transcription factor (Runx2), also known as core-binding factor α1 (Cbfα1), is the major transcription factor responsible for the commitment and differentiation of MSCs towards the osteoblastic lineage (Karsenty and Wagner, 2002). Studies have shown that *Runx2*-deficient mice die of respiratory failure shortly after birth and lack mature osteoblasts and bone formation (Komori et al., 1997; Otto et al., 1997). Osteoprogenitor cells are differentiated further into osteoblasts by Osterix (Osx), a zing finger transcription factor acting downstream of Runx2. Conversely, peroxisome proliferator-activated receptor γ2 (PPARγ2) transcription factor induces adipocyte

differentiation and reduces osteoblast differentiation from MSCs (Lecka-Czernik et al., 1999; Oyajobi et al., 1999).
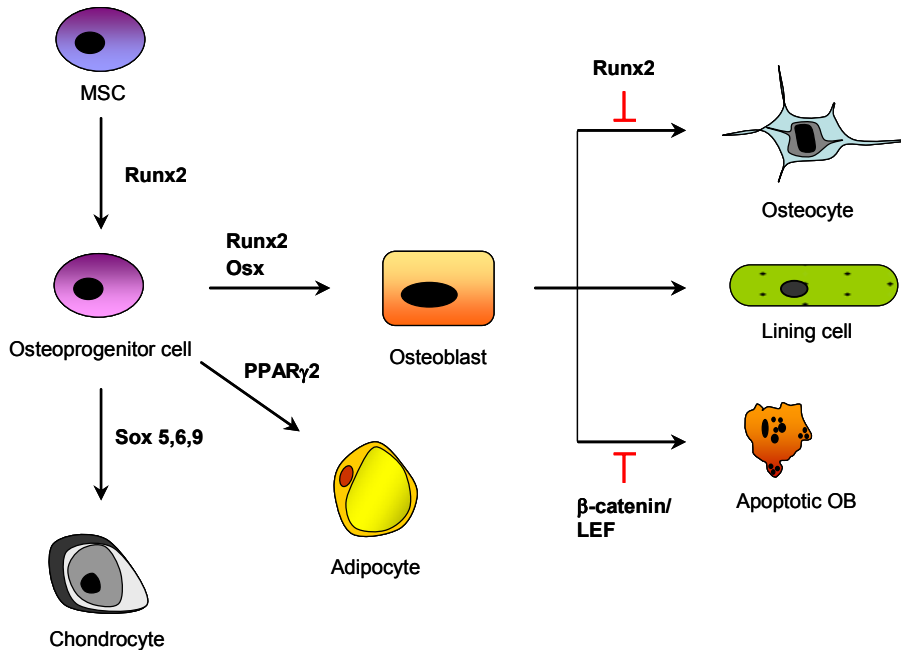
Figure 1.2: Role of transcription factors in lineage determination. See text for more details. *Abbreviations*: MSC, mesenchymal stem cell; Runx, runt-related transcription factor; Osx, osterix; PPARγ, peroxisome proliferator-activated receptor γ; Sox, DNA-binding SRY box found in Sox-family members; LEF, lymphoid-enhancer binding factor .

The endocrine involvement in osteoblast differentiation, survival and function is explained by the expression of receptors such as parathyroid hormone (PTH), oestrogen, glucocorticoid, and 1,25-dihydroxyvitamin D_3 (1,25-$(OH)_2$ vitamin D_3) receptors on mature osteoblasts (Marie, 2008). PTH enhances osteoblast differentiation by phosphorylating and activating Runx2, increasing Osx and reducing PPARγ2 expression in osteoprogenitors and by activating the Wnt/β-Catenin pathway (Krishnan et al., 2003; Wang et al., 2006; Tobimatsu et al., 2006).

Oestrogen on the other hand stimulates Runx2 expression and Wnt/β-Catenin-mediated osteoblast survival (McCarthy et al., 2003). Furthermore, 1,25-(OH)$_2$ vitamin D$_3$ up-regulates the expression of Runx2 and down-regulates PPARγ2 expression (Paredes et al., 2004; Duque et al., 2004). Glucocorticoids have a dual effect on bone formation depending on the duration of the treatment. Short glucocorticoid treatment promotes expression of Runx2 whereas long-term treatment inhibits canonical Wnt signalling and hence has a negative effect on osteoblast differentiation (Smith and Frenkel, 2005).

Osteoblastogenesis is also controlled by growth factors, such as bone morphogenetic proteins (BMPs), transforming growth factor-β (TGF-β), fibroblast growth factors (FGFs), insulin like growth factors (IGFs) and Indian hedgehog (Ihh) [reviewed in (Marie, 2008)]. BMPs, particularly BMP2, promote Osx expression in osteoblastic cells (Lee et al., 2003b) and Runx2 expression in osteoprogenitors and osteoblastic cells (Lee et al., 2000; Lee et al., 2003a). BMP2-deficient mice (*BMP2$^{-/-}$*) are embryonic lethal, but limb-specific conditional *BMP2$^{-/-}$* showed spontaneous fractures that did not heal with time (Tsuji et al., 2006), indicating that BMP2 is important for normal skeletal function. TGF-β stimulates bone formation by increasing the expression of Runx2 and simultaneously decreasing PPARγ2 expression (Ahdjoudj et al., 2002). Ihh increases Runx2 expression in MSCs (Shimoyama et al., 2007) and IGF-1 promotes Osx expression in osteoblastic cells (Celil and Campbell, 2005).

Osteoblasts are responsible for synthesising and secreting osteoid, the unmineralised bone matrix consisting of type I collagen and specialised bone matrix proteins such as OCN, OPN, and BSP (Katagiri and Takahashi, 2002). Osteoblasts also express alkaline phosphatase (ALP), which is involved in mineralisation of bone, by breaking down inhibitors of mineralisation such as pyrophosphate. In addition, osteoblasts express OCN, which appears to be involved in regulating bone formation. Levels of ALP and OCN are used as serum markers of osteoblast activity (Murray J.Favus [Editor], 2006).

Osteoblasts have receptors for prostaglandins, integrins and cytokines and produce cytokines, such as, macrophage colony-stimulating factor (M-CSF), the receptor activator of nuclear factor κB (NF-κB) ligand (RANKL) and interleukin 1 (IL-1). Both RANKL and M-CSF, are essential for the cross-talk between osteoblast and osteoclasts and once expressed they induce osteoclastogenesis in a paracrine manner. Osteoblasts also secrete osteoprotegerin (OPG), a decoy RANK receptor that inhibits osteoclastogenesis (Murray J.Favus [Editor], 2006).

Figure 1.3 shows some of the receptors and signal transduction pathways in osteoblasts.
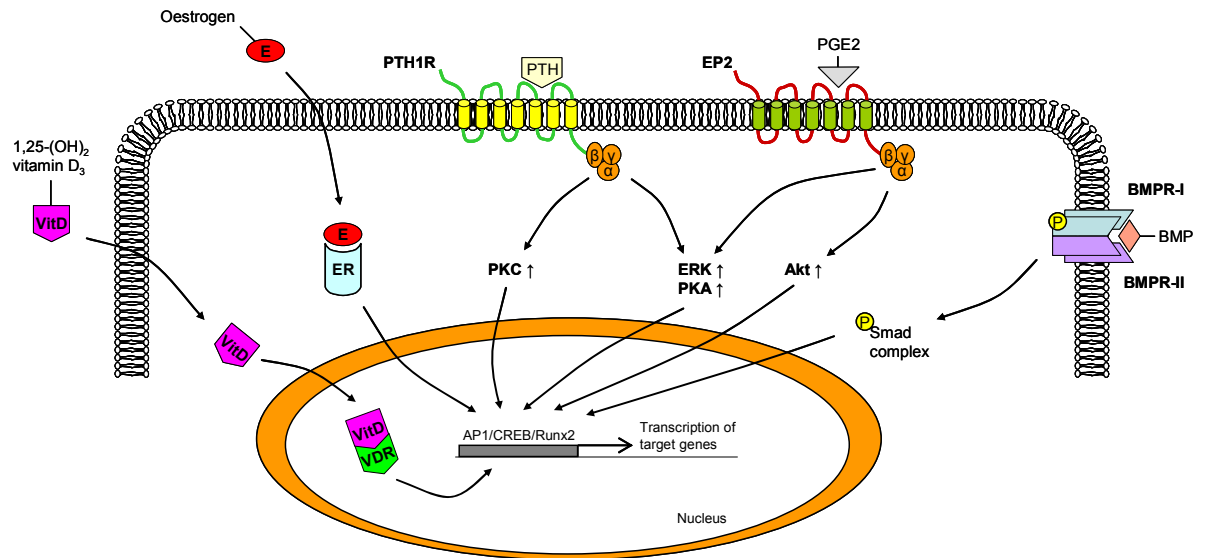
Figure 1.3: Schematic illustration of receptors and signal transduction pathways in osteoblasts. See text for descriptions. *Abbreviations*: VDR, 1,25-(OH)$_2$ vitamin D$_3$ receptor; ER, oestrogen receptor; PTH, parathyroid hormone; PTH1R, PTH receptor; PKC, protein kinase C; PGE2, prostaglandin E$_2$; EP2, PGE2 receptor; ERK, extracellular signal-regulated kinase; PKA, protein kinase A; BMP, bone morphogenetic protein; BMPR, BMP receptor; AP1, activator protein 1; CREB, cAMP response element binding protein; Runx, Runt-related transcription factor.

1.2.2   Osteocytes

Osteocytes are the most abundant cell type in bone (Mullender et al., 1996). Osteocytes are terminally differentiated cells of the osteoblast lineage. During bone formation about 10-20% of mature osteoblasts become embedded in newly formed mineralized bone and differentiate into osteocytes (Murray J.Favus [Editor], 2006), while others differentiate into flattened, quiescent cells lining the bone surface (c.f. Figure 1.2, page 6). The transformation of osteoblasts to osteocytes has been hypothesised to be controlled by osteocytes themselves, possibly by producing signals that decrease bone apposition rate of osteoblasts and facilitate their differentiation into osteocytes (Marotti, 1996).

Osteocytes lie in lacunae and are connected to one another, and with lining cells, through an elaborate network of cytoplasmic filapodial processes that run through canaliculi. Together they form the lacuna/canalicular system in bone (Murray J.Favus [Editor], 2006; Noble, 2008; Palumbo et al., 1990). Although osteocytes were originally considered to be non-migratory because of their location in bone, recently it has been proposed that they might be motile within the lacuna/canalicular system (Bonewald, 2007). It is thought that fluid flows through the canalicular system and the flowing rate is restricted by the size of the lacuna and the canals (Su et al., 2006). Such fluid flow, together with the continuum between lining cells and osteocytes might explain the mechanosensor ability of osteocytes to transduce stress signals in response to mechanical loading (Murray J.Favus [Editor], 2006).

The functional role of osteocytes is still under investigation. Although initially it was proposed that osteocytes were involved in bone resorption (Belanger et al., 1967), it is now clear that they are implicated in mineral homeostasis by modifying the local matrix environment (Aarden et al., 1996). The expression of the Wnt antagonist sclerostin (SOST) in osteocytes, suggests that these cells might have a potential role in inhibiting bone formation (Keller and Kneissel, 2005; Robling et al., 2006). Osteocytes also play a

key role in mineralisation and phosphate metabolism by secreting dentin matrix protein 1 (DMP1), PHEX (phosphate-regulating gene with homologies to endopeptidases on the X chromosome) and fibroblastic growth factor 23 (FGF23) (Strom and Juppner, 2008).

It has been proposed that osteocytes might also regulate recruitment and function of osteoclasts by producing anti-resorptive signals, such as TGF-β (Heino et al., 2002) or pro-resorptive signals, such as RANKL and M-CSF (Zhao et al., 2002).

Osteocytes can remain healthy for long periods in bone that is not turned over (Murray J.Favus [Editor], 2006). However, empty lacunae are indicative of apoptotic osteocytes. Osteocyte apoptosis has been associated with regions of microdamage suggesting that through death osteocytes might generate a signal that targets the resorption process (Noble et al., 2003). Others suggested that this association may be indicative of the necessity of viable osteocytes in order to inhibit osteoclastic resorption (Tatsumi et al., 2007).

1.2.3   Osteoclasts

Osteoclasts are large multinucleated cells of haematopoietic origin that are formed by fusion of mononuclear precursor cells from the myeloid lineage (Murray J.Favus [Editor], 2006). Osteoclasts have been described as terminally differentiated cells from macrophages or myelin precursors (Vaananen and Laitala-Leinonen, 2008), and thus far there is no solid evidence showing a subsequent re-differentiation of osteoclasts to other cells of monocyte/macrophage lineage (Vaananen and Laitala-Leinonen, 2008). Osteoclasts are responsible for bone resorption, a process that involves dissolving hydroxyapatite and degrading the organic bone matrix (Murray J.Favus [Editor], 2006) (Figure 1.4).
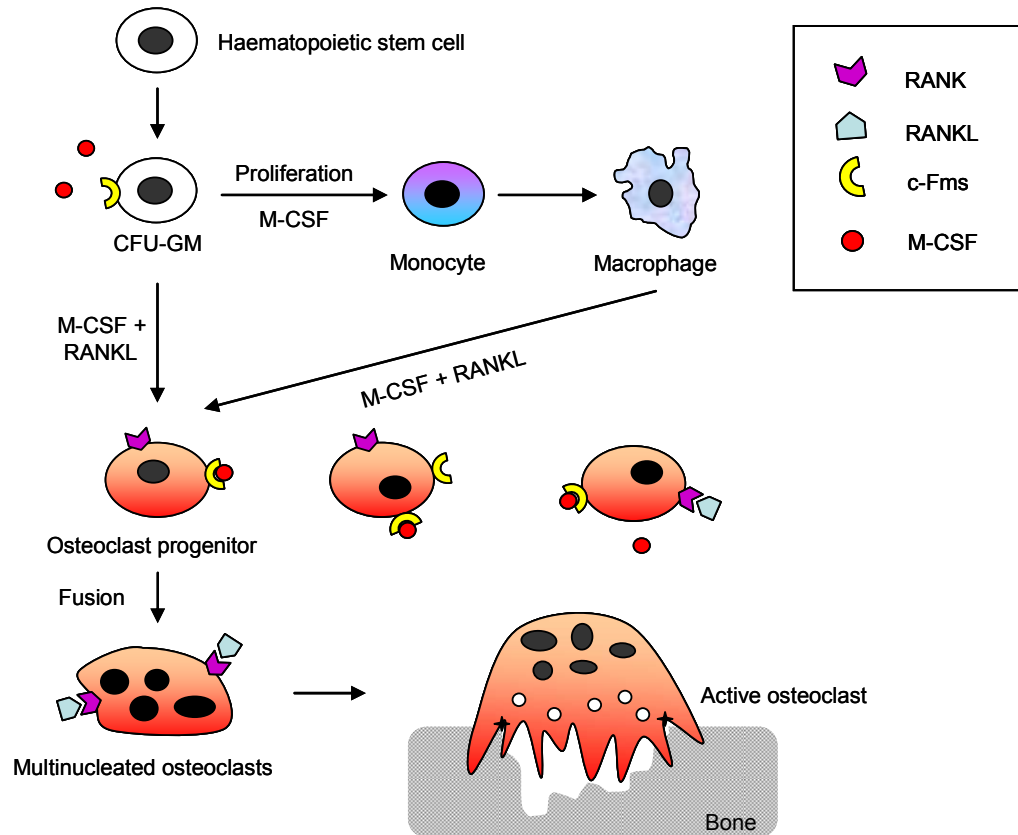
Figure 1.4: Schematic illustration of the differentiation of osteoclasts. See text for descriptions. *Abbreviations*: CFU-GM, colony forming unit-granulocyte-macrophage; M-CSF, macrophage colony stimulating factor; c-Fms, M-CSF receptor; RANK, receptor activator of nuclear factor κB; RANKL, RANK ligand.

Differentiation of precursor cells to functional osteoclasts requires the presence of two essential cytokines, M-CSF and RANKL. Together, these cytokines have the capacity to drive haematopoietic cells to osteoclasts at any stage of their differentiation pathway [reviewed in (Vaananen and Laitala-Leinonen, 2008; Boyce and Xing, 2008)]. M-CSF, which is secreted by osteoblasts or expressed on their membrane, binds to a membrane receptor (c-Fms) expressed on early and committed osteoclast precursors, as well as mature osteoclasts (Weir et al., 1993). This interaction provides signals for osteoclast differentiation and osteoclast survival (Teitelbaum, 2000; Takayanagi, 2005). RANKL is

a membrane-bound cytokine expressed on osteoblasts, dendritic cells, mature T cells, and haematopoietic precursors. In osteoblasts and activated $CD4^+$ and $CD8^+$ T cells RANKL is also produced in a soluble form (Jones et al., 2002). Upon binding to the RANK receptor found on osteoclast precursors, RANKL induces their differentiation into multinucleated osteoclasts (Takayanagi, 2005; Teitelbaum, 2000) (Figure 1.4).

The interaction of RANKL with RANK receptor is blocked by OPG, a soluble decoy receptor for RANKL (Kong et al., 1999). Therefore, the rate of osteoclast differentiation is determined by the ratio of RANKL to OPG (Horowitz et al., 2001). Inflammatory cytokines such as IL-1β and tumour necrosis factor α (TNF-α) are known to affect osteoclast formation, resorption and survival (Pfeilschifter et al., 1989). Moreover, IL-6, and IL-11 act directly on osteoclast progenitors to stimulate proliferation and inhibit apoptosis (Jilka, 1998). Prostaglandins and in particular prostaglandin E2 (PGE2), stimulate osteoclast formation by acting directly on osteoclast precursors (Lacey et al., 1995) or immature osteoblast (Kanematsu et al., 2000), and stimulate bone resorption (Fuller and Chambers, 1989). However, PGE2 was also reported to inhibit osteoclast differentiation and M-CSF production in human bone marrow stromal cells (Besse et al., 1999).

Figure 1.5 illustrates some of the receptors and signal transduction pathways in osteoclasts.
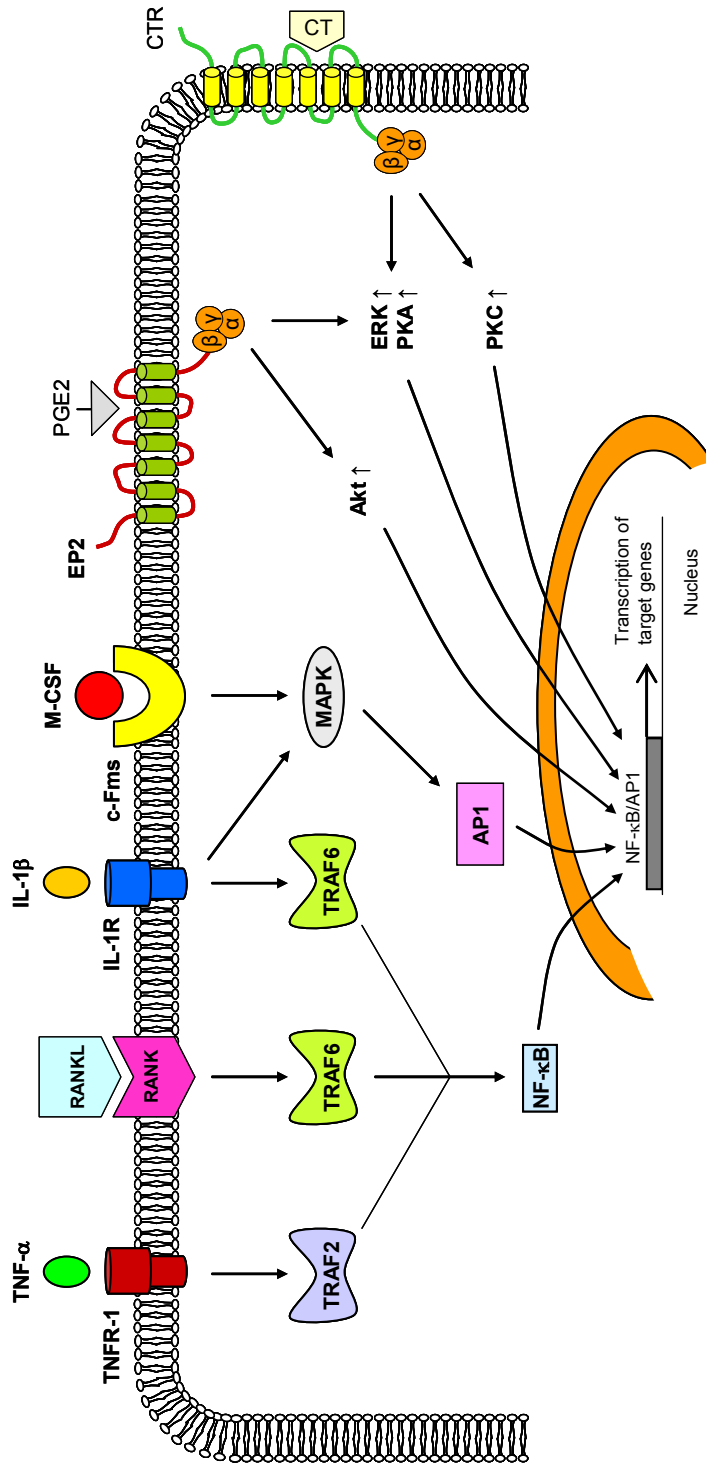
Figure 1.5: Schematic illustration of receptors and signal transduction pathways in osteoclasts. See text for descriptions.

Abbreviations: TNF-α, tumour necrosis factor α; TNFR-1, TNF receptor 1; RANK, receptor activator of nuclear factor (NF) κB; RANKL, RANK ligand; IL-1β, interleukin 1β; IL-1R, IL-1 receptor; TRAF, TNF receptor associated factor; NF-κB, nuclear factor κB; M-CSF, macrophage colony stimulating factor; c-Fms, M-CSF receptor; MAPK, mitogen activated protein kinase; AP1, activator protein 1; PGE2, prostaglandin E$_2$; EP2, PGE2 receptor; PKA, protein kinase A; CT, calcitonin; CTR, calcitonin receptor; PKC, protein kinase C.

Osteoclasts are usually in a close vicinity to mineralised matrix and once attached to the bone surface they become polarised and start resorbing bone (Murray J.Favus [Editor], 2006). During resorption there is an extensive cytoskeletal modulation which is tightly linked to membrane polarisation. The membrane of a resorbing osteoclast is divided into four particular domains: the sealing zone, which is a ring-shape zone securing the osteoclast to the underlying mineralised bone referred to as Howship's lacuna but commonly refer to as resorption lacuna; the ruffled border membrane, which is the main resorbing organelle (Murray J.Favus [Editor], 2006); the basolateral membrane at the non-bone facing side of the osteoclast; and finally the functional secretory domain found at the top of the basal surface (Salo et al., 1996).

At the initial step of resorption, there is an accumulation of podosomes that form actin rings (Murray J.Favus [Editor], 2006; Vaananen and Laitala-Leinonen, 2008). Attachment of podosomes to the matrix is mediated by $\alpha v \beta 3-$integrin, whereas the final tight sealing is mediated by proteins such as CD44 (Chabadel et al., 2007). The essential role of $\alpha v \beta 3-$integrin in matrix degradation is supported by the fact that mice with targeted deletion of the $\beta 3$ chain had dysfunctional osteoclasts (McHugh et al., 2000) and *in vitro* osteoclast cultures from these mice showed defective resorption (Faccio et al., 2003). Microtubules and microfilaments mediate vesicular transport to and from the ruffled border (Mulari et al., 2003). Microtubules also reach the functional secretory domain of the basal membrane, transferring bone resorption products by transcytosis into the extracellular space (Salo et al., 1996) (Figure 1.6).

An important function of the osteoclast is to dissolve hydroxyapatite crystals and this requires lowering of the pH. This is achieved by secretion of protons and chloride ions through the ruffled border (Sundquist et al., 1987; Blair et al., 1989; Vaananen et al., 1990). Generation of protons within osteoclasts is mediated by a cytosolic carbonic anhydrase II (CA II) (Sundquist et al., 1987). This enzyme forms carbonic acid (H_2CO_3) from water and carbon dioxide, which dissociates spontaneously into protons (H^+) and

bicarbonate ions (HCO_3^-). Mice deficient in CA II show growth retardation and renal tubular acidosis, but their bone mass remains unaffected (Lewis et al., 1988). Bicarbonate ions are released from the osteoclast via an anion exchanger whereas the protons are used by the ATP-consuming proton pump known as vacuolar ATPase (V-ATPase) (Blair et al., 1989; Vaananen et al., 1990). V-ATPases are present in intracellular vesicles and ruffled border of osteoclasts (Blair et al., 1989; Vaananen et al., 1990). Mutation in the a3 subunit of V-ATPase causes malignant osteopetrosis in human (Kornak et al., 2000) and genetic inactivation of a3 subunit in mice produces severe osteopetrotic phenotype (Li et al., 1999). Chloride ions are then passively transported into the resorption lacunae mainly via the CIC-7 chloride ion channel, a process that maintains normal intracellular pH (Teti et al., 1989; Schaller et al., 2005). Loss of CIC-7 causes osteopetrosis in human and mice (Kornak et al., 2001). Protons and chloride ions initiate the resorption process in Howship's lacunae. Only after dissolution of bone mineral has occurred will degradation of the organic matrix occur. Matrix metalloproteinases (MMPs) and cathepsins, mainly cathepsin K, are responsible for the degradation of organic matrix (Figure 1.6). It has been shown that the genetic inactivation of cathepsin K in mice leads to osteopetrosis (Gowen et al., 1999) due to the failure of osteoclasts to break down type I collagen (Votta et al., 1997). MMP-9 knockout mice exhibit an abnormal pattern of skeletal growth plate vascularization and ossification indicating the role of MMPs in skeletal maturation (Vu et al., 1998).

Figure 1.6: Schematic illustration of transport mechanisms involved in bone resorption in osteoclast. Hydrogen and chloride ions (H^+ and Cl^-), Cathepsin K and MMP-9 are secreted across the ruffled membrane into the Howship's lacuna by means of vacuolar proton pumps (V-ATPases), chloride channels and secretory transport, respectively. Matrix degradation products are endocytosed though the ruffled border into the cytoplasm and released at the basal surface of the osteoclast membrane.

Tartate resistant acid phosphatase (TRAcP) and specifically the isoform TRAcP5b is used as a cellular marker for osteoclastic resorption activity. However, there is still a dispute about the function of TRAcP in osteoclasts since this gene is also highly expressed in dendritic cells (Hayman et al., 2001). Some studies suggest that in dendritic cells TRAcP might be involved in antigen processing and similarly in osteoclasts it could have a role in preventing autoimmunity against bone, rather than play a role in resorption directly [reviewed in (Vaananen and Laitala-Leinonen, 2008)]. TRAcP-knockout mice showed mild osteopetrosis, deformity of the long bones, impairment of macrophage function and abnormal immunomodulatory cytokine responses, confirming that the *TRAcP* gene plays a role in both the immune system and skeleton (Hayman and Cox, 2003; Hayman et al., 2001).

1.2.4 *Adipocytes*

Adipocytes are derived from multipotent MSCs, in a process known as adipogenesis. The adipogenic transcription factors such as CCAAT-enhancer-binding proteins (C/EBPs) and PPARγ are expressed by MSCs in addition to osteogenic factors such as Runx2 and Osx already mentioned in section 1.2.1, page 5. In an undifferentiated state, the effects of specific lineage factors in MSCs counteract each other (Rosen and MacDougald, 2006; Marie, 2008) until appropriate conditions disrupt this balance. For example PPARγ down-regulates Runx2 expression and favours adipogenesis at the expense of osteogenesis, whereas Runx2 and Osx suppress adipogenesis (c.f. Figure 1.2, page 6).

PPARγ has been described as the adipogenic 'master regulator' because adipogenesis cannot occur in its absence. PPARγ is crucial not only for adipogenesis but also for the viability and survival of adipocytes in the differentiated state (Tamori et al., 2002). There are two protein isoforms, PPARγ1 and PPARγ2, but only PPARγ2 is specifically expressed by adipocytes.

Other pro-adipogenic transcription factors involved in adipocyte differentiation are signal transducer and activator of transcription-5α, cyclic AMP (cAMP) response element-binding protein (CREB); Krüppel-like factors (KLFs), apart from KLF2 and KLF7 that are both anti-adipogenic factors; KROX20, also known as early growth response protein; early B-cell factor 1 (EBF1) and many more [reviewed in (Rosen and MacDougald, 2006)].

1.2.5 Chondrocytes

Chondrocytes are also cells of mesenchymal origin and are the first skeleton-specific cells to appear during embryonic development (c.f. Figure 1.2, page 6). The master transcription factor of chondrogenesis is the sex determining region Y (SRY)-box 9 (Sox9) (Bi et al., 1999). Sox9 induces the condensation and differentiation of MSCs into chondrocytes (Bi et al., 1999) and activates the expression of two major structural components of cartilage matrix, aggrecan and type II collagen (Ng et al., 1997). Sox9 also stimulates the expression of type XI collagen and cartilage-derived retinoic acid-sensitive protein (CD-RAP) (Ng et al., 1997; Xie et al., 1999). Sox5 and Sox6 are also involved in the differentiation of non-hypertrophic chondrocytes, by binding to Sox9 and enhancing its transactivation function (Lefebvre et al., 1998).

As skeletogenesis proceeds, proliferating chondrocytes at the metaphysis of long bone progressively become hypertrophic and express type X collagen. Chondrocyte hypertrophy is positively regulated by the transcription factors Runx2 and Runx3 (Yoshida et al., 2004). However, in perichondrium, the connective tissue surrounding the cartilage of developing bone, Runx2 stimulates the expression of fibroblast growth factor 18 (FGF18), which in turn inhibits chondrocyte hypertrophy (Hinoi et al., 2006). So while Runx2 promotes chondrocyte hypertrophy at the beginning to prepare cells for following events of skeletogenesis, it subsequently inhibits any further chondrocyte proliferation to avoid premature bone formation [reviewed in (Karsenty, 2008)].

Fully differentiated hypertrophic chondrocytes secrete angiogenic factors which induce vascular invasion from the perichondrium. The invading blood vessels carry osteoblasts, osteoclasts and haemopoietic cells, which together form the primary ossification centres. Within these centres, hypertrophic chondrocytes undergo apoptosis and the cartilage matrix is replaced by bone extracellular matrix, rich in type I collagen. This process of bone development is known as endochondral ossification. In regions of the craniofacial skeleton and the clavicle, the mesenchymal condensations bypass the cartilaginous intermediary step and differentiate directly into osteoblasts which produce intramembranous bone. This process of bone development is known as intramembranous ossification [reviewed in (Olsen et al., 2000; Karsenty and Wagner, 2002; Karsenty, 2008)].

1.3   BONE REMODELLING

The skeleton is nearly completely modelled during embryonic development. Throughout life, the skeleton undergoes continuous remodelling in response to local or systemic stimulation, mechanical stresses, after physical exercise or mechanical loading (Raisz, 1999). Bone remodelling is a dynamic process of bone resorption and bone formation where osteoclasts and osteoblasts closely collaborate in what is called a basic multicellular unit (BMU) to maintain the integrity of the skeleton. The remodelling process consists of three consecutive phases: resorption, reversal and formation (Figure 1.7) (Murray J.Favus [Editor], 2006; Hadjidakis and Androulakis, 2006; Lerner, 2006).

1.3.1   Bone resorption

The bone surface is lined with quiescent osteoblasts which are known as bone lining cells. After a prolonged resting period, a new remodelling cycle is initiated through a process that may involve osteocytes, lining cells or pre-osteoblasts in the bone marrow (Hadjidakis and Androulakis, 2006). The first stage of bone resorption is the recruitment of osteoclast precursors from bone marrow and their targeting to bone. Osteoblast/lining cells are thought to secrete a variety of proteolytic enzymes, namely MMPs, collagenase and gelatinase (Meikle et al., 1992), which degrade a thin layer of osteoid that lines the bone surface and eventually facilitate the access of osteoclast precursors to the underlying mineralised bone.

Expansion of the osteoclast progenitor pool, development into multinucleated osteoclasts, survival and activation are controlled by the combined action of RANKL (Boyce and Xing, 2008; Hsu et al., 1999), OPG (Boyce and Xing, 2008; Hofbauer and Schoppet, 2004) and M-CSF (Umeda et al., 1996), which are mainly produced by cells of the osteoblastic lineage.
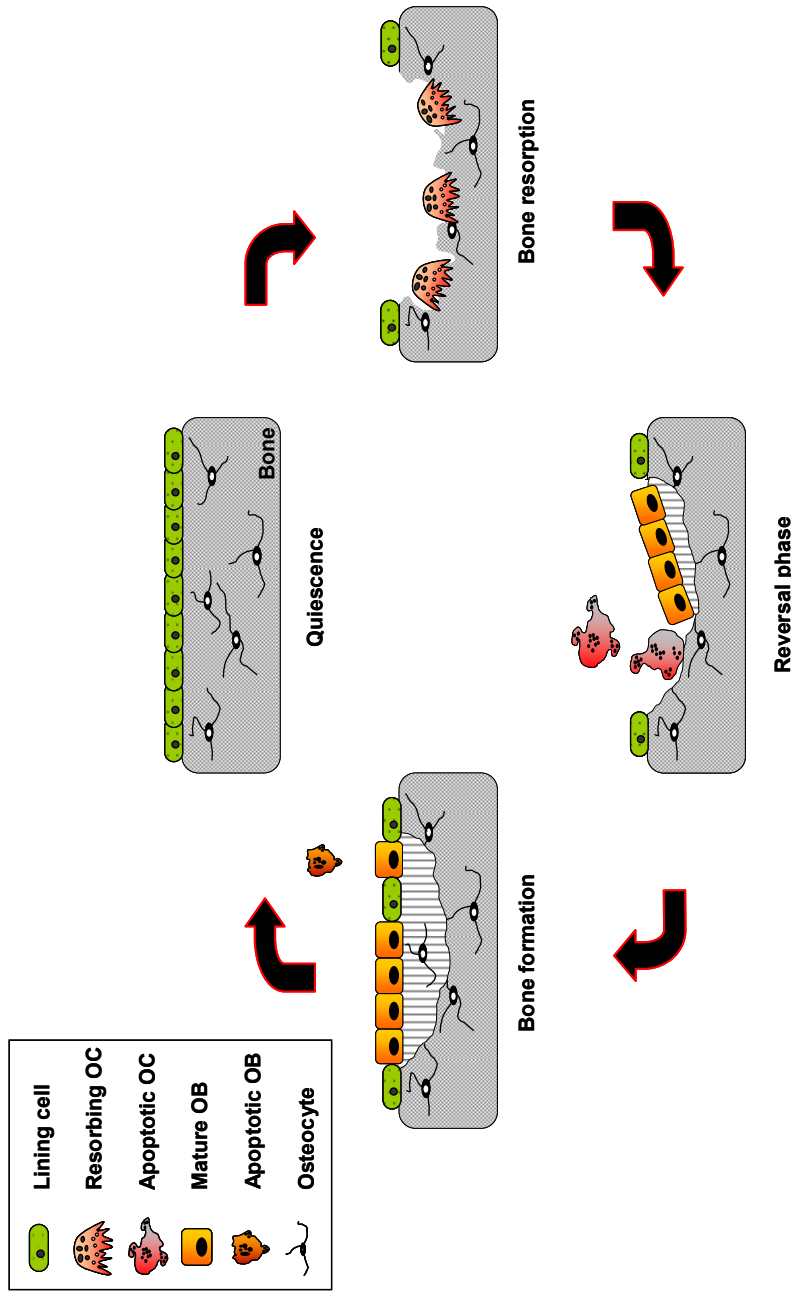
Figure 1.7: Schematic illustration of bone remodelling cycle. Upon stimulus mature osteoclasts appear on bone surface and resorb the mineral components of bone. Following resorption phase and osteoclast apoptosis, there is a reversal phase in which osteoblast recruitment and proliferation occurs. Fully differentiated osteoblasts deposit osteoid on the resorption site, thereby initiating bone formation. Bone formation is followed by a phase in which freshly laid osteoid becomes mineralised and covered by bone lining cells.

In response to these signals, osteoclasts attach to the bone surface and the next step involves recognition of extracellular bone matrix proteins and osteoclast polarisation. It has been suggested that this occurs via members of the integrin superfamily of adhesion receptors, in particular the αvβ3 vitronectin receptor (Lakkakorpi et al., 1991). The vitronectin receptor binds to the extracellular matrix proteins, such as vitronectin, fibronectin and type I collagen, at an Arg-Gly-Asp tripeptide (RGD) exposed on the surface of the underlying mineralised bone. Once bound to bone extracellular matrix, osteoclasts polarise and form the ruffled border and the sealing zone (Roodman, 1996).

The sealing zone is the region of the cytoplasm that is rich in F-actin filaments known as actin rings (Hill, 1998). Actin rings together with integrin receptors form focal adhesions or podosomes which are responsible for the tight sealing of the space beneath, where the ruffled border expands and bone matrix is dissolved.

The ruffled border is the functional resorbing domain of the active osteoclast that enables the transport of protons and chloride ions by means of V-ATPases and chloride channels respectively. Within the sealed resorption cavity, protons and ions create an acidic environment necessary for the demineralisation and degradation of the bone matrix. The demineralised organic matrix of bone is subsequently degraded by proteolytic enzymes including cathepsin K and MMP-9 (Hill, 1998). Both enzymes are highly expressed in osteoclasts and secreted across the ruffled border into the resorption lacuna during bone resorption. MMP-9 releases the carboxyterminal telopeptide of type I collagen, and cathepsin K releases the carboxyterminal cross-linked peptide of type I collagen (Parikka et al., 2001), both of which are used as biochemical markers of bone resorption.

Bone degradation products, both organic and inorganic, are endocytosed from the ruffled border membrane and transported in vesicles through the cell to the functional secretory

domain found at the top of the basal surface (Salo et al., 1996), where they get exocytosed into the extracellular space (Salo et al., 1997).

Ultimately osteoclasts undergo apoptosis and are rapidly removed by phagocytes, at the interface between the resorption and reversal phase.

1.3.2   Reversal phase

Following bone resorption, there is the reversal phase. During this period mononuclear, macrophage-like cells appear in the lacunae and remove residual organic matrix (Hill, 1998; Lerner, 2006). The cement line that marks the limit of resorption and acts to cement together the old and the new bone is formed during the reversal phase (Murray J.Favus [Editor], 2006).

1.3.3   Bone formation

Bone formation is initiated by the recruitment of osteoblast precursors at the freshly resorbed sites. It has been suggested that this process is mediated by local, chemotactic factors produced during the resorption process (Mundy et al., 1982). Such factors are thought to include TGF-β or insulin growth factor 1 (IGF-1), both which are abundant in the extracellular matrix of bone and which are released during the resorption process. Structural proteins such as type I collagen and OCN could also play an important role in this process, since they have been also shown to have chemotactic effects (Lerner, 2006).

The next event involved in the bone formation phase is the proliferation and differentiation of osteoprogenitor cells into committed osteoblast precursors and then into mature osteoblasts. This process is also mediated by factors released during the resorption phase and by osteoblast-derived growth factors. Candidate factors that may mediate this process include members of the TGF-β family, IGF-1 and 2, fibroblast

growth factors (FGFs) and platelet-derived growth factors (PDGFs) (Hill, 1998). In this context, the factors which are involved in the recruitment and activation of osteoblasts in basic multicellular units are referred to as 'coupling factors' which link bone resorption to bone formation (Lerner, 2006).

Differentiated mature osteoblasts produce large amounts of type I collagen (Ducy et al., 2000b; Mackie, 2003) and together with other non-collagenous proteins, such as OPN, OCN, OSN, BSP and proteoglycans, form the extracellular matrix (Murray J.Favus [Editor], 2006). This bone matrix is initially unmineralised and known as osteoid until the mineralisation process is completed. For this, mature osteoblasts secrete ALP, which degrades inhibitors of mineralisation such as pyrophosphates and also releases membrane bound bodies known as matrix vehicles at random sites within the collagen scaffold. These matrix vehicles contain proteins, acidic phospholipids, calcium and phosphate that induce hydroxyapatite formation. Hydroxyapatite crystal deposition turns osteoid into mature mineralised matrix and gives bone its rigidity and stiffness (Murray J.Favus [Editor], 2006; Ducy et al., 2000b; Katagiri and Takahashi, 2002).

The cessation of osteoblast activity is probably mediated by negative regulators of bone formation such as SOST (Sutherland et al., 2004), or due to induction of osteoblast apoptosis by mechanisms that are poorly understood. The average lifespan of osteoblasts is three months, after which approximately 65% of functioning osteoblasts undergo apoptosis (Jilka et al., 1998). The remaining osteoblasts are either buried within the bone matrix as osteocytes or converted into flat, lining cells giving bone surfaces their quiescent nature (Murray J.Favus [Editor], 2006). Bone lining cells remain quiescent until they are activated once again in the next bone remodelling cycle.

1.4   MOLECULAR CONTROL OF BONE REMODELLING

1.4.1   OPG/RANKL/RANK

The receptor activator of NF-κB (RANK) together with its ligand, RANK ligand (RANKL) and the decoy receptor for RANKL called osteoprotegerin (OPG), have been identified as members of the tumour necrosis factor (TNF)/TNF-receptor superfamily proteins. The OPG/RANKL/RANK system has been recognised as the dominant regulator of osteoclastogenesis (Murray J.Favus [Editor], 2006).

OPG was discovered independently by two groups, the Amgen Inc. group while searching for TNF-receptor related molecules (Simonet et al., 1997), and the Snow Brand Milk group while searching for osteoclast stimulatory and inhibitory factors (Yasuda et al., 1998a). Later it became clear that both groups isolated cDNA clones encoding the same protein, OPG. OPG is initially synthesized as a 401-amino acid peptide which is cleaved into a mature protein of 380 amino acids (Simonet et al., 1997; Yasuda et al., 1998a). Unlike all the other TNF receptor superfamily members, OPG lacks transmembrane and cytoplasmic domains and instead is secreted as a soluble protein. OPG mRNA was found to be expressed in various tissues, including lung, heart, kidney, liver, stomach, intestine, brain, spinal cord, thyroid gland and bone (Simonet et al., 1997; Yasuda et al., 1998a). However, the major biologic actions of OPG are to protect bone from excessive osteoclastic resorption by inhibiting osteoclast differentiation and activity (Murray J.Favus [Editor], 2006; Boyce and Xing, 2008), and to protect from vascular calcification (Van Campenhout and Golledge, 2008). Mice lacking OPG exhibited severe osteoporosis due to enhanced osteoclastogenesis (Mizuno et al., 1998).

Soon after the characterisation of OPG, both above-mentioned groups identified the OPG ligand (Lacey et al., 1998; Yasuda et al., 1998b), which was identical to what was already known as TNF-related activation-induced cytokine (TRANCE) (Wong et al.,

1997), and receptor activator of NF-κB ligand (RANKL) (Anderson et al., 1997). RANKL exists as a membrane-bound, 316-amino acid long homotrimeric protein found typically on osteoblasts, and as a soluble protein, derived by cleavage of the full-length form (Lacey et al., 1998). RANKL mRNA is expressed mainly in bone and bone marrow, as well as in lymphoid tissues (Wong et al., 1997; Anderson et al., 1997). RANKL is necessary and sufficient for osteoclast formation, activation and survival. In addition, RANKL is required for immune responses such as, activation of c-Jun N-terminal kinase (JNK) in T cells (Wong et al., 1997), inhibition of apoptosis of dendritic cells (Wong et al., 1997), lymph node development (Dougall et al., 1999) and B cell maturation (Franzoso et al., 1997). *RANKL* knockout mice suffer from severe osteopetrosis with defects in tooth eruption and differentiation of T and B cells (Kong et al., 1999). In human, *RANKL* mutations were also associated with osteopetrosis due to lack of osteoclasts. These individuals showed no improvement following haematopoietic stem cell transplantation but seemed to be cured with exogenous RANKL administration (Sobacchi et al., 2007).

The receptor for RANKL was identified to be RANK (Anderson et al., 1997). RANK is a 616-amino acid transmembrane protein with an N-terminal extracellular domain and a large C-terminal cytoplasmic domain (Anderson et al., 1997). It is mainly expressed on cells of macrophage/monocytic lineage, T and B cells, dendritic cells and fibroblasts (Anderson et al., 1997; Hsu et al., 1999). Mice deficient in *RANK* suffer from profound osteopetrosis since they lack specific signals for the differentiation of myeloid derived osteoclasts (Dougall et al., 1999; Kapur et al., 2004). Such mice also lacked peripheral lymph nodes and had defective B and T cell maturation similarly to *RANKL* knockouts.

The unravelling of the OPG/RANKL/RANK system explained the precise mechanism of osteoblast-osteoclast coupling and the regulatory role of OPG as a RANKL decoy receptor that blocks the effects of RANKL (Figure 1.8). Potential alterations in this

system result in disorders such as age-related osteoporosis, familial Paget's disease and familial expansile osteolysis [reviewed in (Khosla, 2001)].

Other crucial components of the OPG/RANK/RANKL signalling pathway include factors belonging to the TNF family such as TNF receptor-associated factors (TRAFs), the inhibitor of κB kinase (IKK) complex (comprising IKKα, β and γ) and nuclear factor κB (NF-κB), which consists of a family of transcription factors that are important for the regulation of cell growth and survival [reviewed in (Wada et al., 2006)] (c.f. Figure 1.5, page 13 and 1.9, page 29). Genetic experiments have shown that mice deficient in TRAF6, IKKβ or the NF-κB p50 and p52 proteins suffer from severe osteopetrosis (Lomaga et al., 1999; Iotsova et al., 1997; Ruocco et al., 2005). The RANKL/RANK signalling pathway is illustrated in Figure 1.9, page 29.
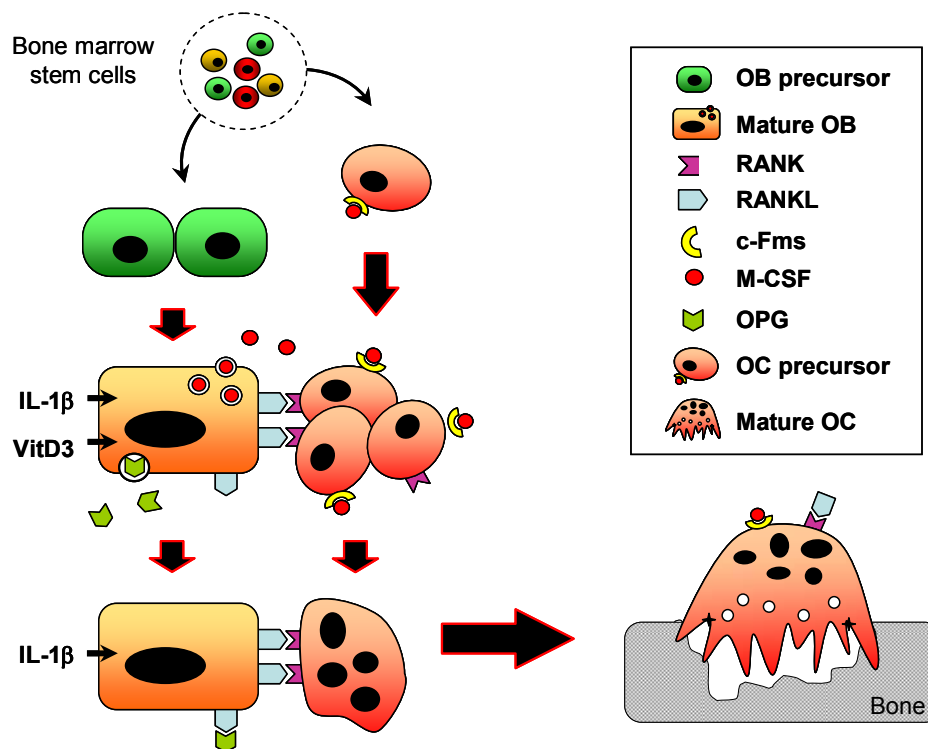
Figure 1.8: Schematic illustration of osteoclast differentiation and cross-talk with osteoblasts. See text for descriptions. *Abbreviations*: RANK, receptor activator of nuclear factor κB; RANKL, RANK ligand; M-CSF, macrophage colony stimulating factor; c-Fms, M-CSF receptor; OPG, osteoprotegerin; IL, interleukin; VitD3, vitamin D3.

1.4.2   M-CSF

Macrophage colony stimulating factor (M-CSF) is a disulphide-linked dimeric glycoprotein with a molecular weight ranging from 45 to 100kDa depending on the glycosylation pattern (Maier et al., 2000). M-CSF can either be secreted into the circulation or expressed as a membrane spanning glycoprotein on the surface of M-CSF producing cells (Cerretti et al., 1988). Osteoblasts produce soluble and cell-surface forms of M-CSF, which function synergistically in stimulating osteoclast formation (Yao et al., 2002).

M-CSF was revealed to be an essential factor for osteoclastogenesis since not only it induces the proliferation of osteoclast precursor cells, but also supports their survival and up-regulates the RANK expression which is essential for osteoclast precursor cells (Arai et al., 1999). M-CSF signalling is also associated with the expression of the anti-apoptotic protein Bcl-2 in the osteoclast lineage and thereby is involved in prolonging osteoclast lifespan (McGill et al., 2002).

The effects of M-CSF are mediated by the M-CSF receptor which is encoded by the *c-fms*, a proto-oncogene (Stanley et al., 1983). Mice with a mutation in the coding region of gene encoding for M-CSF are osteopetrotic (*op/op*) and defective in production of functional M-CSF. These mice are severely deficient in mature macrophages and osteoclasts (Yoshida et al., 1990), have very low numbers of tissue macrophages (Usuda et al., 1994) and no multinuclear osteoclasts, although small numbers of TRAcP-positive mononuclear cells, i.e. pre-osteoclasts, were observed (Umeda et al., 1996). Likewise, targeted disruption of the *c-fms* gene resulted in osteopetrosis, mononuclear phagocyte deficiency and increased primitive haematopoietic progenitor cells (Dai et al., 2002).

Figure 1.9 illustrates the RANKL/RANK and M-CSF/c-Fms signalling pathways.
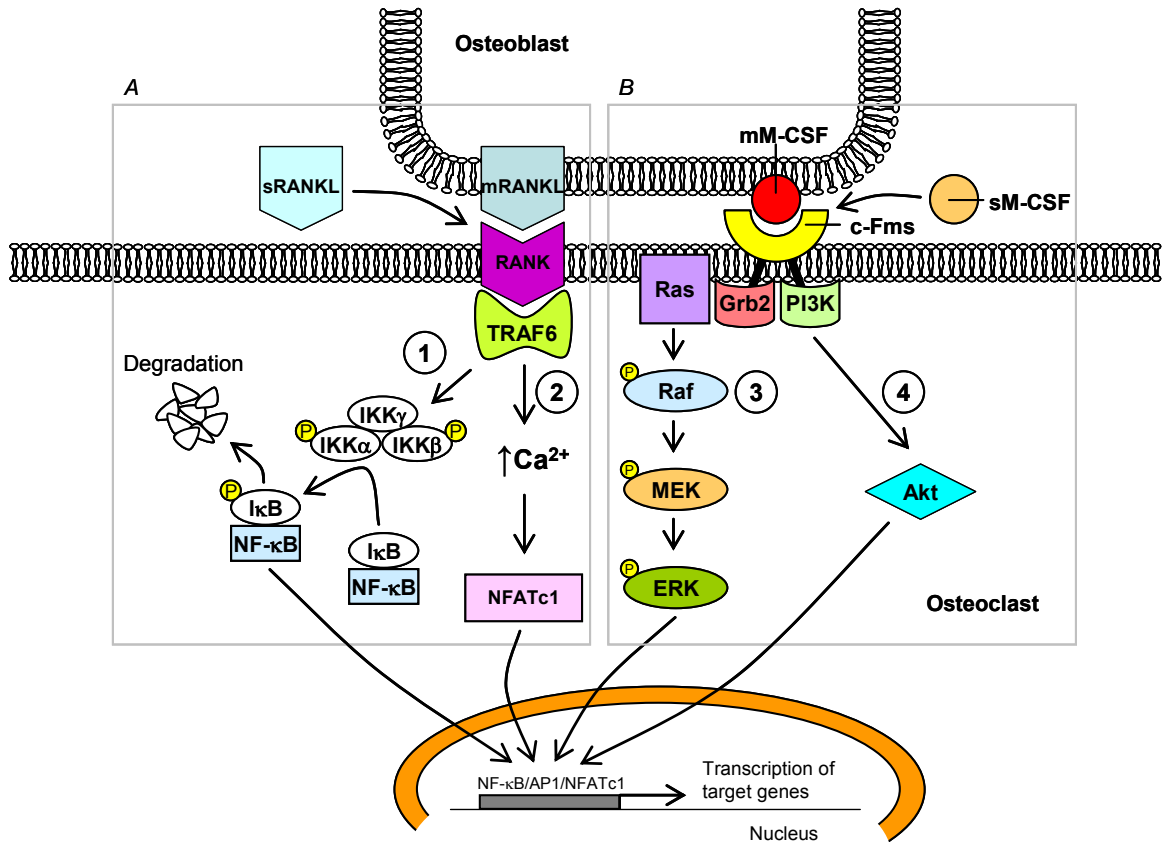
Figure 1.9: RANKL/RANK and M-CSF/c-Fms signalling pathways. *A*. Activation of receptor activator of nuclear factor (NF)-κB (RANK) with membrane-bound (mRANKL) or soluble RANK ligand (sRANKL) induces the recruitment of factors belonging to the tumour necrosis factor (TNF) family such as TNF receptor-associated factor 6 (TRAF6), which consequently recruits and phosphorylates other intracellular signalling proteins, including inhibitor of the κB (IκB) kinase (IKK) complex comprising IKKα, β and γ (1). IKKα and β phosphorylate IκB proteins and target them for proteolytic degradation. This activates NF-κB for nuclear translocation, where it induces the transcription of osteoclast-specific genes including TRAcP, RANK and Cathepsin K (Asagiri and Takayanagi, 2007). TRAF6 function leads to calcium signalling and the induction of NFATc1, which is necessary for osteoclast formation (2) (Takayanagi et al., 2002). *B*. Binding of macrophage colony stimulating factor (M-CSF) to its receptor (c-Fms) recruits the adaptor protein growth factor receptor bound protein 2 (Grb2) which subsequently recruits the small GTPase Ras to the plasma membrane. This complex then generates prolonged signalling through the subsequent Raf/MEK/ERK cascade. ERK is a kinase, which phosphorylates and activates, among other proteins, transcription factors regulating the expression of target genes (Ross, 2006). Phosphatidylinositol-3-Kinase (PI3K) also interacts with c-Fms and activates the anti-apoptotic protein Akt [also known as protein kinase B (Borgatti et al., 2000)] which regulates the transcription of target genes (Ross, 2006).
Abbreviations: ERK, extracellular signal-regulated kinase; MEK, mitogen activated protein kinase (MAPK) kinase/ERK kinase; NFATc1 (NFAT2), nuclear factor of activated T cells; AP1, activator protein 1.

29

1.4.3   Oestrogen

Oestrogen belongs to the gonadocorticoid class of steroid hormones, and is produced by the adrenal cortex and ovary. The effects of oestrogen in reproductive function include the development of female secondary sexual characteristics, the regulation of menstrual cycle, the timing of ovulation in pre-menopausal women and maintenance of pregnancy (Ruggiero and Likis, 2002). The skeleton is one of the main targets of oestrogen as it regulates bone growth and remodelling in both men and women. Decreased levels of oestrogen in post-menopausal women is the main cause of osteoporosis (Ruggiero and Likis, 2002; Riggs et al., 2002; Hawse et al., 2008). Oestrogen replacement has therefore been used for treatment of menopausal symptoms and for the prevention of osteoporosis (Rozenberg et al., 1995).

Two oestrogen receptor isoforms have been identified, ERα and ERβ, with different tissue distributions. Bone cells express both oestrogen receptors and it has been shown that oestrogen treatment of cultured cells has effects on osteoblast and osteoclast differentiation (Turner et al., 1994). However, the oestrogen receptor isoforms and the stage of differentiation influence the response of human osteoblasts to oestrogen (Waters et al., 2001), because these two receptors regulate distinct sets of genes in osteoblasts (Stossi et al., 2004; Monroe et al., 2005). Deletion of both oestrogen receptors results in profound decrease of trabecular bone volume in female mice and significant defects in the cortical bone and bone mineral density (BMD) equally in both sexes (Sims et al., 2002).

It is believed that oestrogen prevents bone loss mainly by reducing bone resorption rather than affecting bone formation. However, it has been shown that oestrogen suppresses the production of the osteoclast-stimulating cytokines IL-6 (Girasole et al., 1992), TNF-α (Srivastava et al., 1999) and M-CSF (Srivastava et al., 1998) in cells of the bone marrow stromal/osteoblastic lineage. Moreover, oestrogen stimulates the

expression of the anti-osteoclastogenic factor OPG in osteoblasts (Hofbauer et al., 1999b), which acts as a decoy receptor of RANKL and hence interrupts osteoclastogenesis. The indirect inhibitory action of oestrogen on bone resorption is also observed in its stimulatory effect for the production of TGF-β, which subsequently induces osteoclast apoptosis (Hughes et al., 1996).

Loss of oestrogen following ovariectomy is associated not only with increased resorption but also with increased numbers of osteoblast progenitors and higher levels of the bone formation marker OCN (Jilka, 1998). However, *in vitro* experiments have shown that addition of oestrogen suppresses osteoblast apoptosis (Kousteni et al., 2001) and increases cell differentiation and collagen type I production (Jilka, 1998).

1.4.4 Vitamin D

Vitamin D is a steroid hormone produced in the skin following exposure to sunlight (Murray J.Favus [Editor], 2006). Vitamin D_3 is also found in oily fish, fish liver oils or foods fortified with vitamin D. In order to become biologically active, Vitamin D_3 undergoes two successive hydroxylations in the liver and kidney and transforms into the hormonally active form 1,25-$(OH)_2$ vitamin D_3.

The main biological effect of 1,25-$(OH)_2$ vitamin D_3 is to help maintain the serum calcium at physiological levels. This is achieved by: a) inducing the expression of the TRPV6 epithelial calcium channel in the small intestine (Song et al., 2003), b) stimulating osteoclastogenesis and c) facilitating the movement and transfer of calcium through the cytoplasm and finally across the basolateral membrane into the circulation (Murray J.Favus [Editor], 2006; Christakos et al., 2003).

In the bone microenvironment, 1,25-$(OH)_2$ vitamin D_3 interacts with its nuclear receptor Vitamin D receptor (VDR) and regulates the transcription of specific genes involved in

bone formation, such as type I collagen and ALP (Owen et al., 1991), osteocalcin (Breen et al., 1994) and osteopontin (Safran et al., 1998), or genes that play a role in osteoclastogenesis, such as RANKL and IL-1β (Lee et al., 2002). *In vitro* studies showed that VDR signalling in chondrocytes promotes osteoclastogenesis by regulating FGF23 production in osteoblasts (Masuyama et al., 2006) and stimulates the expression of vascular endothelial growth factor (VEGF) (Lin et al., 2002).

Amongst these target genes 1,25-$(OH)_2$ vitamin D_3 also induces the expression of the gene encoding the enzyme responsible for its degradation, 25-hydroxyvitamin D-24-hydroxylase (CYP24A1), which helps the regulation of Vitamin D homeostasis (Makin et al., 1989).

1.4.5   *Parathyroid hormone and parathyroid hormone-related peptide*

Parathyroid hormone (PTH) is released from the parathyroid glands and is the principle regulator of calcium homeostasis. In response to a hypocalcaemic stimulus, PTH is secreted and while it enhances calcium re-absorption from the kidney [reviewed in (Friedman, 2000)], it also increases the activity of the epithelial calcium channel TRPV5 (van Abel et al., 2005). Moreover, PTH enhances the conversion of vitamin D to its biologically active metabolite 1,25-$(OH)_2$ vitamin D_3 in the kidney, which in turn increases calcium absorption from the intestine.

Increased secretion of PTH in primary hyperparathyroidism leads to an increase in osteoclast cell number and activity (Murray J.Favus [Editor], 2006). For this reason, endogenous PTH has been considered to be a catabolic agent for bone. However, exogenous PTH when administered intermittently has the property to increase bone mass (Tam et al., 1982; Nishida et al., 1994), because bone formation in this case is predominant over bone resorption.

PTH shares sequence homology with the N-terminal domain of PTH-related peptide (PTHrP), which was initially discovered as the cause of humoral hypercalcaemia of malignancy syndrome (Ikeda et al., 1988; Kemp et al., 1987). Although PTH functions as a circulating endocrine factor, PTHrP acts as an autocrine/paracrine regulator of bone formation [reviewed in (Murray J.Favus [Editor], 2006; Goltzman, 2008)]. PTH and PTHrP bind to the same transmembrane spanning receptor, type 1 PTH/PTHrP receptor (PTHR1) (Mannstadt et al., 1999). PTHR1 is most abundantly expressed in PTH target tissues, such as kidney and bone. PTHR1 is also found in other foetal and adult tissues but similarly to VDR, it is found at particularly high concentrations in growth plate chondrocytes (Murray J.Favus [Editor], 2006). In tissues other than kidney and bone PTHR1 mediates the paracrine/autocrine actions of PTHrP rather than the endocrine actions of PTH (Murray J.Favus [Editor], 2006).

1.4.6   Calcitonin

The calcitonin family consists of calcitonin and the calcitonin gene-related peptides (CGRP), α-CGRP and β-CGRP. Calcitonin and α-CGRP are transcripts of the same gene, known as *Calca* gene, whereas a different gene, *Calcb* encodes for β-CGRP [reviewed in (Huebner et al., 2008)]. Calcitonin is a hormone produced by thyroid C-cells and is responsible for lowering the level of calcium in blood (COPP and CHENEY, 1962). The calcitonin molecule has been identified in the mid 1980's as a 32-amino acid long polypeptide that becomes active following a proteolytic cleavage (Le Moullec et al., 1984).

The calcitonin receptor is a G-protein coupled receptor (Lin et al., 1991) and is mainly expressed in the kidney, neurons of the central nervous system (CNS), placental cells and lymphocytes [reviewed in (Huebner et al., 2008)]. Osteoclasts express high levels of calcitonin receptor as well, reflecting the main skeletal effect of calcitonin, which is the inhibition of osteoclastic bone resorption (Nicholson et al., 1986; Moonga et al., 1992).

Upon administration, calcitonin prevents osteoclast precursor fusion, disrupts actin ring formation and hence reduces osteoclast activity (Suda et al., 1997). Simultaneously, calcitonin causes cAMP production and increase of cytosolic calcium in the osteoclast (Suda et al., 1997; Inzerillo et al., 2002) (c.f. Figure 1.5, page 13).

Calcitonin and α-CGRP knockout mice (*Calca*$^{-/-}$) showed high bone mass phenotype due to increased bone formation rate. However, in mice deficient solely for the α-CGRP peptide, *α-CGRP*$^{-/-}$ mice, bone formation rate was decreased (Hoff et al., 2002; Huebner et al., 2006). In view of this it has been suggested that calcitonin is an inhibitor of bone formation rather than of bone resorption. However, this is still under investigation.

A summary list of the above-mentioned hormones and cytokines, together with some additional systemic and local factors regulating bone remodelling, is shown in Table 1.1.

HORMONE/CYTOKINE	BONE FORMATION	BONE RESORPTION
Systemic hormones		
PTH	↑*	↑
Vitamin D	↑	↑
Sex hormones (Oestrogen/Androgen)	↑	↓
Calcitonin	↓**	↓
Glucocorticoids	↓***	↑ or ↔
Local cytokines and growth factors		
RANKL	↔	↑
OPG	↔	↓
M-CSF	↔	↑
TNF-α	↓	↑
IL-1β	↓	↑
IL-6	↔	↑
IL-15	↔	↑
IL-18	↔	↑
IFN-γ	↔	↓
TGF-β	↑	↑ or ↓
IGF-1	↑	↑
PDGF	↑	↔
PGE2	↑	↑ or ↓

Table 1.1 Systemic and local factors regulating bone remodelling. For simplicity other growth factors are excluded as these mediators have complex actions on both bone resorption and bone formation. * PTH has an anabolic effect when given intermittently at low doses. ** The effect of calcitonin on bone formation is still under investigation. *** Long-term treatment with glucocorticoids has catabolic effects. See text for references. ↑, increase; ↓, decrease; ↔, unchanged.

1.5   BONE DISEASES

1.5.1   *Osteoporosis*

Uncoupling of bone formation from bone resorption in favour of resorption, leads to a reduction of bone mass and a deterioration in bone microarchitecture with a consequent increase in bone fragility and susceptibility to fractures. These are characteristics of osteoporosis, a common bone metabolic disorder [reviewed in (Karasik, 2008)]. Osteoporotic fractures are estimated to affect 75 million people across Europe, the US, and Japan (Karasik, 2008).

Bone turnover during menopause is accelerated and there is an imbalance between the processes of bone resorption and formation, with net bone loss (Manolagas et al., 2002; Bonnick, 2006; Karasik, 2008). The most important factor for the development of osteoporosis at menopause is the loss of ovarian function, which leads to oestrogen deficiency (Manolagas et al., 2002). Oestrogen deficiency in post-menopausal women promotes the expression of IL-1β and TNF-α in bone marrow cells and monocytes (Pacifici, 1999), and IL-6 in stromal cells and osteoblasts (Girasole et al., 1992). These cytokines increase RANKL expression and stimulate bone resorption. A contributing factor to increased bone resorption during menopause is the reduced expression of TGF-β which has anti-proliferative and pro-apoptotic effects in osteoclasts (Hughes et al., 1996; Chenu et al., 1988).

The effect of oestrogen on osteoblasts is less-well-understood, but it has been suggested that during oestrogen deficiency there is decreased osteoblast differentiation due to reduced-expression of TGF-β (Oursler et al., 1991) and IGF-1 (Ernst et al., 1989) and a decreased osteoblast function due to lower expression of *COLIA1* (Ernst et al., 1989). Moreover, it has been observed that oestrogen can decrease osteoblast apoptosis and hence increase osteoblast lifespan (Manolagas, 2000). In humans, oestradiol implants

increased bone density (Studd et al., 1994) and also in rats, 17β oestradiol increased mass markedly (Tobias et al., 1993b), confirming oestrogen's anabolic function.

The most common form of secondary osteoporosis is glucocorticoid-induced osteoporosis (Mazziotti et al., 2006). Glucocorticoids are widely prescribed for inflammatory disorders including rheumatoid arthritis, asthma and inflammatory bowel disease [reviewed in (Mazziotti et al., 2006)]. Although glucocorticoids might ameliorate bone loss by suppressing inflammation in rheumatoid arthritis, they also have direct negative effects on bone which predispose to osteoporosis (Di Munno and Delle, 2008).

At a cellular level, glucocorticoids act directly to inhibit osteoblast function. At pharmacological concentrations, glucocorticoids divert the differentiation of MSCs towards the adipogenic lineage (Canalis et al., 2007b) and inhibit osteoblast cell differentiation by reducing BMP-2 expression (Luppen et al., 2003). At a functional level, glucocorticoids inhibit the synthesis of type I collagen by osteoblasts, by decreasing the amount of bone matrix that is available for mineralisation (Canalis, 2005). The effects of glucocorticoids on osteoclasts are contradictory but it has been reported that glucocorticoids increase expression of RANKL and decrease expression of OPG in stromal and osteoblastic cells (Hofbauer et al., 1999a), contributing to the excessive bone loss that follows long-term glucocorticoid treatment. Other extraskeletal effects of glucocorticoids that may affect bone metabolism are calcium malabsorption from the gastrointestinal tract and suppression on gonadal function in men and women [reviewed in (Mazziotti et al., 2006)].

Osteoporosis in men has also been recognised as an important public health issue although for a long time it was neglected and not considered to be a major threat for men's mobility or independence. Osteoporosis in men is often due to secondary causes, such as corticosteroid use, excessive alcohol use, and hypogonadism (Ebeling, 1998;

Fink et al., 2006). Trabecular bone loss in men occurs at an early stage and is associated with changes in IGF-1, whereas cortical bone loss occurs later and is linked to decreased bioavailability of testosterone and oestrogen (Riggs et al., 2008).

Increases in life expectancy have led to the ageing of world's population. Taking into consideration that fracture risk increases with age, it is predicted that the frequency of osteoporotic hip fractures will increase significantly on a global basis in the years to come (Karasik, 2008).

1.5.2   Rheumatoid arthritis

Rheumatoid arthritis is a chronic, inflammatory, autoimmune disorder. The pathogenesis of rheumatoid arthritis remains unknown but T cells, B cells, macrophages, osteoclasts, neutrophils and synovial fibroblasts have been recognised as key participants in this disease [reviewed in (Firestein, 2003)]. In rheumatoid arthritis patients, these cells accumulate in synovium and stimulate the release of degradative enzymes such as MMPs, serine proteases, and aggrecanases which digest the extracellular matrix and destroy the articular structure (Andersson et al., 2008; Firestein, 2003). Moreover, many pro-inflammatory cytokines are produced within the rheumatoid joint, such as TNF-α, IL-1, IL-6, IL-15, IL-17, IL-18 and granulocyte-macrophage colony stimulating factor (GM-CSF) (Firestein et al., 1990) that maintain the inflammation and stimulate additional cytokine and MMP production from synovial cells.

Various signal transduction pathways, including NF-κB and mitogen activated protein kinase (MAPK), are activated in rheumatoid arthritis synovium, and this contributes to inflammation by up-regulating the cytokine and MMP production. For this reason, these pathways are potential therapeutic targets in rheumatoid arthritis.

1.5.3   Osteoarthritis

Osteoarthritis (OA) is a chronic joint disease that leads to the destruction of articular cartilage and bone (Samuels et al., 2008). OA risk factors include mechanical stress, associated with pathologies such as obesity, joint misalignment or trauma, as well as biochemical abnormalities, such as genetic predisposition (Samuels et al., 2008).

There are varying degrees of synovial inflammation in OA patients (Doherty, 1999), often mild compared to that observed in rheumatoid arthritis, and confined to areas adjacent to pathologically damaged cartilage and bone (Samuels et al., 2008). In such areas, destruction of the articular surfaces is mediated by a variety of cytokines such as TNF-α and IL-1β, which in turn increase the level of production of proteases including MMPs, and other inflammatory mediators such as IL-6, prostaglandin E2 (PGE2) and nitric oxide (NO) (Samuels et al., 2008). Recently, it has been shown that MAPK, AP-1 and NF-κB signalling pathways are involved in the up-regulation of PGE2 and NO release from chondrocytes cultured with IL-1β (Chowdhury et al., 2008).

Current studies focus on the development of biomarkers that could be used as tools to understand the pathophysiologic process of cartilage loss, to characterise the status of the disease or its prognosis, and to measure treatment response (Felson and Lohmander, 2009).

1.5.4   Cancer-associated bone disease

Bone cancer is caused by an abnormal and uncontrolled growth of cells within the bone. Primary bone cancers originate in the bone, such as multiple myeloma, whereas secondary bone tumours include metastatic tumours which have spread from other organs, such as the breast and prostate (Roodman, 2004).

Multiple myeloma is a neoplasm of marrow origin and is characterised by the development of a destructive osteolytic bone disease. Multiple myeloma is associated with lytic lesions, bone pain, pathological fractures on the long bones, osteoporosis and compression fractures in the spine [reviewed in (Terpos et al., 2007; Edwards et al., 2008)].

The principle mechanism responsible for osteolytic lesions in multiple myeloma is increased osteoclastic bone resorption and decreased bone formation (Edwards et al., 2008). Myeloma cells secrete local inflammatory factors such as TNF-α (Lichtenstein et al., 1989), IL-1 (Lichtenstein et al., 1989), IL-3 (Lee et al., 2004) and IL-6 (Kawano et al., 1988), which act directly on osteoclasts, increasing their recruitment and activation. Osteoclast activity in patients is further stimulated by an increase in RANKL expression by stromal cells (Pearse et al., 2001) and malignant cells (Farrugia et al., 2003). Myeloma cells also inhibit the expression of OPG from stromal cells of patients, which favours bone resorption (Pearse et al., 2001).

Myeloma cells have also been shown to suppress bone formation [reviewed in (Terpos et al., 2007)]. Studies reported that serum levels of Dickkopf (Dkk1), one of the inhibitors of Wnt/β-Catenin signalling pathway, are increased in patients with multiple myeloma (Politou et al., 2006), and that Dkk1 from human myeloma cells inhibits the differentiation of osteoblast precursors *in vitro* (Tian et al., 2003). Most recently, it has been shown that treatment of multiple myeloma-bearing mice with anti-Dkk1 antibody, inhibited Dkk1 and prevented the suppression of bone formation, which in turn protected against osteolytic bone disease (Heath et al., 2009). These data offer a potential therapeutic approach for the treatment of myeloma.

While a considerable number of malignant tumours arise from bone and cartilage, the most common cancers with adverse skeletal effects are bone metastases from breast cancer and prostate cancer (Coleman, 2008).

According to the radiographic appearance of the lesions, bone metastases are referred to as osteolytic, ostoblastic or mixed (Coleman, 2008). Skeletal metastases resulting from breast cancer are most often osteolytic (Rose and Siegel, 2006). Once in bone, breast-cancer cells produce factors, such as PTHrP, IL-6, PGE2, TNF-α and M-CSF, which increase the expression of RANKL that directly induces osteoclast formation and function. The enhanced resorption releases factors including TGF-β, IGFs, FGFs, PDGF and BMP which stimulate tumour growth and enhance the production of PTHrP by tumour cells leading to further bone destruction (Roodman, 2004). Such local interactions between bone and breast-cancer cells result in a 'vicious circle' that underlies the development of skeletal osteolytic metastases (Roodman, 2004).

Skeletal metastases from prostate cancer tend to have an osteoblastic phenotype (Logothetis and Lin, 2005). Prostate cancer cells affect bone homeostasis by secreting factors such as BMP2, TGF-α, IGF, PDGF, VEGF, endothelin-1 (ET1), the bone metastasis factor MDA-BF-1, urokinase-type plasminogen activator (uPA) and prostate-specific antigen (PSA) (Logothetis and Lin, 2005). These factors support osteoblast proliferation and promote matrix deposition, resulting in increased numbers of irregular bone trabeculae (Roodman, 2004). In addition to factors that enhance bone mineralisation, prostate cancer cells produce factors that promote osteoclastogenesis and bone resorption, such as RANKL (Zhang et al., 2001). This evidence emphasises the role of osteoclast activity in the establishment of bone metastases, even in typical osteoblastic metastases developed from prostate cancer [reviewed in (Keller and Brown, 2004; Coleman, 2006)].

1.5.5   Paget's disease of bone

Paget's disease of bone (PDB) is a chronic condition that is characterised by focal areas of increased and disorganised turnover, causing bones to expand and become deformed.

These abnormalities are accompanied by bone pain, pathological fractures and osteoarthritis [reviewed in (van Staa et al., 2002; Ralston, 2008)].

Pagetic bone lesions have increased numbers of osteoclasts, containing 3 to 5 times more nuclei than normal osteoclasts and they also contain characteristic intranuclear inclusion bodies [reviewed in (Reddy et al., 2001; Ralston, 2008)]. In response to the increased bone resorption, osteoblasts are recruited to increase bone formation. However, due to the rapidity of this process new collagen fibres are laid down in a disorganised manner creating a mosaic pattern in bone, the so-called woven bone, which is mechanically weak.

The cause of PDB remains incompletely understood. The presence of inclusion bodies that resembled viral nucleocapsids in pagetic osteoclasts, led to the hypothesis that PDB could be triggered by a paramyxovirus infection (Rebel et al., 1974). However, the results of experimental studies regarding this remain conflicting (Ralston et al., 2008). Other environmental factors that could potentially contribute to PDB are low dietary calcium intake or vitamin D deficiency (Ralston et al., 2008).

Family studies have demonstrated that genetic factors play a key role in PDB. Key susceptibility genes include *TNFRSF11A*, which encodes RANK (Hughes et al., 2000; Whyte and Hughes, 2002); *TNFRSF11B*, which encodes OPG (Cundy et al., 2002; Daroszewska et al., 2004; Wuyts et al., 2001); *VCP*, which encodes p97 (Watts et al., 2004; Lucas et al., 2006); and *SQSTM1* which encodes p62 (Laurin et al., 2002; Hocking et al., 2002). All these genes are involved in the RANK/NF-κB signalling pathway which regulates the formation, survival and activity of osteoclasts [reviewed in (Soysa and Alles, 2009)].

1.6 TREATMENTS FOR BONE DISEASES

The prerequisites for treatment and prevention of bone disease include general lifestyle measures, non-pharmacologic and pharmacologic therapy. Sufficient calcium and vitamin D intake together with physical activity can help to diminish the impact of menopause and age on bone mass (Papapoulos and Makras, 2008). Non-pharmacological interventions aim to prevent or reduce the impact of falls. Finally, pharmacological therapy targets bone directly, affecting osteoblasts, osteoclasts or both cell types (Blahos, 2007; Papapoulos and Makras, 2008). Inhibitors of bone resorption and turnover include bisphosphonates, oestrogens and selective oestrogen-receptor modulators, whereas stimulators of bone formation include the parathyroid hormone (Papapoulos and Makras, 2008). Other agents such as strontium ranelate act by mechanisms that are incompletely defined (Papapoulos and Makras, 2008).

1.6.1 *Bisphosphonates*

Bisphosphonates are analogues of pyrophosphate, an endogenous substrate that prevents calcification, where the oxygen atom of pyrophosphate has been replaced by a carbon atom to which are attached various side chains [reviewed in (Coleman, 2008; Redzepovic et al., 2008)]. Different side chains change the potency and side effect profile of the compound. Clodronate and etidronate contain simple alkyl side chains and are known as first-generation bisphosphonates. Nitrogen-containing bisphosphonates such as alendronate and pamidronate are called aminobisphosphonates, and are referred to as second-generation bisphosphonates. Aminobisphosphonates with a cyclic side-chain such as risedronate, zoledronate and ibandronate are known as third-generation bisphosphonates (Blahos, 2007; Rodan and Fleisch, 1996).

All bisphosphonates bind strongly to hydroxyapatite, and especially at sites of high bone turnover (Jung et al., 1973). Bisphosphonates are then released and internalised by the resorbing osteoclasts. Once within the osteoclast, bisphosphonates disrupt a number of

biochemical processes necessary for osteoclast function and typically result in cell apoptosis [reviewed in (Rogers, 2003; Rodan and Fleisch, 1996)].

At the tissue level, bisphosphonates reduce bone turnover by inhibiting bone resorption. At the cellular level, the effects of bisphosphonates are greater in osteoclasts. They inhibit osteoclast recruitment and activity on the bone surface or shorten osteoclasts' life span. At the molecular level, different bisphosphonates have different mechanisms of action [reviewed in (Rodan and Fleisch, 1996)]. Nitrogen-containing bisphosphonates inhibit farnesyl disphosphatase and other enzymes of the mevalonate pathway, whereas non-nitrogen-containing bisphosphonates induce osteoclast apoptosis through the generation of cytotoxic ATP analogues [reviewed in (Roelofs et al., 2006)].

Bisphosphonates have become the standard care for the management and treatment of post-menopausal osteoporosis and for the prevention of skeletal complications associated with bone metastasis (Coleman, 2008). However, a major limiting factor of bisphosphonates is their potential to cause adverse effects. Gastrointestinal upset is the most common complain, with oesophagitis being a potentially serious side effect of bisphosphonate therapy [reviewed in (Blahos, 2007)]. Renal abnormalities have been reported with intravenous administration of high doses of bisphosphonates [reviewed in (Diel et al., 2007)]. Osteonecrosis of the jaw (ONJ) is an extremely rare adverse event related to bisphosphonate therapy. The relationship between bisphosphonate use and ONJ remains uncertain although it is believed that the over-suppression of bone turnover in the jaw and inhibition of angiogenesis by high doses of aminobisphosphonates are possible contributing factors [reviewed in (Coleman, 2008)].

Although it has been reported that bisphosphonates stimulate bone nodule formation *in vitro* and promote differentiation of MSCs into osteoblasts (Giuliani et al., 1998; Duque and Rivas, 2007), there is evidence suggesting that some bisphosphonates inhibit bone formation (Tobias et al., 1993a) and blunt the anabolic effects of PTH (Delmas et al.,

1995; Ettinger et al., 2004). In agreement with this, recent studies from our group and others have also shown that nitrogen-containing bisphosphonates cause osteoblast apoptosis and inhibit bone nodule formation *in vitro* (Idris et al., 2008a; Orriss et al., 2009). This evidence is a cause for a potential concern for the long-term use of bisphosphonates in the management of osteoporosis.

1.6.2   *Hormone replacement therapy*

Hormone replacement therapy (HRT) is used for the management of problems and symptoms associated with oestrogen deficiency, such as vasomotor symptoms, urogenital symptoms such as vaginal dryness, osteoporosis and fractures. HRT refers to the application of oestrogen-alone therapy or oestrogen combined with progesterone therapy (Blahos, 2007).

Oestrogen has been used for a number of years in the prevention and treatment of post-menopausal osteoporosis. The effectiveness of this therapy comes from the fact that oestrogen binds to and activates oestrogen receptor α and β, expressed in both osteoclast and osteoblasts, thereby regulating bone turnover (Lerner, 2006). Activation of oestrogen receptors in osteoblasts inhibits the production of cytokines that stimulate osteoclast formation, whereas activation of oestrogen receptors in terminally differentiated osteoclasts, decreases bone-resorbing activity and increases apoptosis (Lerner, 2006). One of the most commonly used oestrogens in HRT is 17β oestradiol (Rodan and Martin, 2000). Studies have shown that 5 years of HRT decreases the risk of vertebral fractures by 50-80% and the risk of hip, wrist and other fractures by 25% (Blahos, 2007).

However, oestrogen alone is also associated with an increased risk of breast cancer, and with an increased risk of uterine cancer in women that have not undergone hysterectomy or progesterone therapy (Blahos, 2007). Furthermore, the application of

oestrogen/progesterone combination therapy consistently demonstrated an increased risk of stroke (Grodstein et al., 2000) and venous thromboembolism (Miller et al., 2002).

1.6.3 Selective oestrogen-receptor modulators

Oestrogen receptors can also be activated by selective oestrogen-receptor modulators (SERMs). These compounds act as partial agonists at oestrogen receptors and inhibit bone resorption (Oseni et al., 2008). Although these compounds retain some of the beneficial effects of HRT, they act as antagonists of oestrogen receptors in other organs, such as the breast, functioning as anti-cancer agents (Oseni et al., 2008).

Tamoxifen is an oestrogen antagonist in the breast, which is widely used for the treatment of breast cancer and for the prevention of osteoporosis in high risk pre-menopausal women (Jordan, 2003). However, in the uterus tamoxifen acts as an agonist and increases the risk of endometrial cancer in post-menopausal women (Jordan and Morrow, 1994). The desire to find other SERMs that have a similar chemopreventive profile to tamoxifen but with a less undesirable side effect profile, led to human trials with the compound raloxifene (Black et al., 1983). Raloxifene is a polyphenol and is prescribed for both prevention and treatment of osteoporosis (Meier, 1998). It has been shown to have oestrogen agonist effects on bone, and oestrogen antagonistic effects on breast and endometrium, eliminating the associated cancer risk not only to the breast but also in the endometrium (Blahos, 2007).

Recently, it has been discovered that naturally occurring compounds known as phytoestrogens have similar effects to SERMs. These compounds are plant derivatives, but bear structural similarity to 17β oestradiol and act in a similar manner (Oseni et al., 2008).

1.6.4   Calcitonin

Calcitonin was discovered in the early 1960's, as a systemic hormone that lowers calcium level (COPP and CHENEY, 1962). A decade later it was developed as a drug for the treatment of Paget's disease of bone (Douglas et al., 1981). Direct effects of calcitonin on osteoclast function were demonstrated later, in the early 1980's [reviewed in (Zaidi et al., 2002)]. During these forty years, calcitonin from pig, salmon and human, has been used in treating Paget's disease of bone, osteoporosis, painful vertebral fractures and hypercalcaemia (Zaidi et al., 2002).

Parenteral administration of calcitonin to patients with Paget's disease has been reported to be effective in relieving bone pain associated with the disease (Reginster and Lecart, 1995). Intramuscular injection of calcitonin significantly reduces bone turnover in patients with osteoporosis (Gonzalez et al., 1986). However, injectable formulations of calcitonin are effective for less than 24 hours, they cause systemic side effects and may be unpleasant and inconvenient for the patient (Zaidi et al., 2002). Therefore, alternative routes of calcitonin delivery have been explored, such as intranasal administration. The efficacy of intranasal calcitonin formulation has been well-documented and confirmed by meta-analysis of randomized control trials (Cardona and Pastor, 1997). However, others proposed that intranasal administration of calcitonin produces modest effects at best, especially when compared with the newer potent bisphosphonates (Zaidi et al., 2002).

1.6.5   Parathyroid hormone

PTH has been introduced into clinical practice for the treatment of severe osteoporosis as an anabolic agent. Unlike agents that prevent bone loss by inhibiting bone turnover, PTH enhances bone mass through stimulation of bone formation during the bone remodelling cycle (Canalis et al., 2007a; Girotra et al., 2006). The difference in kinetic of changes between biochemical markers of bone turnover with PTH treatment,

demonstrated that there is an 'anabolic window' when PTH affects bone formation to a greater extent than it stimulates bone resorption. During this period the actions of PTH are believed to be maximally anabolic (Rubin and Bilezikian, 2003).

PTH is currently provided for clinical use in two forms. The recombinant human PTH(1-34) fragment known as teriparatide, available throughout most of the world, and the full-length molecule, human recombinant PTH(1-84), available only in Europe (Girotra et al., 2006).

The effects of teriparatide on bone metabolism have been studied in post-menopausal women and men with osteoporosis. Subcutaneous daily injections of teriparatide, increased vertebral and femoral BMD and reduced the incidence of fractures at vertebral and non-vertebral sites, over a 21-month period (Neer et al., 2001). Histomorphometric analysis of bone-biopsy specimens from patients treated with PTH, displayed increases in trabecular bone volume, connectivity, bone microarchitecture and biomechanical properties of bone (Dempster et al., 2001).

Discontinuation of PTH leads to a rapid decline in BMD. For this reason, it is recommended that an anti-resorptive agent, is administered after treatment with teriparatide, in order to maintain the densitometric gains achieved with PTH (Black et al., 2005).

Concomitant use of PTH and anti-resorptive agents, such as OPG and alendronate, has been reported to augment the anabolic action of PTH in ovariectomised mice (Samadfam et al., 2007). Others however, reported that co-treatment of teriparatide with alendronate in human, rather inhibits the anabolic effects of PTH (Finkelstein et al., 2003; Ettinger et al., 2004). Nevertheless, the combination therapy using teriparatide and raloxifene in human (Deal et al., 2005; Ettinger et al., 2004) or teriparatide and calcitonin in ovariectomised rats (Washimi et al., 2007), was reported to be associated

with increased improvement in BMD and better preservation of the trabecular microarchitecture than single-drug therapy using teriparatide alone (Deal et al., 2005; Ettinger et al., 2004; Washimi et al., 2007). Moreover, biphenyl carboxylic acid derivatives, such as ABD350, have been recently identified by our group, as novel anti-resorptive agents that prevent ovariectomy-induced bone loss *in vivo*, without impairing the anabolic response to PTH (Idris et al., 2009).

Possible adverse events with teriparatide include mild hypercalcaemia, whereas with full-length PTH a higher incidence of hypercalcaemia and hypercalciuria have been reported (Canalis et al., 2007a).

1.6.6   Strontium ranelate

Strontium ranelate is a novel therapy for the treatment of post-menopausal osteoporosis, which is currently approved only in Europe. Under the drug name Protelos, strontium ranelate seems to have a unique mechanism of action. On the basis of biochemical marker data it has been suggested to increase bone formation and reduce bone resorption (Canalis et al., 2007a). The anabolic and anti-resorptive actions of strontium ranelate have been reported particularly in preclinical models (Marie, 2006). In clinical trials strontium ranelate, reduced vertebral and non-vertebral fractures and increased BMD (Meunier et al., 2004; Reginster et al., 2005). However, bone-biopsy specimens from these patients treated with strontium ranelate showed a reduction in bone resorption but no evidence of increased bone formation. Strontium ranelate has side effects such as nausea, diarrhoea and headache, but it has also been associated with a slight increase in venous thrombosis (Canalis et al., 2007a). Moreover, it has been suggested that strontium ranelate can compete and replace calcium, particularly if the skeleton is deprived of adequate calcium intake (Fuchs et al., 2008). In keeping with this, high doses of strontium have been found to reduce the amount of calcium in bone and lead to hypocalcaemia (Morohashi et al., 1994) and rickets (Ozgur et al., 1996).

1.7 NEUROGENIC AND SYSTEMIC REGULATORS OF BONE REMODELLING

Apart from local factors and systemic hormones produced by peripheral endocrine glands, which together regulate bone mass through cell-autonomous effects (c.f. section 1.4, page 25), there are also molecules that modulate bone turnover through a central relay. The existence of such neurogenic factors has introduced the concept of a 'neural arm' regulating bone remodelling along with bone resorption and bone formation (Elefteriou, 2008).

1.7.1 Glutamate

Glutamate is one of the 20 amino acids commonly found in animal protein and the primary excitatory neuromediator in the central and peripheral nervous system (Mayer and Westbrook, 1987). Studies showing the presence of glutamate-nerve processes in bone (Serre et al., 1999), as well as the N-methyl-d-aspartate (NMDA) receptor subtype of glutamate receptors in osteoblasts and osteoclasts (Chenu et al., 1998; Laketic-Ljubojevic et al., 1999), suggested that glutamate might be involved in the regulation of bone homeostasis as a neurotransmitter. This hypothesis was supported by later studies showing that glutamate is involved in osteoclastic differentiation, possibly by activating the NF-κB pathway, through the NMDA glutamate receptors expressed on osteoclast precursors (Merle et al., 2003). Glutamate signalling has also been reported to be necessary for normal osteoblast function, since blockade of glutamate receptors in primary osteoblast cultures inhibited bone formation [reviewed in (Taylor, 2002)].

1.7.2 Nitric oxide

Nitric oxide (NO) is a signalling molecule produced by NO synthase (NOS) and plays an important role in many pathological and physiological processes (Hou et al., 1999). All isoforms of NOS, the endothelial isoform (eNOS), the inducible isoform (iNOS) and

the neuronal isoform (nNOS), are important regulators of bone cell function (van't Hof and Ralston, 2001).

The nNOS isoform is highly expressed in the CNS, but even so mice with targeted inactivation of the nNOS gene have increased bone mass due to decreased bone turnover (van't Hof et al., 2004). nNOS expression in bone cells is very low and hence its local effect on bone cell activity seems unlikely (van't Hof et al., 2004). This led to the speculation that nNOS isoform might influence bone metabolism by a neurogenic relay. However, the exact mechanism by which nNOS regulates bone mass and bone turnover remains unclear.

1.7.3 *Thyroid stimulating hormone and follicle stimulating hormone*

Thyroid stimulating hormone (TSH) and follicle stimulating hormone (FSH) are systemic hormones released from a central endocrine gland and have been reported to exert a direct effect on bone metabolism (Blair and Zaidi, 2006; Abe et al., 2003).

TSH is a peptide hormone, released from the thyrotrope cells in the pituitary gland. TSH has been reported to have direct effects on bone turnover. It was shown that high TSH levels suppress osteoclast formation and survival by attenuating JNK/c-jun and NF-κB signalling. Furthermore, TSH inhibits osteoblast differentiation and type 1 collagen expression by down-regulating Wnt signalling (Abe et al., 2003). The effects of TSH are mediated via the TSH receptor (TSHR) found on osteoblast and osteoclast precursors. This explains why a 50% reduction in TSHR expression produces profound osteoporosis together with focal osteosclerosis, in $TSHR^{+/-}$ mice (Abe et al., 2003). Controversial studies have shown that the hypothalamic-pituitary-thyroid axis regulates skeletal development via thyroid hormone receptor α (Bassett et al., 2007) or thyroid hormone excess (Bassett and Williams, 2008; Bassett et al., 2008) and not via TSH circulating

levels. Nonetheless, additional studies are required to distinguish independent effects of thyroid hormones and TSH on bone turnover.

Follicle stimulating hormone (FSH) is a hormone synthesised and secreted by gonadotropes in the anterior pituitary gland. Elevated serum levels of FSH have been traditionally used as an early indicator of menopause, because high circulating levels of FSH go in tandem with low levels of oestrogen [reviewed in (Cromer, 2008)]. Sun and colleagues identified FSH receptors (FSHR) on osteoclasts and their precursors that activate MAPK kinase/extracellular regulated kinase (MEK/ERK), NF-κB, and Akt signalling pathways, enhancing osteoclast formation and function in response to stimulation with FSH (Sun et al., 2006). Furthermore, they showed that FSH is required for hypogonadal bone loss, since FSHR null mice do not have bone loss despite severe hypogonadism (Sun et al., 2006). Goltzman's group however, found that secretory ovarian products, mainly oestrogen, can alter bone homeostasis independent of FSH action (Gao et al., 2007). The proposal that FSH is required for hypogonadal bone loss was also challenged by Seibel and colleagues who found that sex steroids alone, and not FSH, influence bone mass (Seibel et al., 2006).

1.7.4   Neuropeptide Y

Neuropeptide Y (NPY) is a neurotransmitter peptide, expressed widely in the CNS and peripheral nervous systems (Benarroch, 2009). In human, NPY acts via five known G protein-coupled receptors referred to as Y receptors (Y_1, Y_2, Y_3, Y_4, and Y_5) all of which are mainly expressed in the hypothalamus (Benarroch, 2009). Germline deletion of Y_2 receptor and hypothalamus-specific Y_2 receptor deletion in mice led to increased osteoblast activity and a high bone mass phenotype, suggesting that Y_2 receptors are involved in the central regulation of bone metabolism by inhibiting bone formation and without affecting bone resorption (Baldock et al., 2002). Further *in vitro* studies reported that absence of Y_2 receptor increases bone formation by increasing mesenchymal

progenitor numbers and down-regulating Y_1 receptor mRNA in stromal cells and bone tissue (Lundberg et al., 2007). A complementary report explained that Y_1 receptors are also expressed in osteoblasts, they interact with Y_2 receptors and inhibit bone formation with potentially direct effects on bone tissue (Baldock et al., 2007).

1.7.5   Leptin

Leptin has also been identified as a regulator of bone mass acting through a central relay [reviewed in (Takeda and Karsenty, 2008)]. Leptin is a hormone mainly expressed and secreted by white fat cells and is part of a homeostatic loop responsible for controlling food intake and energy expenditure [reviewed in (Whitfield, 2001)]. Once delivered in the brain, leptin binds at the satiety centre of the hypothalamus and reduces appetite. There are six isoforms of leptin receptors (ObRa-f) and are mainly located in the hypothalamus, although one of these isoforms, ObRb, is also found in other cells including osteoblasts [reviewed in (Petzel, 2007)].

Leptin knockout mice showed profound, early onset obesity, decreased energy expenditure, insulin resistance and hypogonadism (Zhang et al., 1994; Strobel et al., 1998). Considering that gonadal failure is a major cause of bone loss leading to osteoporosis (Riggs and Melton, III, 1986), it was hypothesised that bone mass, gonadal function and body weight are players in a common pathway, where leptin could play a crucial role.

This hypothesis was tested by studying the bone phenotype of leptin-deficient and leptin receptor-deficient mice (Ducy et al., 2000a). Despite the fact that both mutant mice models showed hypogonadism and hypercortisolism, two conditions that are expected to favour osteoporosis, the resulting phenotype in both mutant models was high bone mass due to increased bone formation (Ducy et al., 2000a). These data together with the fact that specific deletion of leptin receptor gene in osteoblasts did not affect bone

remodelling or bone mass (meaning that leptin does not affect osteoblasts directly) (Shi et al., 2008), established the fact that leptin is a physiological regulator of bone mass acting through a neuronal pathway.

Recent studies have shown that the sympathetic nervous system (SNS) mediates leptin inhibition of bone formation, via β2-adrenergic receptors (Adrb2), the only adrenergic receptor expressed in osteoblasts (Takeda et al., 2002). The mechanism whereby this anti-osteogenic function occurs is by inhibition of osteoblast proliferation and function (Takeda et al., 2002; Elefteriou et al., 2005). In addition, it has been suggested that bone resorption is also controlled by leptin-regulated neural pathways. Independent studies showed that sympathetic Adrb2 signalling promotes osteoclast differentiation (Elefteriou et al., 2005; Aitken et al., 2009) by increasing the expression of *RANKL* in osteoblast progenitor cells (Elefteriou et al., 2005).

An alternative leptin target in the hypothalamus are the endocannabinoids (Di, V et al., 2001). Endocannabinoids and type 1 cannabinoid receptors (CNR1) are known to be expressed in the hypothalamus (Gonzalez et al., 1999) and the effect of cannabinoids on food intake is also well-established [reviewed in (Mechoulam et al., 1998)]. In view of these studies, Di Marzo et al. showed that hypothalamic endocannabinoids are regulated by leptin signalling and also demonstrated that deletion of CNR1 in mice reduced food intake (Di, V et al., 2001). These findings together suggested that food intake is stimulated by the endocannabinoid system possibly under the control of leptin (Di, V et al., 2001). An obvious hypothesis bearing in mind these studies was that endocannabinoids and their receptors might also be implicated in the regulation of bone remodelling.

1.8   THE ENDOCANNABINOID SYSTEM

Several hypotheses were explored as to the mechanisms by which endocannabinoids exert their physiological effects in the CNS. It was suggested that endocannabinoids act via prostaglandin receptors (Milne, Jr. and Johnson, 1981), secretin receptors (Roth et al., 1984), or α-adrenergic and muscarinic cholinergic receptors (Howlett, 1984). The first clue to the likely mechanism of cannabinoid action came from the observation that cannabinoids decreased prostaglandin-induced cAMP in neuroblastoma cells (Milne, Jr. and Johnson, 1981). Then using membrane preparations from neuroblastoma cells it was shown that pertussis toxin blocked cannabimimetic responses by attenuating the inhibition of adenylate cyclase (Howlett, 1985; Howlett et al., 1986). Knowing that pertussis toxin is able to block receptor-mediated inhibition of adenylate cyclase and also that it can block enzyme inhibition via a guanine nucleotide-binding protein complex (G_i), it seemed logical to propose that the cannabimimetic action requires a functional G_i-protein coupled receptor that could be referred to as a 'cannabinoid receptor'.

1.8.1   Cannabinoid receptors

In 1990, Matsuda and colleagues reported the cloning and expression of a cDNA encoding for a G protein-coupled receptor (GPCR) that inhibited adenylate cyclase activity in a dose-dependent and pertussis toxin-sensitive manner, and also responded to psychoactive rather than non-psychoactive cannabinoids (Matsuda et al., 1990). This was the cDNA of the brain-abundant cannabinoid receptor that was later known as type 1 cannabinoid receptor or CNR1.

CNR1 are primarily found on neurones in the brain, spinal chord and peripheral nervous system (Pertwee, 1997). Within the CNS, CNR1 distribution is not homogeneous. Significant numbers of CNR1 are found in cerebral cortex and hippocampus, where they affect cognition and short-term memory, as well as in basal ganglia and cerebellum,

affecting motor function and movement (Pertwee, 1997). Although present in lower abundance than in CNS, CNR1 is also expressed in spleen, tonsils, immune cells, reproductive tissues, gastrointestinal tissues, heart, lung and adrenal gland (Pertwee, 1997; Schatz et al., 1997).

Additionally there is evidence for the existence of a CNR1 subtype in mammalian tissue. A splice variant of CNR1 cDNA from a human lung cDNA library has been isolated (Shire et al., 1995). This variant, CNR1A, is predicted to translate into an amino-terminal modified isoform of CNR1 (Shire et al., 1995), but its mRNA distribution pattern is the same as that of CNR1 mRNA (Pertwee, 1997). The full extent to which cannabinoid pharmacology is influenced by the presence of cannabinoid CNR1 receptor subtype remains to be established.

The clinical application of cannabinoid compounds was rather limited because these agents were highly psychoactive and their peripheral effects had an unknown mechanism of action. At this point it seemed possible that the peripheral effects of cannabinoids were either indirect or mediated via an alternative pathway (Reichman et al., 1991; Martin, 1986).

In light of these observations, a novel GPCR was cloned in the early 1990's from cDNA prepared from the human promyelocytic leukemic cell line HL60 (Munro et al., 1993). The newly found cDNA clone, named type 2 cannabinoid receptor or CNR2, showed only 44% sequence homology with CNR1 but their resemblance in the transmembrane region reached 68% (Munro et al., 1993).

CNR2 mRNA is mainly expressed in cells of the immune system, such as B cells, natural killer cells, CD8^{+} cells, monocytes and CD4^{+} cells (Pertwee, 1997). CNR2 mRNA, although in far smaller amounts, is also found in thymus gland, bone marrow, adrenal gland, heart, lung, prostate gland, uterus, pancreas, ovary and testis (Galiegue et

al., 1995). Recent studies have reported that CNR2 is also expressed in cerebellar white matter (Nunez et al., 2004; Ashton et al., 2006), in Purkinje neurones (Skaper et al., 1996) as well as in the vagus nerve in the brainstem (Van Sickle et al., 2005).

1.8.2   Signal transduction pathways associated with cannabinoid receptors

Both cannabinoid receptors are GPCRs and interact with the pertussis toxin-sensitive G_i class of G proteins (Pertwee, 1997), which initiate several intracellular responses.

Both receptors share some common signal transduction pathways, including; the inhibition of adenylate cyclase leading to a reduction of cAMP (Pertwee, 1997); stimulation of MAPK (Bouaboula et al., 1997); activation of protein kinase B (PKB)/Akt (Gomez et al., 2000); activation of inwardly rectifying K^+ channels (Mackie et al., 1995; Ho et al., 1999); and activation of phospholipase C (PLC), which catalyses the production of inositol triphosphate (IP_3) leading to the release of intracellular Ca^{2+} (Sugiura et al., 1996; Sugiura et al., 1997; Zoratti et al., 2003) (Figure 1.10).

In addition, CNR1 has been shown to affect ion channels. For instance, activation of CNR1 inhibits certain types of Ca^{2+} channels (Caulfield and Brown, 1992; Mackie and Hille, 1992; Mackie et al., 1995) and enhances voltage-sensitive outwardly rectifying K^+ channels (Deadwyler et al., 1993). Other CNR1-induced cellular effects include activation of the JNK cascades via a common upstream mechanism (Rueda et al., 2000) and ERK (Bouaboula et al., 1997).
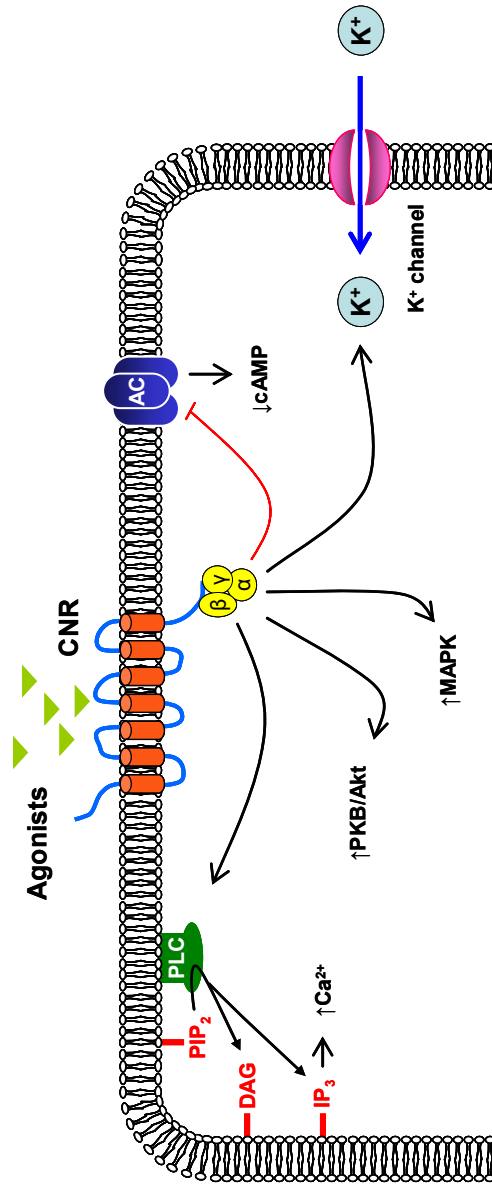
Figure 1.10: Schematic representation of the main signal transduction pathways associated with CNR1 and CNR2. *Abbreviations*: CNR, cannabinoid receptor; AC, adenylate cyclase; cAMP, cyclic AMP; MAPK, mitogen activated protein kinase; PKB/AKT, protein kinase B also called Akt; PLC, phospholipase C; PI$_3$, inositol triphosphate; DAG, diacylglycerol; PIP$_2$, phosphatidylinositol bisphosphate; Ca^{2+}, calcium ions; K$^+$, potassium ions. See text for descriptions.

1.8.3   The endocannabinoids

Initially the term 'cannabinoid' was used to describe a group of structurally related substances found in the plant *Cannabis sativa* (Burstein et al., 1995). Among them, the only cannabinoid that is both highly psychoactive and present in large amounts, is Δ^9-tetrahydrocannabinol (Δ^9-THC) (Dewey, 1986). However, the discovery of the cannabinoid receptors raised the possibility that endogenous cannabinoid ligands (endocannabinoids) may exist.

Mass spectrometry and nuclear magnetic resonance spectroscopy identified a ligand that exhibited competitive behaviour for the binding site of cannabinoid receptors on synaptosomal membranes of porcine brain (Devane et al., 1992). This was identified as arachidonyl ethanolamide (AEA) (Devane et al., 1992). Shortly after, a second endogenous cannabinoid, 2-arachidonyl glycerol (2-AG) was isolated from canine gut (Mechoulam et al., 1995). Both endocannabinoids were also considered to be eicosanoids since they are metabolites of arachidonic (eicosatetraenoid) acid and their biosynthetic pathways are common to other members of the eicosanoid family (Burstein and Hunter, 1995).

With the use of gas chromatography – mass spectrometry (GC-MS), endocannabinoids have been detected both in central (Schmid et al., 1995; Schmid et al., 1997) and peripheral tissues, such as heart, spleen, liver, kidney and testis (Martin et al., 1999; Schmid et al., 1997; Goutopoulos and Makriyannis, 2002). Endocannabinoids concentrations in blood are very low (Monteleone et al., 2005), and plasma levels of 2-AG are slightly lower than plasma levels of AEA (Martin et al., 1999).

AEA acts only as a partial cannabinoid receptor agonist, whereas 2-AG is a full cannabinoid receptor agonist (Savinainen et al., 2001). Although both endocannabinoids exhibit greater affinity for CNR1 than CNR2 (Appendix 4, page 275), 2-AG differs from

AEA in exhibiting higher-efficacy in mediating CNR2- and probably CNR1-dependent G-protein signalling (Pertwee and Ross, 2002; Hanus et al., 2001; Pertwee, 1999; Gonsiorek et al., 2000). Both endocannabinoids may serve as neurotransmitters or neuromodulators as there is evidence that they mediate retrograde signalling from post-synaptic neurons to pre-synaptic terminals via cannabinoid receptors (Ohno-Shosaku et al., 2001; Wilson and Nicoll, 2001).

1.8.4 Endocannabinoid metabolism

Endocannabinoids are arachidonic acid derivatives (Burstein and Hunter, 1995) that are synthesised and extracellularly released 'on demand' (Pertwee and Ross, 2002). AEA is formed from pre-existing N-arachidonoyl phosphatidylethanolamine (NArPE) through the action of a specific phospholipase D (PLD) (Di, V et al., 1994). 2-AG can be formed from arachidonic acid-enriched membrane phospholipids, such as inositol phospholipids through the actions of phospholipase C and diacyl glycerol lipase (Sugiura et al., 1995) (Figure 1.11).

Endocannabinoids are removed from the extracellular space via a membrane transport molecule, the 'AEA' membrane transporter (AMT) (Di, V et al., 1994; Maccarrone et al., 2000; De Petrocellis et al., 2004). This process however, is yet to be fully characterised. Once inside the cell, the endocannabinoids are hydrolysed by a membrane-bound enzyme known as fatty acid amide hydrolase (FAAH) (Cravatt et al., 1996). FAAH degrades anadamide and 2-AG to arachidonic acid and ethanolamine or glycerol, respectively (Sugiura et al., 2002). 2-AG breakdown is also catalysed by another hydrolase, the monoacylglycerol lipase (MGL) (Di, V et al., 1999; Karlsson et al., 1997) (Figure 1.11). Both hydrolases are expressed in brain regions where CNR1 receptors are also highly expressed (Egertova et al., 1998).

The cannabinoid receptors and the family of endogenous ligands, together with the molecular machinery for the endocannabinoid synthesis, transport and metabolism, are collectively known as the endocannabinoid system.
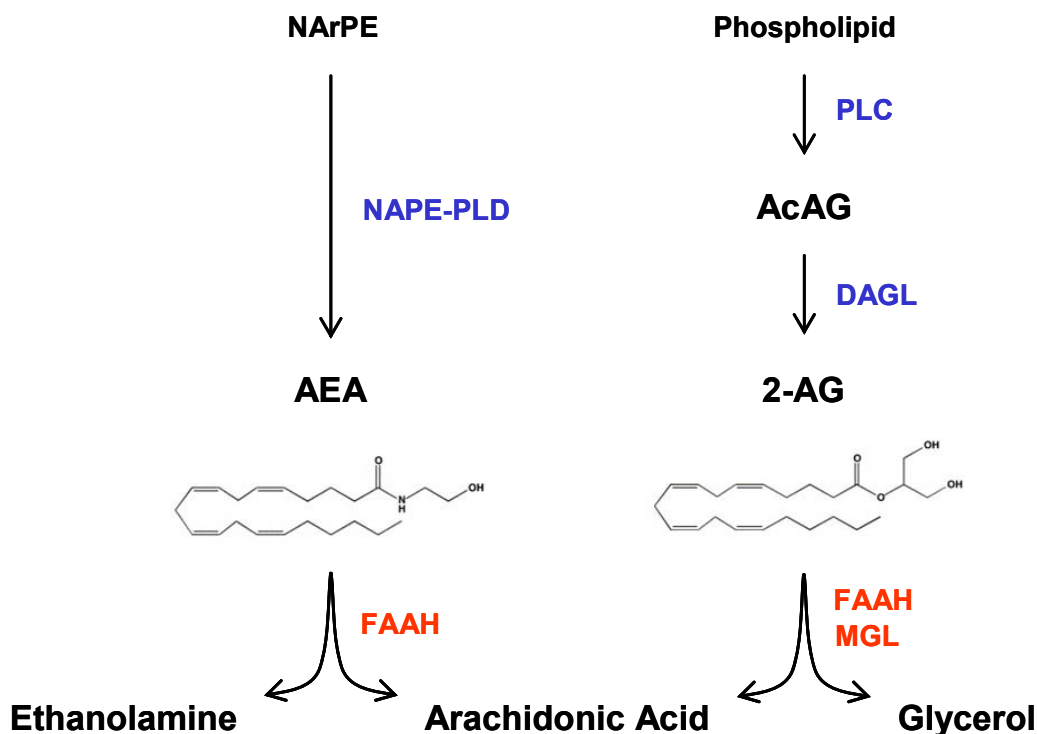
Figure 1.11: Schematic illustration of endocannabinoid synthesis and breakdown. In blue are the enzymes involved in the endocannabinoid synthesis and in red are the enzymes involved in their breakdown. *Abbreviations*: NArPE, N-arachidonoyl phosphatidylethanolamine; NAPE-PLD, N-acyl phosphatidylethanolamine phospholipase D; AEA, arachidonoyl ethanolamide; PLC, phospholipase C; AcAG, sn-1-diacyl arachidonoyl glycerol; DAGL, sn-1-diacyl glycerol lipase; 2-AG, 2-arachidonoyl glycerol; FAAH, fatty acid amide hydrolase; MGL, monoacylglycerol lipase. See text for descriptions.

1.8.5 Synthetic cannabinoid receptor ligands

In addition to endocannabinoids, synthetic cannabinoid receptor ligands are widely used in cannabinoid research. Some of these compounds are mixed CNR1/CNR2 receptor

agonists, meaning that they activate CNR1 and CNR2 receptors with approximately equal potency, such as CP55940 (Griffin et al., 1998). Other synthetic cannabinoid receptor ligands are CNR1-selective, like arachidonyl-2´-chloroethylamide (ACEA) and arachidonyl-cyclopropylamide (ACPA) (Hillard et al., 1999). Potent CNR2-selective cannabinoid receptor agonists include the synthetic compounds JWH133 (Huffman et al., 1999) and HU308 (Hanus et al., 1999), both which are very attractive therapeutic agents as they can be applied without any undesirable psychotropic effects. Another group of synthetic cannabinoid receptor ligands have the capacity to block the effects of cannabinoid receptor agonists and exert the opposite pharmacological effects on downstream signalling pathways (Pertwee, 1999). These compounds are referred to as cannabinoid receptor antagonists/inverse agonists and include the cannabinoid receptor ligands AM251 and AM630, which are selective for CNR1 and CNR2 cannabinoid receptors, respectively. CNR1 and CNR2 binding properties of these compounds are summarised in Appendix 4, page 275.

1.8.6   *Alternative cannabinoid binding sites*

Cannabinoid effects might also be mediated through other non-cannabinoid receptors, including the transient receptor potential vallinoid type 1 (TRPV1) (De Petrocellis et al., 2000; Smart et al., 2000; Hermann et al., 2003), the orphan G-protein coupled receptor GPR55 [reviewed in (Begg et al., 2005; Brown, 2007)] and other receptors collectively known as non-CNR1/CNR2 receptors [reviewed in (Begg et al., 2005; Brown, 2007)].

The TRPV1 is a non-selective cation channel with high calcium permeability (Pingle et al., 2007). Ligands for TRPV1 include capsaicin, olvanil and resinoferatoxin, but also the endocannabinoid, anandamide (Smart et al., 2000). The fact that CNR1/CNR2 and TRPV1 are frequently co-expressed in neural and non-neural cells provided further evidence about the cross-talk between these receptors (De Petrocellis et al., 2000; Hermann et al., 2003; Ahluwalia et al., 2003; Rossi et al., 2009). Recent studies have

also shown that osteoclast formation and osteoclastic bone resorption are regulated by TRPV receptors (Rossi et al., 2009; van der Eerden et al., 2005).

GPR55 is an orphan receptor that is mainly expressed in brain but also found in spleen (Sawzdargo et al., 1997). Evidence for the association between GPR55 and cannabinoids was initially provided in 2001, using yeast host strains that co-expressed yeast/human chimeric proteins [reviewed in (Brown, 2007)]. This and other studies showed that GPR55 is activated by Δ^9-THC, AEA, 2-AG, CP55940 and AM251 (Brown, 2007; Ryberg et al., 2007). Recently it has been reported that GPR55 is expressed in human and mouse osteoblast and osteoclasts and that treatment of GPR55 with a synthetic ligand stimulates osteoclast function *in vitro* (Whyte et al., 2009). The same group has also shown that *GPR55$^{-/-}$* mice have increased trabecular volume and trabecular thickness as well as increased numbers of morphologically-inactive osteoclasts (Whyte et al., 2009). These results together suggest that endocannabinoid action that was previously considered to be mediated via CNR1/CNR2 mechanism may actually be mediated via GPR55 mechanism.

Endocannabinoids have multiple *in vivo* sites-of-action additional to CNR1, CNR2 and TRPV1, referred to as non-CNR1/CNR2 sites. Most extensively-studied non-CNR1/CNR2 sites occur in the vasculature, the CNS and immune cells [reviewed in (Brown, 2007)].

1.8.7 *Role of the endocannabinoid system*

Extensive research on the main aspects of the endocannabinoid system has revealed that it is a ubiquitous lipid signalling system, with a profound impact on the main physiological systems that control body functions. It appears that the endocannabinoid system is a modulator of physiological functions in the central and autonomous nervous system (Di, V et al., 1998), the immune system (Cabral et al., 2008), the gastrointestinal

tract (Izzo et al., 2001), and in the microcirculation (Kunos et al., 2002). It has also been shown that the endocannabinoid system has a pathophysiological role in the modulation of pain (Calignano et al., 2001; Pertwee, 2001) and a homeostatic control over the motivation for appetite stimuli, including food (Di, V et al., 2001), drugs (Navarro et al., 2001) and alcohol (Rodriguez et al., 2005). Recent studies indicate that the endocannabinoid system is also involved in the regulation of bone homeostasis (section 1.9).

1.9 THE ENDOCANNABINOID SYSTEM AND BONE

1.9.1 Presence of endocannabinoid system in bone

Several components of the endocannabinoid machinery have been detected in the skeleton. Recently CNR1 and CNR2 were found to be expressed in bone marrow derived osteoclasts and osteoblasts (Idris et al., 2005; Ofek et al., 2006), RAW 264.7-derived osteoclast-like cells (Ofek et al., 2006), MC3T3 E1 osteoblast-like cells (Ofek et al., 2006) and osteocytes (Lian et al., 2004). In addition, the endocannabinoids AEA and 2-AG, have been detected in bone and MC3T3 E1 osteoblasts (Tam et al., 2008), in cultured mouse osteoblasts and osteoclasts (Ridge et al., 2007) and in cultured human osteoclasts (Rossi et al., 2009). The fact that 2-AG is present in bone at similar levels to those found in the brain (Tam et al., 2008) but the blood 2-AG levels are negligible (Monteleone et al., 2005), confirmed that 2-AG is synthesised locally in bone (Bab et al., 2008).

1.9.2 Type 1 cannabinoid receptor and bone

The earliest investigation on the role of the endocannabinoid system on bone metabolism was performed by Idris and colleagues, using both genetic and pharmacological approaches (Idris et al., 2005). They showed that young CNR1 knockout ($CNR1^{-/-}$) mice on an ABH background [congenic strain from CD1 (Ledent et al., 1999)], had an increased BMD and were resistant to bone loss induced by ovariectomy due to a reduction in osteoclast activity. Ageing experiments have shown that $CNR1^{-/-}$ mice a CD1 genetic background also have increase peak bone mass but develop age-related osteoporosis due to increased accumulation of adipocytes in bone marrow at the expense of osteoblasts (Idris et al., 2008b).

In vitro studies showed that osteoblasts from $CNR1^{-/-}$ mice had reduced expression of *RANKL* mRNA, which lead to a reduction in osteoclast formation in osteoblast-bone marrow co-cultures from $CNR1^{-/-}$ mice (Idris et al., 2008b). In addition, bone marrow

stromal cells from *CNR1*^{-/-} mice had increased mRNA levels of the adipogenic transcription factor *PPARγ*, explaining the increased adipocyte accumulation in bone marrow of 12-month old *CNR1*^{-/-} mice (Idris et al., 2008b).

Pharmacological approaches showed that cannabinoid receptor antagonists/inverse agonists selective for CNR1 or CNR2 prevented bone loss in C57BL/6 mice following ovariectomy in a dose-dependent manner by inhibiting bone resorption (Idris et al., 2005). In RANKL-stimulated osteoclast cultures, cannabinoid receptor antagonists/inverse agonists inhibited osteoclasts by stimulating apoptosis and inhibiting the release of osteoclast survival factors (Idris et al., 2005). As expected, osteoclast cultures generated from *CNR1*^{-/-} mice were resistant to the inhibitory effects of the CNR1 selective antagonist AM251 on osteoclast survival confirming a CNR1-mediated effect (Idris et al., 2005). On the other hand, the CNR2 selective antagonist/inverse agonist AM630 was equally potent in inhibiting osteoclast formation in cultures generated from both wild type and the *CNR1*^{-/-} mice. This was early evidence that the effect of the endocannabinoid system on bone metabolism may be mediated by central as well as peripheral cannabinoid receptors (Idris et al., 2005).

Tam and colleagues studied CNR1-deficient mice on C57BL/6 and CD1 genetic backgrounds (Tam et al., 2006). It was illustrated that *CNR1*^{-/-} mice backcrossed to a C57BL/6 background had lower bone mass than their wild type littermates. In both genders the CNR1 knockout on a C57BL/6 background had decreased bone formation and increased osteoclast numbers (Tam et al., 2006). Nevertheless, *CNR1*^{-/-} mice on a CD1 background demonstrated different findings. Young female *CNR1*^{-/-} mice had a normal trabecular bone volume while male *CNR1*^{-/-} mice displayed a high bone mass phenotype with increased trabecular thickness in agreement with the work of Idris and colleagues (Idris et al., 2005). These observations led the authors to suggest that CNR1 signalling regulates bone mass differentially in different mouse strains.

The effects of CNR1 were partly attributed to the regulation of norepinephrine release from sympathetic nerve fibres. Sympathetic fibres are abundant in trabecular bone (Mach et al., 2002) and norepinephrin released from them has the property to inhibit bone formation and stimulate bone resorption (Elefteriou et al., 2005). Because sympathetic CNR1 signalling inhibits norepinephrine release, it was suggested that the absence of CNR1 in bone might increase sympathetic tone and decrease bone formation (Tam et al., 2006). However, a recent study from our group showed that although norepinephrin indeed stimulates osteoclast formation and bone resorption, it does not have a direct effect on bone formation or osteoblast function (Aitken et al., 2009).

1.9.3   Type 2 cannabinoid receptor and bone

A study by Ofek and colleagues showed that the peripheral CNR2 also regulates bone mass (Ofek et al., 2006). This study demonstrated that CNR2-deficient ($CNR2^{-/-}$) mice on a C57BL/6 genetic background, suffer from accelerated age-related trabecular bone loss and cortical expansion, unlike their wild type littermates. These changes were thought to be the consequence of increased bone remodelling, especially affecting the trabecular compartment of the bone. All these phenotypic characteristics were considered to be similar to post-menopausal osteoporosis in humans. In fact, genetic association studies reported the involvement of CNR2, but not CNR1, in inherited human osteoporosis (Karsak et al., 2005; YAMADA et al., 2007), suggesting that *CNR2* is a susceptibility gene for reduced bone mineral density.

Ofek et al. have also shown that the CNR2-selective non-psychotropic agonist HU308 stimulated osteoblast number and activity in the endocortical part of the bone, whereas osteoclastogenesis in the trabecular region was reduced (Ofek et al., 2006). Moreover, in ovariectomy experiments it was shown that HU308 prevented bone loss resulting from oestrogen deficiency, possibly by inhibiting osteoclast formation, and stimulating bone formation in the endocortical region (Ofek et al., 2006). Overall, it was suggested that

HU308 has pro-osteoblastic and anti-osteoclastic activities *in vitro* and it was regarded as a possible candidate for the treatment of post-menopausal osteoporosis (Ofek et al., 2006).

Although the two distinct studies with *CNR1*$^{-/-}$ and *CNR2*$^{-/-}$ mice implicate that pharmacological modulation of the endocannabinoid system has a role in regulating bone mass and bone turnover *in vivo*, their results are rather contradictory (Idris et al., 2005; Ofek et al., 2006). The contrasting phenotypes in *CNR1*$^{-/-}$ and *CNR2*$^{-/-}$ mice indicate that these receptors affect bone metabolism in different ways. Whether this inconsistency is due to the different genetic background strains of these knockouts or a consequence of the absence of CNR1 or CNR2 only, remains unclear.

The current models of the regulation of bone remodelling by the endocannabinoid system are summarised in Figure 1.12.
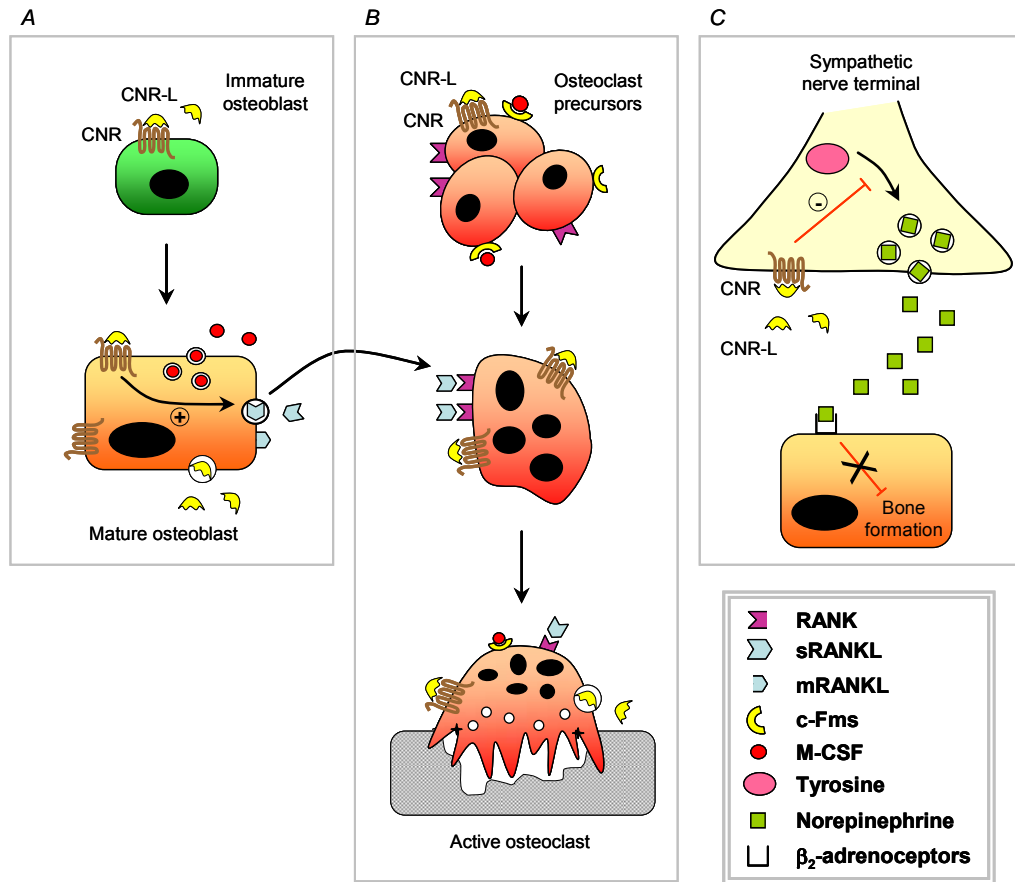
Figure 1.12: Schematic representation of the current models of the regulation of bone remodelling by cannabinoid ligands. *A*. Endocannabinoids (CNR-L) act on type 1 and type 2 cannabinoid receptors (CNR) expressed on immature osteoblasts from bone marrow, thereby enhancing osteoblast differentiation and function. Cytokines released from mature osteoblasts (RANKL and M-CSF) stimulate osteoclast formation, an event which is enhanced by the activation of cannabinoid receptors (*B*). *C*. Endocannabinoids are also able to regulate bone formation indirectly by inhibiting the production of norepinephrine, an inhibitor of osteoblast differentiation and function. Reproduced and adapted from (Idris, 2008).

1.10 TREATMENT OF BONE DISEASES WITH CANNABINOID RECEPTOR LIGANDS

In the last couple of decades cannabis has been used for both recreational and medical purposes due to its psychoactive, analgesic, anti-anxiety, anti-emetic and anti-inflammatory properties (c.f. section 1.8.7, page 63).

1.10.1 Treatment of inflammatory bone diseases with cannabinoid ligands

Cannabis-based drugs have been reported to have immunomodulatory effects and therefore their potential for treatment of inflammatory diseases is being assessed [reviewed in (Idris, 2008; Klein, 2005; Klein et al., 2003)]. Studies reported contradictory roles for the effect of cannabinoid ligands on cytokine production. Earlier studies suggested that cannabinoid receptor agonists may have anti-inflammatory qualities and hence could be applied for arthritis therapy. For example, work by Baldwin and colleagues, showed that lipopolysaccharide-stimulated alveolar macrophages from habitual marijuana smokers, produced lower than normal levels of cytokines such as TNF-α, GM-CSF and IL-6 (Baldwin et al., 1997). Similarly Smith et al. showed that cannabinoid receptor agonists prevented the lipopolysaccharide-induced production of TNF-α and IL-12 in mice (Smith et al., 2000). Moreover, Malfait et al. (Malfait et al., 2000) demonstrated that cannabidiol, the major non-psychoactive component of cannabis, suppressed the progression of collage-induced arthritis (CIA) in arthritic mice, by inhibiting TNF-α production from synovial cells (Malfait et al., 2000). In addition a randomised, double-blind, placebo-controlled trial of Sativex [a drug consisting of tetrahydrocannabinol (THC) and cannabidiol (CBD)] for treatment of pain due to rheumatoid arthritis, showed that Sativex treatment significantly improved pain in movement, pain at rest and quality of sleep in comparison with placebo treatment (Blake et al., 2006).

However, other studies showed that endocannabinoids may posses pro-inflammatory qualities. For example, the endocannabinoid 2-AG was reported to increase the production of chemokines in human promyelocytic leukaemia HL-60 cells (Kishimoto et al., 2004), and activation of the type 2 cannabinoid receptor *in vitro* up-regulated genes involved in the synthesis of cytokines (Derocq et al., 2000). In keeping with this, the expression of *RANKL* mRNA was found to be reduced in osteoblasts from *CNR1*$^{-/-}$ mice, indicating the role of cannabinoid receptor signalling in cytokine production (Idris et al., 2008b). Finally, the CNR2-selective inverse agonist Sch.036 reversed bone damage in arthritic rats (Lunn et al., 2008). These studies together suggest that cannabinoid ligands may have pro-inflammatory qualities, whereas inverse agonists may have therapeutic properties for the treatment of inflammatory bone diseases. However, further work is required to address the role of cannabinoid ligands in inflammation.

1.10.2 *Treatment of cancer-associated bone disease with cannabinoid ligands*

Bone is the most common site for metastasis in patients with advanced tumours arising from breast and prostate cancer (Coleman, 2008). Studies have shown that cannabinoids have the potential to become novel chemotherapeutic agents for suppression of tumour growth and metastasis. The earliest evidence related to this was in the 1970's when Δ^9-THC was shown to inhibit growth of lung adenocarcinoma (Munson et al., 1975). Subsequent studies showed that plant-derived, synthetic and endogenous cannabinoids had anti-proliferative effects in prostate, breast, lung, skin and pancreatic cancer cells [reviewed in (Guzman, 2003; Bifulco et al., 2008; Sarfaraz et al., 2008)]. Thus far, cannabinoids are thought to exert their anti-tumour effects by different mechanisms including modulation of main survival pathways for tumour cells, such as MAPK/ERK and PI3K/Akt; stimulation of ceramide synthesis which can then induce apoptosis and cell-cycle arrest; reduction of VEGF expression, which results in inhibition of tumour angiogenesis and metastasis (Guzman, 2003; Bifulco et al., 2008; Sarfaraz et al., 2008) and also by induction of autophagic death in cancer cells (Salazar et al., 2009). On the

contrary, other groups reported that cannabinoids stimulate the growth and metastasis of cancer cells (Hart et al., 2004; McKallip et al., 2005), possibly by suppressing the anti-tumour immune response (McKallip et al., 2005).

Although the precise mechanism of cannabinoid action in cancer cells still needs to be fully clarified, evidence thus far suggests that cannabinoids may represent a potential new drug therapy for the treatment of cancer.

1.11 HYPOTHESIS AND AIMS OF THIS STUDY

This thesis was designed to test the hypothesis that type 2 cannabinoid receptors (CNR2) are involved in regulating bone metabolism, by affecting both osteoclastic bone resorption and osteoblastic bone formation.

The general aim of this study was to use genetic and pharmacological approaches to examine the role of CNR2 in bone metabolism *in vitro* and *in vivo*.

The specific aims of the work reported in this thesis were:

- To examine the expression of CNR2 and other components of the endocannabinoid machinery in the bone microenvironment.
- To investigate the effect of *CNR2* genetic inactivation on bone mass of C57BL/6 mice at age 3, 6 and 12 months.
- To define the functional role of CNR2 in osteoclast formation *in vitro* and to investigate the effect of a CNR2-selective antagonist/inverse agonist on ovariectomy-induced bone loss *in vivo*.
- To analyse the functional role of CNR2 in osteoblast differentiation and function *in vitro* and to examine the effect of a CNR2-selective agonist on ovariectomy-induced bone loss *in vivo*.

CHAPTER TWO
MATERIALS AND METHODS

2   MATERIALS AND METHODS

2.1   PREPARATION OF CANNABINOID COMPOUNDS TESTED

The cannabinoid receptor ligands AEA, 2-AG, JWH133, AM251, and AM630 were purchased from Tocris Bioscience (UK). HU308 was a kind gift from Dr. Roel J. Arends (Organon). For *in vitro* studies the compounds were dissolved in dimethyl sulfoxide (DMSO) or absolute ethanol according to the manufacturer's instructions at a concentration of 10mM. Once made into solutions, the commercially available compounds were stored at -20°C and the HU308 solution was stored at 4°C. For *in vivo* studies the compounds were dissolved in the minimum possible volume of DMSO (i.e. 1mg AM630 in 47.2μl DMSO, 1mg HU308 in 200μl DMSO) and then made up in corn oil (AM630) or in a solution of 5% (w/v) mannitol and 0.5% (v/v) gelatine in distilled H$_2$O (dH$_2$O) (HU308) to obtain doses of 0.1 or 1.0mg/kg. The solutions of AM630 in corn oil vehicle were stored at room temperature, whereas the suspension of HU308 in mannitol/gelatine vehicle was stored at 4°C. Fresh solutions and suspensions were prepared weekly.

2.2   TISSUE CULTURE

2.2.1   *Cell culture medium and standard conditions*

Murine calvarial osteoblasts and bone marrow cells were cultured in alpha-Minimum Essential Medium (αMEM) supplemented with 10% foetal calf serum (FCS), 5% L-Glutamine, 100U/ml penicillin and 100μg/ml streptomycin (standard αMEM). All cultures were kept under standard conditions of 5% CO$_2$: 95% air at 37°C in a humidified atmosphere, unless stated otherwise. All media preparation and cell culture work was performed in a laminar flow hood, which was sprayed with 70% (v/v) ethanol prior to use. All solutions were warmed to 37°C before use and plastic-ware was bought pre-sterilised or autoclaved prior to use. A phase-contrast microscope was used regularly during the culture period, to assess confluence or contamination of cultures.

2.2.2 Bone marrow macrophage cultures

Bone marrow cells were isolated from the long bones (tibia and femur) of 6-10 week-old mice sacrificed by cervical dislocation according to Schedule 1 of the Animals (Scientific Procedures) Act. The isolation procedure was performed under tissue culture conditions with sterilised equipment. Using sterile scissors, the legs were isolated and transferred to universals containing ice-cold sterile PBS. Once in the laminar flow cabinet, the legs were placed in a Petri dish and the soft tissue that surrounds the bone was removed using a scalpel. The isolated bones were transferred to a fresh Petri dish containing standard αMEM. Bone marrow cells were flushed out with standard αMEM using a syringe fitted with a 25-gauge (G) needle. To achieve a homogenous cell suspension the mixture of bone marrow cells and αMEM was pushed through needles of decreasing size (19G – 25G) prior to centrifugation. Following a 3-minute centrifugation at 300g, bone marrow cells were resuspended in standard αMEM supplemented with 100ng/ml M-CSF and plated in Petri dishes. Cultures were kept under standard conditions for 48 hours when adherent cells were scraped off the Petri dish using a rubber-tipped scraper. Mouse macrophages were plated in 96-well plates at 15×10^3 cells/well in 125μl of standard αMEM supplemented with 25ng/ml M-CSF. The plates were kept under standard conditions for 72 hours. Then the cultures were treated with the desired compounds while changing 50% of the medium. Cultures were terminated 24-48 hours following treatment.
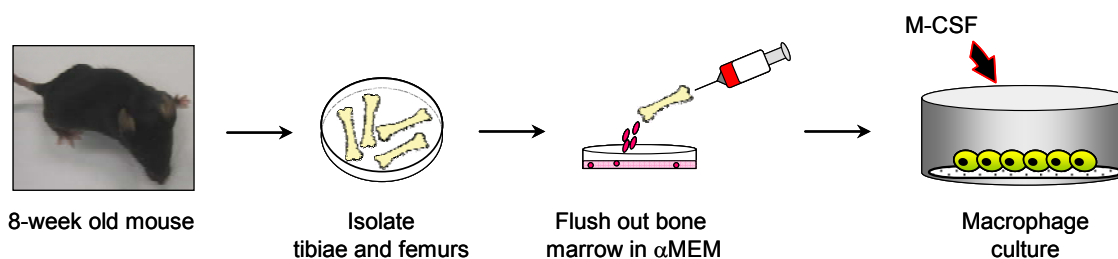
Figure 2.1: Schematic illustration of isolation of bone marrow cells. See text under section 2.2.2 for more details.

2.2.3   Bone marrow osteoclast cultures

Bone marrow macrophages generated as described in section 2.2.2, were plated in 96-well plates at 15 x 10^3 cells/well in αMEM supplemented with 100ng/ml human recombinant RANKL and 25ng/ml M-CSF, in order to generate osteoclasts. The plates were cultured under standard conditions for 72 hours and treated with the desired compounds for 24-48 hours, while changing 50% of the medium supplemented with M-CSF and RANKL.

2.2.4   Fixation and Tartrate-resistant Acid Phosphatase (TRAcP) staining

Upon termination of osteoclast cultures the culture medium was removed and the adherent cells were rinsed twice with PBS. Cells in 96-well plates were then incubated with 150μl of 4% (v/v) formaldehyde in PBS for 10 minutes at room temperature. Following fixation, cells were rinsed twice with sterile PBS and stored at 4^oC in 70% (v/v) ethanol until further use.

Multinucleated osteoclasts in mouse bone marrow cultures were identified using TRAcP staining as previously described by van't Hof et al. (van't Hof et al., 1995). Following fixation the adherent cells were rinsed twice with PBS and then incubated with TRAcP staining solution (Appendix 2.1, page 271) at 37^oC for 45 minutes. Subsequently, the cultures were rinsed with PBS and then stored at 4^oC in 70% (v/v) ethanol. TRAcP positive multinucleated cells were manually counted on a Zeiss Axiovert light microscope using a 10x objective lens.

2.2.5   Calvarial osteoblast cultures

Primary calvarial osteoblasts were isolated from the calvarial bones of 2 day-old mice sacrificed by decapitation according to Schedule 1 of the Animals (Scientific Procedures) Act. The calvariae were removed, washed thoroughly in Hank's balanced salt solution (HBSS) and transferred to a sterilised universal tube containing 2ml of

collagenase type 1 (1mg/ml) in HBSS and incubated for 10 minutes at 37°C in a shaking water bath. The supernatant was discarded and the calvariae were incubated in 4ml of collagenase type 1 (1mg/ml) in HBSS for 30 minutes. The cell suspension was removed and mixed with 6ml of standard αMEM (cell suspension 1). The remaining tissues were washed in PBS and treated for 10 minutes with 4ml of ethylenediaminetetraacetic acid (EDTA) (4mM) in PBS. The cell suspension was removed and mixed with 6ml of standard αMEM (cell suspension 2). The remaining tissues were incubated in 4ml of collagenase type 1 (1mg/ml) in HBSS for 20 minutes. The cell suspension was removed and mixed with 6ml of standard αMEM (cell suspension 3). Cell suspensions were pooled and centrifuged at 300g for 3 minutes. The supernatant was discarded and cell pellets were resuspended in standard αMEM. The cell suspension was cultured under standard conditions in 75cm^2 tissue culture flasks at a density of 3 calvariae per flask. The medium was changed 24 hours after seeding to remove non-adherent cells, and then every 48 hours until cells reached 100% confluence.

When osteoblasts reached confluence, the tissue culture medium was removed from the flasks and the osteoblast monolayer was carefully rinsed with sterile PBS to remove any traces of serum. The adherent cells were incubated with Trypsin (4ml/75cm^2 flask) for 3 minutes at 37°C after which microscopic examination was performed to ensure cell detachment. To inactivate Trypsin, 6ml of standard αMEM was added to the flask. The cell suspension was transferred to a fresh tube and centrifuged at 300g for 3 minutes. The pellet was resuspended in standard αMEM and osteoblasts were plated in 96- or 12- well plates at 8 x 10^3 cells/well in 100μl of standard αMEM, or 100 x 10^3 cells/well in 1ml standard αMEM, respectively. The plates were incubated for 72 hours. Cell cultures in 96-well plates were then treated with the desired compounds while changing 50% of the medium and finally terminated 24 hours following treatment. From day 3, cell cultures in 12-well plates were treated with the desired compounds while replacing the medium with standard αMEM supplemented with 50μg/ml Vitamin C and 3mM beta-

glycerophosphate (β−GP) (osteogenic medium). The cultures were kept under standard conditions and the medium was refreshed three times per week. The cultures were finally fixed in 70% (v/v) ethanol in week 3.
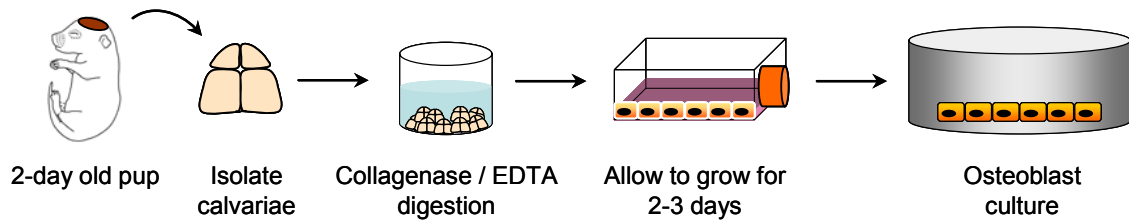
Figure 2.2: Schematic illustration of isolation of mouse calvarial osteoblasts. See text under section 2.2.5 for more details.

2.2.6   Bone marrow osteoblast cultures

Osteoblasts were generated from bone marrow which was flushed out from murine long bones as previously described in section 2.2.2, page 76. Following a 3-minute centrifugation at 300g, bone marrow cells were resuspended in standard αMEM supplemented with 50μg/ml Vitamin C and 3mM β−GP (osteogenic medium) and plated in Petri dishes at a density of 1 mouse per Petri dish. Cultures were kept under standard conditions for 72 hours when non-adherent cells were removed. Adherent cells were maintained under standard conditions in osteogenic medium for 5 to 7 days and considered to consist of osteoblast precursors. These cells were trypsinised, plated and treated as described previously for calvarial osteoblasts in section 2.2.5, page 77.

2.2.7   Alizarin Red staining and quantitative destaining procedure

Mineralisation nodules were detected using Alizarin Red S staining, which is a common histochemical technique used to detect calcium deposits in mineralised tissues and cultures (Chang et al., 2000; Coelho et al., 2000). Alizarin Red reacts with calcium via its sulfonate and hydroxyl groups and forms an Alizarin Red-calcium complex during a chelation process. Calcium ions then precipitate and form brick-red deposits.

Alizarin Red was dissolved in dH_2O to a final concentration of 40mM. The solution was mixed well and the pH was adjusted to 4.1-4.3 with 10% (v/v) ammonium hydroxide. Fixed osteoblasts in 12-well plates were rinsed with dH_2O to remove traces of 70% (v/v) ethanol and then incubated with 0.8ml/well of Alizarin Red staining solution for 20 minutes with gentle rocking at room temperature. Unincorporated stains were rinsed off with dH_2O three times. Excess of dH_2O was removed by inverting the plates on several layers of paper towels three times. Plates were then left to air-dry overnight.

Images of the stained cultures were taken using a standard scanner. To destain and quantify the mineralised nodules, a destaining solution made of 10% (w/v) cetylpyridinium chloride in 10mM sodium phosphate (pH 7.0) was used. Plates with destaining solution were kept at room temperature for 30 minutes. Alizarin Red concentration was determined by absorbance measured at 562nm on a Bio-Tek Synergy HT plate reader using an Alizarin Red standard curve (concentration range 0-10mM) in the same solvent.

2.2.8   Alamar Blue viability assay

The viability of osteoblasts and macrophages was determined using the Alamar Blue assay. This assay is based on the use of an oxidation/reduction (redox) growth indicator which fluoresces and changes colour in an appropriate range relating to the metabolic reduction of the growing medium caused by cell growth (alamarBlue[TM] Assay Protocol).

The amount of the redox indicator that changes from oxidised (non-fluorescent, blue) to a reduced form (fluorescent, red) is directly proportional to the number of the viable, active cells that maintain a reduced environment (Ahmed et al., 1994).

AlamarBlue^{TM} reagent equal to 10% of the volume of the medium per well was added in cultured cells and left for 2 hours under standard conditions. Fluorescence was measured using a plate reader at an excitation wavelength of 540nm and an emission wavelength of 590nm. Data were corrected for background fluorescence by repeating the assay in wells containing medium but lacking cells or treatment.

2.2.9   Alkaline phosphatase assay

The Alkaline Phosphatase (ALP) assay is based on the conversion of p-nitrophenol phosphate (colourless) into p-nitrophenol (yellow) by the enzyme ALP, which is mainly expressed by cells of the osteoblastic lineage.

Cells were cultured in 96-well plates at 8×10^3 cells per well in 100μl of standard αMEM for 72 hours. The cell monolayer was rinsed with PBS and then incubated with 150μl ALP lysis buffer (Appendix 2.2, page 272) for 20 minutes. A standard curve was generated by preparing series of dilutions of p-nitrophenol (1.25 – 30nM). In a fresh 96-well plate, 50μl of the standard solutions and test samples were plated in triplicate and an equal amount of substrate solution was added. A plate reader was used to measure the absorbance readings at 405nm, with reference at 960nm, at 2 minute intervals for 20 minutes. ALP activity was determined from the slope of the linear part of the kinetics curve and was expressed as fold stimulation over the vehicle control.

2.3   GENE EXPRESSION USING QUANTITATIVE REAL-TIME PCR

Quantitative real-time PCR (qPCR) was used to detect expression of genes of interest in brain, bone marrow and bone cell cultures.

2.3.1   RNA extraction

Macrophages and osteoblasts were cultured under standard conditions in 12-well plates, until confluence was reached. Osteoclasts were also cultured in 12-well plates until a large number of osteoclast precursors or osteoclasts were visible in each well. The culture medium was removed and cells were washed with 500µl of cold PBS. Then 500µl of Total RNA Isolation (Trizol®) reagent was used to lyse the cells in each plate by sequentially transferring it from well to well. To ensure that all cells were lysed another 500µl aliquot of Trizol® reagent was used to rinse all 12-wells of the same plate and then combined with the first Trizol® reagent aliquot. Bone marrow was directly flushed out with 1ml of Trizol® reagent. Brain was initially frozen and then homogenised with a pestle and mortar prior to total RNA extraction with TRizol® reagent (1ml TRizol® per 50-100mg of brain tissue).

All lysates were transferred into Diethyl Pyrocarbonate (DEPC)–treated 1.5ml Eppendorf tubes and mixed thoroughly by pipetting up and down. The homogenised sample was incubated for 5 minutes at room temperature. 200µl of chloroform was added to each lysate and mixed by shaking vigorously for 15 seconds. The mixture was then incubated at room temperature for 3 minutes before the samples were centrifuged at 12000g for 15 minutes at 4°C. The aqueous phase was transferred carefully into a fresh DEPC-treated 1.5ml Eppendorf tube. For RNA precipitation, 500µl of isopropanol was added to each sample and mixed by inverting. The mixture was incubated for 10 minutes at room temperature and then centrifuged at 12000g for 10 minutes at 4°C. The supernatant was discarded and the RNA pellet was washed once with 1ml of 75% (v/v) cold ethanol and then centrifuged at 7500g for 5 minutes at 4°C. After removing the

supernatant, the RNA pellet was air-dried for 5 minutes. 25µl of cold DEPC-treated water was added into each sample and the pellet was allowed to dissolve while on ice for 10 minutes. After the pellet had completely dissolved, samples were heated at 65°C for 5 minutes. All RNA samples were stored at -80°C.

2.3.2   Measuring RNA concentration

The RNA concentration was determined using the Molecular Probes RiboGreen kit. A standard curve was generated by preparing a series of dilutions of an RNA standard (0.3125 - 2ng/µl) in Tris EDTA (TE) buffer. In a fresh black 96-well clear bottom plate, 50µl of the standard dilutions and 50µl of RiboGreen dye (1:200 diluted in TE buffer) were mixed to generate the standard curve. In the same plates RNA samples (1:4000 and 1:5000 diluted in TE buffer) were plated in duplicate and an equal amount of RiboGreen dye added. The fluorescence was measured using a plate reader, at an excitation wavelength of 485nm and an emission wavelength of 528nm.

2.3.3   Reverse Transcription

The RNA samples were then used for the production of cDNA by reverse transcription. The following 20µl reaction volume was used for 10pg-5µg of total RNA in a nuclease-free microcentrifuge tube:

Xµg of total RNA
1µl of oligo(dT)$_{20}$ (50µM)
1µl of 10mM dNTP mix (10mM each)
Topped up to 13µl with DEPC-treated H_2O

The mixture was heated to 65°C for 5 minutes and then incubated on ice for at least 1 minute. After a brief centrifugation to spin down samples, the following components were added:

4μl of 5X first-strand buffer

1μl of 0.1M DTT

1μl of RNaseOut Recombinant RNase Inhibitor (40U/μl)

1μl of SuperScript III Reverse Transcriptase (200U/μl)

For the negative control reaction, SuperScript III Reverse Transcriptase was eliminated and replaced by dH$_2$O. All reagents were mixed by pipetting gently up and down. The mixtures were incubated at 50°C for 60 minutes in a MJ Research cycler, and then the reaction was terminated by heating at 70°C for 15 minutes.

2.3.4   *qPCR amplification using a fluorescent probe*

Polymerase chain reactions (PCR) were performed on the cDNA using mouse targeted primer/probe combination sets (Table 2.1) designed following the Roche Universal Probe Library (UPL) method (www.universalprobelibrary.com). Intron-spanning primers were mainly designed in order to prevent amplification of contaminating genomic DNA (Table 2.2). In the absence of introns, an intron spanning assay could not be designed. Instead, non-intron spanning solutions suggested by the UPL Assay Design Center were used (Table 2.2). The Roche universal probes have two labels, a fluorescent reporter and a quencher. During the extension phase of PCR, the polymerase cleaves the probe from its target sequence, separating reporter and quencher. The unquenched reporter emits a fluorescent signal which is automatically quantified.

Table 2.1: qPCR primers and the universal probe library number and sequence

GENE	Universal Probe Library (UPL) Forward and Reverse Primer	Probe no. (UPL)	Probe seq. (UPL)
CNR1	GAC GGT GTT TGC CTT CTG TAG GAG CAT AGA TGA TGG GGT TCA	40	GCC TGC TG
CNR2	GGC AGT GTG ACC ATG ACC TT GGT CAA CAG CGG TTA GCA G	110	AGC CTC TG
NAPE-PLD	CAT GGC CAA CAT GGA AAA A GGA GCT CTT TGT CAA GTT CCT C	58	CTC CAT CC
DAGLα	GAG CAC CAA GCC CAA ATG AGC TCC GAC TTG GGG ATA C	49	GGC CAC CA
DAGLβ	AGG ATT GGT GGC GAC TGT TGG TCA CCT TCC ACT GCA T	21	CAG AGC CA
FAAH	CGC TTG GAC TCC ACC ATC CAC GAA GGG GTC GAG AAC T	52	GGG AGG AG
MGL	TTC TGG CAT GGT CCT GAT TT ATT GAG CAG TTT GGC AGC A	93	TCT GGT CC

Table 2.2: Amplicon length and the sequence identification number (ID) for each gene

GENE	Amplicon length (nt)	Length of intron spanned (nt)	Sequence ID (EMBL/GenBank, Ensembl, RefSeq)
CNR1	68	No intron spanned	BC079564
CNR2	61	No intron spanned	ENSMUST00000068830.2
DAGLα	63	1091	NM_198114
DAGLβ	62	2467	NM_144915.3
NAPE-PLD	111	7051	AB112350
FAAH	70	1250	NM_010173
MGL	88	9123	NM_011844.3

The PCR reaction was set up as following:

<table>
<tr><td><u>Master mix</u></td><td></td><td><u>Final concentration</u></td></tr>
<tr><td>25μl of 2X SensiMix(dT) Taq polymerase</td><td>→</td><td>1X</td></tr>
<tr><td>0.5μl of Universal ProbeLibrary Probe (10μM)</td><td>→</td><td>100nM</td></tr>
<tr><td>0.5μl of Forward Primer (20μM)</td><td>→</td><td>200nM</td></tr>
<tr><td>0.5μl of Reverse Primer (20μM)</td><td>→</td><td>200nM</td></tr>
<tr><td>1μl of MgCl$_2$ (50mM)</td><td>→</td><td>4mM</td></tr>
<tr><td>17.5μl of RNase-free H$_2$O</td><td></td><td></td></tr>
</table>

5μl of cDNA template was added to each well of the microplate and then the master mix was aliquoted in volumes of 45μl per well. The amplification of all fragments was performed in a MJ Research Chromo 4 Real Time PCR thermocycler. The thermal cycling protocol consisted of an initial incubation for 10 minutes at 95°C, followed by 35 cycles of 15 seconds at 95°C, then 30 seconds at 60°C and 15 seconds at 72°C.

The qPCR products yielding the highest signal with no noise during qPCR optimising runs, were cleaned using the QIAquick PCR Purification Kit and then loaded on gel to verify the successful amplification of the cDNA into clean amplicons of the expected size (Figure 2.3). The amount of these products was quantified using the Quant-iT^{TM} PicoGreen® assay following the manufacturer's instructions.

The copy number of the products was calculated using the following formula: **[amplicon size (bp) x (330 Da x 2 nucleotide/bp)] / 6.022 x 10^{23} = g/molecule.** Knowing the concentration of these products and their copy number is possible to calculate the precise number of molecule in each reaction as follows: **Concentration of product (g/μl)/copy number (g/molecule) = molecule/μl.** Results were plotted as mean percentages of maximal mRNA expression from one experiment.
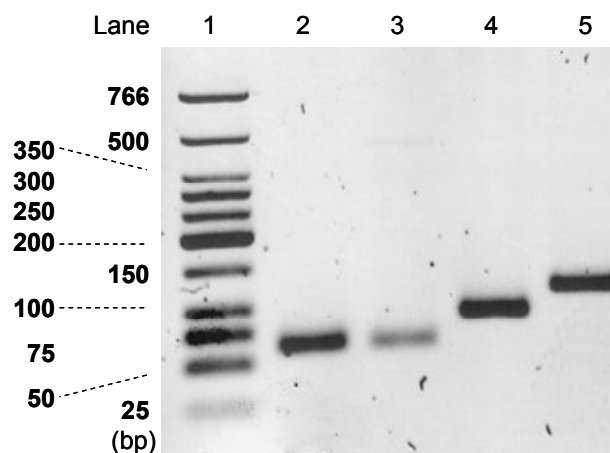
Figure 2.3: qPCR products. Lane 1: Low Molecular Weight DNA ladder; lane 2: DAGLα, lane 3:DAGLβ; lane 4: MGL; lane 5: NAPE-PLD.

Standard curves were generated by serial 10-fold dilutions of the quantified cDNA products and were run alongside samples during the qPCR. The copy number of each sample was calculated according to fluorescence intensity using the programme Opticon Monitor version 3. Briefly, each standard curve was plotted in a linear plot of the logarithm of the amount of DNA against the cycle number (C(T) cycle) (Figure 2.4*B*) at which the fluorescence intensity reached a set cycle threshold (dashed lined in Figure 2.4*A*). The copy numbers of the unknown samples should lie within the range of the dilutions used to fit the standard curve (grey dots in Figure 2.4*D*).

Quantitation graph   C(T) Control graph
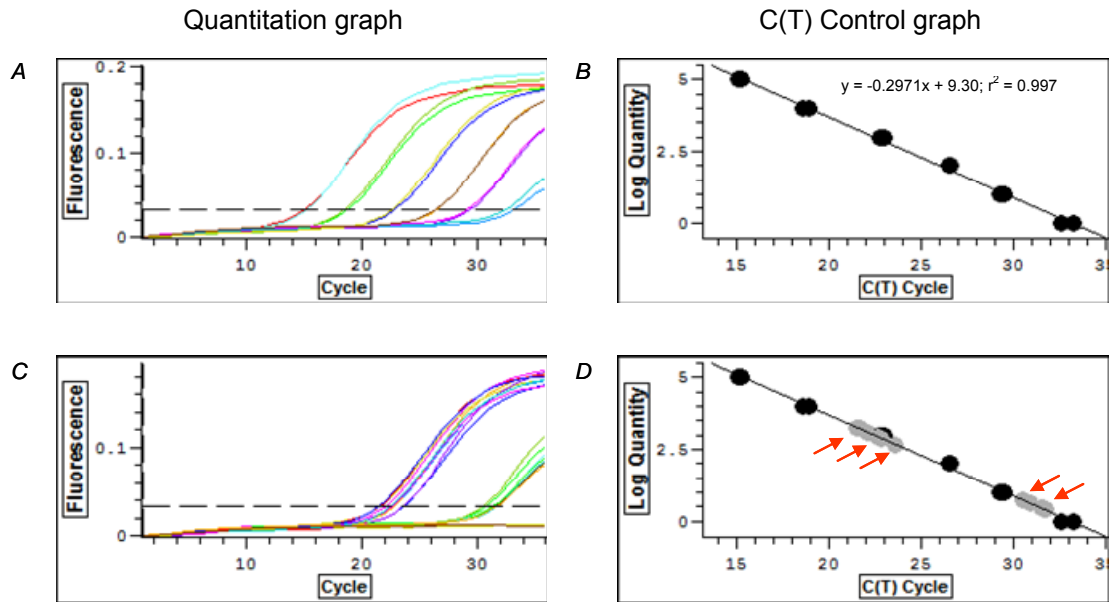
Figure 2.4: Amplification plots and standard curve from Opticon Monitor 3. *A*. Sigmoidal-shaped amplification plot of standard dilutions, in which fluorescence is plotted against the number of cycles. The dashed line indicates the threshold cycle (C(T) cycle) in which the first significant increase in fluoresce is detected. *B*. Standard curve plot, in which the logarithm of the amount of DNA is plotted against the C(T) cycle. *C*. Amplification plot of unknown samples. *D*. The range of concentrations in the unknown samples (pointed by red arrows) lies within the range of the standard dilutions.

2.3.5   Normalisation

The housekeeping gene 18S ribosomal RNA was investigated as reference gene for normalisation of relative gene expression levels. 18S ribosomal RNA standard curve dilutions and cDNA samples were run alongside.

The PCR reaction was set up as following:

5μl of template

25μl of 2X SensiMix(dT) Taq polymerase

2.5μl of TaqMan® Gene Expression Assay Mix for 18S ribosomal RNA

1μl of $MgCl_2$

16.5μl of RNase-free H_2O

88

The amplification procedure and the copy number calculation were performed as described in section 2.3.4, page 84.

2.4 WESTERN BLOT

2.4.1 Preparation of cell lysates

Cells were cultured in 6-well plates at 250 x 10^3 cells/well in 2.5ml of standard αMEM until they reached 80% confluence. Then the medium was removed and the monolayer was rinsed with ice-cold PBS. Adherent cells were then gently scraped in 150μl of RIPA lysis buffer (Appendix 2.3, page 272) supplemented with 2% (v/v) protease inhibitor cocktail and 0.4% (v/v) phosphatase inhibitor cocktail and left on ice for 10 minutes. For preparation of bone marrow cell lysates, bone marrow cells were isolated from long bones of mice as described in section 2.2.2, page 76. Following a 3-minute centrifugation at 300g, bone marrow cells were washed twice in PBS, then resuspended in 250μl of RIPA lysis buffer supplemented with 2% (v/v) protease inhibitor cocktail and 0.4% (v/v) phosphatase inhibitor cocktail, and left on ice for 10 minutes. All lysates were transferred to a centrifuge tube and centrifuged at 12000g for 10 minutes at 4°C. The supernatant was collected and stored at -20°C until further use.

2.4.2 Measuring protein concentration

The protein concentration was determined using the bicinchoninic acid (BCA) Pierce protein assay. A standard curve was generated with dilutions of bovine serum albumin (BSA) (2000μg/μl). In a fresh 96-well plate, 10μl of standard dilutions and protein samples (1:5 diluted in H_2O) were plated in duplicates. 200μl of copper (II)-sulfate (diluted 1:50 with BCA) were added in each well and incubated for 15 minutes at 37°C. The absorbance was measured at 562nm on a plate reader and the protein concentration in each sample was calculated from the BSA standard curve.

2.4.3 Gel electrophoresis

Gel electrophoresis was performed using Criterion^{TM} XT BioRad (12% Bis-Tris) pre-cast gels, which were placed into a vertical electrophoresis tank filled with

electrophoresis running buffer (Appendix 2.4, page 272). Cell lysates were mixed with the appropriate volume of 5X sample loading protein buffer (Appendix 2.4, page 272), heated at 100°C for 3 minutes and loaded carefully into the well. A Kaleidoscope pre-stained standard and a Magic Marker XP western standard were used to identify molecular weights. Gels were run at constant voltage of 200V for 40 minutes.

2.4.4   Electrophoretic transfer

This procedure allows the recovery of proteins from the polyacrylamide gel to a solid protein-binding membrane. The gel was removed from the pre-cast gel cassette and immersed into transfer buffer (Appendix 2.4, page 272) for 5 minutes. Meanwhile, a Hybond™-P membrane was cut to the size of polyacrylamide gel, immersed in 100% methanol and then allowed to equilibrate in transfer buffer for 5 minutes. A blotting sandwich was prepared with the following successive layers; pre-soaked extra thick blot paper, membrane, polyacrylamide gel, pre-soaked extra thick blot paper. The sandwich was orientated to ensure that the negatively charged proteins was moved out of the polyacrylamide gel and transferred across to the membrane. The transfer was carried out at a constant current of 90mA for 2.5 hours.

2.4.5   Immunostaining and antibody detection

The polyvinyliden difluoride (PVDF) membrane was incubated at room temperature for 1 hour in blocking solution [5% (w/v) dried non-fat milk in TBST (Appendix 2.4, page 272)]. This step is essential to ensure blocking of non-specific binding sites. Once completed, the membrane was washed in TBST for 30 minutes, while changing the buffer every 10 minutes. Membranes were incubated overnight at 4°C with continuous agitation, with a CNR2 polyclonal antibody developed in rabbit, at a concentration of 1:2000 in 3% BSA in TBST. The membrane was washed three times in TBST for 15 minutes and incubated with an anti-rabbit secondary antibody at a concentration of 1:5000 in 5% w/v dried non-fat milk in TBST for 1 hour at room temperature.

Membranes were again washed three times with TBST. To visualise immunoreactivity the Pierce SuperSignal® West Dura Extended Duration chemiluminescent detection system was used and the signal was detected on a Syngene Genegnome Bio Imaging System. The intensities of the bands were quantified using the GeneSnap software from Syngene.

Membranes were then incubate in stripping buffer (Appendix 2.4, page 272) for 15 minutes at 50°C in order to remove all antibodies, then blocked and re-probed with an actin primary antibody developed in rabbit [1:1000 in 5% (w/v) dried non-fat milk in TBST] and an anti-rabbit secondary antibody [1:5000 in 5% (w/v) dried non-fat milk in TBST] as described above. Immunoreactivity was visualised and bands were quantified as described above.

2.5   ANIMAL EXPERIMENTATION

All experimental protocols were approved by the Ethics Committee at the University of Edinburgh and were conducted in accordance with the UK Home Office regulations (personal licence number 60/10983, project licence number 60/3981).

2.5.1   Animals

C57BL/6 mice were housed in a designated animal facility, in pathogen-free rooms maintained at constant temperature, with 12 hours light/12 hours dark cycles. All animals had free access to water and pelleted standard commercial diet (SDS, Special Diets Service).

Mice with CNR2 deficiency ($CNR2^{-/-}$) were obtained from Dr. Susana Winfield at the National Institutes of Health and were generated from an 129 embryonic stem cell line carrying a targeted knockout of the *CNR2* gene, as previously described (Buckley et al., 2000). To create a congenic strain on a C57BL/6 background, these mice had been crossed with wild type C57BL/6 mice for at least 10 generations. The $CNR2^{-/-}$ mice used in this study were generated by mating heterozygote breeding pairs.

2.5.2   Genotyping Methods

Genomic DNA was extracted from murine ear snips using the commercially available Invisorb® Spin Tissue Mini Kit according to the manufacturer's instructions. The purity of the extracted DNA was determined from the A_{260}/A_{280} ratio and the concentration was determined using UV-transparent plates and a plate reader. The extracted DNA was stored at $-20^{o}C$.

Genotyping of mice was carried out by PCR analysis of genomic DNA. All PCR reactions were performed in 96-well plates and consisted of the following reagents. The volume for each reaction was adjusted to 50μl with sterile dH_2O.

5.0μl of 10x Taq buffer mix

2.0μl of dNTPs

1.0μl of $MgCl_2$

6.0μl of Primer mix (10μM each of forward and reverse primers)

1.0μl of Taq Polymerase

0.5 – 2.0μl of Genomic DNA

Identifying CNR2-deficient mice

CNR2-deficient mice have the neomycin (*NEO*) gene incorporated into their genome, which has replaced 391 base pairs (bp) of the 3' end of the coding sequence (CDS) of exon 2 of the *CNR2* gene. The disruption of the *CNR2* gene by the *NEO* gene eliminated part of intracellular loop 3 (i3), the transmembrane domains 6 and 7 (TM6 and TM7), and the carboxy terminus (Buckley et al., 2000) (Figure 2.5).
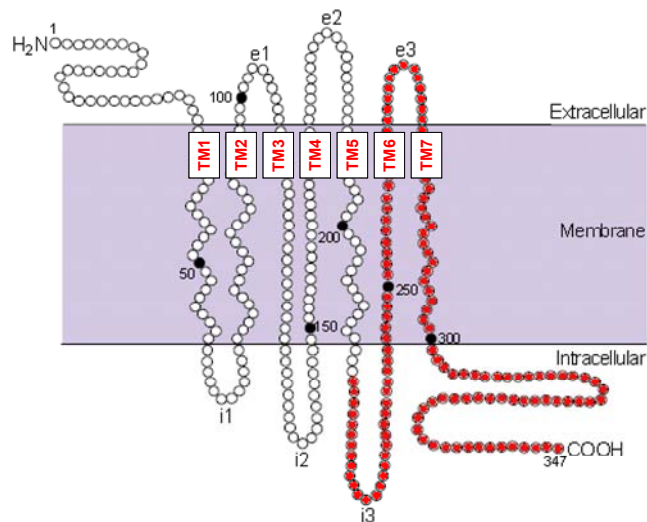
Figure 2.5: Mouse cannabinoid receptor 2 protein (CNR2). CNR2 is a single polypeptide with seven transmembrane α-helices and has an extracellular N-terminus and an intracellular C-terminus. The residues in red indicate the deleted part of the protein following the *NEO* gene insertion. e1-e3 are the extracellular loops 1-3; i1-i3 are the intracellular loops 1-3; TM1-TM7 are the transmembrane domains 1-7. The image is adapted from Klein et al. (Klein et al., 1998).

94

To identify this mutation, a 643bp fragment was generated, encoding entirely part of the *NEO* gene, using the following primers: 5'-TTGGGTGGAGAGGCTATTCGGCTATG-3' and 5'-GCCCATTCGCCGCCAAGCTCTT-3'. To identify wild type mice in the same PCR reaction, a 790bp fragment encoding part of the *CNR2* gene coding sequence was generated using the following primers: 5'-GAGGGATGCCGGGAGACAGAAGTGACC-3' and 5'-CATGAGAGCCAGTGCAGGGAACCAGC-3'. The latter primer was binding on the region of CDS of exon 2 of the *CNR2* gene that was deleted upon insertion of the *NEO* gene (Figure 2.6). Genomic DNA from heterozygote mice was expected to yield both fragments after amplification.

Figure 2.6: PCR design for identifying CNR2-deficient mice. *A.* The coding sequence (CDS) for the *CNR2* gene is on exon 2, is 1041bp long and is translated into a functional CNR2 protein of 347 amino acids. *B.* Primers (1) and (2) annealed within the region of the CDS. Amplification of a 790 bp product was successful in animals having at least one intact copy of the *CNR2* gene, i.e. in wild type mice and heterozygotes for the CNR2 mutation. *C.* Primers (3) and (4) annealed within the *NEO* gene sequence which replaced only the 3' end of the *CNR2* CDS, leaving only 650bp from the original CDS sequence. Amplification of a 643 bp fragment was successful in mice having at least one copy of mutant *CNR2* gene, i.e. in homozygote (*CNR2$^{-/-}$*) or heterozygote (*CNR2$^{+/-}$*) mice for the *CNR2* mutation.

95

Amplification of both fragments was performed in a MJ Research thermocycler. The thermal cycling protocol consisted of an initial incubation for 2.5 minutes at 95°C, followed by 30 cycles of 20 seconds at 95°C and 3 minutes at 68°C and then by a final extension step at 68°C for 5 minutes in the last cycle (Figure 2.7).
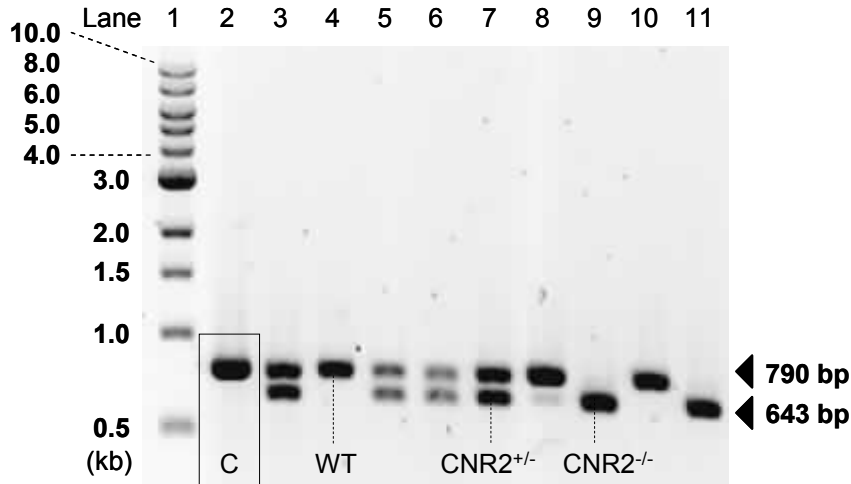
Figure 2.7: Gel electrophoresis analysis to identify CNR2-deficient mice. Lane 1: 1kb DNA ladder; lane 2: Control; lane 4: wild type; lane 7: heterozygote for the CNR2 mutation; lane 9: homozygote for the CNR2 mutation.

2.5.3 SNP genotyping of wild type and CNR2-deficient mice

A genome scan was performed to compare the genotypes of wild type and *CNR2$^{-/-}$* C57BL/6 mice to pure C57BL/6 genotypes provided by Illumina Inc. DNA was extracted from mouse tails using the commercially available Invisorb® Spin Tissue Mini Kit. Genotyping services were provided by the Wellcome Trust Clinical Research Facility (WTCRF, Western General Hospital, Edinburgh, UK), using a commercially available medium density linkage panel to genotype 1449 evenly distributed single nucleotide polymorphisms (SNPs) with a uniform coverage across the mouse genome.

2.5.4   Ovariectomy and sham operations

Eight week-old female mice, weighing approximately 20g underwent bilateral ovariectomy or sham operation as previously described by Idris et al. (Idris et al., 2008c). Briefly, anaesthesia was induced by an intraperitoneal injection of ketamine hydrochloride (Vetalar, 76mg/kg) and medetomidine hydrochloride (Dormitor, 1mg/kg) cocktail. Anaesthesia was reached once the animal did not response to gentle pressure on the hind paws. Before operating, the fur over the lumbar spine was wiped with 70% (v/v) ethanol. Using autoclaved sharp scissors a midline dorsal incision of 10mm was made at the bottom of the rib cage and the skin at each side of the cut was separated from the underlying muscle. To gain access to the two ovaries that were lying under the thin muscle layer, a 5mm incision was made on each side of the peritoneal wall. The edge of the incision was held open with autoclaved tooth forceps and the ovarian fat pad surrounding the ovaries were retracted with blunt forceps making the ovary identifiable. The exposed ovaries and part of the oviduct were carefully removed. The same procedure was followed for sham operations except that the ovaries were identified and placed back. The skin cut was closed using metal clips. Anaesthesia was reversed by an intraperitoneal injection of atipamezole hydrochloride (Antisedan, 1mg/kg). Animals were left undisturbed in a warm, quiet place for recovery. They were housed in groups of 8 in large cages, at constant temperature and free access to water and standard laboratory diet.

2.5.5   Treatment regiments

After a two-day recovery period all ovariectomised and sham-operated animals, received a 100μl intraperitoneal injection on a daily basis that consisted of either vehicle or the designated drug prepared as described in section 2.1, page 75. All animals also received two 0.2% (w/v) calcein injections, 4 days apart, with the last injection administered on the second-last day of the experiment. The intraperitoneal injection volume of calcein was 200μl. Mice from all groups were sacrificed by cervical dislocation on day 21.

2.5.6   Posterior vena cava blood collection for serum

Blood was collected from the posterior vena cava of mice as previously described (Hoff, 2000). Mice were killed by CO_2 asphyxiation and the abdominal cavity was immediately opened by making a V-cut through the skin and abdominal wall. The intestines and liver were pushed to one side and the widest part of posterior vena cava was located (between the kidneys). A 25G needle and a 1ml syringe were used to collect blood from the posterior vena cava by carefully inserting the needle into the vein and drawing blood slowly until no more blood was available.

Blood samples were transferred to Eppendorf tubes and placed on ice until sera were separated by a 10-minute centrifugation at 4^oC. Sera were collected and stored at -20^oC until further use.

2.5.7   PINP and CTX serum assays

The PINP serum assay is an enzyme immunoassay for the quantitative determination of N-terminal propeptide of type I procollagen (PINP), which are released during collagen synthesis. The PINP assay is considered to be a specific and sensitive marker of bone formation and is used for determining the bone formation rate from serum samples. The commercially available PINP kit is a competitive enzyme immunoassay using a polyclonal rabbit anti-PINP antibody coated onto the inner surface of microtitre wells. According to manufacturer's instructions, controls, calibrators and samples were added into the wells followed by biotin-labelled PINP, and incubated for 1 hour at room temperature before aspiration and washing. Horseradish peroxidase (HRP)-labelled avidin was added to the wells and bound selectively to complexed biotin. After a wash step, colour was developed using the aqueous formulation of tetramethylbenzidine (TMB) and hydrogen peroxide as a chromogenic substrate. The reaction was stopped by 0.5M hydrochloric acid and the absorbance of each well was measured at 450nm using a

plate reader. The colour intensity developed was inversely proportional to the concentration of PINP.

The CTX serum assay is an enzyme immunoassay used for the quantitative determination of C-terminal telopeptide fragments of type I collagen (CTX), released in circulation during bone matrix degradation. Thus, serum CTX is used as a marker of osteoclastic bone resorption. The CTX kit is a competitive enzyme immunoassay using a polyclonal antibody raised against a synthetic peptide having a sequence specific for a part of the C-terminal telopeptide $\alpha 1$ chain of rat type I collagen (CTX antigen). During the pre-incubation step, biotinylated CTX antigen was added and immobilised in streptavidin-coated microtitre wells for 30 minutes at room temperature. After aspiration and washing, standards, control and samples were added into the wells followed by a solution of the polyclonal rabbit antibody mentioned above. Following an overnight incubation at 4°C wells were emptied and washed. In the second incubation step a solution of goat anti-rabbit antibody conjugated with peroxidase was added into the wells for 1 hour at room temperature. After washing, the chromogenic substrate solution TMB was added. After a 15-minute incubation at room temperature the colour reaction was stopped by 0.18M sulphuric acid. The absorbance was measured at 450nm using a plate reader and was inversely proportional to the concentration of CTX antigens in the samples.

2.5.8   *Micro computed tomography (μCT)*

Animals were sacrificed by cervical dislocation and hind legs were isolated, fixed in 4% (v/v) parafolmadehyde in PBS and stored in 70% (v/v) ethanol. Left tibias were dissected and gently cleaned from the surrounding muscle tissue using a scalpel. The tibia was separated from the fibula and cut at the tibial crest using a Dremel rotary tool. Each bone was tightly wrapped in parafilm to avoid desiccation and placed in an upright position in 1ml syringe with both ends cut. Each wrapped sample was pushed to the

bottom of the hollow tube using a plunger, allowing 5 or 6 samples to fit in at once. Whole 2 day-old mouse neonates were carefully but loosely wrapped in parafilm and placed in a 15ml falcon tube with both ends cut.

The µCT was performed on the left proximal tibial metaphysis and diaphysis for trabecular and cortical bone analysis respectively, or on 2 day-old whole mouse neonates using a SkyScan 1172 scanner. Stacks of 5 or 6 dissected tibias (Figure 2.8*A*) and mouse neonates one at a time were fixed in an upright position on a platform within the scanner. Using SkyScan scanner µCT software, the x-ray radiation source was set at 60kV and 150µA. A 0.5mm aluminium filter was added for a 180 degree scan with a rotation step of 0.6 degrees. The pixel size was set at 5µm for scanning tibias and 10µm for scanning mouse neonates.

The 3D image stacks were reconstructed from the rotation image projections, using the NRecon software by SkyScan and a 5-piece computer cluster. The reference line was chosen at the growth plate. For measurements at the proximal tibial metaphysis, which comprises mainly trabecular bone, 500 frames distal to the growth plate at baseline were chosen to be reconstructed (Figure 2.8*B*i). For measurements of proximal diaphysis, which comprises mainly cortical bone, 100 frames lying 700 frames distal to the reference line were selected to be reconstructed (Figure 2.8*B*ii). Images for the entire 2 day-old mouse neonates were reconstructed. Reconstruction settings involved the parameters shown in Table 2.3. All reconstructed images were saved as *.bmp* files.

Table 2.3: Reconstruction parameters by NRecon software

Parameter	Description	Setting
Smoothing	Smoothes images and removes noise	Width; 1 pixel
Beam Hardening factor correction	Corrects for the absorption of lower energy x-ray on the outside of specimen	9%
Ring correction level	Corrects for the non-linear behaviour of pixels causing ring artifacts	3

The reconstructed images were analysed using the CTAn software by SkyScan. The region of interest (ROI) was selected using a free-hand drawing tool at 3-7 different levels. Auto-interpolation between these levels produced the total ROI.

The reference line for the trabecular bone was set at the point where the calcified cartilage ridges of growth plate fuse together. Measurements were performed on 200 frames distal to the reference point, 5µm apart, at the trabecular bone specified by ROI (Figure 2.8*C*i). For cortical bone analysis ROI was specified by an 8-figure drawing, which included only the cortex as a hollow tube (Figure 2.8*C*ii). Measurements were performed on all 100 frames selected previously for 3D-reconstruction. These reconstructed frames were also subjected to a total bone analysis at the cortical level (Figure 2.8*C*iii). For the analysis of 2 day-old mouse neonates, ROI stretched along the entire reconstructed skeleton images. Analysing parameters such as smoothing, threshold, despeckle, 3D-analysis and configuration, were set as shown in Table 2.4.

Table 2.4: Analysing parameters by CTAn software

Parameter	Description	Setting
Smoothing	Smoothes images and removes noise	Median filter; 2D space, radius 1
Threshold	Segments the foreground from background to binary images	Global; low level 100, high level 255
Despeckle	Removes speckles from binary images	Image; remove white speckles <150 voxels
3D-Model	Creates a 3D surface from binary images	Adaptive rendering; file saved as *.p3g*
3D-Analysis	Calculates 3D parameters of binary images	Requested for basic values, trabecular thickness, number and separation

Analysis was performed on trabecular bone volume, trabecular thickness, trabecular separation, trabecular number and trabecular pattern factor as shown in Table 2.5. Cortical bone analysis was performed on cortical bone volume, cortical thickness, cortical diameter, medullary cavity diameter and cross-sectional diaphyseal area. All calculations were saved as *.csv* files. 3D models of tibias and 2 day-old pup skeletons were visualised using the CTVol software by SkyScan (Figure 2.8*D*).

Table 2.5: Analysing parameters and abbreviations

Parameter	Abbreviation (unit)
Trabecular bone volume	BV/TV (%)
Trabecular Thickness	Tb.Th (μm)
Trabecular Separation	Tb.Sp (μm)
Trabecular Number	Tb.N (1/mm)
Trabecular Pattern factor	Tb.Pf (1/mm)
Cortical bone volume	Ct.BV (mm^3)
Cortical Thickness	Ct.Th (μm)
Cortical diameter	Ct.Dm (μm)
Medullary cavity diameter	Med.Cav.Dm (μm)
Cross-sectional diaphyseal area	Ct.Ar (mm^2)

The μCT scanning procedure is summarised in Figure 2.8.
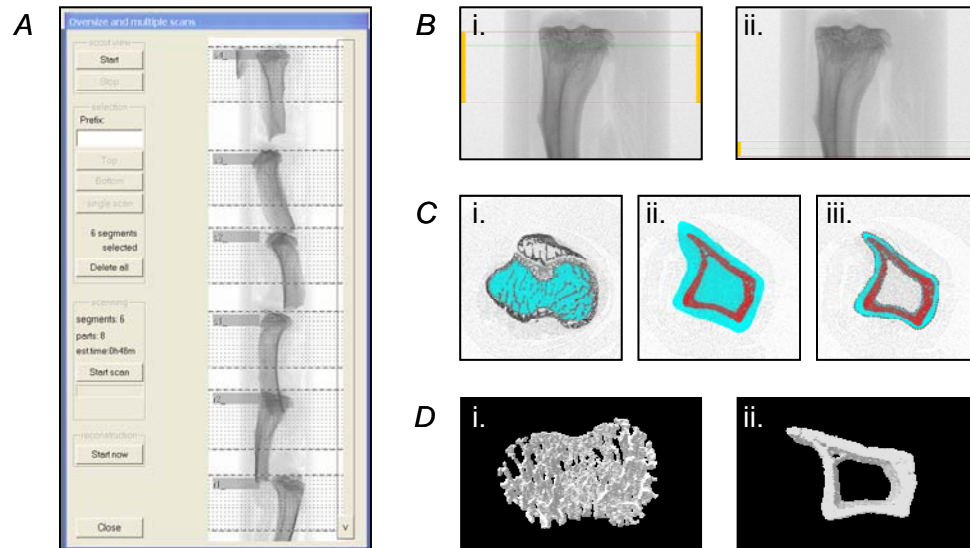
Figure 2.8: µCT scan procedure. *A*. Scanning of dissected tibiae in groups of 6 bones. *B*. Reconstruction of a tibia at the proximal tibial metaphysis (i) or proximal diaphysis (ii) in scout view. *C*. Selection of region of interest (ROI) in a cross sectional view. The ROI for the proximal tibial metaphysis is the trabecular bone (i), whereas for the proximal diaphysis could be the cortical bone including the medullar cavity (ii) or simply the cortex (iii). *D*. 3D model viewings of trabecular bone (i) or cortical bone (ii) in cross sectional view.

2.5.9 *Bone histomorphometric analysis*

Left proximal tibia, including metaphysis and part of diaphysis, were carefully dissected and fitted into an embedding basket (Figure 2.9*A*i) which in turn was placed in a vial with PBS. The vial was then placed in a Leica automatic tissue processor at room temperature for about 28 hours (Figure 2.9*A*ii). During this period the samples underwent various stages of dehydration with ethanol dilutions and defatting with xylene as shown in Table 2.6.

103

Table 2.6: Stages and reagents for Leica tissue processor programme

Stage	Reagent	Time (hours)
1	PBS	45min
2	50% Ethanol	02.00
3	70% Ethanol	02.00
4	80% Ethanol	02.00
5	96% Ethanol	02.00
6	100% Ethanol	03.00
7	100% Ethanol	03.00
8	Xylene	01.00
9	Xylene	12.00

Following processing, the samples were placed in freshly-prepared methyl methacrylate (MMA)-based infiltration solution (Appendix 2.5, page 273). The samples were kept in an air-tight vacuum desiccator, at 4°C for 1 week (Figure 2.9*B*i).

Once infiltrated, the samples were transferred individually into embedding molds and covered with 3ml of MMA-based embedding solution which had been stored for 1 week at 4°C. The molds were then shut airtight and immersed in a water bath at 30°C. Polymerisation of MMA-based resin was completed within 9-15 hours. Resin blocks were then mounted on embedding rings using a quick-hardening mounting medium made of 2 parts of dibenzoylperoxide (powder) and 1 part of N,N-dimethyl-p-toluidine (liquid).

Each resin block was clamped onto an appropriate holder and with a low speed microtome steel knife, the specimens were trimmed to a bone-section width of 600-1000μm depending on the size of the bone, reaching approximately the sagittal plane of

the tibia (Figure 2.9Ci). The specimens were then cut into 5μm thick sections. Sections were collected and placed on a drop of 96% (v/v) ethanol on a silane coated microscope slide and then covered with Kisol foil. The excess ethanol was removed using a small piece of filter paper and to improve adhesion of the sections they were left to dry under pressure at 37°C for 1-2 days.

Prior to resin removal, the Kisol foil was carefully removed from the slide. Then the slides were immersed into 2-Methoxyethyl acetate (MEA) for 20 minutes. This was repeated three times using fresh MEA each time. Slides were then immersed twice into xylene, for 10 minutes each time. For rehydration the sections were washed in a series of ethanol solutions of decreasing concentration, i.e. 100% (twice), 96%, 80%, 70%, and 50% (v/v) ethanol. Finally the slides were washed in dH$_2$O.

The sections were initially stained with Von Kossa. Sections were immersed in 1.5% (v/v) aqueous silver nitrate and incubated in the dark for 5 minutes. Following the incubation period, sections were carefully rinsed in three changes of dH$_2$O and then immersed in 0.5% (w/v) aqueous hydroquinone for 2 minutes. Finally, all sections were washed in three changes of dH$_2$O.

Following Von Kossa staining, the sections were counterstained with Paragon stain, a 1:5 mixture of Paragon solution : Borax buffer solution (Appendix 2.5, page 273) and incubated at room temperature for 1 minute. Once stained, all sections were washed in three changes of dH$_2$O.

After counterstaining, sections were air dried in a fume hood and then immersed in xylene for up to 5 minutes. Excess xylene was removed by a paper towel and finally the sections were coverslipped with DPX mounting medium (Figure 2.9Cii).

The process of bone histology is summarised in Figure 2.9.
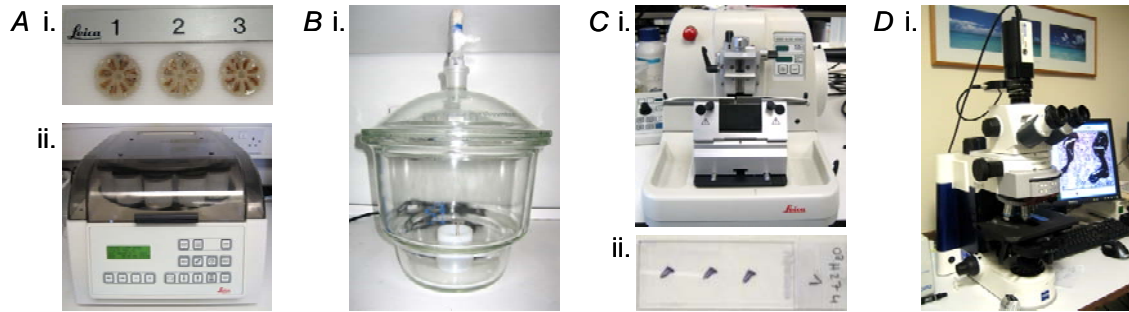
Figure 2.9: Histology and histomorphometry procedures. *A*. Dissected tibias were placed in baskets (i) and then in a tissue processor (ii) for dehydration and defatting. *B*. Samples were kept in MMA-based infiltration solution in a vacuum desiccator at 4°C for a week. Infiltrated samples were embedded in MMA-based embedding solution which polymerised into resin blocks (not shown). *C*. Blocks were trimmed and cut into 5μm thick sections using a microtome steel knife (i). Sections were placed on silane coated microscope slides and then went through Von Kossa and Paragon staining (ii). *D*. Sections were analysed using a Zeiss Axio Image microscope.

2.5.10 Image analysis

Tibial sections of the proximal metaphysis distal to the epiphysial growth plate were visualised at 10x magnification using a Zeiss Axio Imager microscope fitted with a QImaging Retiga 4000R camera (Figure 2.9*D*). Static and dynamic bone histomorphometry was performed on the trabecular bone in the area between 0.1mm and 1.0mm distal to the growth plate, using a custom software developed by Dr. Rob J. van't Hof using the Aphelion Image Analysis tool kit (Adcis SA, Hérouville-Saint-Clair, France) as previously described (van't Hof et al., 2004) (Figure 2.10). Parameters such as bone volume, active resorption area, osteoclast and osteoblast number, bone formation rate and mineral apposition rate, were calculated according to the ASBMR Histomorphometry Nomenclature Committee (Parfitt et al., 1987) and are shown in Table 2.7.
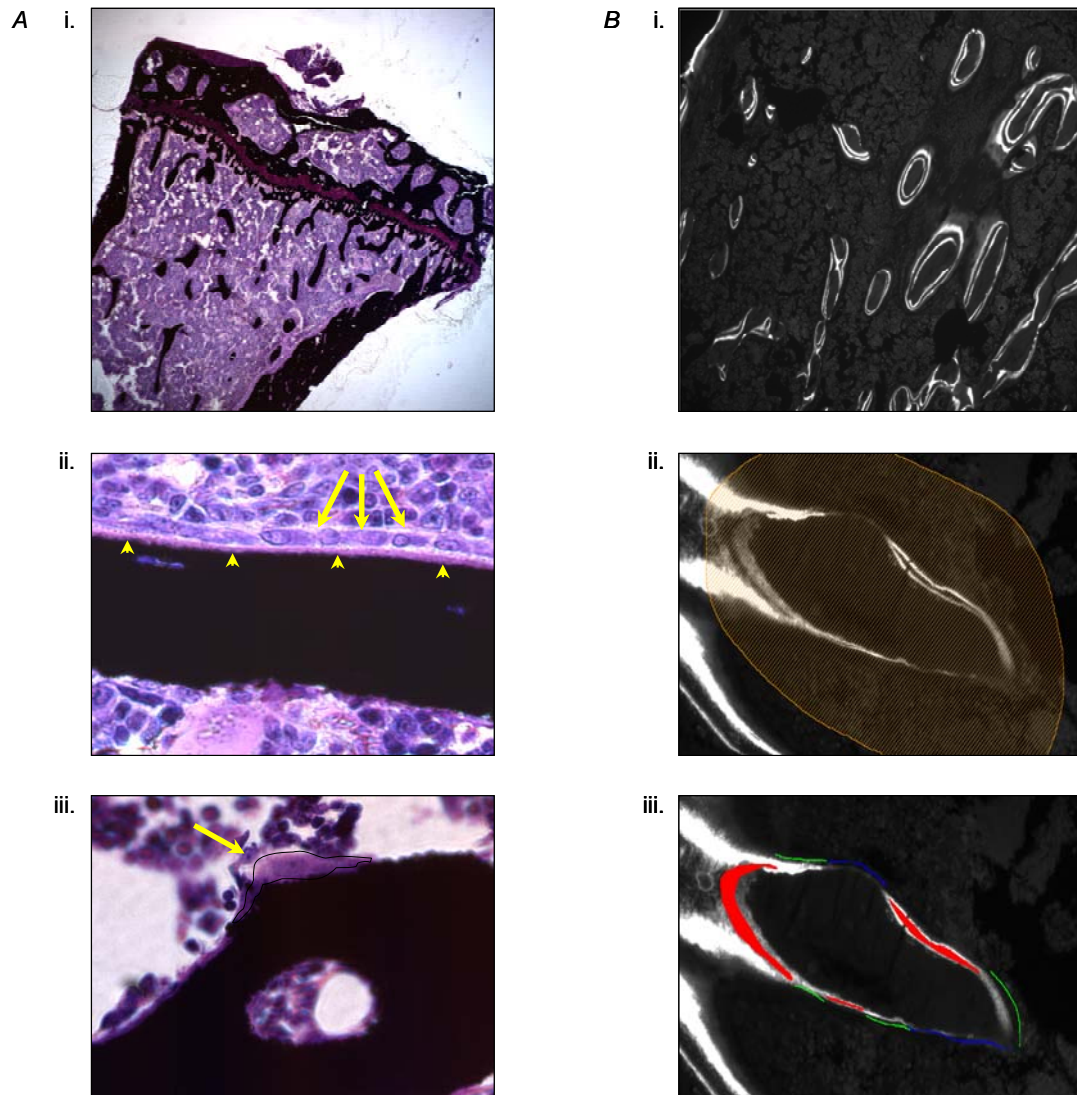
Figure 2.10: Static and dynamic histomorphometric analysis. *A*i. Von Kossa and Paragon stained section at 5X magnification. ii. Arrows and arrowheads point to osteoblasts and osteoid, respectively (x40 magnification). iii. Arrow points to an osteoclast at x40 magnification. *B*. Picture of calcein labelling visualised by fluorescent microscope at x20 magnification (monochrome capture) (i). Trabecular bone surface is selected (ii) and traced in blue, indicating unlabelled surface, in green, indicating single labelled surface, or in red, while filling the space between the two lines, indicating double labelled surface (x20 magnification).

Table 2.7: Static and dynamic bone histomorphometric parameters

Parameter	Abbreviation (unit)	Calculation/Expression
Bone Volume per Total Volume	BV/TV (%)	Value x 100
Active resorption area per Bone Surface	Oc.S/BS (%)	Value x 100
Osteoclast Number per Bone Surface	Oc.N/BS (# of cells/mm)	Osteoclast number/Bone surface
Osteoblast Number per Bone Surface	Ob.N/BS (# of cells/mm)	Osteoblast number/Bone surface
Osteoclast Number per total section area	Oc.N/T.Ar (# of cells/mm^2)	Osteoclast number/Section area
Osteoblast Number per total section area	Ob.N/T.Ar (# of cells/mm^2)	Osteoblast number/Section area
Single Labelled Surface	sLS (μm)	Calculated by software
Double Labelled Surface	dLS (μm)	Calculated by software
Bone Surface	BS (μm)	sLS + dLS + unlabelled surface
Labelled Width	L.Wi (μm)	Calculated by software
Mineral Apposition Rate	MAR (μm/day)	L.Wi /# of days
Mineralising Surface per Bone Surface	MS/BS (ratio)	(dLS + sLS/2)/BS
Bone Formation Rate (at bone surface level)	BFR (μm^2/μm/day)	MAR*(MS/BS)

2.6   DATA ANALYSIS

Statistical analysis was performed using SPSS version 13.0. Differences between mean scores for drug-treated cultures and control cultures were analysed for significance by one-way analysis of variance (ANOVA) followed by Dunnett's post hoc test. Significant differences between groups were assessed using ANOVA followed by Tukey's post hoc test (for equal variances) or Games-Howell post hoc test (for unequal variances). Differences between wild type and *CNR2*$^{-/-}$ mice, or cultures derived from wild type and *CNR2*$^{-/-}$ mice were analysed by independent-samples *t* test. All data are presented as means ± standard error of means (sem) unless stated otherwise. Values of *p* less than 0.05 were considered significant.

The *half maximal effective concentration* (EC$_{50}$) and *half maximal inhibitory concentration* (IC$_{50}$) values were calculated by non-linear regression analysis using the equation for a sigmoidal concentration-response curve (GraphPad Prism version 4.0).

CHAPTER THREE
ENDOCANNABINOID SYSTEM IN BONE CELLS

3 ENDOCANNABINOID SYSTEM IN BONE CELLS

3.1 SUMMARY

Type 1 (CNR1) and type 2 (CNR2) cannabinoid receptors have been previously reported to be expressed on mouse osteoblasts and osteoclasts. Shortly after, studies showed that bone cells also expressed some of the enzymes critically involved in the metabolism of AEA and 2-AG. The expression of CNR2 and enzymes involved in the endocannabinoid biosynthesis and degradation in the bone microenvironment was concurrently investigated by our group, using qPCR and Western blot analysis.

CNR2 mRNA and protein levels were found to be expressed in bone marrow, M-CSF-stimulated macrophages, M-CSF- and RANKL-stimulated osteoclasts and calvarial osteoblasts. CNR2 protein levels were found to be expressed in two different forms most likely representing a glycosylated and a non-glycosylated form of CNR2. Bone marrow and calvarial osteoblasts mainly expressed the non-glycosylated form of CNR2 whereas macrophages and osteoclasts mainly expressed the glycosylated CNR2 form. Regardless whether CNR2 was glycosylated or not, it was most highly expressed in bone marrow and osteoclasts suggesting a possible role of CNR2 in osteoclast differentiation and function. In bone marrow-derived osteoblasts, *CNR2* mRNA expression increased progressively as cells differentiated from osteoblast precursors to mature osteoblasts, indicating a potential role of CNR2 in osteoblast differentiation. In addition, bone cells were found to express *NAPE-PLD* and *DAGL*s (α and β), enzymes involved in the biosynthesis of AEA and 2-AG respectively, and *FAAH* and *MGL*, enzymes involved in endocannabinoid degradation, at comparable levels to those expressed in the brain.

In conclusion, cells within the bone microenvironment express *CNR2* mRNA and protein, as well as mRNA levels of the enzymes responsible for the biosynthesis and degradation of endocannabinoids.

3.2   INTRODUCTION

The endocannabinoid system comprises two known receptors; the type 1 cannabinoid receptor (CNR1) and the type 2 cannabinoid receptor (CNR2), a family of endogenous ligands and a molecular machinery for ligand synthesis, transport and inactivation [reviewed in (Goutopoulos and Makriyannis, 2002; Griffin et al., 2000; Howlett, 2002; Lutz, 2002)].

The CNR1 and CNR2 receptors exhibit 44% homology at the protein level and share common signal transduction pathways (Lutz, 2002; Schatz et al., 1997) (c.f. Figure 1.10, page 58). Both cannabinoid receptors are G protein-coupled receptors and are highly expressed in the brain (CNR1), immune system (CNR2) and in a number of other peripheral tissues (Pertwee, 1997). Osteoclasts, osteoblasts, osteocytes and bone marrow have been recently reported to express CNR1 and CNR2, with CNR2 being higher than CNR1 [reviewed in (Idris, 2008; Bab and Zimmer, 2008; Bab et al., 2008)].

Two well-characterised endocannabinoids, arachidonoyl ethanolamide (AEA) and 2-arachidonoyl glycerol (2-AG), have also been detected in the brain and peripheral tissues (Schmid et al., 1997). Recent studies have shown that bone cells express endocannabinoids at levels similar to those found in the brain [reviewed in (Bab et al., 2008)]. Finally, the presence of enzymes involved in the endocannabinoid metabolism (c.f. Figure 1.11, page 61), in osteoclasts, osteoblasts, osteocytes and bone lining cells, provided further evidence for the existence of a skeletal endocannabinoid system (Tam et al., 2008; Bab and Zimmer, 2008; Rossi et al., 2009).

The aim of the work reported in this chapter was to investigate further the presence and distribution of CNR2 and other components of the endocannabinoid system, such as enzymes involved in the synthesis/breakdown of endocannabinoids, in the bone microenvironment. mRNA expression levels of the endocannabinoid machinery components and CNR2 protein levels were measured by means of qPCR and Western blot analysis, respectively.

3.3   RESULTS

3.3.1   *Osteoclasts and osteoblasts express type 2 cannabinoid receptors*

The expression of *CNR2* mRNA was measured in M-CSF- and RANKL-generated osteoclasts and calvarial osteoblasts, using Reverse Transcription PCR (RT-PCR) (c.f. section 2.3.3, page 83) followed by quantitative real time PCR (qPCR) (c.f. section 2.3.4, page 84). As shown in Figure 3.1 the *CNR2* mRNA expression was most abundant in osteoclasts, which exceeded that in calvarial osteoblasts by 4-fold.
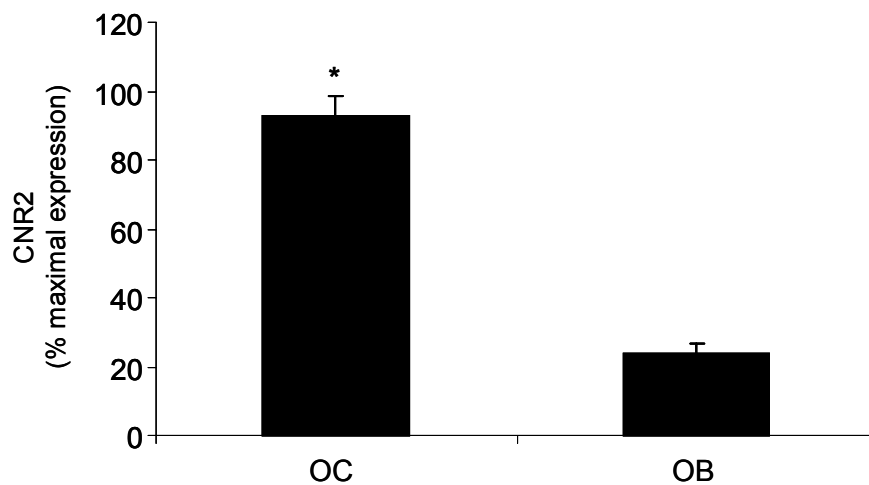
Figure 3.1: mRNA expression of *CNR2* in osteoclasts and osteoblasts. *CNR2* mRNA expression in M-CSF- and RANKL-stimulated osteoclasts (OC) and calvarial osteoblasts (OB). The amount of total RNA used for cDNA synthesis was 25ng. mRNA levels were expressed as a percent of values from maximal expression. Values are means ± sem from 3 independent experiments. *$p < 0.05$ from OB.

To determine the protein level of CNR2 in bone cells, Western blot analysis was used (c.f. section 2.4, page 90). CNR2 protein was detected in M-CSF- and RANKL-generated osteoclasts and calvarial osteoblasts in two different forms, most likely representing a non-glycosylated and a glycosylated form of the receptor (Figure 3.2*A*i). Both bone cell types expressed a 41kDa peptide. In addition, a second peptide with the molecular weight of 45kDa was mainly expressed by osteoclasts (Figure 3.2*A*i).

Following protein normalisation to the 42kDa actin, the expression of the 41kDa CNR2 peptide in osteoclasts and osteoblasts was not significantly different (Figure 3.2*B*), whereas the 45kDa CNR2 peptide in osteoclasts was clearly more abundant than in osteoblasts, where this peptide was expressed in far smaller amounts (Figure 3.2*C*).
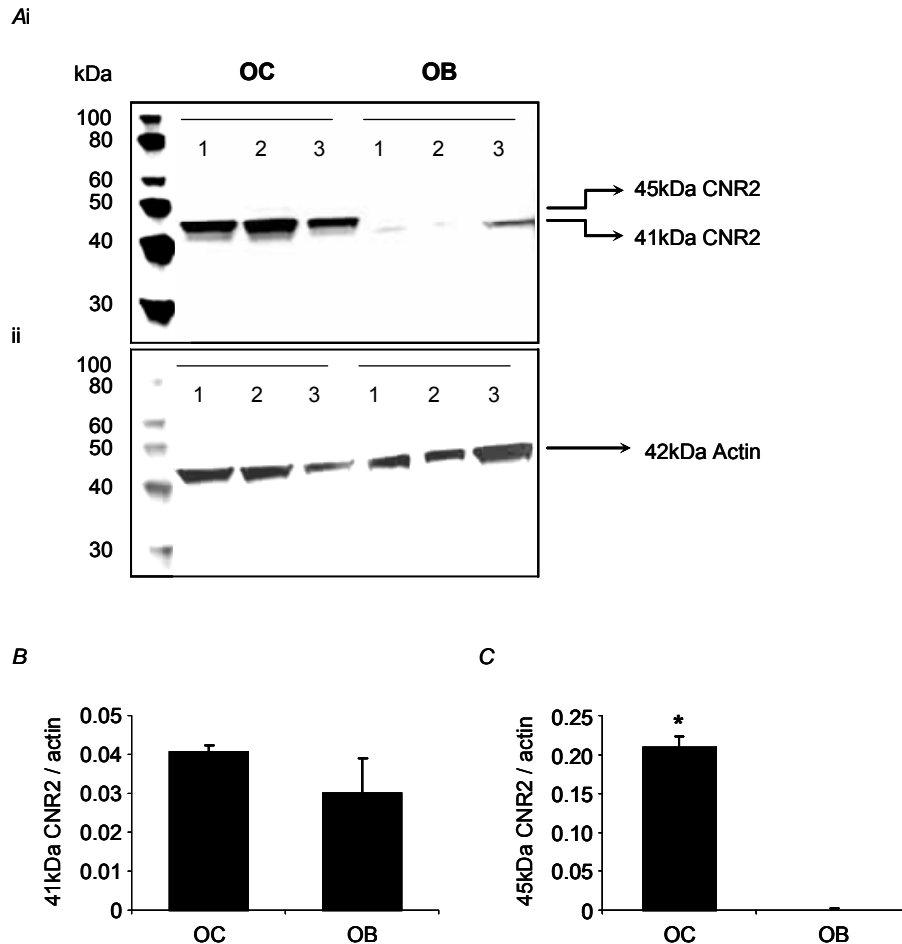
Figure 3.2: CNR2 protein expression in osteoclasts and osteoblasts. *A*. CNR2 (i) and actin (ii) expression in M-CSF- and RANKL-stimulated osteoclasts (OC) and calvarial osteoblasts (OB). Lanes are replicates from 3 mice (for OC) or 3 litters (for OB). Quantification of 41kDa CNR2 peptide (*B*) and 45kDa CNR2 peptide (*C*) in OC and OB expressed as a ratio of CNR2 over actin. The amount of total protein used for western blotting was 47μg. Values in *B* and *C* are means ± sem from 3 independent experiments. *p < 0.001 from OB.

3.3.2 Bone marrow-derived macrophages and osteoclasts express type 2 cannabinoid receptors

To determine the mRNA levels of *CNR2* in bone marrow cells differentiating towards osteoclasts, qPCR was performed on bone marrow and bone marrow-derived macrophages (treated with M-CSF) and osteoclasts (treated with M-CSF and RANKL) (c.f section 2.3.4, page 84). As shown in Figure 3.3, there was decreasing *CNR2* mRNA expression from bone marrow to macrophages to osteoclasts. The mRNA levels of *CNR2* in bone marrow exceeded those in macrophages by almost 2-fold and those in osteoclast by 6-fold.
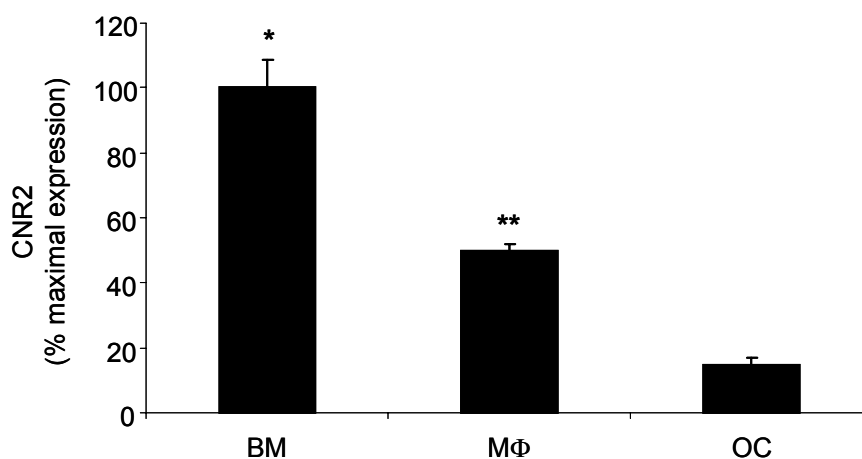
Figure 3.3: mRNA expression of *CNR2* in bone marrow and bone marrow-derived macrophages and osteoclasts. *CNR2* mRNA expression in bone marrow (BM), M-CSF-stimulated macrophages (MΦ) and M-CSF- and RANKL-stimulated osteoclasts (OC). The amount of total RNA used for cDNA synthesis was 25ng. mRNA levels were expressed as a percent of values from maximal expression. Values are means ± sem from 3 independent experiments. *$p < 0.05$ from all samples, **$p < 0.05$ from OC.

To determine the protein level of CNR2 in bone marrow cells differentiating towards osteoclasts, Western blot analysis was performed on bone marrow, M-CSF-stimulated macrophages and M-CSF- and RANKL-stimulated osteoclasts (c.f. section 2.4, page 90). Consistent with section 3.3.1, page 113, Western blot analysis yielded two forms of CNR2, most likely representing a non-glycosylated and a glycosylated form of the

receptor (Figure 3.4*A*i). Bone marrow mainly expressed a 41kDa peptide of CNR2, whereas macrophage and osteoclasts mainly expressed a CNR2 peptide with the molecular weight of 45kDa (Figure 3.4*A*i). Following protein normalisation to actin, the expression of the 41kDa CNR2 peptide in bone marrow exceeded the expression in macrophages and osteoclasts by at least 10-fold (Figure 3.4*B*). The 45kDa CNR2 peptide was expressed in increasing order from bone marrow to macrophages to osteoclasts (Figure 3.4*C*). However, regardless of the glycosylation state of the receptor, this data shows that bone marrow and osteoclasts express comparable protein levels of CNR2, which are significantly higher than those expressed in macrophages.
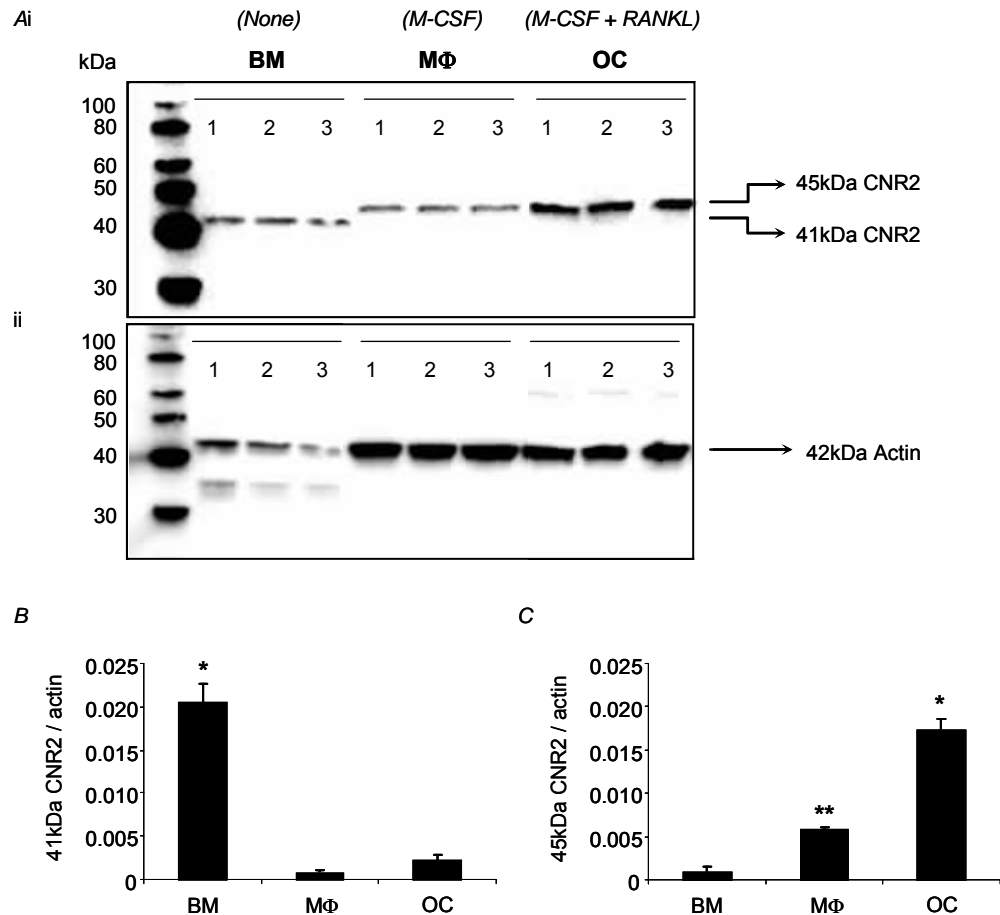
Figure 3.4: CNR2 protein expression in bone marrow and bone marrow derived-macrophages and osteoclasts. *A*. CNR2 (i) and actin (ii) expression in bone marrow (BM), M-CSF-stimulated macrophages (MΦ) and M-CSF- and RANKL-stimulated osteoclasts (OC). Lanes are replicates from 3 mice. Quantification of 41kDa CNR2 peptide (*B*) and 45kDa CNR2 peptide (*C*) in BM, MΦ and OC expressed as a ratio of CNR2 over actin. The amount of total protein used for western blotting was 47μg. Values in *B* and *C* are means ± sem from 3 independent experiments. *p < 0.05 from all samples, **p < 0.05 from BM.

3.3.3   *Bone marrow-derived mature osteoblasts express high levels of CNR2 mRNA*

To investigate the presence of CNR2 in differentiating osteoblasts, *CNR2* mRNA expression was also analysed in bone marrow-derived stromal cells grown in medium supplemented with 50μg/ml Vitamin C and 3mM β-GP (osteogenic medium) (c.f. section 2.2.6, page 79). Expression of *CNR2* mRNA increased progressively during the culture period of 20 days (Figure 3.5). The mRNA levels of *CNR2* were much lower when bone marrow-derived stromal cells were grown in non-osteogenic medium for 20 days (Figure 3.5). At the end of the culture period, *CNR2* mRNA expression in cultures propagated with osteogenic medium for 20 days was 4-fold higher than in cultures in non-osteogenic medium (Figure 3.5).
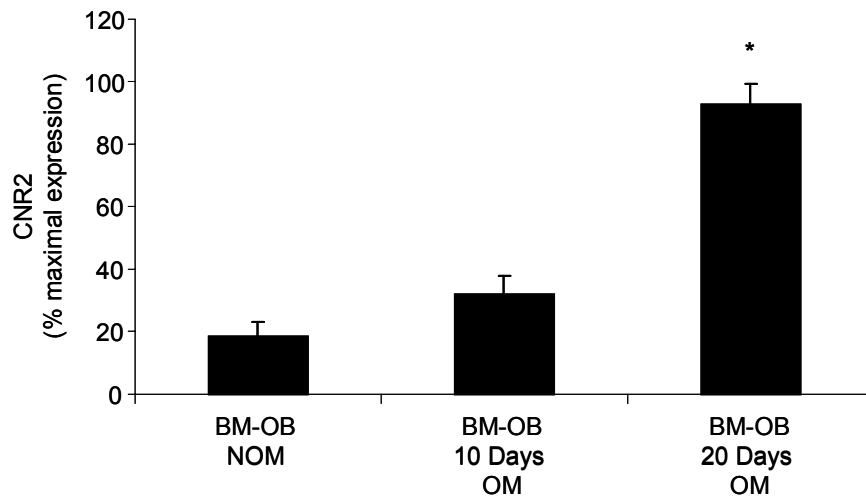
Figure 3.5: mRNA expression of *CNR2* in bone marrow-derived osteoblasts. *CNR2* mRNA expression in bone marrow-derived osteoblasts (BM-OB) in non-osteogenic medium (NOM) for 20 days and in medium supplemented with Vitamin C and β-GP [osteogenic medium – (OM)] for 10 or 20 days. The amount of total RNA used for cDNA synthesis was 100ng. mRNA levels were expressed as a percent of values from maximal expression. Values are means ± sem from 3 independent experiments. *p < 0.05 from all samples.

3.3.4 Bone cells express the mRNA of endocannabinoid synthesising and breakdown enzymes

To investigate the presence of other components of the endocannabinoid machinery in bone cells, qPCR was used to investigate the mRNA expression of enzymes involved in the synthesis and breakdown of the endocannabinoids AEA and 2-AG. The mRNA levels of these enzymes in the bone microenvironment were of the same order of magnitude as in the brain (Figure 3.6, 3.7 and 3.8).

The mRNA levels of the AEA-synthesising enzyme, N-acyl phosphatidylethanolamine phospholipase D (*NAPE-PLD*), in osteoclasts exceeded those in brain by 3-fold and those in bone marrow, macrophages and osteoblasts by almost 4-fold (Figure 3.6).
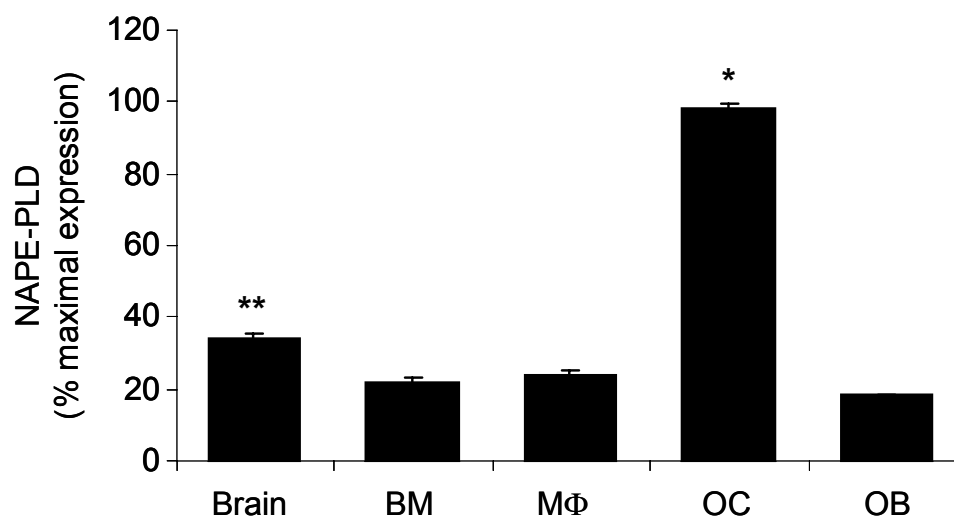
Figure 3.6: mRNA expression of the enzyme involved in the synthesis of AEA in brain and bone microenvironment. *NAPE-PLD* mRNA expression in brain, bone marrow (BM), macrophages (MΦ), osteoclasts (OC) and calvarial osteoblasts (OB). The amount of total RNA used for cDNA synthesis was 5μg. mRNA levels were expressed as a percent of values from maximal expression. Values are means ± sem from 3 independent experiments. *$p < 0.05$ from all samples, **$p < 0.05$ from BM, MΦ and OB.

Two enzymes are involved in 2-AG synthesis, sn-1-diacyl glycerol lipase α (*DAGLα*) and *DAGLβ*. Unlike *DAGLβ*, *DAGLα* was most abundant in the brain. Bone marrow had extremely low levels of *DAGLα* mRNA compared to bone cells which expressed *DAGLα* mRNA in increasing order from macrophages to osteoclasts to osteoblasts (Figure 3.7*A*). *DAGLβ* however, was more highly expressed in the bone microenvironment than in brain. Macrophages and bone marrow had the highest mRNA levels of *DAGLβ*, whereas osteoclasts and osteoblasts expressed *DAGLβ* mRNA at similar levels as brain (Figure 3.7*B*).
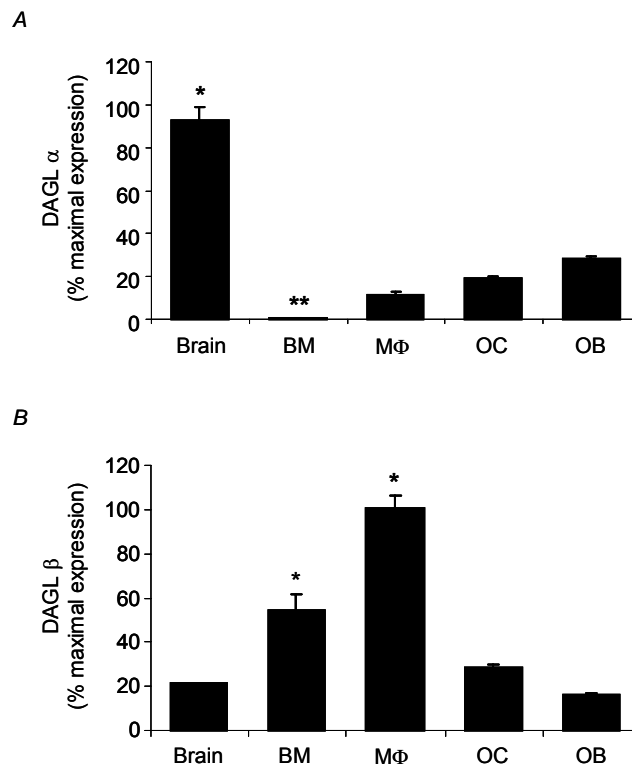
Figure 3.7: mRNA expression of enzymes involved in the synthesis of 2-AG in brain and bone microenvironment. *DAGLα* (*A*) and *DAGLβ* (*B*) mRNA expression in brain, bone marrow (BM), macrophages (MΦ), osteoclasts (OC) and calvarial osteoblasts (OB). The amount of total RNA used for cDNA synthesis was 5µg. mRNA levels were expressed as a percent of values from maximal expression. Values are means ± sem from 3 independent experiments. *p < 0.05 from all samples, **p < 0.05 from OC and OB.

The mRNA of both enzymes responsible for endocannabinoid breakdown, fatty acid amide hydrolase (*FAAH*) and monoacylglycerol lipase (*MGL*), were most abundant in brain and at levels at least twice as high as in the bone microenvironment (Figure 3.8*A,B*). Expression of *FAAH* mRNA in bone marrow was 2-fold higher than in osteoclasts and 4-fold higher than in osteoblasts. In macrophages *FAAH* mRNA was found to be expressed in far smaller amounts (Figure 3.8*A*). In the bone microenvironment, *MGL* mRNA was most highly expressed in bone marrow, where levels were twice as high as in osteoblasts. The expression of *MGL* mRNA in macrophages and osteoclasts was very low (Figure 3.8*B*).
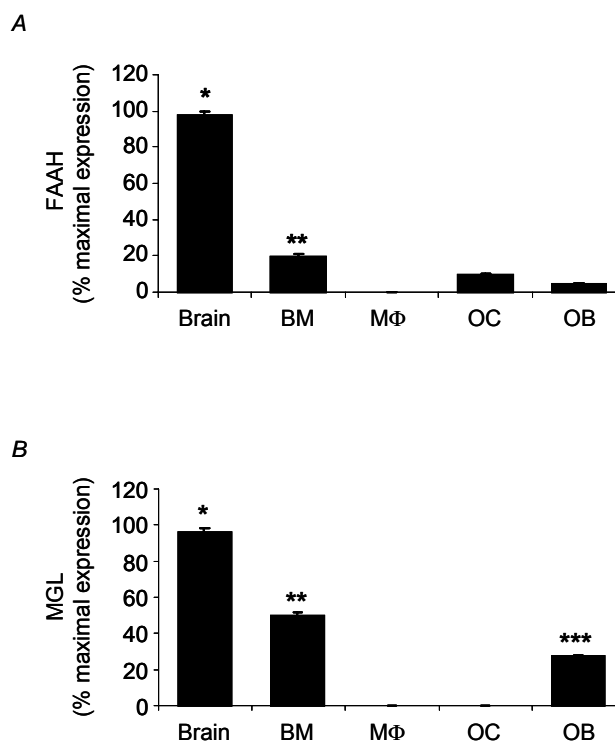
Figure 3.8: mRNA expression of enzymes involved in the breakdown of AEA and 2-AG in brain and bone microenvironment. *FAAH* (*A*) and *MGL* (*B*) mRNA expression in brain, bone marrow (BM), macrophages (MΦ), osteoclasts (OC) and calvarial osteoblasts (OB). The amount of total RNA used for cDNA synthesis was 5μg. mRNA levels were expressed as a percent of values from maximal expression. Values are means ± sem from 3 independent experiments. *p < 0.05 from all samples, **p < 0.05 from MΦ, OC and OB, ***p < 0.05 from MΦ and OC.

3.4   DISCUSSION

The discovery of the central type 1 cannabinoid receptor (CNR1) (Matsuda et al., 1990) was followed by the characterisation of the peripheral type 2 cannabinoid receptor (CNR2) (Munro et al., 1993). A search of endogenous ligands for cannabinoid receptors led to the identification of AEA and 2-AG (Devane et al., 1992; Mechoulam et al., 1995). Cannabinoid receptors, their endogenous ligands and enzymatic systems for their biosynthesis and degradation together form the endocannabinoid system.

CNR1 is highly expressed in brain tissue and to lesser extent in peripheral tissues (Matsuda et al., 1990; Bouaboula et al., 1993), whereas CNR2 is mainly expressed by immune and haematopoietic cells (Munro et al., 1993; Schatz et al., 1997). In this study *CNR2* mRNA expression was detected in bone marrow, macrophages and osteoclasts. This was in agreement with previous findings of our group and others showing that *CNR2* mRNA was expressed in mouse osteoclasts (Idris et al., 2005; Ofek et al., 2006), in RAW 264.7-derived osteoclast-like cells (Ofek et al., 2006) and in human osteoclasts (Rossi et al., 2009). The detection of *CNR2* mRNA in cells of the osteoclast lineage suggests that CNR2 could mediate the effects of cannabinoid ligands on osteoclast formation and function.

Western blot analysis yielded two bands corresponding to CNR2. Bone marrow mainly expressed a 41kDa peptide that could correspond to the predicted size of the CNR2 protein based on its amino acid sequence. Macrophages and osteoclasts mainly expressed a second CNR2 peptide with an apparent molecular weight of 45kDa, most likely to represent a glycosylated form of CNR2 as previously detected in human dendritic cells (Matias et al., 2002) and in Sf21 insect cells expressing human CNR2 using the baculovirus expression system (Filppula et al., 2004).

Glycosylation is a common structural feature of G protein-coupled receptors (GPCRs) (Howlett et al., 1991). Murine CNR2 contains one potential glycosylation site in the extracellular N-terminal domain (Olson et al., 2003). N-glycosylation is a post-translational modification occurring as a series of enzymatic reactions initiated in the endoplasmic reticulum and completed during transport through the Golgi apparatus [reviewed in (Duvernay et al., 2005)]. N-glycosylation in GPCRs may be absolutely necessary for their cell-surface expression, may facilitate their transport to the cell surface, or may have no effect on their expression at all (Duvernay et al., 2005). For cannabinoid receptors it has been shown that oligosaccharide groups are not necessary for agonist-binding or the subsequent inhibition of adenylate cyclase, suggesting that glycosylation is unimportant for cannabinoid receptor activity (Howlett et al., 1991). However, the authors mentioned that the rate of receptor synthesis and degradation had not been taken into consideration (Howlett et al., 1991). With no more evidence regarding the role of glycosylation in cannabinoid receptors, it has been accepted that glycosylation modification yields different forms of cannabinoid receptors, but does not affect the receptor expression at the cell surface, or receptor activity. The expression of different forms of CNR2 in bone marrow and bone marrow-derived cells suggests that CNR2 may be subjected to different post-translation modifications in distinct cell populations. Whether these modifications are important for the rate of CNR2 synthesis or degradation is yet to be established.

Regardless of the glycosylation state of the receptor, it was obvious that bone marrow and osteoclasts had comparable CNR2 protein levels, while macrophages had 4 times lower levels. This data suggest a possible role of CNR2 in osteoclast formation, maturation and function. However, these results were not entirely reflected by quantitative real time PCR (qPCR) analysis, which showed that *CNR2* mRNA expression was least abundant in osteoclasts. Taking into consideration that qPCR analysis can only predict the amount of a protein according to the mRNA levels at the

exact time of RNA isolation, Western blot analysis is believed to be a more suitable method for determining the presence/absence or levels of a protein.

CNR2 mRNA expression in calvarial osteoblasts was very low but in bone marrow-derived osteoblasts grown in osteogenic medium, mRNA levels of *CNR2* were progressively increased as previously described (Ofek et al., 2006). These results indicate that *CNR2* mRNA expression is increased as osteoblasts mature and start forming bone matrix, suggesting a possible role of CNR2 in osteoblast differentiation.

Western blot analysis showed that calvarial osteoblasts mainly expressed the non-glycosylated form of CNR2. The detection of CNR2 in calvarial osteoblasts together with the increasing expression of *CNR2* mRNA levels in differentiating bone marrow-derived osteoblasts, suggest that CNR2 could mediate the effects of cannabinoid ligands on osteoblast differentiation and function. Due to the difficulty in recovering adequate amount of protein from mature bone marrow-derived osteoblasts grown in osteogenic medium, Western blot analysis was not repeated in these cells.

Previous studies have shown that AEA and 2-AG are produced in the bone microenvironment (Tam et al., 2008; Bab et al., 2008; Ridge et al., 2007; Rossi et al., 2009). This chapter shows that the mRNA of the enzymes involved in the endocannabinoid synthesis (*NAPE-PLD*, *DAGLα* and *DAGLβ*) and degradation (*FAAH* and *MGL*) are expressed in cells of the bone microenvironment at levels comparable to those expressed in the brain, in agreement with previously studies (Tam et al., 2008; Bab and Zimmer, 2008; Rossi et al., 2009).

Throughout this study qPCR analysis was carried out without normalisation. Although control genes can be used to correct sample-to-sample variation within the same cell type, they are not always relevant for normalisation between distinct cell types (SUGAHARA et al., 2006). Recent and previous work from our group showed that the

mRNA expression levels of *18S rRNA, ß-actin* and *GAPDH* were variable among bone marrow-derived cells and significantly affected with M-CSF and RANKL treatment (Landao-Bassonga, E., personal communication). In view of this, qPCR data in this chapter were not normalised to house keeping genes, but instead a sensitive method for measuring RNA concentration was used (c.f section 2.3.2, page 83). However, for Western blot analysis, actin was used as a loading control. The second protein detected alongside the 42kDa actin in bone marrow samples could be attributed to the likely presence of impurities in total bone marrow lysates. When this experiment was repeated with bone marrow mononuclear cells isolated by density centrifugation using Ficoll [previously described in (Majumdar et al., 1998)], no additional peptide was detected adjacent to actin (data not shown).

In conclusion, this chapter reports that CNR2 expression is enhanced in mature osteoclasts and osteoblasts indicating a significant role of this receptor in both osteoclast and osteoblast differentiation and function. Moreover, cells of the bone microenvironment also express the enzymatic machinery involved in the synthesis and breakdown of endocannabinoids, providing evidence for the existence of a skeletal endocannabinoid system.

CHAPTER FOUR
SKELETAL PHENOTYPE OF CNR2-DEFICIENT MICE

4   SKELETAL PHENOTYPE OF CNR2-DEFICIENT MICE

4.1   SUMMARY

Recent studies have shown that the endocannabinoid system plays a key role in regulating bone turnover. Mice lacking CNR2 (*CNR2$^{-/-}$*) were previously reported to have reduced bone mass, but the mechanisms responsible remain poorly understood.

Analysis by μCT showed that *CNR2$^{-/-}$* neonates had normal skeletal development and 3-month old *CNR2$^{-/-}$* mice had normal peak trabecular bone volume (BV/TV). Further analysis on bone morphometric parameters showed that 3-month old *CNR2$^{-/-}$* female mice had significantly lower trabecular number and significantly higher cortical bone volume and cross-sectional diaphyseal area than wild type littermates. Nonetheless, histomorphometric analysis demonstrated that young *CNR2$^{-/-}$* male and female mice had normal bone turnover. At 12 months of age *CNR2$^{-/-}$* mice developed accelerated osteoporosis. Comparison between 12-month old wild type and *CNR2$^{-/-}$* female mice showed that *CNR2$^{-/-}$* female mice had significantly lower BV/TV and trabecular number and significantly higher trabecular thickness and trabecular separation. Twelve-month old *CNR2$^{-/-}$* male mice showed the same trend for all morphometric parameters. Histomorphometric analysis showed that 12-month old *CNR2$^{-/-}$* mice had significantly lower osteoblast number than wild type controls. In keeping with this, 12-month old *CNR2$^{-/-}$* male mice had significantly lower serum PINP levels than wild type littermates, but surprisingly there was no difference in serum PINP levels between wild type and *CNR2$^{-/-}$* female mice. No difference was observed in osteoclast number or serum CTX levels between wild type and *CNR2$^{-/-}$* mice.

This chapter shows that type 2 cannabinoid receptors protect against accelerated age-related bone loss mainly by regulating osteoblast numbers and bone formation.

4.2 INTRODUCTION

Over recent years, there has been increasing interest in the role that neurotransmitters play in the regulation of bone remodelling (Patel and Elefteriou, 2007). Reflecting this fact, the endocannabinoid system has recently been implicated as a potentially important regulator of bone turnover and bone mass (Idris et al., 2005; Ofek et al., 2006; Tam et al., 2006; Tam et al., 2008).

The expression of cannabinoid receptors together with other components of the endocannabinoid system in bone cells (Chapter 3), indicates that signalling through cannabinoid receptors may be involved in the regulation of bone mass. Previous work from our group showed that genetic inactivation of *CNR1* in young ABH mice, resulted in high bone mass phenotype at several skeletal sites (Idris et al., 2005). We and others also reported that young *CNR1*^{-/-} mice on a CD1 background also exhibited high bone mass phenotype (Idris et al., 2008b; Tam et al., 2006), but mice with CNR1 deficiency on a C57BL/6 background had low bone mass (Tam et al., 2006). Finally, ageing experiments showed that 12-month old CD1 *CNR1*^{-/-} mice suffered from age-related osteoporosis due to reduced osteoblast numbers and increased accumulation of adipocytes in bone marrow (Idris et al., 2008b). These results indicate that CNR1 is involved in regulating bone mineral density and age-related bone loss but genetic differences between background strains may influence the effects of CNR1 on bone (Tam et al., 2006).

Evidence for the involvement of CNR2 in regulating bone remodelling and bone mass was reported by Ofek et al. (Ofek et al., 2006). This study showed that 8-week old female *CNR2*^{-/-} mice on a C57BL/6 genetic background, had a low bone mass phenotype with significantly reduced trabecular number and cortical expansion, as a result of increased bone turnover. Ageing experiments showed that 12-month old *CNR2*^{-/-} mice had a progressive trabecular bone loss accompanied with transition from plate- to rod-

like trabecular structures, associated with a net increased of bone resorption (Ofek et al., 2006). On the basis of these observations, Ofek and colleagues suggested that an important function of CNR2 is to suppress bone turnover and regulate osteoblast-osteoclast coupling (Ofek et al., 2006; Bab and Zimmer, 2008).

The aim of the work reported in this chapter was to investigate the effects of *CNR2* deletion in C57BL/6 mice at ages 3, 6 and 12 months. Structural parameters and cellular changes at the tibial metaphyses of these mice and wild type age-matched controls were measured by means of μCT and histomorphometric analysis.

4.3 RESULTS

4.3.1 Wild type and CNR2-deficient mice are 96% identical to 'pure' C57BL/6 mice

To investigate the level of similarity between the congenic mouse strain used in this study (C57BL/6 background and 129 embryonic stem cell line) and a pure C57BL/6 reference strain provided by Illumina Inc., SNP genotyping was performed using a commercially available mouse medium-density linkage panel (c.f. section 2.5.3, page 96). The congenic wild type and $CNR2^{-/-}$ mice used in this study were 96% identical to pure C57BL/6 mice (Appendix 5, page 276), whereas wild type and $CNR2^{-/-}$ littermates derived from heterozygote breeding pairs were 98% identical among themselves. None of the SNPs tested that differed between pure C57BL/6 mice and wild type and $CNR2^{-/-}$ littermates lay in the CNR2 locus.

4.3.2 CNR2-deficient mouse neonates have normal bone volume

To establish the role of CNR2 on skeletal development during embryogenesis, the bone volume of 2-day old wild type and $CNR2^{-/-}$ mouse neonates was examined using μCT analysis (c.f. section 2.5.8, page 99). As shown in Figure 4.1*A*, $CNR2^{-/-}$ mouse neonates had normal bone volume.
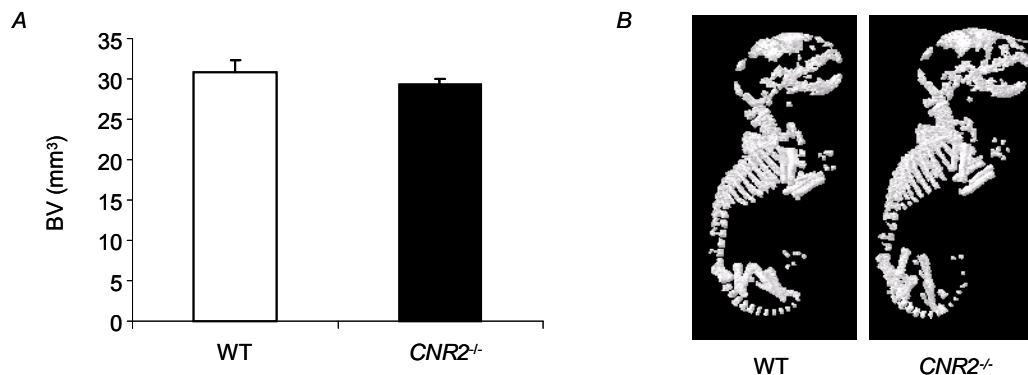
Figure 4.1: CNR2-deficient mouse neonates have normal bone volume. *A*. Bone volume (BV) of wild type and $CNR2^{-/-}$ mouse neonates at 2 days of age assessed by μCT. *B*. Representative μCT images showing the lateral view of wild type and $CNR2^{-/-}$ mouse neonates. Values are means ± sem from 6 neonates per group.

4.3.3   CNR2-deficient mice exhibit normal peak trabecular bone mass

Structural parameters of trabecular bone are normal in young CNR2-deficient mice

To investigate the role of CNR2 in bone mass of young mice, bone architectural parameters were measured within isolated tibiae from wild type and $CNR2^{-/-}$ mice at 3 months of age (c.f. section 2.5.8, page 99). μCT analysis showed that trabecular bone from $CNR2^{-/-}$ mice did not significantly differ from wild type mice of the same gender with regard to standard morphological structure parameters such as trabecular bone volume (BV/TV), trabecular thickness (Tb.Th) or trabecular pattern factor (Tb.Pf) (Figure 4.2). However, in $CNR2^{-/-}$ female mice the trabecular number (Tb.N) was significantly reduced (Figure 4.2*C*) and in $CNR2^{-/-}$ male mice the trabecular separation (Tb.Sp) was significantly increased over wild type controls (Figure 4.2*D*), suggesting that $CNR2^{-/-}$ mice have a modest bone phenotype at young age.

Comparison of the above-mentioned morphometric parameters between the two genders showed that female C57BL/6 mice had lower trabecular bone volume and trabecular number than male mice of the same strain, as shown previously (Glatt et al., 2007) (Figure 4.2*A,C*). Consequently, trabecular separation and hence trabecular pattern factor in male were significantly lower than in female specimen, indicating better trabecular connectivity (Figure 4.2*D,E*). Trabecular thickness was also different by gender, higher in male than in female mice, but this was less noticeable (Figure 4.2*B*).

No defective bone turnover in young CNR2-deficient mice

To establish whether *CNR2* deletion has an effect on cellular events occurring at the trabecular compartment of the bone, histomorphometric analysis was performed at the tibial metaphysis of 3-month old wild type and $CNR2^{-/-}$ mice (c.f. section 2.5.9, page 103). As shown in Figure 4.3*A,C*, no significant differences with respect to osteoblast numbers, osteoclast numbers or active resorption surfaces were observed between wild type and $CNR2^{-/-}$ mice at 3 months of age.
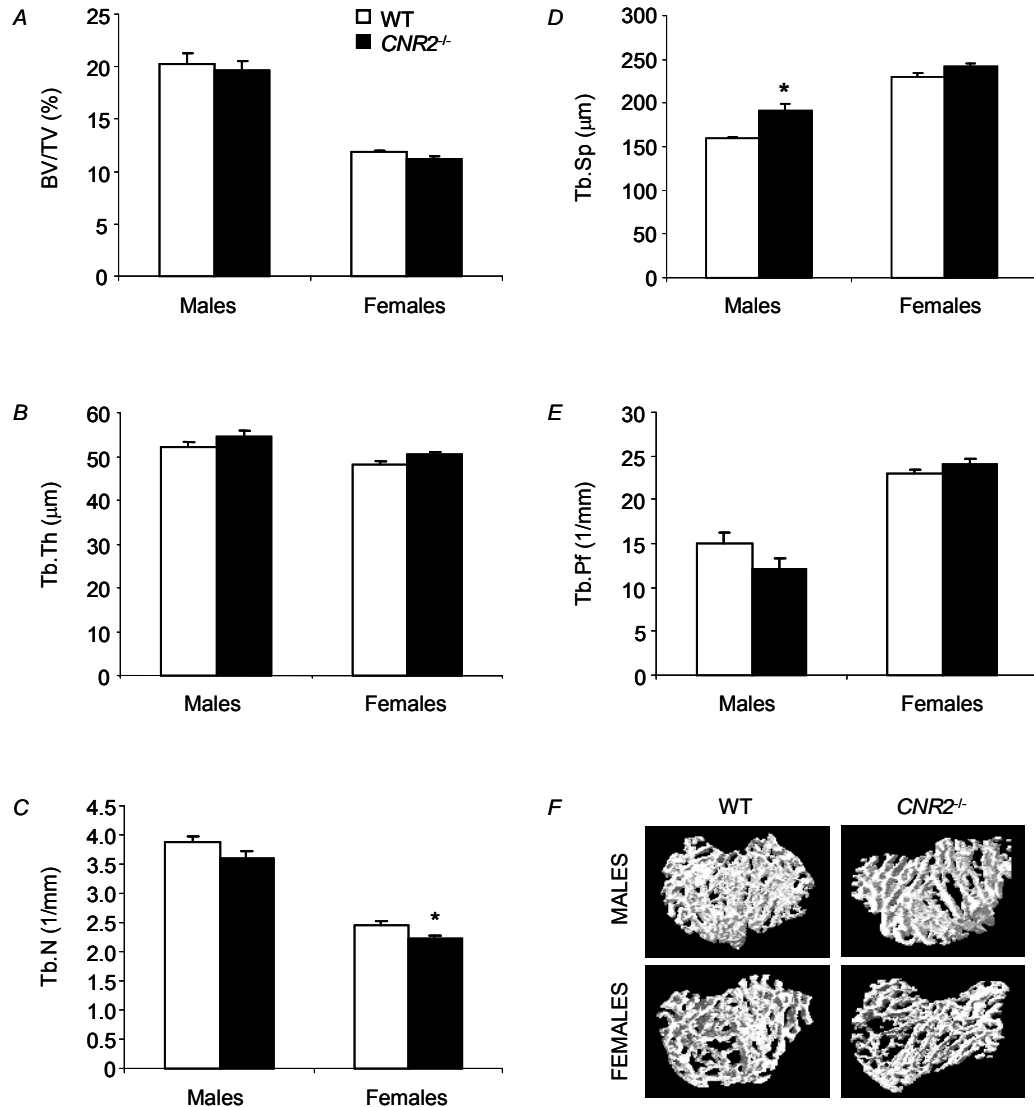
Figure 4.2: Trabecular bone mass in 3-month old wild type and CNR2-deficient mice. *A*. Trabecular bone volume (BV/TV) in wild type and *CNR2*$^{-/-}$ mice, of both genders at 3 months of age, assessed by μCT of the tibia. Trabecular thickness (Tb.Th) (*B*), trabecular number (Tb.N) (*C*), trabecular separation (Tb.Sp) (*D*), and trabecular pattern factor (Tb.Pf) (*E*) of the same experiment. *F*. Representative μCT images from the tibial metaphysis of wild type and *CNR2*$^{-/-}$ mice, of both genders. Values are means ± sem from 7-8 mice per group. *$p < 0.05$ from wild type mice of same gender.

A

Male	BV/TV (%)	Ob.N/T.Ar (cells/mm²)	Oc.N/T.Ar (cells/mm²)	Oc.S/BS (%)
WT	17.7 ± 1.0	182.6 ± 10.7	3.5 ± 0.3	1.0 ± 0.1
CNR2-/-	18.0 ± 0.7	203.1 ± 12.2	3.1 ± 0.5	1.0 ± 0.2

Bi

ii

Male WT

Male CNR2-/-

C
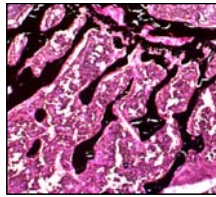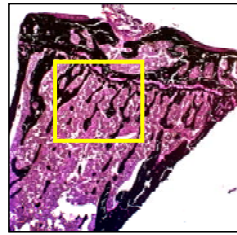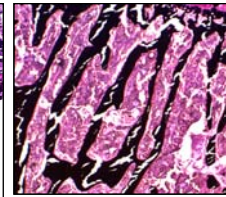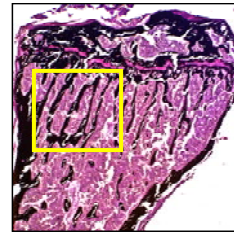
Female	BV/TV (%)	Ob.N/T.Ar (cells/mm²)	Oc.N/T.Ar (cells/mm²)	Oc.S/BS (%)
WT	9.7 ± 0.8	245.7 ± 16.0	2.2 ± 0.3	0.9 ± 0.1
CNR2-/-	12.0 ± 1.5	242.2 ± 21.8	2.6 ± 0.6	1.2 ± 0.1

Di

ii
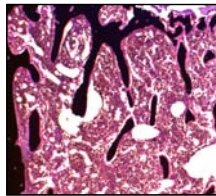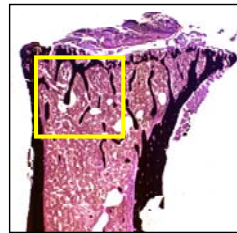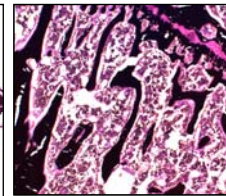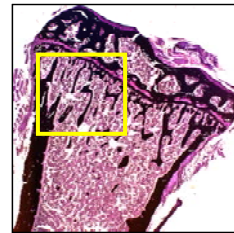
Female WT

Female CNR2-/-

Figure 4.3: Bone histomorphometry in 3-month old wild type and CNR2-deficient mice. Summary tables of bone histomorphometry from male and female mice are shown in *A* and *C*, respectively. BV/TV, trabecular bone volume (%); Ob.N/T.Ar, osteoblast number/total area (cells/mm^2); Oc.N/T.Ar, osteoclast number/total area (cells/mm^2); Oc.S/BS, osteoclast surface/bone surface (%). Values are expressed as means ± sem from 4 mice per group. Representative sections of the proximal tibia from wild type and *CNR2$^{-/-}$* male (*Bi,ii*) and female (*Di,ii*) mice, stained with von Kossa/Paragon staining (c.f. section 2.5.9, page 103). The areas of the photomicrographs in high-power images are indicated by boxes in lower-power images.

4.3.4 CNR2-deficient female mice exhibit higher cortical bone volume and cross-sectional diaphyseal area

To examine the role of CNR2 in cortical bone of young mice, cortical architectural parameters were studied at the tibial proximal diaphysis of wild type and $CNR2^{-/-}$ female mice at 3 months of age (c.f. section 2.5.8, page 99). μCT analysis showed that $CNR2^{-/-}$ female mice had significantly higher cortical bone volume (Ct.BV) (Figure 4.4*A*) and cross-sectional diaphyseal area (Ct.Ar) (Figure 4.4*B*) compared to wild type controls, whereas cortical thickness (Ct.Th) was not significantly different between wild type and $CNR2^{-/-}$ female mice (Figure 4.4*C*).
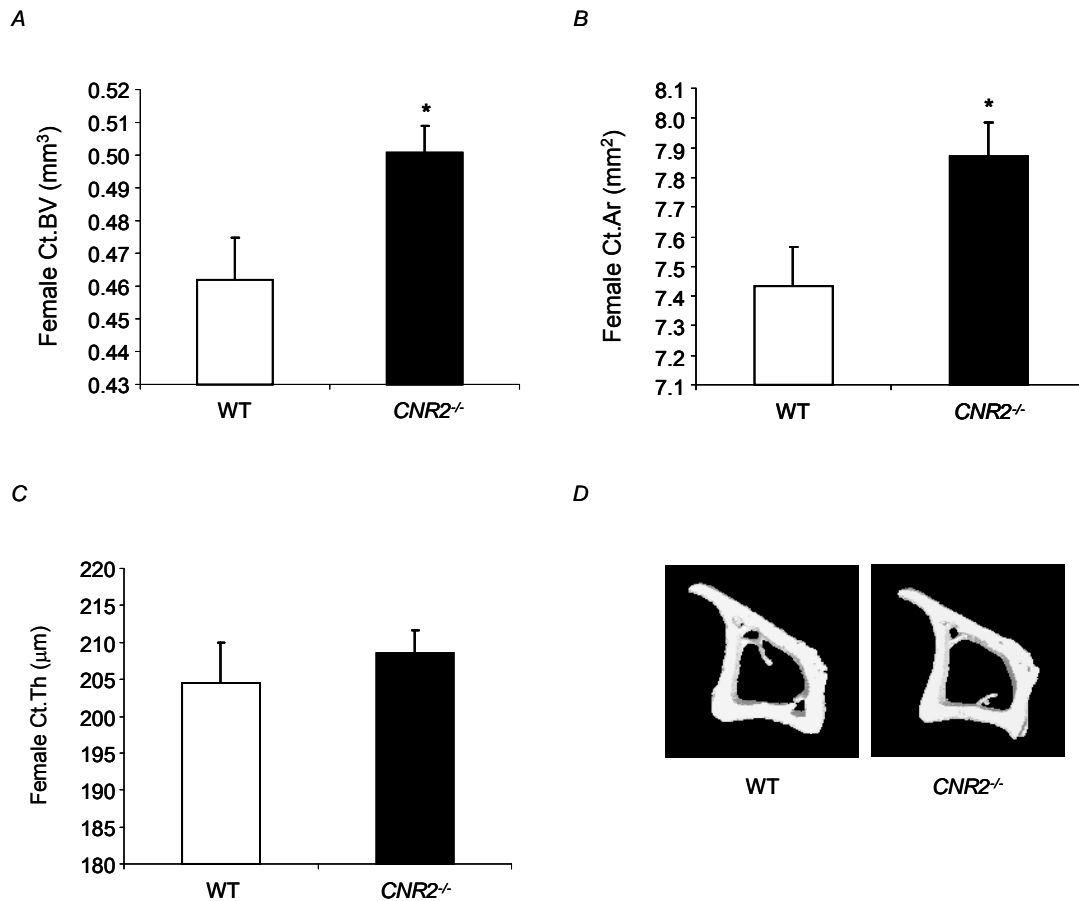
Figure 4.4: Cortical bone in 3-month old wild type and CNR2-deficient female mice. Cortical bone volume (Ct.BV) (*A*), cross-sectional diaphyseal area (Ct.Ar) (*B*) and cortical thickness (Ct.Th) (C) of wild type (WT) and $CNR2^{-/-}$ female mice at age 3 months, assessed by μCT of the tibial proximal diaphysis. *D*. Representative μCT images from the proximal diaphysis of wild type and $CNR2^{-/-}$ female mice at 3 months of age. Values are means ± sem from 7-8 mice per group. *p < 0.05 from wild type controls.

133

4.3.5   CNR2-deficient mice develop a low bone mass phenotype with age

To investigate the role of CNR2 in bone mass of ageing mice, µCT analysis was performed on tibial metaphysis of wild type and *CNR2$^{-/-}$* mice aged 6 and 12 months.

Results showed that increasing age was associated with trabecular bone loss in wild type and *CNR2$^{-/-}$* mice (Figure 4.5). At 6 months of age, *CNR2$^{-/-}$* male mice had significantly higher trabecular bone volume than wild type littermates (Figure 4.5*A*). Trabecular bone volume of *CNR2$^{-/-}$* female mice at 6 months of age was not different from age-matched wild type female mice (Figure 4.5*B*).

However, 12-month old *CNR2$^{-/-}$* female mice had significantly lower trabecular bone volume than wild type controls (Figure 4.5*B,D*). In comparison to peak levels, *CNR2$^{-/-}$* female mice experienced 74% trabecular bone loss, whereas wild type female mice experienced only 57% loss (Figure 4.5*B,D*). The trabecular bone loss with ageing in male mice was not significantly different between genotypes (Figure 4.5*A,C*). Nevertheless, male *CNR2$^{-/-}$* mice showed a trend towards reduced trabecular bone volume compared to wild type controls. In comparison to peak levels, male *CNR2$^{-/-}$* mice experienced 62% trabecular bone loss, while wild type male mice experienced 53% loss (Figure 4.5*A,C*).

Regardless of genotypic differences in bone mass with age, *CNR2$^{-/-}$* mice were healthy and their size and weight were indistinguishable from age-matched wild type littermates throughout their lives (Appendix 6, page 278).
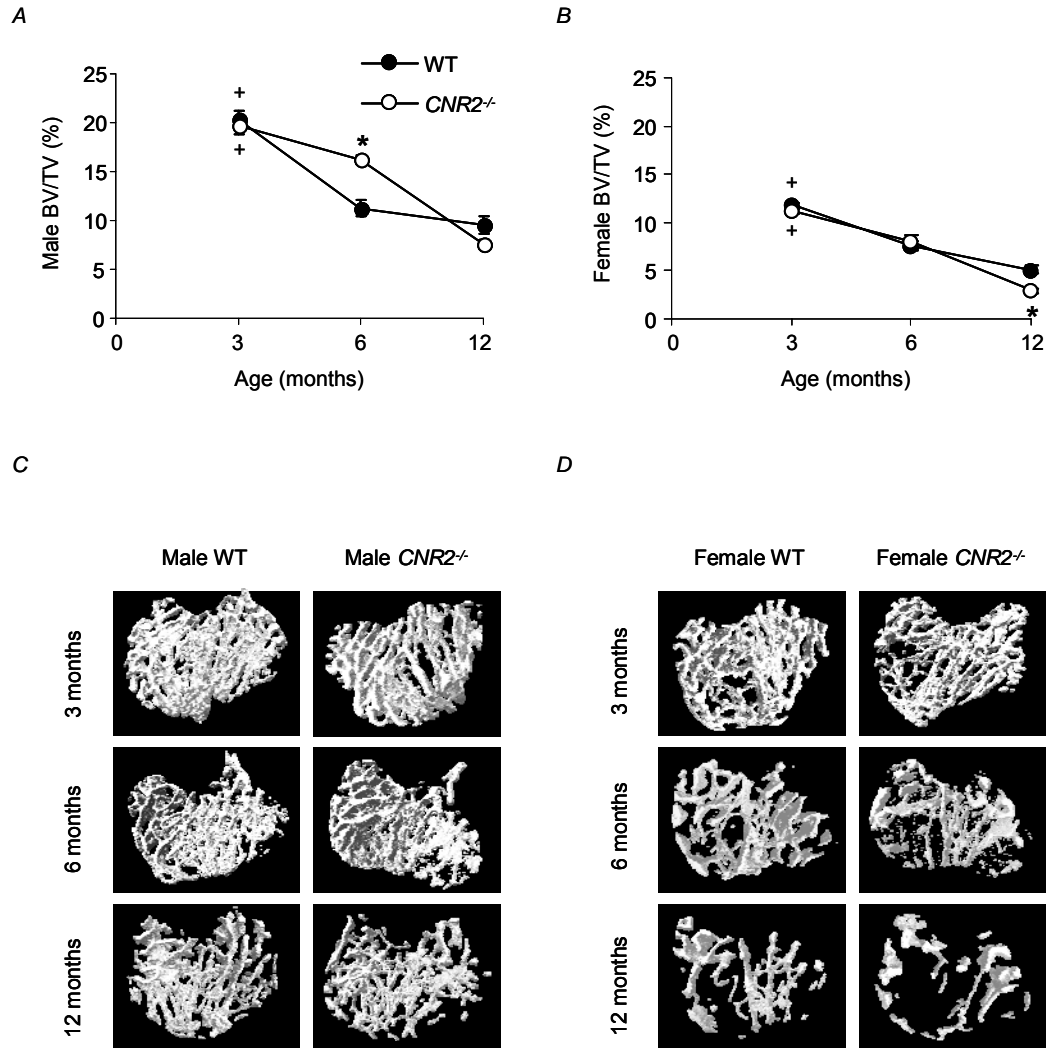
Figure 4.5: CNR2-deficient mice develop age-related osteoporosis. *A,B*. Trabecular bone volume at age 3, 6 and 12 months of wild type and *CNR2-/-* mice of both genders, assessed by μCT of tibial metaphysis. *C,D*. Representative μCT images showing the trabecular bone of wild type and *CNR2-/-* mice at age 3, 6 and 12 months of both genders. Values are means ± sem from 7-8 mice per group. *p < 0.05 from age-matched wild type mice, +p < 0.05 from 6 and 12-month old mice of same genotype.

To examine the role of CNR2 in cortical bone of ageing mice, μCT analysis was performed at the proximal tibial diaphysis of wild type and *CNR2$^{-/-}$* female mice aged 3, 6 and 12 months (c.f. section 2.5.8, page 99).

μCT analysis showed a trend towards decreased cortical bone volume (Ct.BV) with age, whereas cross-sectional diaphyseal area (Ct.Ar) remained unchanged (Figure 4.6*A,B*). Analysis of cortical bone from *CNR2$^{-/-}$* female mice displayed a trend towards increased values for both parameters throughout ageing compared to age-matched controls (Figure 4.6*A,B*). Although *CNR2$^{-/-}$* female mice at 3 months of age had significantly higher cortical volume (Figure 4.6*A*) and higher cross-sectional diaphyseal area compared to wild type controls (Figure 4.6*B*), at 6 and 12 months of age, this difference between wild type and *CNR2$^{-/-}$* female mice was blunted.
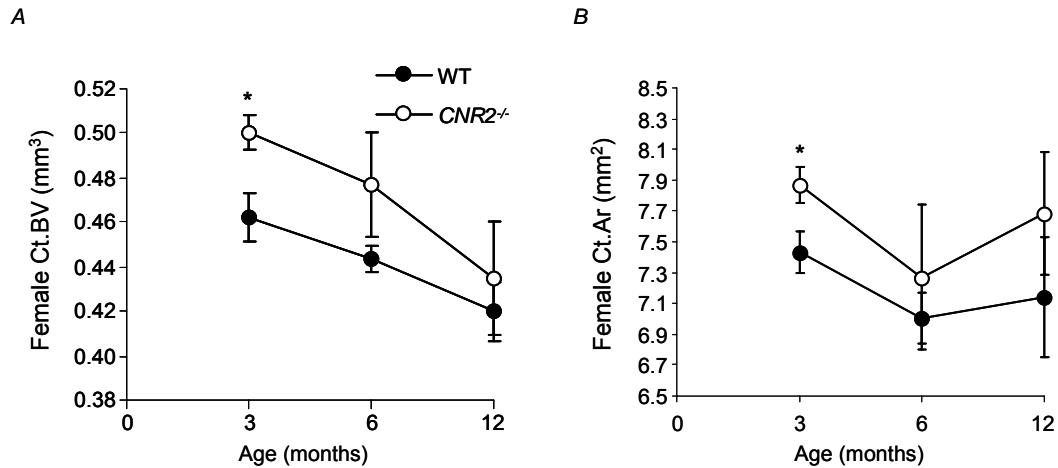
Figure 4.6: Cortical bone of wild type and CNR2-deficient female mice. Cortical bone volume (Ct.BV) (*A*) and cross-sectional diaphyseal area (Ct.Ar) (*B*) of wild type (WT) and *CNR2$^{-/-}$* female mice at age 3, 6 and 12 months, assessed by μCT of tibial proximal diaphysis. Values are means ± sem from 7-8 mice per group. *p < 0.05 from age-matched wild type mice.

With ageing, there was also a trend towards reduced cortical thickness (Ct.Th). Although this was not significant in wild type female mice, it was significant for $CNR2^{-/-}$ female mice between the age of 6 and 12 months (Figure 4.7*A*). In keeping with this, the medullary cavity diameter (Med.Cav.Dm) remained unchanged in ageing wild type mice, whereas in 12-month old $CNR2^{-/-}$ female mice the medullary cavity diameter increased, but due to large error bars this was not statistically significant (Figure 4.7*B*). Although the analyses of cortical thickness and medullary cavity diameter in 12-month old mice suggested that $CNR2^{-/-}$ female mice may experience greater endocortical bone resorption than wild type littermates, this was not accompanied by a significant difference in cortical diameter (Figure 4.7*C*).
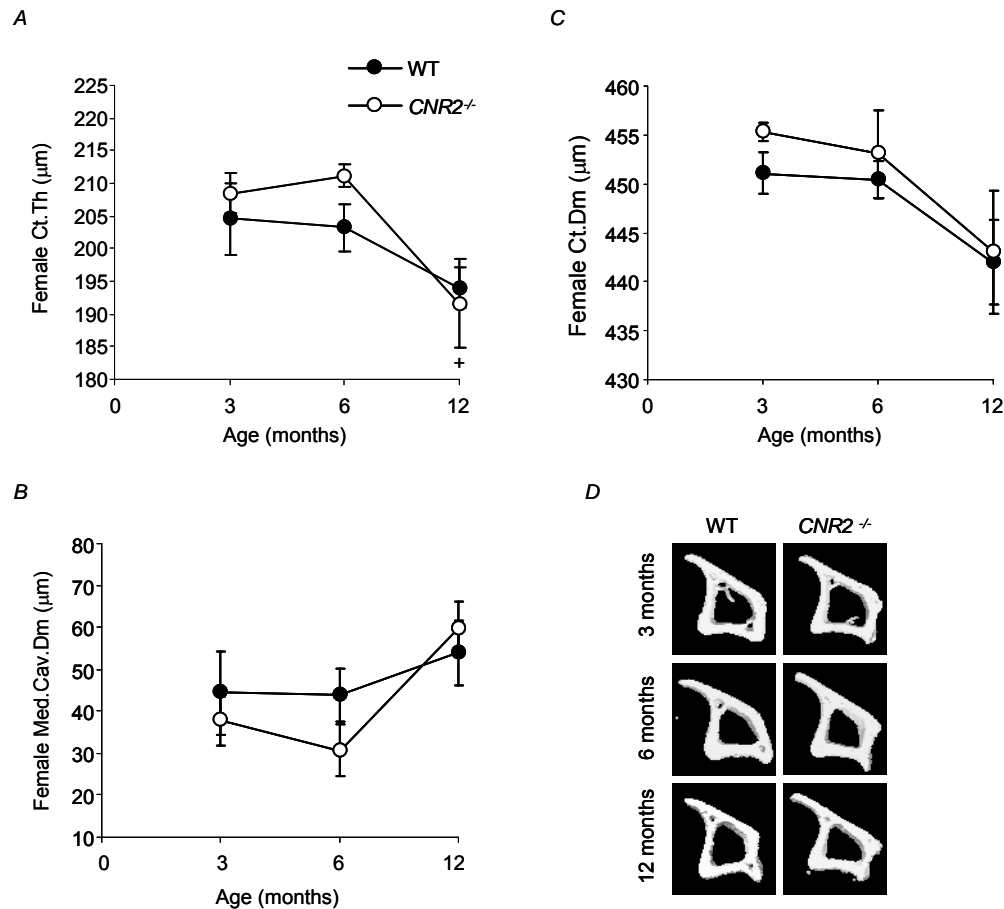
Figure 4.7: Cortical bone of wild type and CNR2-deficient female mice. *A.* Cortical thickness (Ct.Th) of wild type (WT) and $CNR2^{-/-}$ female mice at age 3, 6 and 12 months, assessed by μCT of tibial proximal diaphysis. Medullary cavity diameter (Med.Cav.Dm) (*B*) and cortical diameter (Ct.Dm) (*C*) of the same experiment. *D*. Representative μCT images from the proximal diaphysis of wild type and $CNR2^{-/-}$ female mice at age 3, 6, and 12 months. Values are means ± sem from 7-8 mice per group. $^{+}$p < 0.05 from 6-month old mice of same genotype.

4.3.6 Changes in bone mass at 6 months of age

Male CNR2-deficient mice are protected from age-related osteoporosis at 6 months of age

Detailed μCT analysis of tibial morphometric parameters from 6-month old wild type and *CNR2*^{-/-} mice revealed that *CNR2*^{-/-} male mice had increased trabecular bone volume, trabecular thickness and trabecular number over wild type controls (Figure 4.8*A*,*B*,*C*). In addition, the trabecular connectivity in *CNR2*^{-/-} male mice was better than in wild type mice (Figure 4.8*E*). No significant differences were observed in trabecular bone volume or trabecular number across wild type and *CNR2*^{-/-} female mice (Figure 4.8*A*,*C*). However, the trabeculae of *CNR2*^{-/-} female mice were thicker (Figure 4.8*B*) and more dense (Figure 4.8*D*) but not as well connected as the trabeculae in wild type controls (Figure 4.8*E*).

Comparison across gender showed that female mice at 6 months of age had lower trabecular bone volume and trabecular number than male mice regardless of genotype (Figure 4.8*A*,*C*). The reverse was true for trabecular separation, indicating less dense trabeculae in female cancellous bone (Figure 4.8*D*), whereas the differences in trabecular thickness by gender were less noticeable (Figure 4.8*B*).
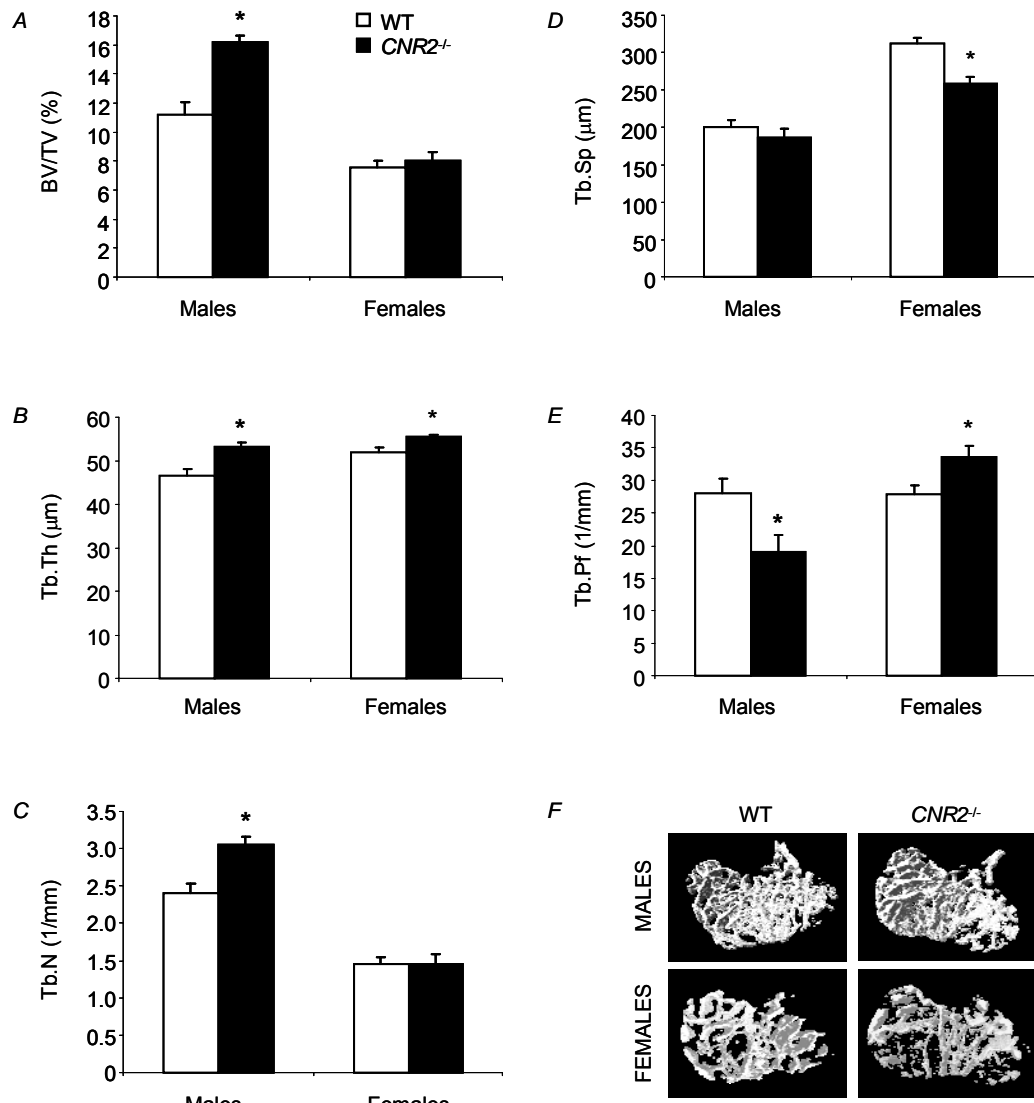
Figure 4.8: Trabecular bone mass in 6-month old wild type and CNR2-deficient mice. *A*. Trabecular bone volume (BV/TV) in wild type and *CNR2*^{-/-} mice, of both genders at 6 months of age assessed by μCT of the tibia. Trabecular thickness (Tb.Th) (*B*), trabecular number (Tb.N) (*C*), trabecular separation (Tb.Sp) (*D*), and trabecular pattern factor (Tb.Pf) (*E*) of the same experiment. *F*. Representative μCT images from the tibial metaphysis of wild type and *CNR2*^{-/-} mice, of both genders. Values are means ± sem from 7-8 mice per group. *$p < 0.05$ from wild type mice of same gender.

Increased osteoblast numbers and decreased active resorption surfaces in 6-month old CNR2-deficient male mice

Bone histomorphometry showed that trabecular bone from $CNR2^{-/-}$ male mice at 6 months of age had significantly higher osteoblast numbers and fewer active resorption surfaces (Figure 4.9*A*). This suggests that the increased trabecular bone volume of $CNR2^{-/-}$ male mice observed from μCT and histomorphometric analysis (Figure 4.8*A* and 4.9*A*) was a result of a combined effect of increased osteoblast function and reduced osteoclast activity.

Bone histomorphometric analysis on tibias from adult female mice at 6 months of age showed that trabecular bone volume was slightly but not significantly decreased in $CNR2^{-/-}$ mice (p > 0.05) (Figure 4.9*C*). No significant differences were observed in osteoblast or active resorption surfaces across wild type and $CNR2^{-/-}$ female mice. However, there was a trend towards reduced osteoclast numbers in $CNR2^{-/-}$ female mice (Figure 4.9*C*).

A

Male	BV/TV (%)	Ob.N/T.Ar (cells/mm²)	Oc.N/T.Ar (cells/mm²)	Oc.S/BS (%)
WT	9.7 ± 1.1	91.6 ± 9.0	3.4 ± 0.5	1.7 ± 0.2
CNR2⁻/⁻	14.5 ± 1.0*	124.5 ± 7.7*	2.4 ± 0.3	1.0 ± 0.1*

Bi ␣␣␣␣␣␣␣␣ *ii*

Male WT ␣␣␣␣␣␣␣␣ Male *CNR2⁻/⁻*

C
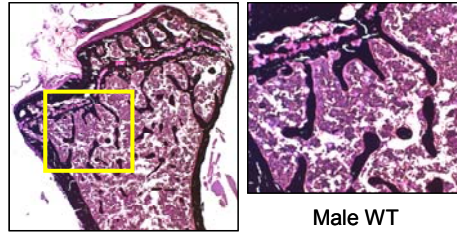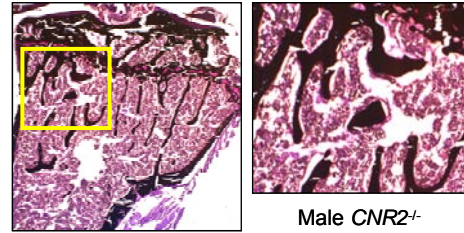
Female	BV/TV (%)	Ob.N/T.Ar (cells/mm²)	Oc.N/T.Ar (cells/mm²)	Oc.S/BS (%)
WT	8.6 ± 1.3	105.0 ± 4.7	3.9 ± 0.7	2.4 ± 0.6
CNR2⁻/⁻	6.8 ± 0.7	98.2 ± 21.0	2.9 ± 0.4	2.3 ± 0.4

Di ␣␣␣␣␣␣␣␣ *ii*
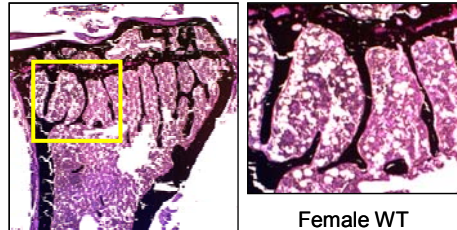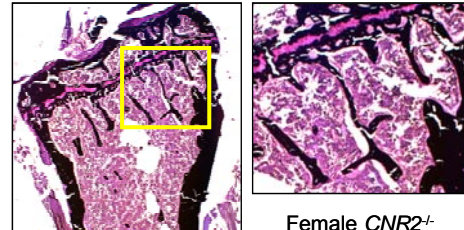
Female WT ␣␣␣␣␣␣␣␣ Female *CNR2⁻/⁻*

Figure 4.9: Bone histomorphometry in 6-month old wild type and CNR2-deficient mice. Summary tables of bone histomorphometry from male and female mice are shown in *A* and *C*, respectively. BV/TV, trabecular bone volume (%); Ob.N/T.Ar, osteoblast number/total area (cells/mm^2); Oc.N/T.Ar, osteoclast number/total area (cells/mm^2); Oc.S/BS, osteoclast surface/bone surface (%). Values are expressed as means ± sem from 4 mice per group. Representative sections of the proximal tibia from wild type and *CNR2⁻/⁻* male (*Bi,ii*) and female (*Di,ii*) mice, stained with von Kossa/Paragon staining. The areas of the photomicrographs in high-power images are indicated by boxes in lower-power images. *p < 0.05 from wild type mice of same gender.

4.3.7   Changes in bone mass at 12 months of age

Female CNR2-deficient mice develop accelerated age-related osteoporosis

μCT analysis of tibiae from 12-month old male and female mice demonstrated that wild type C57BL/6 mice at this age suffer from severe trabecular bone loss, regardless of genotype (Figure 4.10*A*, c.f. Figure 4.5, page 135). However, *CNR2*$^{-/-}$ female mice had a more aggressive osteoporotic phenotype when compared to their wild type littermates, with significantly lower trabecular bone volume and trabecular number (Figure 4.10*A,C*), and significantly higher trabecular thickness and trabecular separation (Figure 4.10*B,D*). Moreover, *CNR2*$^{-/-}$ female mice had poorer trabecular connectivity than wild type controls (Figure 4.10*E*). Although there was a trend towards reduced trabecular bone volume and trabecular number in *CNR2*$^{-/-}$ male mice, it was not significant (Figure 4.10*A,C*). No significant differences were observed in trabecular separation between wild type and *CNR2*$^{-/-}$ male mice (Figure 4.10*D*).

Gender comparison of male and female mice at 12 months of age showed that female mice had lower trabecular bone volume and trabecular number than male mice (Figure 4.10*A,C*). However, the reverse was true for trabecular thickness and trabecular separation, indicating that trabeculae in female mice were thicker and further apart from one another than in male mice (Figure 4.10*B,D*).

Decreased osteoblast numbers in 12-month old CNR2-deficient mice

Bone histomorphometric analysis showed that *CNR2*$^{-/-}$ mice had significantly lower osteoblast numbers than wild type controls, whereas osteoclast numbers were not significantly different (Figure 4.11*A,C*). However, active resorption surfaces in *CNR2*$^{-/-}$ female mice appeared to be significantly higher than in wild type littermates (Figure 4.11*C*). The same pattern was also observed in male *CNR2*$^{-/-}$ mice, but this was not significant (Figure 4.11*A*). A summary table of the histomorphometric data from 3, 6 and 12-month old mice is shown in Figure 4.12.
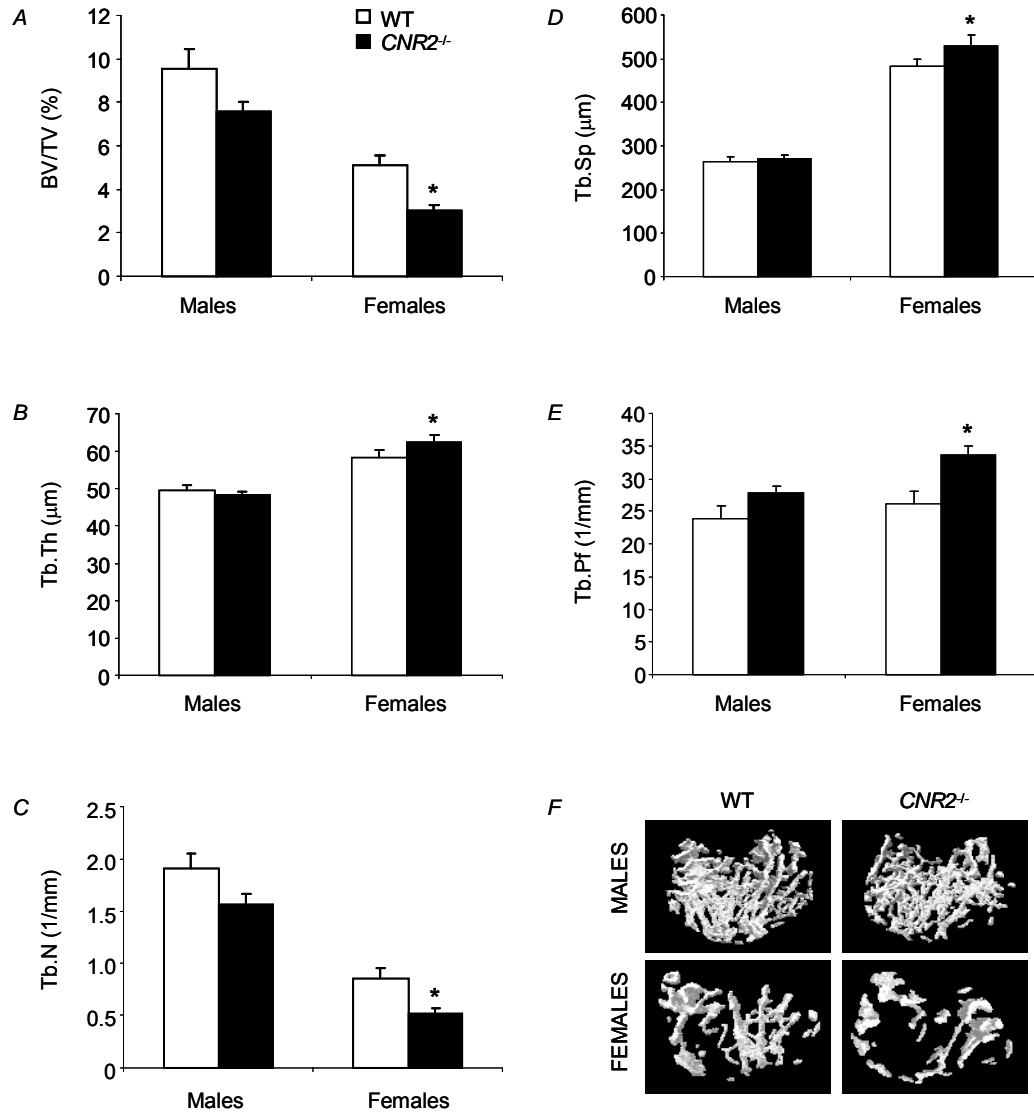
Figure 4.10: Trabecular bone mass in 12-month old wild type and CNR2-deficient mice.
A. Trabecular bone volume (BV/TV) in wild type and *CNR2$^{-/-}$* mice, of both genders at 12 months of age assessed by μCT of the tibia. Trabecular thickness (Tb.Th) (*B*), trabecular number (Tb.N) (*C*), trabecular separation (Tb.Sp) (*D*), and trabecular pattern factor (Tb.Pf) (*E*) of the same experiment. *F*. Representative μCT images from tibial metaphysis of wild type and *CNR2$^{-/-}$* mice, of both genders. Values are means ± sem from 7-8 mice per group. *p < 0.05 from wild type mice of same gender.

A

Male	BV/TV (%)	Ob.N/T.Ar (cells/mm²)	Oc.N/T.Ar (cells/mm²)	Oc.S/BS (%)
WT	9.7 ± 0.9	63.9 ± 3.6	7.8 ± 1.9	4.8 ± 0.9
CNR2⁻/⁻	6.1 ± 1.2*	49.4 ± 3.1*	7.5 ± 0.7	6.6 ± 0.6

Bi *ii*

Male WT

Male *CNR2⁻/⁻*

C
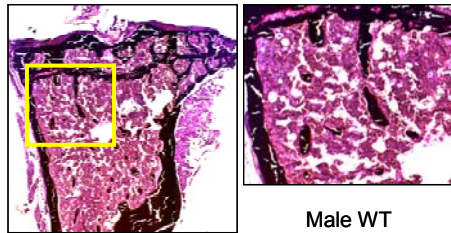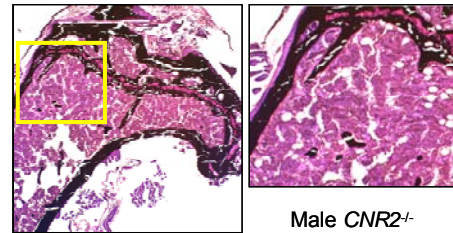
Female	BV/TV (%)	Ob.N/T.Ar (cells/mm²)	Oc.N/T.Ar (cells/mm²)	Oc.S/BS (%)
WT	4.9 ± 0.3	46.5 ± 2.6	5.7 ± 0.4	7.1 ± 0.8
CNR2⁻/⁻	2.4 ± 0.6*	29.2 ± 5.2*	4.6 ± 1.2	10.2 ± 1.0*

Di *ii*
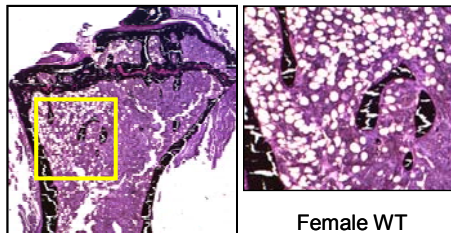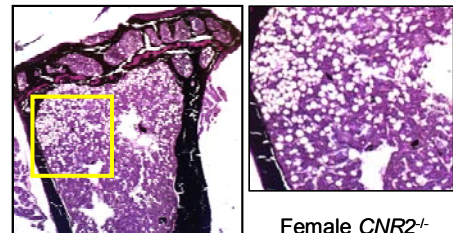
Female WT

Female *CNR2⁻/⁻*

Figure 4.11: Bone histomorphometry in 12-month old wild type and CNR2-deficient mice. Summary tables of bone histomorphometry from male and female mice are shown in *A* and *C*, respectively. BV/TV, trabecular bone volume (%); Ob.N/T.Ar, osteoblast number/total area (cells/mm^2); Oc.N/T.Ar, osteoclast number/total area (cells/mm^2); Oc.S/BS, osteoclast surface/bone surface (%). Values are expressed as means ± sem from 4 mice per group. Representative sections of the proximal tibia from wild type and *CNR2⁻/⁻* male (*Bi,ii*) and female (*Di,ii*) mice, stained with von Kossa/Paragon staining. The areas of the photomicrographs in high-power images are indicated by boxes in lower-power images. *p < 0.05 from wild type mice of same gender.

A

Male		BV/TV (%)	Ob.N/T.Ar (cells/mm²)	Oc.N/T.Ar (cells/mm²)	Oc.S/BS (%)
WT	3M	17.7 ± 1.0	182.6 ± 10.7	3.5 ± 0.3	1.0 ± 0.1
	6M	9.7 ± 1.1+	91.6 ± 9.0+	3.4 ± 0.5	1.7 ± 0.2
	12M	9.7 ± 0.9+	63.9 ± 3.6+	7.8 ± 1.9+	4.8 ± 0.9+
CNR2-/-	3M	18.0 ± 0.7	203.1 ± 12.2	3.1 ± 0.5	1.0 ± 0.2
	6M	14.5 ± 1.0 +,*	124.5 ± 7.7+,*	2.4 ± 0.3	1.0 ± 0.1*
	12M	6.1 ± 1.2+,*	49.4 ± 3.1+,*	7.5 ± 0.7+	6.6 ± 0.6+

B

Female		BV/TV (%)	Ob.N/T.Ar (cells/mm²)	Oc.N/T.Ar (cells/mm²)	Oc.S/BS (%)
WT	3M	9.7 ± 0.8	245.7 ± 16.0	2.2 ± 0.3	0.9 ± 0.1
	6M	8.6 ± 1.3	105.0 ± 4.7+	3.9 ± 0.7	2.4 ± 0.6
	12M	4.9 ± 0.3+	46.5 ± 2.6+	5.7 ± 0.4+	7.1 ± 0.8+
CNR2-/-	3M	12.0 ± 1.5	242.2 ± 21.8	2.6 ± 0.6	1.2 ± 0.1
	6M	6.8 ± 0.7+	98.2 ± 21.0+	2.9 ± 0.4	2.3 ± 0.4+
	12M	2.4 ± 0.6+,*	29.2 ± 5.2+,*	4.6 ± 1.2	10.2 ± 1.0+,*

Figure 4.12: Summary tables for bone histomorphometry in 3, 6 and 12-month old wild type and CNR2-deficient male (*A*) and female (*B*) mice. BV/TV, trabecular bone volume (%); Ob.N/T.Ar, osteoblast number/total area (cells/mm^2); Oc.N/T.Ar, osteoclast number/total area (cells/mm^2); Oc.S/BS, osteoclast surface/bone surface (%). Values are expressed as means ± sem from 4 mice per group. *p < 0.05 from wild type mice of same age, +p < 0.05 from 3-month old mice of same genotype.

4.3.8 Low serum levels of bone formation marker in CNR2-deficient male mice

To establish whether *CNR2* deletion also affects biochemical markers of bone turnover, serum levels of amino (N)-terminal propeptides of type I procollagen (PINP) (a marker of bone formation) and cross-linked carboxy (C)-telopeptides of type I collagen (CTX) (a marker of bone resorption) were measured using commercially available kits (c.f. section 2.5.7, page 98).

Serum levels of PINP in *CNR2*$^{-/-}$ male mice were significantly lower than in wild type age-matched controls, but this was not observed between wild type and *CNR2*$^{-/-}$ female mice (Figure 4.13*A*). Further analysis showed a trend towards reduced CTX serum levels in *CNR2*$^{-/-}$ male and female mice but this was not significant (Figure 4.13*B*).
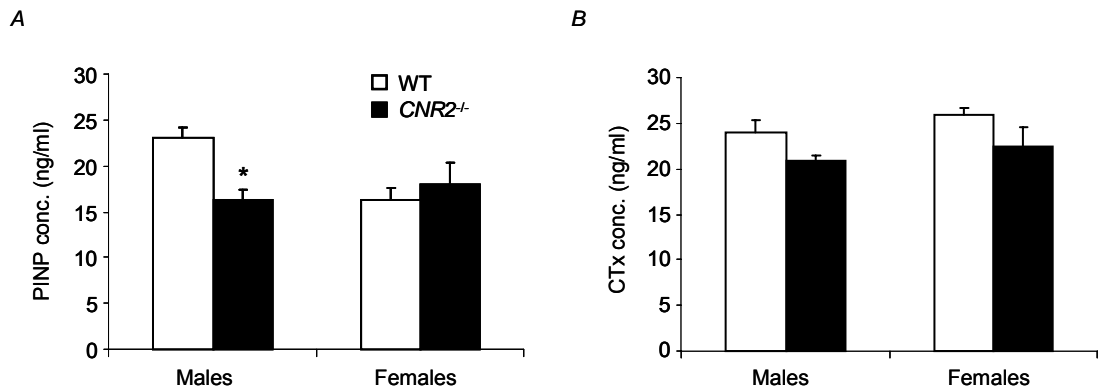
Figure 4.13: Biochemical markers of bone turnover in 12-month old wild type and CNR2-deficient mice. Amino (N)-terminal propeptides of type I procollagen (PINP) serum concentration (*A*) and cross-linked carboxy (C)-telopeptides of type I collagen (CTX) serum concentration (*B*) in wild type and *CNR2*$^{-/-}$ mice of both genders. Values are means ± sem from 5-6 mice per group. *p < 0.05 from wild type mice of same gender.

4.4   DISCUSSION

Recent studies have shown that the endocannabinoid system plays a vital role in bone remodelling and that mice with deficiency in type 2 cannabinoid receptor ($CNR2^{-/-}$ mice) have low bone mass phenotype and accelerated age-related bone loss (Ofek et al., 2006). In view of this, the aim of this chapter was to further characterise the effects of $CNR2$ deletion in ageing mice.

This chapter demonstrates that $CNR2^{-/-}$ mouse neonates have normal bone volume and that $CNR2^{-/-}$ mice had normal peak trabecular bone mass. Further bone morphometric analysis showed that 3-month old $CNR2^{-/-}$ female mice had significantly lower trabecular number in agreement with Ofek and colleagues (Ofek et al., 2006). Although young $CNR2^{-/-}$ female mice in the Ofek et al. study were also reported to have a low bone mass phenotype with greater total diaphyseal and medullary cavity diameters (Ofek et al., 2006), such differences were not observed between young wild type and $CNR2^{-/-}$ female mice in the study described here. Instead, young $CNR2^{-/-}$ female mice in the present study had indistinguishable trabecular bone volume to that of wild type mice, a significantly higher cortical bone volume and a greater cross-sectional diaphyseal area, compared to wild type controls. The fact that Ofek and colleagues performed trabecular and cortical analysis on different skeletal sites than us [femurs (Ofek) *vs.* tibiae (current study)] may have contributed to the differences observed. Regarding the trabecular structure in young male $CNR2^{-/-}$ mice, there was significantly higher trabecular separation than wild type littermates and a trend towards reduce trabecular number, in accordance with what was previously published by Ofek et al. (Ofek et al., 2006).

At 6 months of age variable effects were found depending on gender. Although trabecular bone volume appeared to be normal in female $CNR2^{-/-}$ mice, males showed a high bone mass phenotype resulting from increased trabecular thickness and increased trabecular number. Histomorphometric analysis revealed that $CNR2^{-/-}$ male mice at 6

months of age had significantly higher osteoblast numbers than wild type littermates. Although no difference was observed in osteoclast numbers between wild type and $CNR2^{-/-}$ male mice, active resorption surfaces were shown to be significantly lower in $CNR2^{-/-}$ mice. Considering that bone surface was significantly increased in $CNR2^{-/-}$ male mice due to increased trabecular number, the ratio of active resorption surface resulting from osteoclast numbers over bone surface, is expected to be greater in $CNR2^{-/-}$ male mice than in wild type littermates. A gender bias was also observed in the skeletal phenotype of $CNR1^{-/-}$ mice on a CD1 genetic background (CD1$^{CNR1-/-}$) (Tam et al., 2006). Young male CD1$^{CNR1-/-}$ mice (~3 months old) had increased bone mass compared to wild type controls, whereas no differences were observed between female CD1$^{CNR1-/-}$ and wild type littermates (Tam et al., 2006). Yet this model targets a different receptor, CNR1 rather than CNR2, and it is on a different genetic background than $CNR2^{-/-}$ mice, CD1 rather than C57BL/6, therefore no clear conclusions can be drawn about the relevance of these comparisons.

Twelve-month old $CNR2^{-/-}$ female mice developed accelerated osteoporosis, characterised by decreased trabecular bone volume and trabecular number and increased trabecular thickness and trabecular separation when compared to wild type littermates. Overall, there was poorer trabecular connectivity in $CNR2^{-/-}$ female mice indicated by the increased trabecular pattern factor compared to wild type littermates. Although $CNR2^{-/-}$ male mice also showed a trend towards reduced trabecular bone volume and trabecular number compared to wild type littermates, differences were less significant. Bone histomorphometric analysis at 12 months of age showed that $CNR2^{-/-}$ mice had a low bone mass phenotype as a result of decreased osteoblast numbers, even though active resorption surfaces appeared to be significantly higher in female $CNR2^{-/-}$ mice than in wild type controls at this age. Such outcome was expected, since osteoclast numbers were indistinguishable between wild type and $CNR2^{-/-}$ female mice, but there was a marked drop in trabecular bone volume, and hence in bone surface, of $CNR2^{-/-}$ female mice compared to wild type controls. Therefore, the ratio expressing active

resorption surfaces in *CNR2*$^{-/-}$ female mice, i.e. osteoclast number over bone surface, appeared to be significantly higher than in wild type controls. Male *CNR2*$^{-/-}$ mice also showed a trend towards increased active resorption surfaces compared to wild type littermates at 12 months of age, but this was not significant.

Serum analysis using biochemical markers of bone turnover, was in agreement with the histomorphometric analysis. CNR2-deficient male mice at 12 months of age had significantly lower serum levels of PINP (a marker of bone formation) than wild type littermates, whereas serum levels of CTX (a marker of bone resorption) were not significantly different between wild type and *CNR2*$^{-/-}$ controls. These results together support the idea that CNR2 protects from age-related bone loss mainly by regulating osteoblastic bone formation. Unexpectedly, serum levels of biochemical markers of bone turnover in female mice did not display the same pattern, since neither PINP or CTX levels were significantly different between wild type and *CNR2*$^{-/-}$ female mice. This could be attributed to the fact that serum samples were taken from non-fasting female mice, which most likely were at different phases of the oestrous cycle. These are two well-documented factors that strongly influence serum levels of bone turnover markers (Calvo et al., 1996).

Collectively, histomorphometry and biochemical markers of bone turnover showed that low bone mass phenotype in 12-month old *CNR2*$^{-/-}$ mice was the result of decreased osteoblast numbers and decreased bone formation. These results were in agreement with previous findings from our group showing that *CNR1*$^{-/-}$ mice on a CD1 background suffered from severe osteoporosis at 12 months of age due to reduced osteoblast numbers and increased marrow fat accumulation compared to wild type littermates (Idris et al., 2008b). While Ofek and colleagues also reported that *CNR2*$^{-/-}$ mice at 12 months of age suffered from accelerated osteoporosis compared to wild type littermates, such phenotypic changes were attributed to high bone turnover (Ofek et al., 2006). Nevertheless, this assumption was based on histomorphometric measurements carried

out on young, 8-week old mice and not on 12-month old mice, perhaps explaining the discrepancy of the histomorphometric data between the two studies.

Regardless of the mechanism through which CNR2 regulates bone mass and bone turnover in mice, the concept that CNR2 protects from age-related bone loss is well-established by us and others. Given that the C57BL/6 background strain of the *CNR2*^{-/-} mice used in this study is associated with age-related osteopenia, regardless of gender (Ferguson et al., 2003), *CNR2*^{-/-} mice have been backcrossed to the CD1 strain which does not experience substantial bone loss with age (Beamer et al., 1996). With these mice in hand, additional experiments will be conducted in the near future to gain further insight into the mechanism by which CNR2 deficiency affects bone mass.

In conclusion, this chapter demonstrates that *CNR2*^{-/-} mice have normal peak bone mass but suffer from age-related osteoporosis due to decreased osteoblast numbers and defective bone formation. Therefore, type 2 cannabinoid receptor protects from bone loss with ageing by regulating osteoblast numbers and bone formation.

CHAPTER FIVE
ROLE OF CNR2 IN OSTEOCLAST DIFFERENTIATION AND FUNCTION

5 ROLE OF CNR2 IN OSTEOCLAST DIFFERENTIATION AND FUNCTION

5.1 SUMMARY

Conflicting results have been reported with regard to the role of cannabinoid receptors in bone resorption and osteoclast function. Our group has previously shown that the endocannabinoid AEA stimulates osteoclast formation, whereas the CNR1-selective antagonist/inverse agonist AM251 is a potent inhibitor of osteoclast formation and bone resorption *in vitro* and *in vivo*. However, others reported that the CNR2-selective agonist HU308 inhibits osteoclast formation *in vitro* and *in vivo*. In view of this, the aim of this chapter is to investigate the role of CNR2 in regulating bone mass and osteoclast function, using a combination of pharmacological and genetic approaches.

The CNR2-selective agonists HU308 and JWH133 stimulated osteoclast formation and nuclearity *in vitro*, whereas the CNR2-selective antagonist/inverse agonist AM630 inhibited osteoclast formation in a concentration-dependent manner. Osteoclasts generated from *CNR2^{-/-}* mice were resistant to the stimulatory effects of HU308 and JWH133 and to the inhibitory effects of AM630, consistent with a CNR2-mediated mechanism. Furthermore, AM630 rescued ovariectomy-induced bone loss in wild type mice, by preventing the increase in osteoclast numbers and active resorption surfaces and without affecting osteoblast numbers. *CNR2^{-/-}* mice were partly protected from ovariectomy-induced bone loss as a result of reduced osteoclast number compared to wild type littermates. Moreover, *CNR2^{-/-}* ovariectomised mice were not responsive to the protective effects of AM630 at a low dose (0.1 mg/kg/day), suggesting a CNR2-mediated effect. However, at a higher dose (1.0 mg/kg/day), AM630 was equally effective in preventing ovariectomy-induced bone loss in *CNR2^{-/-}* mice and wild type littermates, indicating a non-CNR2 mediated mechanism.

These observations indicate that CNR2 regulates osteoclast formation *in vitro* and contributes to ovariectomy-induced bone loss *in vivo*, and demonstrate that cannabinoid receptor antagonists/inverse agonists have anti-osteoclast activities.

5.2   INTRODUCTION

Cannabinoid receptor ligands have been shown to be important for the regulation of bone resorption/formation balance *in vivo* and *in vitro* (Idris et al., 2005; Ofek et al., 2006; Ridge et al., 2007; Rossi et al., 2009). However, conflicting results have been reported regarding their effects on osteoclast formation and function (Idris et al., 2005; Ofek et al., 2006). This chapter investigates the *in vitro* and *in vivo* effects of pharmacological activation and blockade of CNR2 on osteoclast differentiation and function.

Cannabinoid receptor agonists such as AEA, 2-AG and Δ^9-tetrahydrocannabinol bind to the cannabinoid receptors causing inhibition of adenylate cyclase, activation of ERK kinases and initiation of other intracellular responses (Demuth and Molleman, 2006) (cf. Figure 1.10, page 58). Cannabinoid receptor antagonists/inverse agonists such as AM251 and AM630, block the effects of cannabinoid receptor agonists and exert opposite pharmacological effects (Pertwee, 1999). AM251 shows selectivity for CNR1, whereas AM630 shows selectivity for CNR2 (Pertwee and Ross, 2002).

A recent study from our group, has shown that the endocannabinoid AEA increased osteoclast formation, whereas blockade of cannabinoid receptors with AM251 and AM630 inhibited RANKL-induced osteoclast formation in a concentration dependent manner (Idris et al., 2005). Cultures prepared from *CNR1*$^{-/-}$ mice were resistant to the inhibitory effects of AM251 on osteoclast formation, when compared with wild type cultures, whereas AM630 was equally potent in wild type and *CNR1*$^{-/-}$ cultures (Idris et al., 2005). These results indicate that CNR1 mediates the effects of AM251, the CNR1-selective antagonist/inverse agonist. Furthermore, *in vivo* experiments showed that AM251 rescued ovariectomy-induced bone loss in a dose-dependent manner, by inhibiting bone resorption (Idris et al., 2005). Together these results demonstrate that cannabinoid receptor antagonists/inverse agonists inhibit osteoclast formation and bone

resorption *in vitro* and *in vivo*. Conversely, the CNR2-selective agonist HU308, was reported to have anti-osteoclastic effects *in vitro*, and anti-resorptive properties in ovariectomised mice (Ofek et al., 2006). Likewise, the CNR1-selective agonist ajulemic acid has been shown to suppress osteoclastogenesis *in vitro*, at concentrations in the micromolar range (George et al., 2008). In contrast to the earlier study by Idris and colleagues, the latter two studies suggest that cannabinoid receptors agonists, and not antagonists/inverse agonists, have an inhibitory effect on osteoclast formation.

Although all studies suggest that pharmacological modulation of the endocannabinoid system has a role in regulating bone mass and bone turnover, the CNR2 signalling mechanism and its role in bone resorption are poorly-understood. The aims of the work reported in this chapter were to investigate further the role of CNR2 in osteoclast formation *in vitro* by means of pharmacological activation/inactivation of the receptors, to analyse the effect of a CNR2-selective antagonist/inverse agonist on ovariectomy-induced bone loss *in vivo* and to examine the potential use of this ligand as an anti-resorptive agent in conditions of increased bone turnover.

5.3   RESULTS

5.3.1   *Bone marrow cultures from CNR2-deficient mice have less osteoclasts*

To investigate whether defective CNR2 in bone cells affects osteoclast formation *in vitro*, wild type and *CNR2$^{-/-}$* monocyte cultures were stimulated with 25ng/ml M-CSF and 0-200ng/ml RANKL for 4 days (c.f. section 2.2.3, page 77). Osteoclast numbers were assessed by counting multinucleated TRAcP-positive cells with three or more nuclei (c.f. section 2.2.4, page 77). *CNR2$^{-/-}$* cultures stimulated with 100 and 200ng/ml of RANKL had 15-20% fewer TRAcP-positive osteoclasts than wild type cultures. With RANKL concentrations lower than 100ng/ml there was also a trend towards fewer osteoclasts in *CNR2$^{-/-}$* cultures, but this was not statistically significant (Figure 5.1).
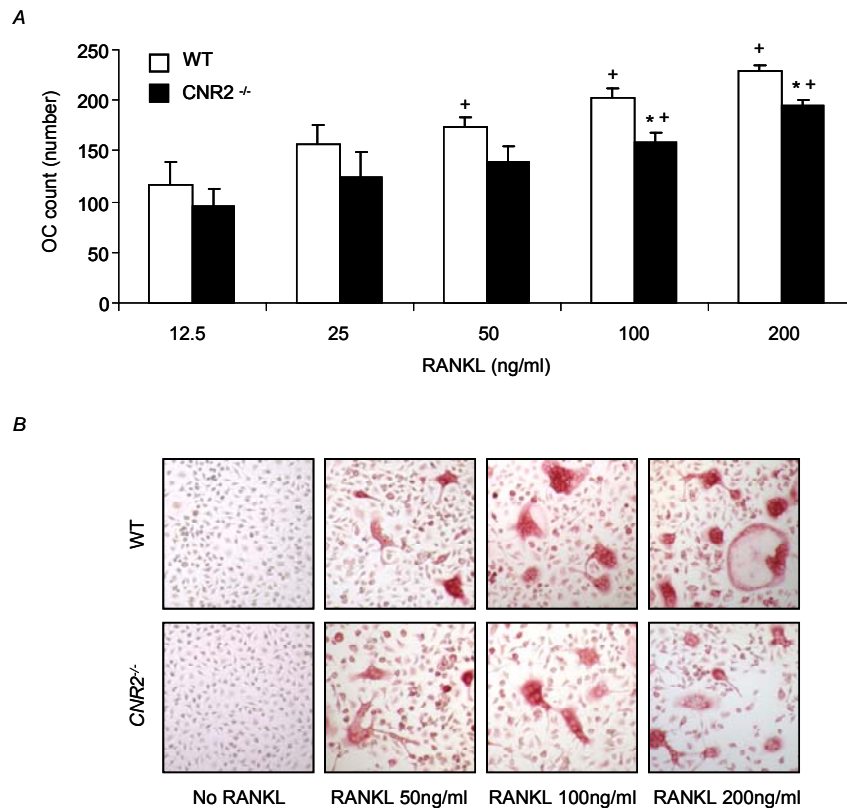
Figure 5.1: M-CSF- and RANKL-stimulated bone marrow cultures from wild type and CNR2-deficient mice. *A*. Number of multinucleated TRAcP-positive osteoclasts (OC) in wild type and *CNR2$^{-/-}$* bone marrow cultures stimulated with M-CSF (25ng/ml) and RANKL at the indicated concentrations, for 4 days. *B*. Representative photomicrographs of wild type and *CNR2$^{-/-}$* bone marrow cultures stimulated with M-CSF (25ng/ml) and RANKL (0-200ng/ml) stained for TRAcP. Values are means ± sem and were obtained from 3 independent experiments. *p < 0.05 from wild type cultures of same RANKL-treatment, $^{+}$p < 0.05 from same genotype cultures treated with 12.5ng/ml of RANKL.

5.3.2 Bone marrow cultures from CNR2-deficient mice have normal macrophage viability

To examine whether the defective osteoclast formation in *CNR2*$^{-/-}$ bone marrow cultures was the result of defective osteoclastogenesis or the consequence of limited availability of osteoclast precursors/macrophages, wild type and *CNR2*$^{-/-}$ monocyte cultures were stimulated with 5-100ng/ml M-CSF for 4 days (c.f. section 2.2.2, page 76). Macrophage number was determined by the Alamar Blue assay as previously described in section 2.2.8, page 80. Throughout the concentration range of M-CSF (5-100ng/ml), the viability of wild type and *CNR2*$^{-/-}$ bone marrow-derived macrophages was indistinguishable (Figure 5.2). Together with section 5.3.1, these data suggest that *CNR2*$^{-/-}$ bone marrow cultures experience defective osteoclastogenesis, in the presence of normal macrophages.
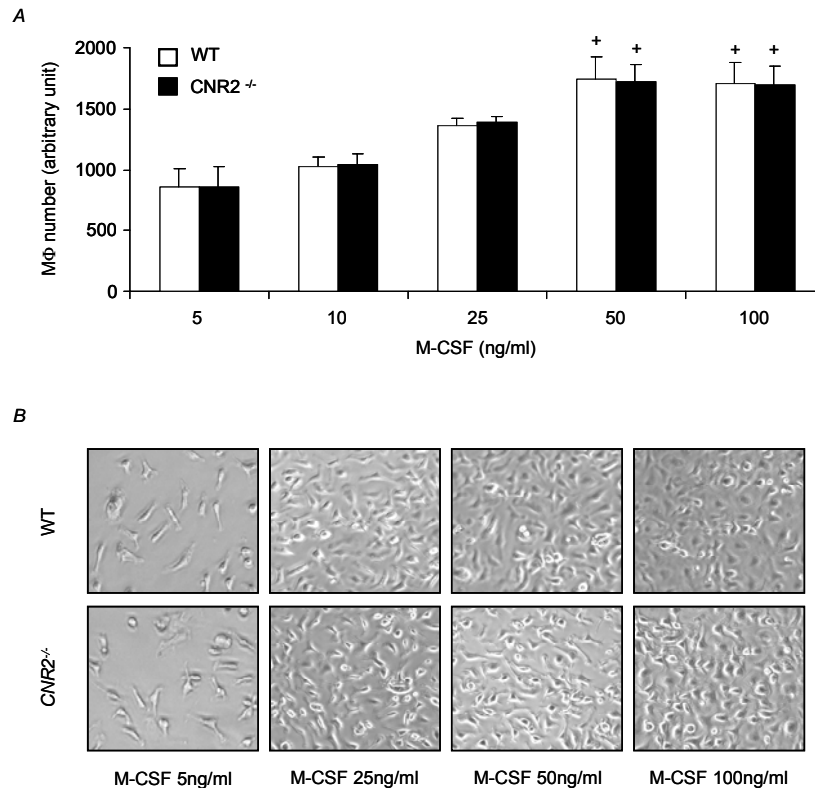
Figure 5.2: M-CSF-stimulated bone marrow cultures from wild type and CNR2-deficient mice. *A*. Number of macrophages (MΦ) in wild type and *CNR2*$^{-/-}$ bone marrow cultures stimulated with M-CSF at the indicated concentrations for 4 days, as assessed by Alamar Blue assay. *B*. Representative photomicrographs of wild type and *CNR2*$^{-/-}$ macrophage cultures from *A*. Values are means ± sem and were obtained from 3 independent experiments. $^{+}$p < 0.05 from same genotype cultures treated with 5ng/ml of M-CSF.

5.3.3 Cannabinoid receptor ligands regulate osteoclast formation in vitro

To examine the effect of cannabinoid receptor ligands on osteoclast formation, bone marrow cultures treated with 25ng/ml M-CSF and 100ng/ml RANKL for 72 hours were exposed to the CNR2-selective agonists, HU308 and JWH133, the endocannabinoids, AEA and 2-AG, and the cannabinoid receptor antagonists/inverse agonists, AM251 and AM630, at concentrations varying from 0.1nM to 10μM, for 24-48 hours (c.f. section 2.2.3, page 77). Osteoclasts were identified by TRAcP staining (section 2.2.4, page 77).

The CNR2-selective agonists HU308 and JWH133, significantly enhanced osteoclast formation at concentrations as low as 0.25nM for JWH133 and 1nM for HU308 (Figure 5.3*A*). JWH133 increased osteoclast numbers by about 100% over the concentration range 0.5nM-10μM. HU308 reached maximal stimulation at 30nM, and increased osteoclast numbers by about 70%. No significant stimulatory effects were observed at concentrations of HU308 higher than 300nM. Surprisingly, HU308 at 10μM significantly inhibited osteoclast formation (Figure 5.3*A*). The mean ± SEM concentration of HU308 and JWH133 that half-maximally increased osteoclast formation (**EC$_{50}$**) was 0.23±0.11nM and 0.19±0.09nM, respectively. The mean ± SEM concentration of HU308 that half-maximally inhibited osteoclast formation (**IC$_{50}$**) was 4.2±2.4μM. The endogenous cannabinoid receptor agonists, AEA and 2-AG, also stimulated osteoclast formation at concentrations as low as 0.25nM (Figure 5.3*B*). Their stimulatory effect on osteoclast formation remained constant up to 10μM. The mean ± SEM **EC$_{50}$** values of AEA and 2-AG were 0.16±0.06nM and 0.12±0.06nM, respectively.

Exposure of M-CSF- and RANKL-stimulated bone marrow cultures to the cannabinoid receptor antagonists/inverse agonists AM251 (CNR1-selective) and AM630 (CNR2-selective) inhibited osteoclast formation in a concentration-dependent manner (Figure 5.3*C*). The mean ± SEM **IC$_{50}$** values of AM251 and AM630 were 819±317nM and 175±67nM, respectively.
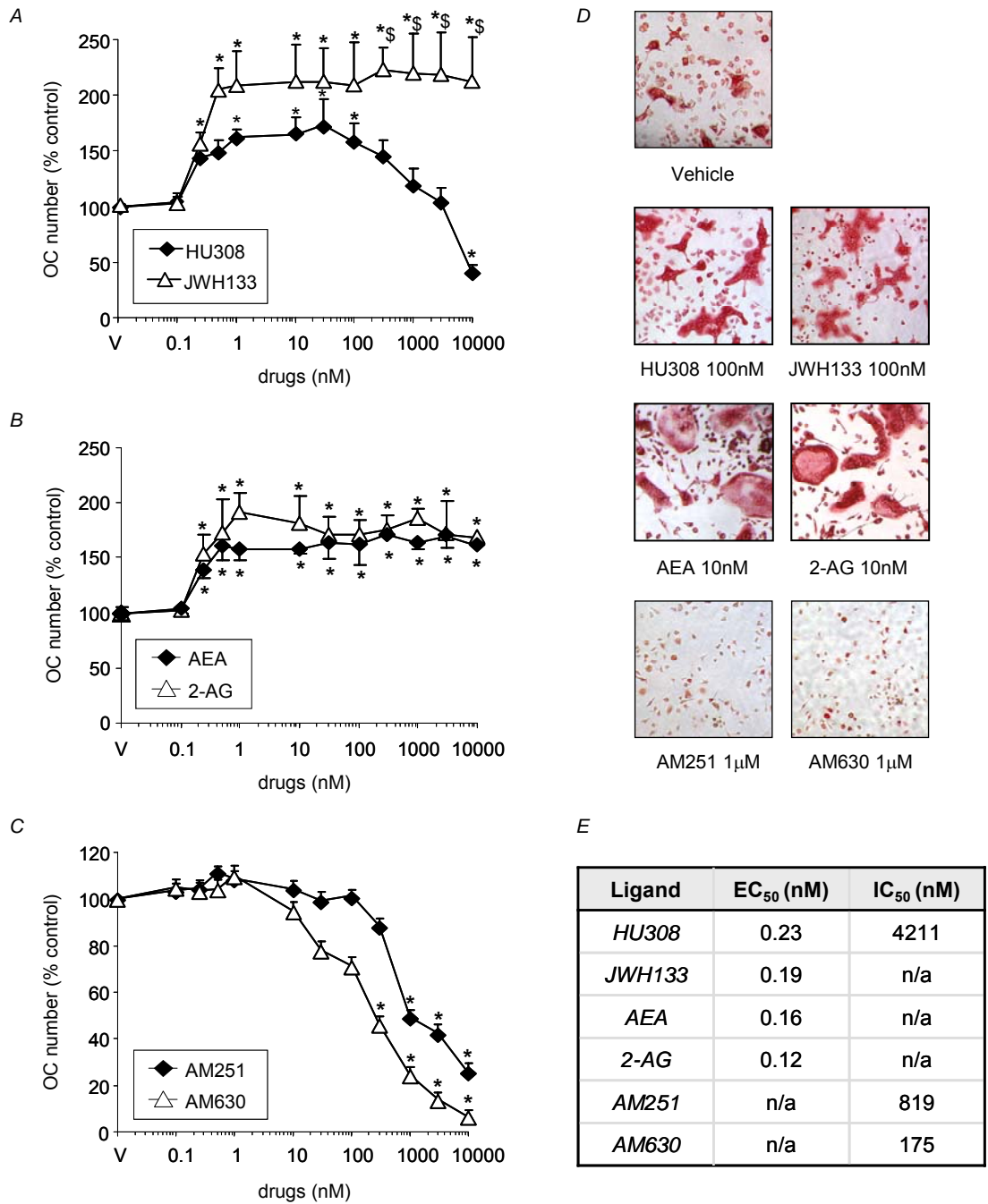
Figure 5.3: Effect of cannabinoid receptor ligands on osteoclast formation *in vitro*.
A. Number of multinucleated TRAcP-positive osteoclasts (OC) in bone marrow cultures stimulated with M-CSF (25ng/ml) and RANKL (100ng/ml) for 72 hours and then exposed to vehicle (V), HU308 or JWH133, at the indicated concentrations for 24 hours. Changes in osteoclast number were expressed as a percent of values in vehicle-treated cultures. Osteoclast number in cultures exposed to vehicle, AEA or 2-AG (*B*) for 24 hours, or to vehicle, AM251 or AM630 (*C*) for 48 hours, from similar experiments, expressed in the same way. *D*. Representative photomicrographs of osteoclasts stained for TRAcP from cultures in *A*, *B* and *C*. *E*. Summary table of EC_{50} or IC_{50} values of the cannabinoid receptor ligands tested for osteoclast formation *in vitro*. Values in *A*, *B* and *C* are means ± sem and were obtained from 3 independent experiments. *p < 0.05 from vehicle-treated cultures, $^\$$p < 0.05 from HU308-treated cultures. *Abbreviations*: n/a, not applicable.

158

5.3.4 Cannabinoid receptor ligands influence osteoclast fusion

To establish whether cannabinoid receptor ligands have an effect on osteoclast fusion, osteoclasts with more than 20 nuclei from cultures in section 5.3.3, were counted. Both CNR2-selective agonists, HU308 and JWH133 (30nM), significantly increased osteoclast size and nuclearity such that the proportion of cells with more than 20 nuclei rose from about 7% in vehicle-treated cells to 14% in HU308-treated cells and from 14% to 27% in JWH133-treated cells (Figure 5.4*A,B*). The endocannabinoids, AEA and 2-AG (30nM) also increased osteoclast nuclearity and raised the proportion of cells with more than 20 nuclei from 13% in vehicle-treated cells to 17% in AEA-treated cells, and from 14% to 26% in 2-AG-treated cells (Figure 5.4*C,D*).
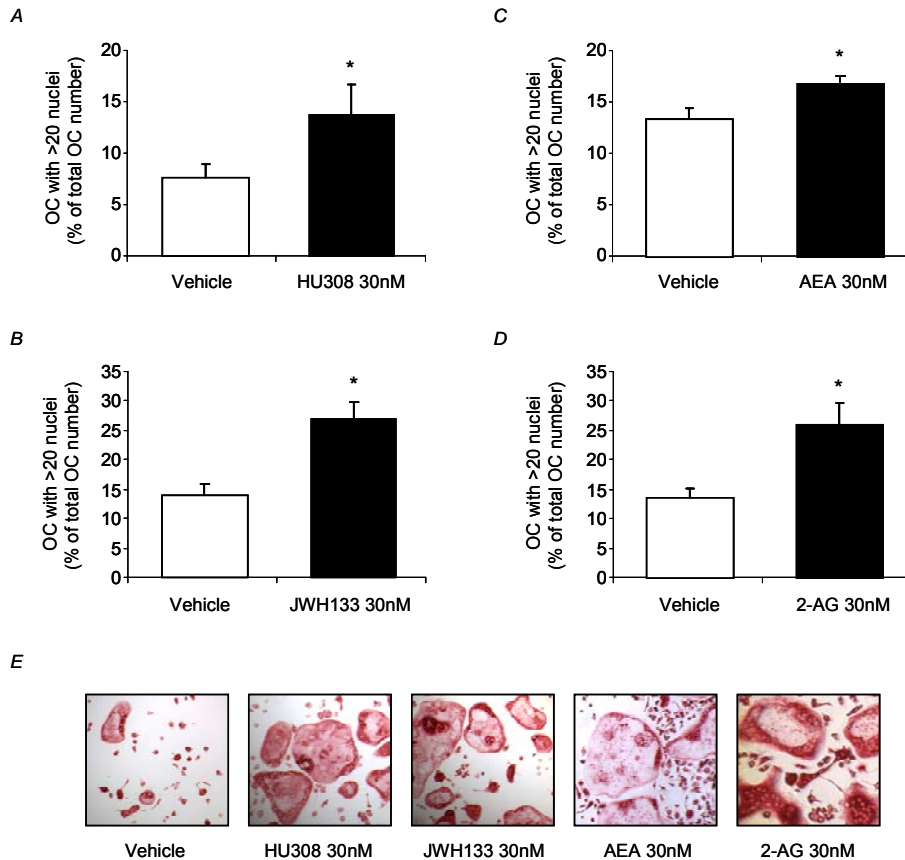
Figure 5.4: Effect of cannabinoid receptor agonists on osteoclast nuclearity. *A*. Number of multinucleated TRAcP-positive osteoclasts (OC) per well with 20 or more nuclei in bone marrow cultures stimulated with M-CSF (25ng/ml) and RANKL (100ng/ml) for 72 hours and then exposed to vehicle (V) or HU308 (30nM) for 24 hours. Changes in OC number were expressed as a percent of total OC number. Number of OC with more than 20 nuclei in cultures exposed to vehicle, JWH133 (*B*), AEA (*C*) or 2-AG (*D*) at the indicated concentrations, from similar experiments, expressed in the same way. Representative photomicrographs of large OC stained for TRAcP from the cultures in *A*, *B*, *C* and *D*. Values are means ± sem and were obtained from 3 independent experiments. *p < 0.05 from vehicle-treated cultures.

159

Conversely, AM251 and AM630 (300nM and 1000nM) significantly reduced osteoclast size and nuclearity in a concentration-dependent manner following a 48 hour-treatment. As shown in Figure 5.5*A* and *B*, the proportion of cells with more than 20 nuclei decreased from 20% in vehicle-treated cells to 12% and 8% in cells treated with AM630 at 300nM and 1000nM, respectively; and from 16% in vehicle-treated cells to 9% and 7% in cells treated with AM251 at 300nM and 1000nM, respectively.
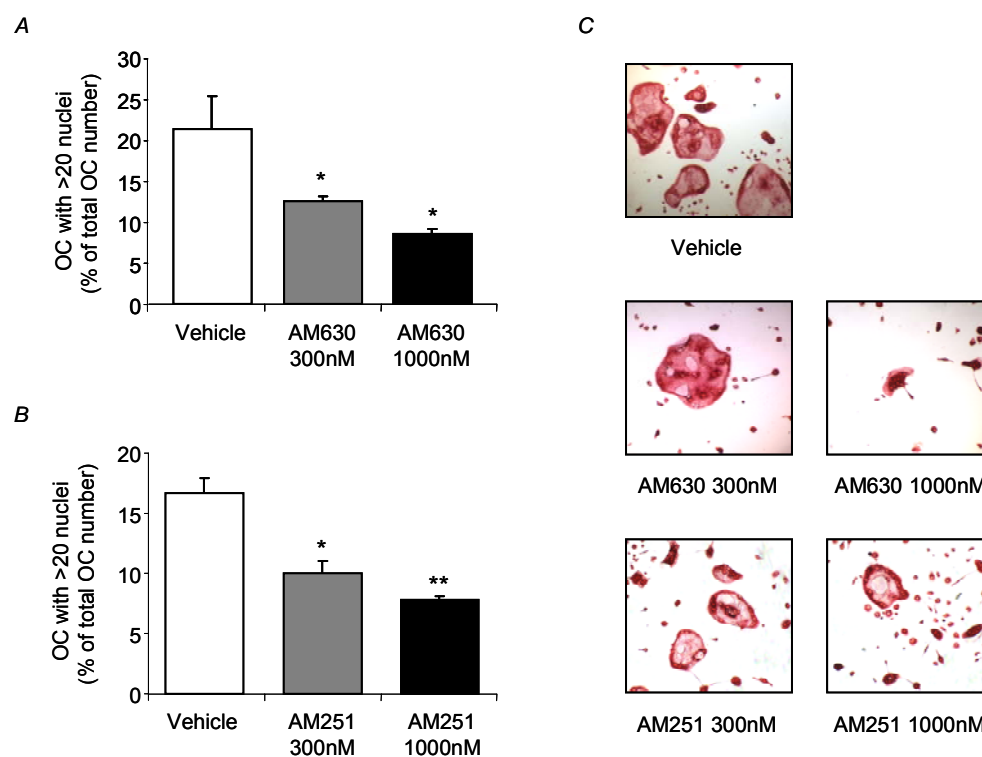
Figure 5.5: Effect of cannabinoid receptor antagonists/inverse agonists on osteoclast nuclearity. *A*. Number of multinucleated TRAcP-positive osteoclasts (OC) per well with 20 or more nuclei in bone marrow cultures stimulated with M-CSF (25ng/ml) and RANKL (100ng/ml) for 72 hours and then exposed to vehicle (V) or AM630 at the indicated concentrations for 48 hours. Changes in osteoclast number were expressed as a percent of total osteoclast number. *B*. Number of osteoclasts with more than 20 nuclei in cultures exposed to vehicle or AM251 at the indicated concentrations, from similar experiments, expressed in the same way. Representative photomicrographs of large osteoclasts stained for TRAcP from the cultures in *A* and *B*. Values are means ± sem and were obtained from 3 independent experiments. *p < 0.05 and **p < 0.005 from vehicle-treated cultures.

5.3.5 Effect of cannabinoid receptor ligands on macrophage viability

To determine whether cannabinoid receptor ligands are affecting directly the process of osteoclastogenesis or the viability of monocytic osteoclast precursors, macrophage cultures generated from bone marrow cells stimulated with M-CSF (25ng/ml) for 72 hours, were exposed to a concentration range of cannabinoid receptor ligands for 24-48 hours (c.f. section 2.2.2, page 76).

As shown in Figure 5.6*A* and *B*, none of the CNR2-selective agonists, HU308 and JWH133, or the endocannabinoids, AEA and 2-AG, had an effect on macrophage viability at the concentration range of 0.25nM - 10μM.
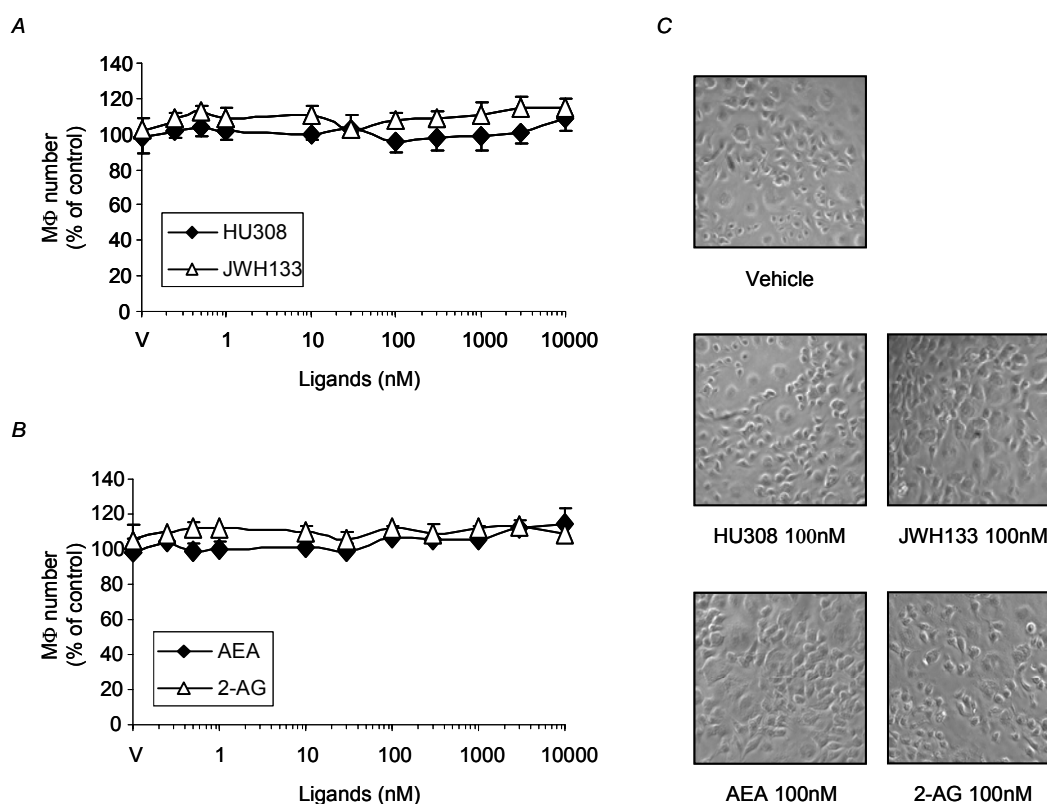
Figure 5.6: Effect of cannabinoid receptor agonists on macrophage number.
A. Macrophage (MΦ) number in bone marrow cultures stimulated with M-CSF (25ng/ml) for 72 hours and then exposed to vehicle (V), HU308 or JWH133, at the indicated concentrations for 24 hours, as assessed by Alamar Blue assay. Changes in macrophage number were expressed as a percent of values in vehicle-treated cultures. Macrophage number in cultures exposed to vehicle, AEA or 2-AG (*B*) from similar experiments, expressed in the same way. *C*. Representative phase contrast photomicrographs from the cultures in *A* and *B*. Values are means ± sem and were obtained from 3 independent experiments.

Likewise, neither of the cannabinoid receptor antagonist/inverse agonists, AM251 (CNR1-selective) or AM630 (CNR2-selective) had an effect on macrophage viability at the concentration range of 0.25nM - 3μM, as shown in Figure 5.7*A*. Even at the highest concentration tested of 10μM, AM630 did not have an effect on macrophage number. Surprisingly, the CNR1-selective antagonist/inverse agonist AM251, significantly increased macrophage number at 10μM (Figure 5.7*A*). Whether this is a noteworthy result or an irrelevant consequence of the extremely high concentrations of AM251, is still to be determined.
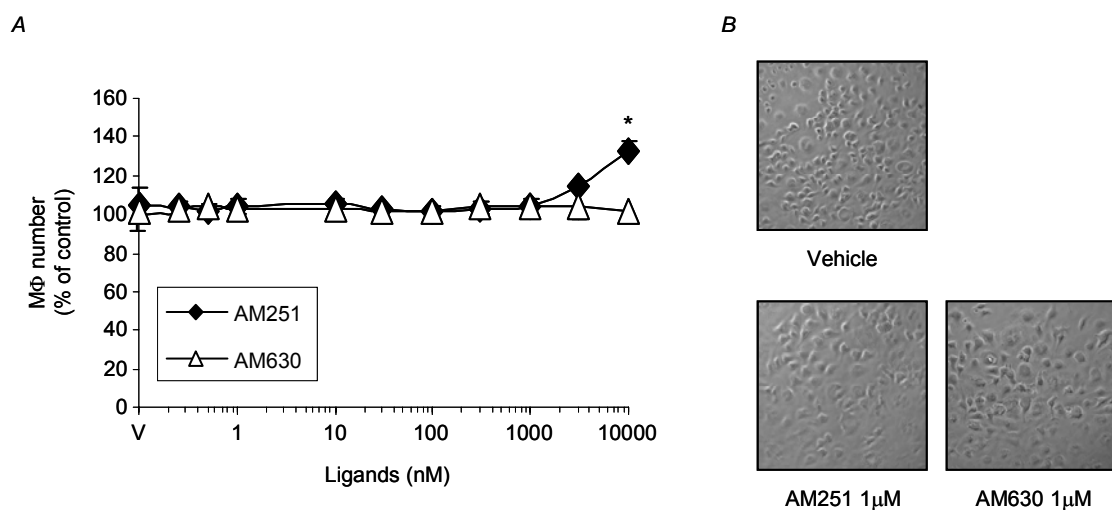
Figure 5.7: Effect of cannabinoid receptor antagonists/inverse agonists on macrophage number. *A*. Macrophage (MΦ) number in bone marrow cultures stimulated with M-CSF (25ng/ml) for 72 hours and then exposed to vehicle (V), AM251 or AM630, at the indicated concentrations for 48 hours, as assessed by Alamar Blue assay. Changes in macrophage number were expressed as a percent of values in vehicle-treated cultures. *B*. Representative phase contrast photomicrographs from the cultures in *A*. Values are means ± sem and were obtained from 3 independent experiments. *p < 0.05 from vehicle-treated cultures.

5.3.6 Effects of cannabinoid receptor ligands on osteoclasts from bone marrow of wild type and CNR2-deficient mice

To establish whether the effects of cannabinoid ligands on osteoclast number were mediated via the CNR2, osteoclast formation was assessed in cultures generated from wild type and *CNR2*$^{-/-}$ mice. These cultures were treated with M-CSF (25ng/ml) and RANKL (100ng/ml) for 72 hours and then exposed to cannabinoid receptor ligands for 24-48 hours (c.f. section 2.2.3, page 77).

As shown in Figure 5.8, vehicle-treated bone marrow cultures from *CNR2*$^{-/-}$ mice have significantly fewer osteoclasts than wild type cultures as already mentioned in section 5.3.1, page 155. The CNR2-selective agonists, HU308 and JWH133, stimulated osteoclast formation, with maximal stimulation at 30nM for HU308 and 30-1000nM for JWH133, in cultures derived from wild type but not from *CNR2*$^{-/-}$ mice. Cultures prepared from *CNR2*$^{-/-}$ mice were resistant to the stimulatory effects of HU308 and JWH133 at all concentrations tested, confirming a CNR2-mediated mechanism (Figure 5.8*A,B*).

The endocannabinoid AEA stimulated osteoclast formation in both wild type and *CNR2*$^{-/-}$ bone marrow cultures. Although AEA increased the osteoclast numbers significantly from concentrations as low as 30nM in wild type cultures, in *CNR2*$^{-/-}$ cultures AEA had a stimulatory effect only at a 10-fold higher concentration (Figure 5.8*C*). AEA had a maximal stimulatory effect at 300nM, causing 60% increase in osteoclast numbers in both wild type and *CNR2*$^{-/-}$ cultures (Figure 5.8*C*).

The endocannabinoid 2-AG stimulated osteoclast formation in *CNR2*$^{-/-}$ cultures in a manner indistinguishable from wild type cultures. The stimulatory effect of 2-AG on osteoclast number was significant from the concentration of 30nM, with maximal stimulation at 100nM in both wild type and *CNR2*$^{-/-}$ cultures (Figure 5.8*D*).
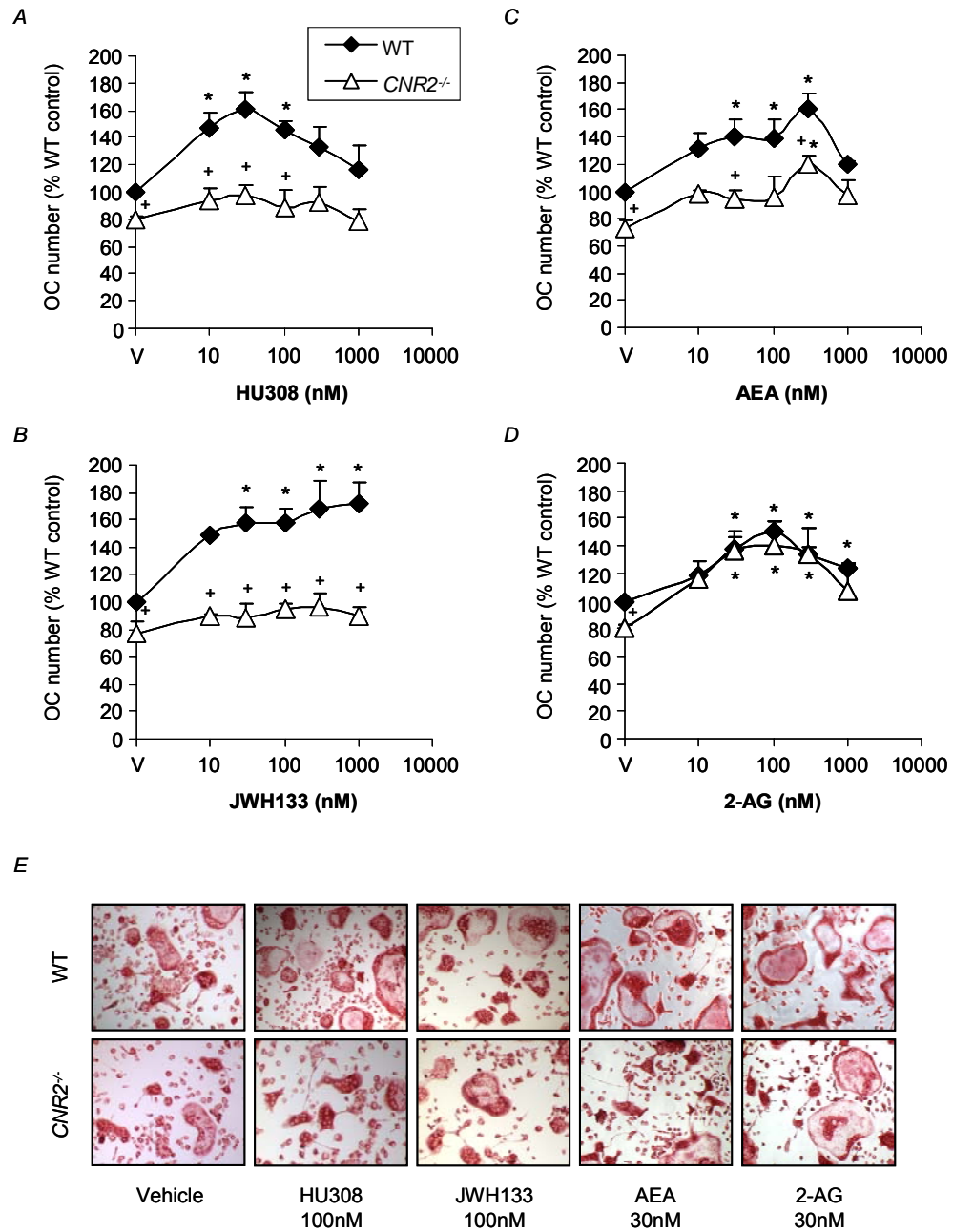
Figure 5.8: Effect of cannabinoid receptor agonists on osteoclasts from wild type and CNR2-deficient mice. *A*. Number of multinucleated TRAcP-positive osteoclasts (OC) in wild type and *CNR2-/-* bone marrow cultures stimulated with M-CSF (25ng/ml) and RANKL (100ng/ml) for 72 hours and then exposed to vehicle (V) or HU308 at the indicated concentrations for 24 hours. Changes in osteoclast number were expressed as a percent of values in wild type, vehicle-treated cultures. Osteoclast number in cultures exposed to vehicle, JWH133 (*B*), AEA (*C*) or 2-AG (*D*), from similar experiments, expressed in the same way. Representative photomicrographs of osteoclasts stained for TRAcP from the cultures in *A*, *B*, *C* and *D*. Values are means ± sem and were obtained from 3 independent experiments. *p < 0.05 from vehicle-treated cultures of same genotype, +p < 0.05 from wild type cultures treated in the same way.

The CNR2-selective antagonist/inverse agonist AM630 significantly inhibited osteoclast formation in wild type bone marrow cultures from concentrations as low as 30nM. Increasing concentrations of AM630 further inhibited osteoclast number in a concentration-dependent manner (Figure 5.9*A*). *CNR2*^{-/-} bone marrow cultures were not responsive to the inhibitory effects of AM630 at concentrations up to 300nM, but at higher concentrations of 1-3μM, AM630 inhibited osteoclast formation in a concentration dependent manner as in wild type cultures (Figure 5.9*A*). The IC_{50} of AM630 in wild type cultures was 199 ± 55nM, whereas in *CNR2*^{-/-} cultures it significantly increased to 1713 ± 804nM. The CNR1-selective antagonist/inverse agonist AM251 was less potent than AM630, but inhibited osteoclast formation in *CNR2*^{-/-} cultures to a similar extent as in wild type cultures (Figure 5.9*B*). The IC_{50} of AM251 in wild type and *CNR2*^{-/-} cultures was 1165 ± 598nM and 1500 ± 788nM, respectively.
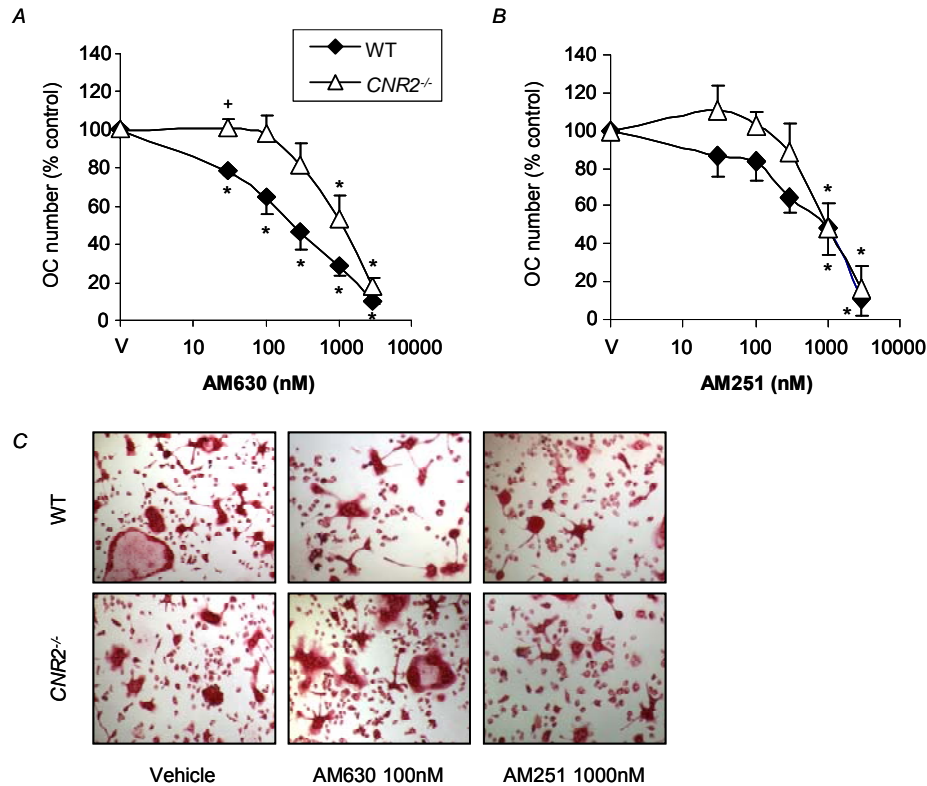
Figure 5.9: Effect of cannabinoid receptor antagonists/inverse agonists on osteoclasts from wild type and CNR2-deficient mice. Number of multinucleated TRAcP-positive osteoclasts (OC) in wild type and *CNR2*^{-/-} bone marrow cultures stimulated with M-CSF (25ng/ml) and RANKL (100ng/ml) for 72 hours and then exposed to vehicle (V), AM630 (*A*) or AM251 (*B*) at the indicated concentrations for 48 hours. Changes in osteoclast number were expressed as a percent of values in vehicle-treated cultures. Values are means ± sem and were obtained from 3 independent experiments. *p < 0.05 from vehicle-treated cultures of same genotype, [+]p < 0.05 from wild type cultures treated in the same way.

5.3.7 Cannabinoid receptor ligands have no effect on macrophage viability from bone marrow of wild type or CNR2-deficient mice

The effect of cannabinoid receptor ligands was also tested on M-CSF (25ng/ml) generated macrophage cultures from bone marrow of wild type and *CNR2$^{-/-}$* mice (c.f. section 2.2.2, page 76). As shown in Figure 5.10, none of the CNR2-selective ligands, HU308 and JWH133, or the endocannabinoids, AEA and 2-AG, had an effect on macrophage viability in cultures derived either from wild type or *CNR2$^{-/-}$* mice.
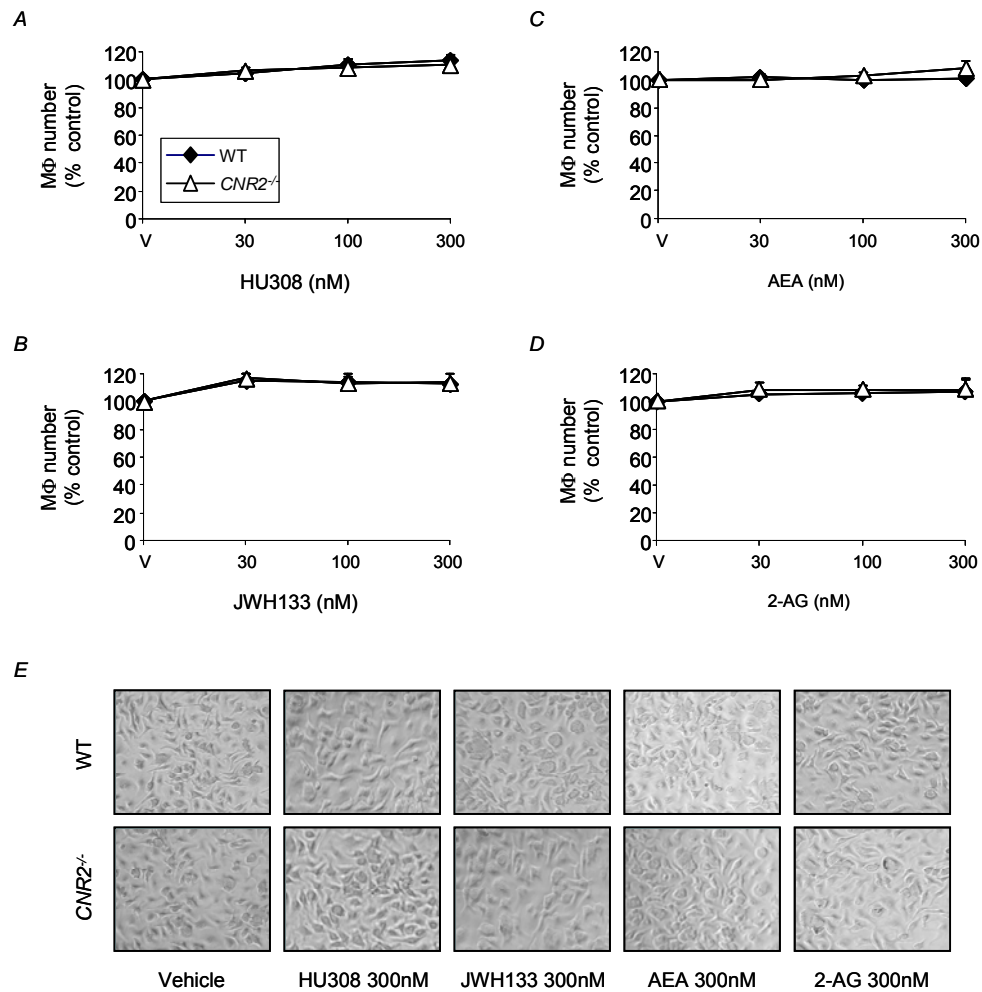
Figure 5.10: Effect of cannabinoid receptor agonists on macrophages from wild type and CNR2-deficient mice. *A*. Number of macrophages (MΦ) in wild type and *CNR2$^{-/-}$* bone marrow cultures stimulated with M-CSF (25ng/ml) for 72 hours and then exposed to vehicle (V) or HU308 at the indicated concentrations for 24 hours, as assessed by Alamar Blue assay. Changes in macrophage number were expressed as a percent of values in vehicle-treated cultures. Macrophage number in cultures exposed to vehicle, or JWH133 (*B*), AEA (*C*) or 2-AG (*D*), from similar experiments, expressed in the same way. *E*. Representative phase contrast photomicrographs of macrophages from the cultures in *A*, *B*, *C* and *D*. Values are means ± sem and were obtained from 3 independent experiments.

166

Similarly, the CNR2-selective antagonist/inverse agonist AM630 and the CNR1-seletive antagonist/inverse agonist AM251, did not have an effect on macrophage viability in M-CSF-stimulated cultures from wild type or $CNR2^{-/-}$ mice at the concentrations tested (Figure 5.11).
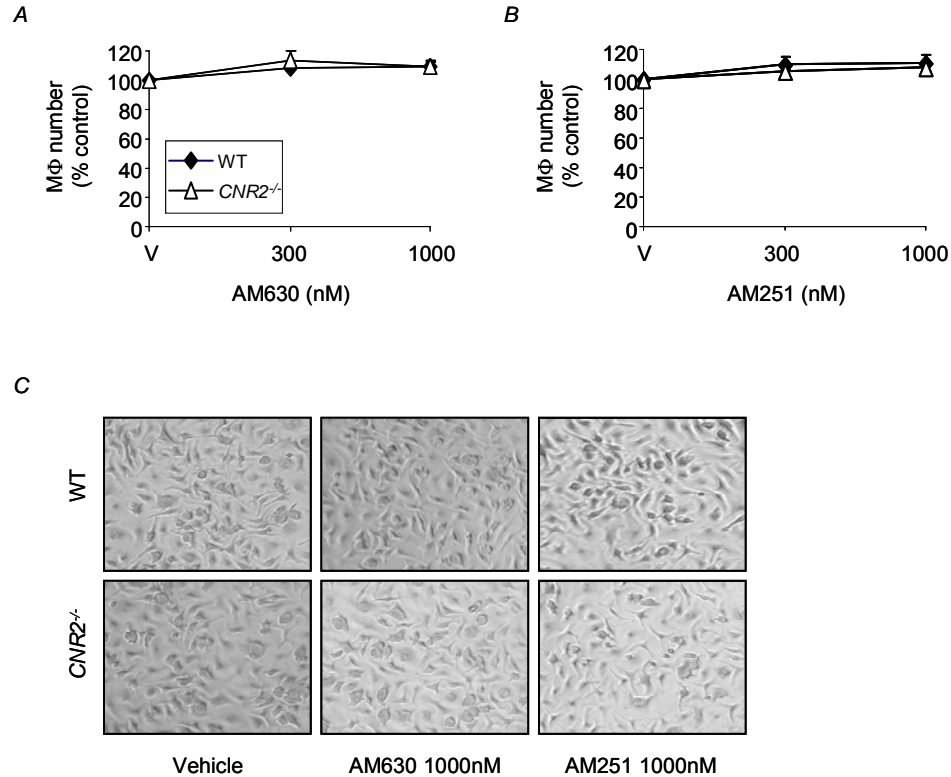
Figure 5.11: Effect of cannabinoid receptor antagonists/inverse agonists on macrophages from wild type and CNR2-deficient mice. Number of macrophages (MΦ) in wild type and $CNR2^{-/-}$ bone marrow cultures stimulated with M-CSF (25ng/ml) for 72 hours and then exposed to vehicle (V), AM630 (*A*) or AM251 (*B*) at the indicated concentrations for 48 hours, as assessed by Alamar Blue assay. Changes in macrophage number were expressed as a percent of values in vehicle-treated cultures. *C*. Representative phase contrast photomicrographs of macrophages from cultures in *A* and *B*. Values are means ± sem and were obtained from 3 independent experiments.

167

5.3.8 CNR2-deficient mice are partially protected from ovariectomy induced bone loss

Genetic inactivation of CNR2 partially rescues bone loss in ovariectomised mice

To determine the role CNR2 in bone mass due to oestrogen deficiency, 8-week old wild type and *CNR2$^{-/-}$* female littermates were subjected to ovariectomy or sham operation (c.f. section 2.5.4, page 97). Following a 3-week period, mice were sacrificed and μCT analysis was performed at the trabecular compartment of isolated tibiae (c.f. section 2.5.8, page 99).

As shown in Figure 5.12*A*, ovariectomised *CNR2$^{-/-}$* mice were partly protected from ovariectomy-induced bone loss, since they experienced less trabecular bone loss than wild type littermates. Although *CNR2$^{-/-}$* female mice also experienced less trabecular number loss than wild type controls, this difference did not achieve statistical significance (Figure 5.12*C*). Wild type ovariectomised mice suffered from loss of trabecular thickness (Figure 5.12*B*) and a subsequent increase in trabecular separation (Figure 5.12*D*), while in *CNR2$^{-/-}$* littermates trabecular thickness and trabecular separation were reserved (Figure 5.12*B,D*). Moreover, trabecular pattern factor was lower in *CNR2$^{-/-}$* mice than in wild type mice following ovariectomy, indicating better trabecular connectivity (Figure 5.12*E*).

The actual values of all parameters from ovariectomised and sham-operated wild type and *CNR2$^{-/-}$* mice are shown in Appendix 7, page 279.
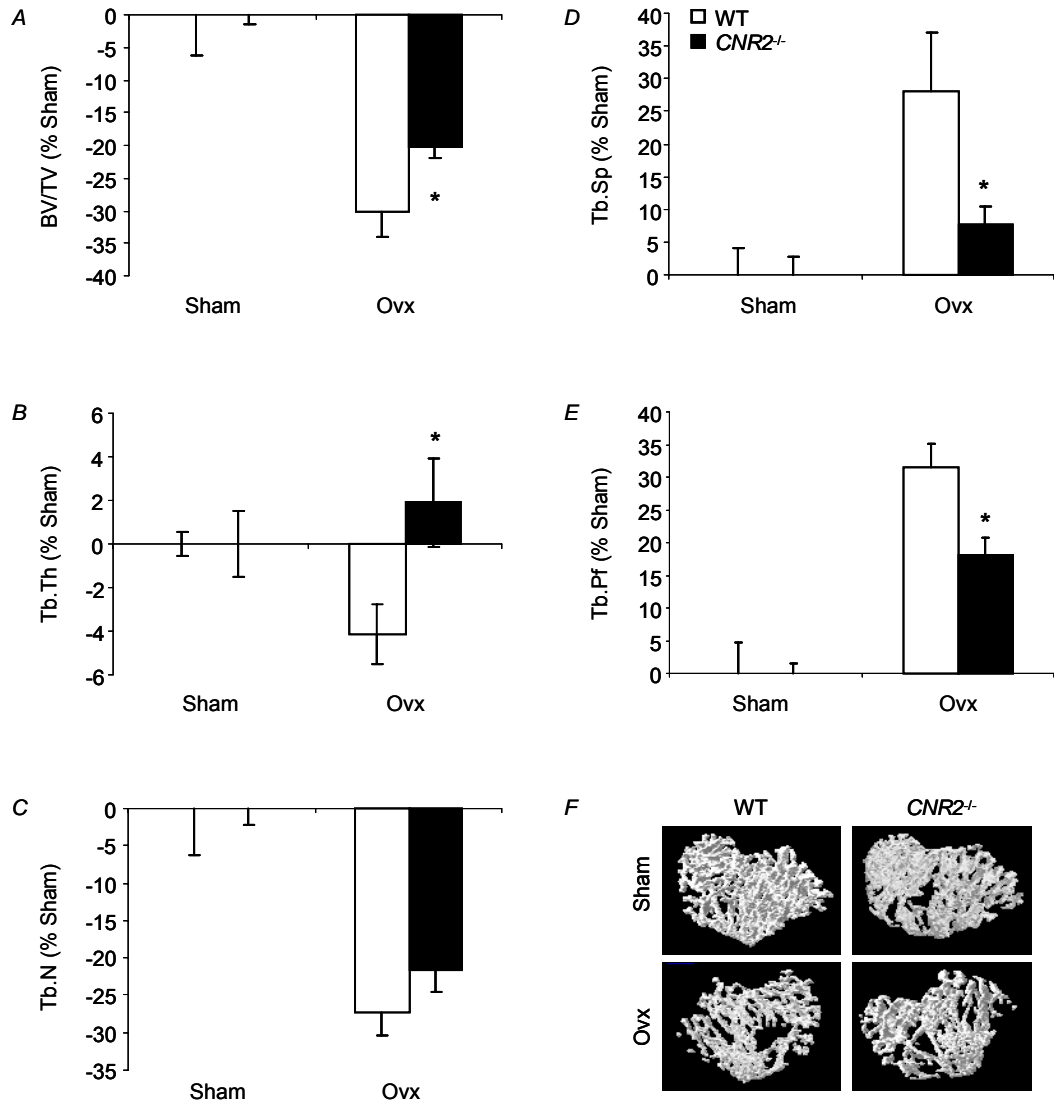
Figure 5.12: Effect of ovariectomy (Ovx) on trabecular bone in wild type and CNR2-deficient mice. *A*. Trabecular bone volume (BV/TV) in wild type and *CNR2$^{-/-}$* littermates subjected to ovariectomy or sham operation for 3 weeks, assessed by μCT of the tibia. Changes in BV/TV were normalised to those in sham operated mice of the same genotype and expressed as percent change. Trabecular thickness (Tb.Th) (*B*), trabecular number (Tb.N) (*C*), trabecular separation (Tb.Sp) (*D*), and trabecular pattern factor (Tb.Pf) (*E*) of the same experiment, expressed in the same way. *F*. Representative μCT images from the tibial metaphysis of wild type and *CNR2$^{-/-}$* mice, subjected to ovariectomy or sham operation. Values are means ± sem from 7-8 mice per group. *$p < 0.05$ from wild type ovariectomised mice.

Genetic inactivation of CNR2 partially rescues bone loss in ovariectomised mice due to low osteoclast number

To investigate the cellular events at the trabecular compartment of the bone, histomorphometric analysis was performed at the tibial metaphysis of wild type and *CNR2*^{-/-} ovariectomised mice (c.f. section 2.5.9, page 103). As shown in Table 5.1 osteoblast and osteoclast numbers increased in wild type mice following ovariectomy. However, in *CNR2*^{-/-} ovariectomised mice osteoclast numbers and active resorption surfaces were indistinguishable from sham-operated mice (Table 5.1), indicating a significant inhibition on osteoclast formation and function. Osteoblast numbers on the other hand, increased in *CNR2*^{-/-} mice following ovariectomy compared to sham-operated mice, but this increase did not achieve statistical significance. These results suggest that *CNR2*^{-/-} female mice are partially protected from ovariectomy-induced bone loss due to reduced osteoclast numbers and defective bone resorption (Table 5.1).

		BV/TV (%)	Ob.N/BS (cells/mm)	Oc.N/BS (cells/mm)	Oc.S/BS (%)
WT	SHAM	9.1 ± 1.3	33.2 ± 0.5	0.39 ± 0.03	1.1 ± 0.1
	OVX	5.5 ± 0.8^a	39.3 ± 2.5^a	0.74 ± 0.10^a	2.0 ± 0.3^a
CNR2^{-/-}	SHAM	9.1 ± 1.0	31.6 ± 1.7	0.56 ± 0.08	1.8 ± 0.3
	OVX	8.3 ± 0.7^b	36.7 ± 2.7	0.47 ± 0.07	1.6 ± 0.2

Table 5.1: Effect of ovariectomy (Ovx) on static histomorphometry in wild type and CNR2-deficient mice. BV/TV, trabecular bone volume (%); Ob.N/BS, osteoblast number/bone surface (cells/mm); Oc.N/BS, osteoclast number/bone surface (cells/mm); Oc.S/BS, osteoclast surface/bone surface (%). Values are expressed as means ± sem from 3-4 mice per group. [a]p < 0.05 from sham-operated mice, [b]p < 0.05 from wild type ovariectomised mice.

Genetic inactivation of CNR2 does not affect body weight gain in ovariectomised mice

To investigate whether lack of CNR2 has an effect on body weight gain after loss of ovarian function, ovariectomised and sham-operate wild type and *CNR2-/-* mice were weighed at the beginning and the end of the 3-week period. As shown in Figure 5.13, all mice in this study showed an increase in body weight regardless of genotype or type of operation. As expected, weight gain was greater in both wild type and *CNR2-/-* ovariectomised mice compared to sham-operated mice. However, no significant difference in body weight gain was observed among wild type and *CNR2-/-* mice subjected to the same type of operation (Figure 5.13).
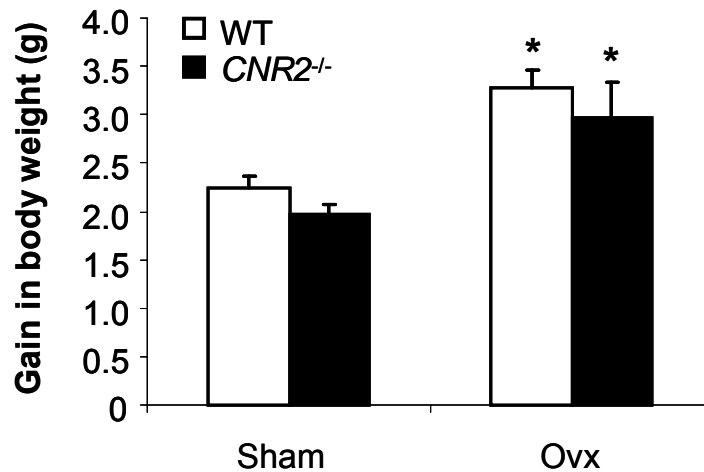
Figure 5.13: Effect of ovariectomy on body weight gain in wild type and CNR2-deficient mice. Actual gain in body weight of wild type and *CNR2-/-* mice subjected to ovariectomy or sham operation for 3 weeks. Values are means ± sem from 7-8 mice per group. *p < 0.05 from sham-operated mice of same genotype.

Genetic inactivation of CNR2 does not affect uterine or spleen weights in ovariectomised mice

The success of the ovariectomy operation was confirmed by comparing the uterine weight from sham-operated and ovariectomised mice. As shown in Figure 5.14*A*, ovariectomy significantly reduced the weight of uterus in wild type and *CNR2*^{-/-} mice by approximately 70% compared to the respective sham-operated mice. No significant difference in spleen weight was observed between the groups (Figure 5.14*B*).
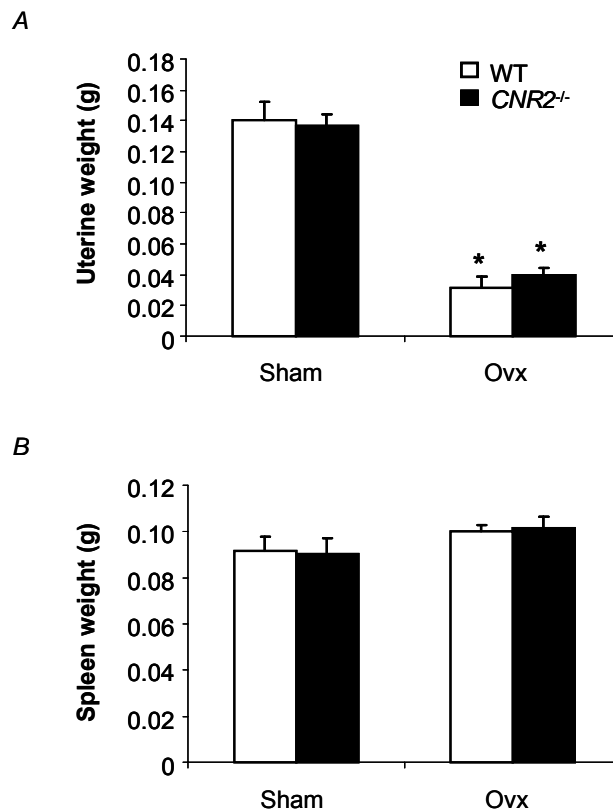
Figure 5.14: Effect of ovariectomy on uterine and spleen weights in wild type and CNR2-deficient mice. Weight of uterus (*A*) and spleen (*B*) isolated from wild type and *CNR2*^{-/-} mice subjected to ovariectomy or sham operation for 3 weeks. Values are means ± sem from 7-8 mice per group. *p < 0.05 from sham-operated mice of same genotype.

5.3.9 Effect of the CNR2-selective antagonist/inverse agonist AM630, on ovariectomy-induced bone loss

In view of the anti-osteoclast activities of the CNR2-selective antagonist/inverse agonist *in vitro*, and the genetic inactivation of *CNR2 in vivo*, the effects of AM630 were also studied in 8-week old wild type and *CNR2^{-/-}* female mice subjected to ovariectomy (c.f. section 2.5.4, page 97). Mice received daily intraperitoneal injections of either vehicle, 0.1 or 1.0mg/kg of AM630 for 3 weeks (c.f. section 2.5.5, page 97). Mice were then sacrificed and μCT analysis was performed on isolated tibiae (c.f. section 2.5.8, page 99).

Pharmacological inactivation of CNR2 protects from ovariectomy-induced bone loss

As shown in Figure 5.15*A*, treatment of wild type mice with the CNR2-selective antagonist/inverse agonist AM630, rescued ovariectomy-induced bone loss at a dose as low as 0.1mg/kg. Wild type mice treated with AM630 at 0.1mg/kg lost 65% less trabecular bone volume than vehicle-treated mice ($p < 0.05$), and with AM630 treatment at 1.0mg/kg, wild type mice lost 55% less trabecular bone volume compared to vehicle-treated controls ($p < 0.05$) (Figure 5.15*A*).

CNR2^{-/-} female mice were resistant to the protective effects of AM630 at a low dose of 0.1mg/kg. However, at a higher dose of 1.0mg/kg, AM630 rescued ovariectomy-induced bone loss in *CNR2^{-/-}* mice to a similar extent as in wild type mice. The maximum rescue of bone loss in *CNR2^{-/-}* mice following treatment with AM630 at 1.0mg/kg was 65% when compared to the vehicle-treated *CNR2^{-/-}* mice ($p < 0.05$) (Figure 5.15*A*).
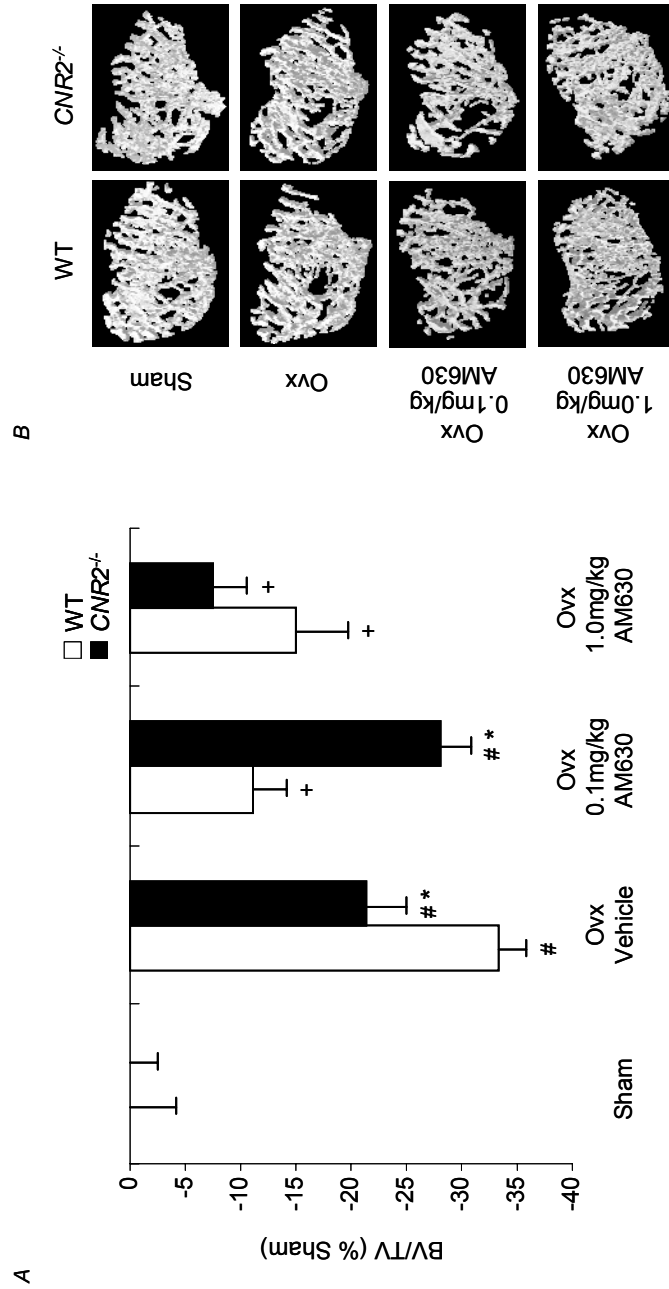
Figure 5.15: Effect of AM630 on ovariectomy-induced bone loss in wild type and CNR2-deficient mice. *A.* Trabecular bone volume (BV/TV) in wild type and *CNR2*^{-/-} mice subjected to ovariectomy or sham operation and treated with vehicle or AM630 (0.1 and 1.0mg/kg) for 3 weeks. Changes in trabecular bone volume were normalised to those in sham operated mice of same genotype and expressed as percent change. *B.* Representative μCT images from the tibial metaphysis of wild type and *CNR2*^{-/-} mice, from *A.* Values are means ± sem from 7-8 mice per group. *p < 0.05 from wild type mice, [†]p < 0.05 from ovariectomised, vehicle-treated mice of the same genotype, [#]p < 0.05 from sham-operated mice of the same genotype.

174

Further μCT analysis showed that the CNR2-selective antagonist/inverse agonist AM630, rescued trabecular bone loss in wild type mice at a dose as low as 0.1mg/kg, by reversing the loss of trabecular number (Figure 5.16*B*) and moderately protecting trabecular thickness (Figure 5.16*A*). Accordingly, the trabecular separation of wild type mice treated with AM630 at 0.1 and 1.0mg/kg was rescued to levels that were significantly lower from those in vehicle-treated ovariectomised controls (Figure 5.16*C*). Overall, AM630 treatment increased the trabecular connectivity in wild type mice, as indicated by the reduction in trabecular pattern factor (Figure 5.16*D*).

The trabecular thickness of *CNR2*$^{-/-}$ mice did not significantly change after AM630 treatment and was indistinguishable from wild type controls at all times (Figure 5.16*A*). However, the trabecular number of *CNR2*$^{-/-}$ mice treated with AM630 at 1.0mg/kg was rescued to levels that were no longer significantly different from wild type littermates, unlike *CNR2*$^{-/-}$ mice treated with the low dose of AM630 (Figure 5.16*B*). Similarly, ovariectomised *CNR2*$^{-/-}$ mice treated with AM630 at 0.1mg/kg had significantly higher trabecular separation than wild type controls and *CNR2*$^{-/-}$ mice treated with AM630 at 1.0mg/kg after ovariectomy (Figure 5.16*C*). Nonetheless, the trabecular connectivity in AM630-treated *CNR2*$^{-/-}$ mice did not significantly change from vehicle-treated controls, but at 1.0mg/kg AM630 treatment trabecular connectivity was reduced to levels that were no longer statistically different from sham-operated *CNR2*$^{-/-}$ mice (Figure 5.16*D*).

The actual values of all μCT parameters for the trabecular bone analysis of ovariectomised and sham-operated wild type and *CNR2*$^{-/-}$ female mice treated with the CNR2-selective antagonist/inverse agonist AM630, are shown in Appendix 8, page 280.
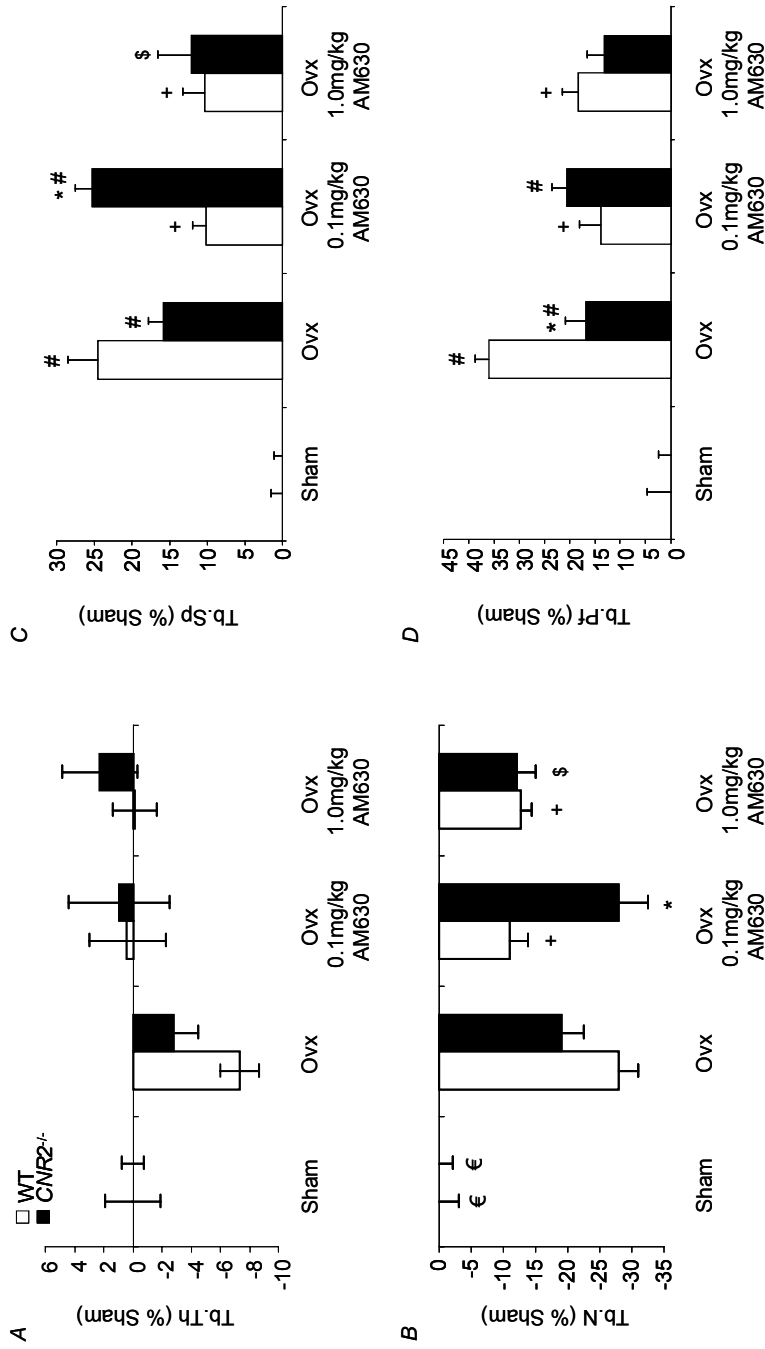
Figure 5.16: Effect of AM630 on other µCT parameters of trabecular bone following ovariectomy in wild type and CNR2-deficient mice. *A.* Trabecular thickness (Tb.Th) in wild type and *CNR2⁻ᐟ⁻* littermates subjected to ovariectomy or sham operation and treated with vehicle or AM630 at 2 doses for 3 weeks. Changes in Tb.Th were normalised to those in sham operated mice of the same genotype and expressed as percent change. Trabecular number (Tb.N) (*B*), trabecular separation (Tb.Sp) (*C*), and trabecular pattern factor (Tb.Pf) (*D*) of the same experiment, expressed in the same way. Values are means ± sem from 7-8 mice per group. *p < 0.05 from wild type mice, ⁺p < 0.05 from ovariectomised, vehicle-treated mice of the same genotype, $p < 0.05 from *CNR2⁻ᐟ⁻* mice treated with AM630 at 0.1mg/kg, #p < 0.05 from sham-operated mice of the same genotype, €p < 0.05 from all ovariectomised groups of the same genotype.

Pharmacological inactivation of CNR2 protects from ovariectomy-induced bone loss by inhibiting osteoclasts and bone resorption

Bone histomorphometric analysis (c.f. section 2.5.9, page 103) at the trabecular compartment of tibial metaphyses from wild type ovariectomised mice showed that AM630 blocked the increase in osteoclast numbers and active resorption surfaces that usually follow ovariectomy, without affecting osteoblast numbers (Table 5.2). These data indicate that prevention of ovariectomy-induced bone loss with AM630 was due to an inhibitory effect on osteoclasts and bone resorption rather than an effect on osteoblasts and bone formation.

		BV/TV (%)	Ob.N/BS (cells/mm)	Oc.N/BS (cells/mm)	Oc.S/BS (%)
Sham	Vehicle	13.3 ± 0.5	14.9 ± 0.9	0.30 ± 0.07	1.11 ± 0.26
OVX	Vehicle	6.8 ± 0.2^a	21.5 ± 2.1^a	0.75 ± 0.09^a	3.04 ± 0.49^a
OVX	AM630 0.1mg/kg	9.8 ± 0.3^b	20.7 ± 2.8^a	0.63 ± 0.08^a	$2.14 \pm 0.31^{a,b}$
OVX	AM630 1.0mg/kg	13.1 ± 0.5^b	18.0 ± 1.7^a	0.24 ± 0.04^b	1.15 ± 0.21^b

Table 5.2: Static histomorphometry in wild type mice following ovariectomy (OVX) and AM630 treatment at 0.1 and 1.0mg/kg for 3 weeks. BV/TV, trabecular bone volume (%); Ob.N/BS, osteoblast number/bone surface (cells/mm); Oc.N/BS, osteoclast number/bone surface (cells/mm); Oc.S/BS, osteoclast surface/bone surface (%). Values are expressed as means ± sem from 4-5 mice per group. [a]$p < 0.05$ from sham-operated mice; [b]$p < 0.05$ from vehicle-treated ovariectomised mice.

Pharmacological inactivation of CNR2 does not affect body weight gain in ovariectomised mice

To establish whether pharmacological inactivation of CNR2 with the CNR2-selective antagonist/inverse agonist AM630, has an effect on body weight gain following ovariectomy, the weight of all mice used in this study was measured before the operation and 3 weeks after when mice were sacrificed. As shown in Figure 5.17, no significant difference in body weight gain was observed between wild type and *CNR2-/-* mice subjected to the same type of operation and same drug treatment. As expected, all groups subjected to ovariectomy, regardless of treatment, had at least a 2-fold increase in body weight gain when compared with sham-operated mice (Figure 5.17).
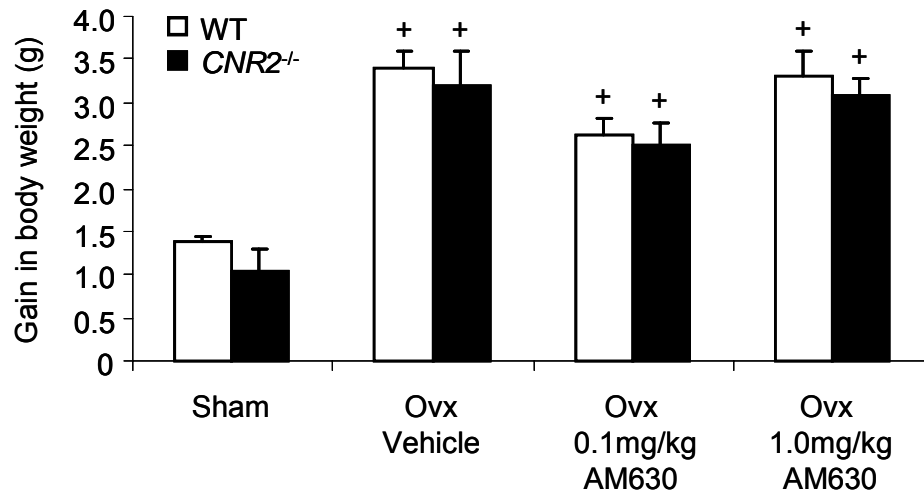
Figure 5.17: Effect of ovariectomy and AM630-treatment on body weight gain in wild type and CNR2-deficient mice. Actual gain in body weight of wild type and *CNR2-/-* mice, treated with vehicle or AM630 (0.1 and 1.0mg/kg), following ovariectomy or sham operations for 3 weeks. Values are means ± sem from 7-8 mice per group. $^+$p < 0.05 from sham-operated mice of the same genotype.

Pharmacological inactivation of CNR2 does not affect uterine or spleen weights

The mean uterine weight from all ovariectomised groups was reduced by about 75% compared to the respective sham-operated mice, indicating that ovariectomy was carried out successfully (Figure 5.18*A*). Although all mice remained healthy throughout the treatment period, all ovariectomised groups had slightly heavier spleens than sham operated mice, possibly due to an inflammatory response after surgery (Figure 5.18*B*).
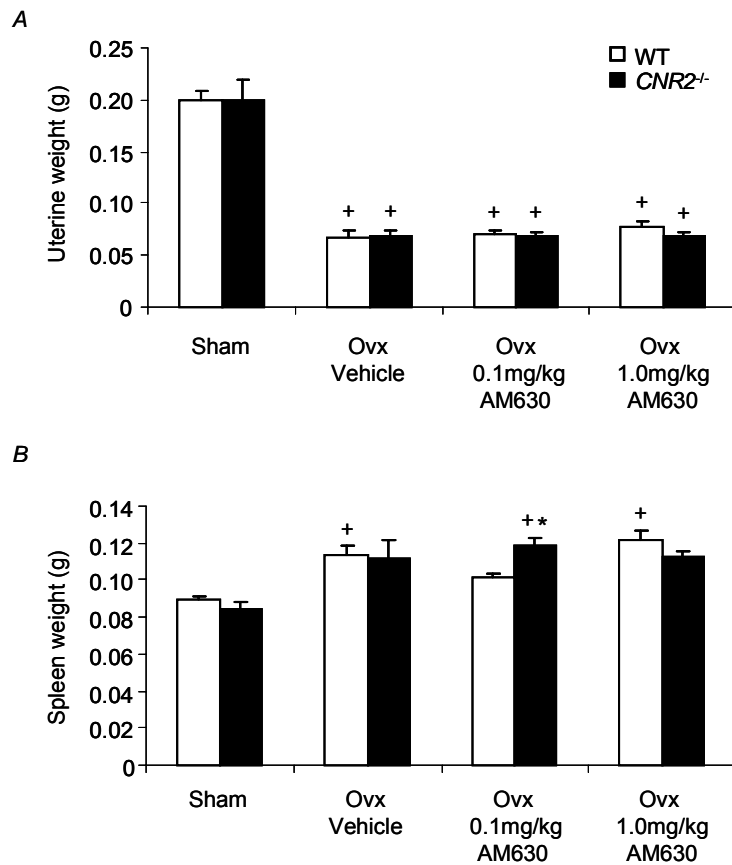
Figure 5.18: Effect of ovariectomy and AM630-treatment on uterine and spleen weights in wild type and CNR2-deficient mice. Weight of uterus (*A*) and spleen (*B*) isolated from wild type and *CNR2*^{-/-} mice treated with vehicle or AM630 (0.1 and 1.0mg/kg), following ovariectomy or sham operations for 3 weeks. Values are means ± sem from 7-8 mice per group. [+]p < 0.05 from sham-operated mice of the same genotype, *p <0.05 from wild type mice subjected to the same treatment.

5.4   DISCUSSION

We and others have previously reported that endocannabinoids and cannabinoid receptor agonists stimulate osteoclast formation (Idris et al., 2005; Ridge et al., 2007), whereas Ofek and colleagues proposed that the CNR2-seletive agonist HU308 inhibits osteoclast formation *in vitro* and *in vivo* (Ofek et al., 2006). In view of these observations, the aim of this chapter was to further investigate the role of CNR2 on osteoclast formation *in vitro* and ovariectomy-induced bone loss *in vivo*.

This chapter demonstrates that although bone marrow macrophages from *CNR2$^{-/-}$* mice responded normally to M-CSF, they have a defect in RANKL-induced osteoclast formation. In keeping with this, the two cannabinoid receptor antagonists/inverse agonists, AM251 and AM630, selective for CNR1 and CNR2 respectively (Pertwee and Ross, 2002), inhibited osteoclast formation and nuclearity in a concentration-dependent manner, with AM630 being more potent than AM251. Conversely, the endocannabinoids AEA and 2-AG, as well as the CNR2-selective agonists HU308 and JWH133, stimulated osteoclast formation with an EC$_{50}$ of <1nM, and increased nuclearity at concentrations in the nanomolar range. Although AEA, 2-AG and JWH133 had a stimulatory effect on osteoclast formation even at 10- and 100-fold higher concentrations, HU308 did not increase osteoclast numbers at concentrations higher than 100nM and caused osteoclast inhibition at 10μM with an IC$_{50}$ value of 4.2μM. However, HU308 concentration of 10μM, is approximately 2000 times greater than the concentration of HU308 required for CNR2-mediated adenylyl cyclase inhibition in CNR2-transfected cells (Hanus et al., 1999). This suggests that the inhibitory effects of HU308 at these concentrations may have been non-specific and mediated by an interaction with pathways other than CNR2. The stimulatory effects of HU308 and JWH133 on osteoclast formation are consistent with previous work which has shown that non-selective cannabinoid receptor agonists including AEA, 2-AG and CP55940 stimulate osteoclast formation and bone resorption *in vitro* at nanomolar concentrations

(Idris et al., 2005; Ridge et al., 2007). However, the observations reported in this chapter differ from previous work of Ofek and colleagues, who found that HU308 caused osteoclast inhibition at concentrations in the nanomolar range (Ofek et al., 2006). These differences cannot be readily explained but it should be noted that the observations of Ofek et al. were based in part on studies of RAW 264.7 cells rather than primary osteoclasts. Although Ofek et al. also studied M-CSF- and RANKL-stimulated bone marrow cultures, the numbers of osteoclasts generated were very low (an average of 15 cells per culture), and cannabinoid agonist treatments were kept for a long period of time (6 days) (Ofek et al., 2006). These factors might have also contributed to the differences observed between the two studies.

Because all pharmacological ligands used in this study are non-specific and can interact with both CNR1 and CNR2 (Appendix 4, page 275), further studies were conducted with osteoclasts derived from wild type and $CNR2^{-/-}$ mice to determine whether the effects of these ligands on osteoclast activity were truly mediated by CNR2. The stimulatory effect of HU308 and JWH133 on osteoclast formation was only observed in wild type cultures, since neither of these compounds increased osteoclast differentiation in cultures from $CNR2^{-/-}$ mice. However, cultures from both wild type and $CNR2^{-/-}$ mice responded to the endocannabinoids AEA and 2-AG, probably because of their well-documented activity towards CNR1 (Pertwee and Ross, 2002) (Appendix 4, page 275). Moreover, endocannabinoids are likely to have a stimulatory effect on osteoclast formation, via the transient receptor potential vallinoid type 1 (TRPV1) (De Petrocellis et al., 2000; Smart et al., 2000; Hermann et al., 2003; Rossi et al., 2009), or other G-protein coupled receptors such as GPR55 (Whyte et al., 2009). Further studies showed that osteoclasts generated from $CNR2^{-/-}$ mice were resistant to the inhibitory effects of AM630 at low concentrations but inhibited osteoclast formation in cultures from $CNR2^{-/-}$ mice at higher concentrations. In contrast, the CNR1-selective antagonist/inverse agonist AM251 was an equally potent inhibitor of osteoclast formation in cultures from wild

type and $CNR2^{-/-}$ mice, showing that its effects are mainly mediated by CNR1 or other available receptors, such as GPR55.

To confirm that pharmacological or genetic inactivation of CNR2 indeed leads to osteoclast inhibition, osteoclastogenesis should also be studied in co-cultures of osteoblast and bone marrow. Such system will enable the mixing and matching of cell populations from wild type and $CNR2^{-/-}$ mice in order to determine whether osteoblasts lacking CNR2 or osteoclast precursors from bone marrow of $CNR2^{-/-}$ mice are most likely to be responsible for the defective osteoclastogenesis observed. Defective osteoclast formation could be due to the fact that bone marrow from CNR2-deficient mice is less responsive to osteoclastogenic stimuli, as also seen in RANKL and M-CSF stimulated bone marrow cultures, or that osteoblasts from $CNR2^{-/-}$ mice cannot support osteoclast formation due to reduced production of osteoclastogenic cytokines, as previously shown with osteoblasts derived from $CNR1^{-/-}$ mice (Idris et al., 2008b). Such experiments will be performed in the near future.

Oestrogen deficiency was studied in ovariectomised mice, a well-established model of post-menopausal osteoporosis (Turner, 1999). Unlike ageing experiments, which allow the study of hormonal changes and the natural transition from cycling to acycling mice (Nelson et al., 1981; Felicio et al., 1984; Nelson and Felicio, 1990), ovariectomy addresses the transition phase of bone loss due to oestrogen deficiency (Kalu, 1991). $CNR1^{-/-}$ female mice were previously shown to be resistant to trabecular bone loss following ovariectomy (Idris et al., 2005). Consistent with this, 8-week old $CNR2^{-/-}$ female mice subjected to ovariectomy in the current study were partly protected from bone loss, due to defective osteoclast formation. These results suggested that CNR2 plays a role in regulating bone loss after ovariectomy and that genetic inactivation of CNR2 may protect from bone loss following ovariectomy.

To determine whether pharmacological inactivation/blockade of CNR2 can also prevent bone loss resulting from oestrogen deficiency, the effects of the CNR2-selective antagonist/inverse agonist AM630 were studied on ovariectomy-induced bone loss in wild type and *CNR2*$^{-/-}$ mice. Administration of AM630 in ovariectomised wild type mice at a dose of 0.1 and 1.0mg/kg prevented ovariectomy-induced bone loss, with identical results to those observed with the CNR1-selective antagonist/inverse agonist AM251 as previously reported (Idris et al., 2005). Analysis of bone histomorphometry showed that AM630 blocked the increase in osteoclast numbers and active resorption surfaces that followed ovariectomy, demonstrating that prevention of bone loss with AM630 was due to an inhibitory effect on osteoclast and bone resorption rather than an effect on osteoblast and bone formation. This findings together with Idris et al. (Idris et al., 2005) indicate that CNR1 or CNR2 blockade prevent ovariectomy-induced bone loss by inhibiting osteoclast formation and function. Mice lacking CNR2 were resistant to the protective effects of AM630 at a low dose (0.1mg/kg), consistent with a CNR2-mediated mechanism. However, at higher dose of 1.0mg/kg, AM630 was equally effective at preventing ovariectomy-induced bone loss in *CNR2*$^{-/-}$ mice and wild type littermates, possibly through non-specific binding on CNR1.

In summary, the results reported in this chapter indicate that type 2 cannabinoid receptors regulate osteoclast differentiation *in vitro* and ovariectomy-induced bone loss *in vivo*. Antagonists/inverse agonists of cannabinoid receptors inhibit osteoclast differentiation and bone resorption by a CNR2 mediated pathway as well as interacting by CNR1 as previously reported (Idris et al., 2005). Conversely, it appears that the stimulatory effects of CNR2-selective agonists on osteoclast formation, at the concentrations tested here, are mediated only by an interaction with CNR2. These data suggest that cannabinoid receptor antagonists/inverse agonists may have potential value as anti-resorptive drugs.

CHAPTER SIX
ROLE OF CNR2 IN OSTEOBLAST DIFFERENTIATION AND FUNCTION

6   ROLE OF CNR2 IN OSTEOBLAST DIFFERENTIATION AND FUNCTION

6.1   SUMMARY

Cannabinoid receptor agonists stimulate osteoclast formation *in vitro*, but paradoxically, the CNR2-selective agonist HU308 has also been found to partially protect against ovariectomy-induced bone loss *in vivo*. In an attempt to resolve these discrepancies, the role of CNR2 in osteoblast differentiation and function was investigated further using a combination of pharmacological and genetic approaches.

Bone marrow-derived osteoblasts and calvarial osteoblasts from *CNR2*$^{-/-}$ mice, showed defective bone nodule formation in comparison to wild type osteoblasts even though they proliferated normally. Bone nodule cultures with different cell seeding densities showed that calvarial osteoblasts from *CNR2*$^{-/-}$ neonates are slower in becoming matrix-secreting osteoblasts than wild type osteoblasts, suggesting a defect in differentiation. The CNR2-selective agonists HU308 and JWH133 stimulated bone nodule formation in wild type osteoblast cultures at concentrations of 10 and 30nM. Partial stimulatory effects were also observed in cultures from *CNR2*$^{-/-}$ mice, indicating that the enhancement of bone nodule formation was mediated by CNR2 dependent and independent effects. Studies *in vivo* showed that administration of HU308 (0.1 and 1.0mg/kg) in wild type mice, reversed ovariectomy-induced bone loss and preserved trabecular number in a dose-dependent manner. This was accompanied by an increase in osteoblast numbers and bone formation rate but no change in osteoclast numbers or bone resorption. Administration of HU308 in *CNR2*$^{-/-}$ mice at 0.1mg/kg had no significant effect on ovariectomy-induced bone loss, consistent with a CNR2-mediated effect. Treatment with HU308 at a higher dose (1.0mg/kg) had a moderate but yet not significant effect on bone loss in *CNR2*$^{-/-}$ mice.

In conclusion, these data shows that CNR2-selective agonists stimulate nodule formation *in vitro* and prevent ovariectomy-induced bone loss *in vivo* by promoting bone formation. Therefore, the CNR2 pathway may have an anabolic effect on bone, raising the possibility that CNR2 agonists might be of value as new treatments for osteoporosis.

6.2 INTRODUCTION

Recent studies have shown that the endocannabinoid system is implicated in bone remodelling via osteoclastic and osteoblastic CNR1 and CNR2 signalling. Idris and colleagues have previously shown that CNR1 mediates the effects of cannabinoid receptor ligands on osteoclast activity (Idris et al., 2005), whereas Ofek et al. reported that CNR2 regulates bone mass by stimulating osteoblasts and inhibiting osteoclasts (Ofek et al., 2006). This chapter investigates further the role of CNR2 in osteoblast differentiation and function, *in vitro* and *in vivo*.

The CNR2-selective agonist HU308, has previously been found to inhibit osteoclast formation *in vitro* and to partially protect from ovariectomy-induced bone loss *in vivo*, by inhibiting bone resorption and stimulating endocortical bone formation (Ofek et al., 2006). In addition, HU308 was found to stimulate growth and proliferation of primary osteoblasts from wild type mice but not from $CNR2^{-/-}$ mice. And finally, HU308 was shown to stimulate nodule formation in wild type calvarial osteoblast cultures kept in osteogenic medium, whereas $CNR2^{-/-}$ cultures showed no response to HU308 (Ofek et al., 2006). Together these results suggested that the CNR2-selective agonist HU308, enhances osteoblast differentiation and activity *in vivo* and *in vitro*, and suppresses trabecular osteoclastogenesis via a CNR2 mediated mechanism (Ofek et al., 2006).

The aim of the work reported in this chapter was to investigate further the role of CNR2 in osteoblast number, differentiation and function *in vitro* by pharmacological activation and inactivation of CNR2 in wild type and CNR2-deficient primary osteoblasts cutures. In addition, the activation of type 2 cannabinoid receptors with a CNR2-selective agonist was used to study the role of CNR2 on ovariectomy-induced bone loss and the potential use of CNR2-selective agonists as anabolic agents.

6.3 RESULTS

6.3.1 Osteoblasts from bone marrow of CNR2-deficient mice are defective in PTH-induced differentiation

To investigate the effects of CNR2 on osteoblastogenesis, osteoblast differentiation and growth were investigated, using the Alkaline phosphatase (ALP) assay (c.f. section 2.2.9, page 81) and Alamar Blue assay (c.f. section 2.2.8, page 80), respectively. Osteoblasts were generated from bone marrow in medium supplemented with 50μg/ml Vitamin C and 3mM β-GP (osteogenic medium) for 8-10 days. Cells were then re-plated and allowed to proliferate for 72 hours, before they were exposed to PTH for 24 hours (c.f. section 2.2.6, pages 79).

As shown in Figure 6.1*A*, ALP activity (a marker of osteoblast differentiation) increased with PTH treatment in a concentration-dependent manner in cultures from wild type mice. However, ALP activity in cultures from *CNR2*$^{-/-}$ mice was not significantly increased, suggesting that bone marrow osteoblasts from *CNR2*$^{-/-}$ mice were unresponsive to PTH treatment and hence defective in differentiation (Figure 6.1*A*). Figure 6.1*B*, shows that the proliferation of osteoblasts derived from bone marrow of wild type and *CNR2*$^{-/-}$ mice was similar and increased in the same manner following treatment with increasing concentrations of PTH (25-100nM).

To study the role of CNR2 on osteoblast function, nodule formation was investigated in osteoblast cultures from bone marrow of wild type and *CNR2*$^{-/-}$ mice. Cultures were kept in osteogenic medium for up to 3 weeks (c.f. section 2.2.6, page 79) and mineralised nodules were detected with Alizarin Red staining (section 2.2.7, page 80). As shown in Figure 6.1*C*, bone nodule formation was diminished in cultures from *CNR2*$^{-/-}$ mice when compared with wild type cultures. This was not a consequence of difference in cell numbers between wild type and *CNR2*$^{-/-}$ bone marrow osteoblast cultures as shown in Figure 6.1*D*.
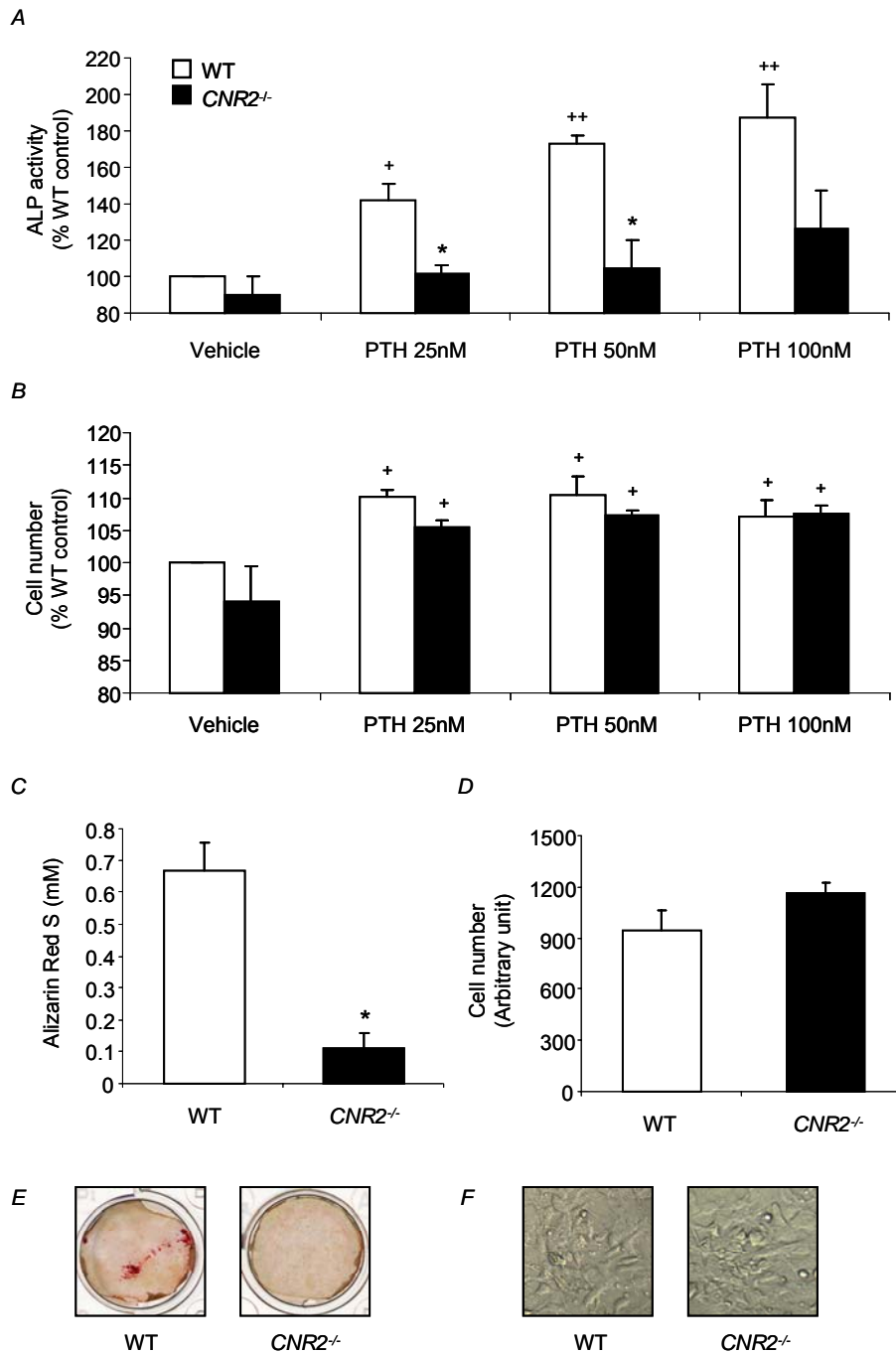
Figure 6.1: Bone marrow osteoblasts from CNR2-deficient mice have reduced ALP activity and defective bone nodule formation. *A*. Alkaline phosphatase (ALP) activity of bone marrow osteoblasts from wild type and *CNR2*^{-/-} mice exposed to PTH (25-100nM) for 24 hours, assessed by ALP assay. ALP levels were normalised to cell number and expressed as a percent of values in wild type vehicle-treated cultures. *B*. Number of bone marrow osteoblasts from cultures in *A*, assessed by Alamar Blue assay. Changes in osteoblast number were expressed as a percent of values in wild type vehicle-treated cultures. *C*. Quantification of Alizarin Red concentration from bone nodules of bone marrow osteoblast cultures from wild type and *CNR2*^{-/-} mice, grown in osteogenic medium for 3 weeks. *D*. Number of bone marrow osteoblasts from cultures in *C*, determined by Alamar Blue assay. Representative photomicrographs of mineral staining with Alizarin Red (*E*) and phase contrast images (*F*) of wild type and *CNR2*^{-/-} bone marrow osteoblasts. Values are means ± sem and were obtained from 3 independent experiments. *p < 0.05 from wild type cultures, [+]p < 0.05 and [++]p < 0.005 from vehicle-treated cultures of the same genotype.

188

6.3.2 *Calvarial osteoblasts from CNR2-deficient mice form defective bone nodules*

The role of CNR2 in osteoblast function was also studied in nodule assays using calvarial osteoblasts from wild type and *CNR2*^{-/-} mouse neonates (c.f. section 2.2.5, page 77). Osteoblasts were cultured in osteogenic medium for 3 weeks (c.f. section 2.2.5, page 77) and mineralised nodules were stained with Alizarin Red (section 2.2.7, page 80). Figure 6.2*A,C* shows that *CNR2*^{-/-} calvarial osteoblast cultures formed fewer bone nodules and had a slower nodule formation rate over the period of 3 weeks, compared to wild type cultures. Alamar Blue assay showed that osteoblast numbers in wild type and *CNR2*^{-/-} cultures did not vary significantly ruling out the possibility that the difference in nodule formation was secondary to a difference in cell number (Figure 6.2*B*).
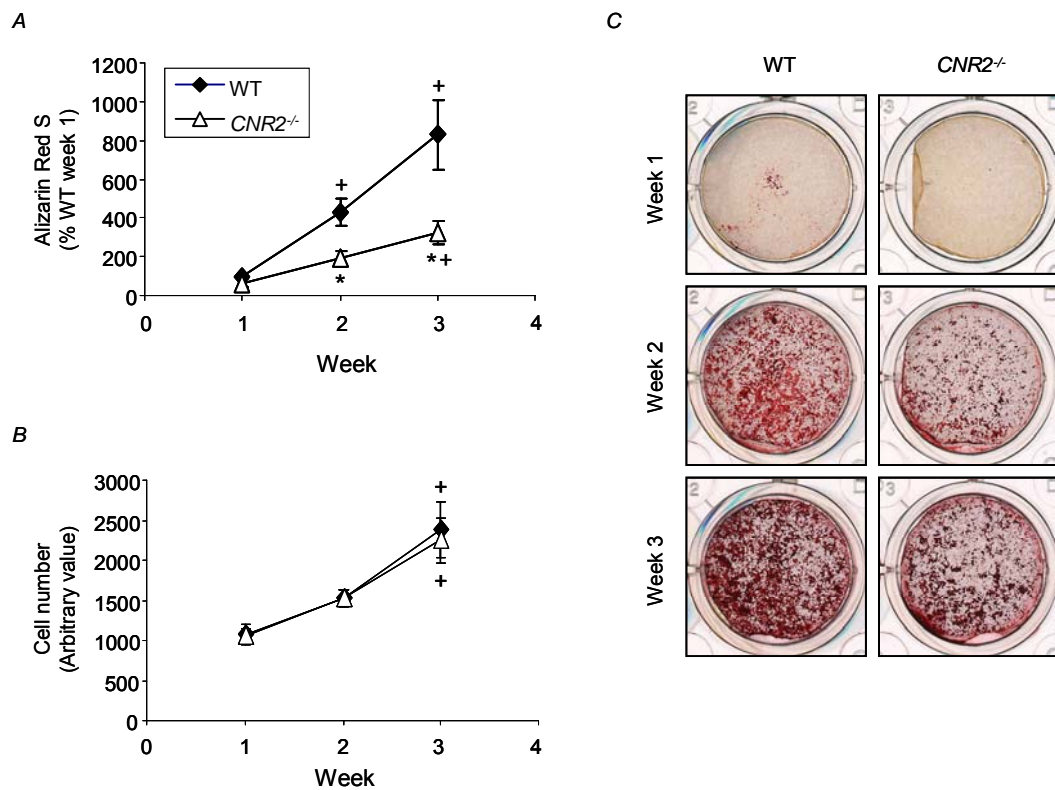
Figure 6.2: Calvarial osteoblasts from CNR2-deficient mice form defective bone nodules.
A. Quantification of Alizarin Red staining concentration from bone nodules of calvarial osteoblasts from wild type and *CNR2*^{-/-} neonates, grown in osteogenic medium over the period of 3 weeks. Changes in Alizarin Red staining concentration were expressed as a percent of values in wild type (WT)-week 1 cultures. *B*. Number of calvarial osteoblasts in bone nodule cultures from wild type and *CNR2*^{-/-} neonates, assessed by Alamar Blue assay. Changes in osteoblast number were normalised to those of wild type-week 1 cultures. *C*. Representative photomicrographs of mineral staining with Alizarin Red. Values are means ± sem and were obtained from 3 independent experiments. *p < 0.05 from wild type cultures, [+]p < 0.05 from week 1 cultures of same genotype.

6.3.3 *Nodule formation by calvarial osteoblasts from CNR2-deficient mice is defective as a result of defective osteoblast differentiation*

To investigate the role of CNR2 on osteoblast differentiation, calvarial osteoblasts isolated from wild type and *CNR2$^{-/-}$* mouse neonates (c.f. section 2.2.5, page 77) were cultured in 4 different cell seeding densities (50, 100, 200 and 300 x 10^3 cells/well) in 12-well plates, with 50μg/ml Vitamin C and 3mM β-GP (osteogenic medium) for the period of 3 weeks. Bone nodule formation was detected with Alizarin Red staining (c.f. section 2.2.7, page 80).

As shown in Figure 6.3*A*, *CNR2$^{-/-}$* osteoblast cultures starting from a low seeding density, such as 50 or 100 x 10^3 cells/well, had defective nodule formation compared to wild type osteoblast cultures. However, *CNR2$^{-/-}$* cultures starting with higher seeding densities than 100 x 10^3 cells/well, that is at 200 and 300 x 10^3 cells/well, had normal nodule formation (Figure 6.3*A*). These results suggest that at low seeding densities, when cells were at a sub-confluent state, *CNR2$^{-/-}$* calvarial osteoblasts were slower in differentiating to matrix-secreting osteoblasts than wild type osteoblasts. However, when cells were seeded at higher and nearly confluent seeding densities, matrix deposition occurred simultaneously in wild type and *CNR2$^{-/-}$* cultures, allowing *CNR2$^{-/-}$* osteoblasts to form bone nodules at the same extent as wild type osteoblasts. Alamar Blue assay showed that after 3 weeks, all cultures had similar cell number regardless of the initial cell seeding density (Figure 6.3*B*), suggesting that the variability in nodule formation was not due to difference in cell number.

Together these data indicate that calvarial osteoblasts from *CNR2$^{-/-}$* mice experience defective differentiation which leads to defective nodule formation.
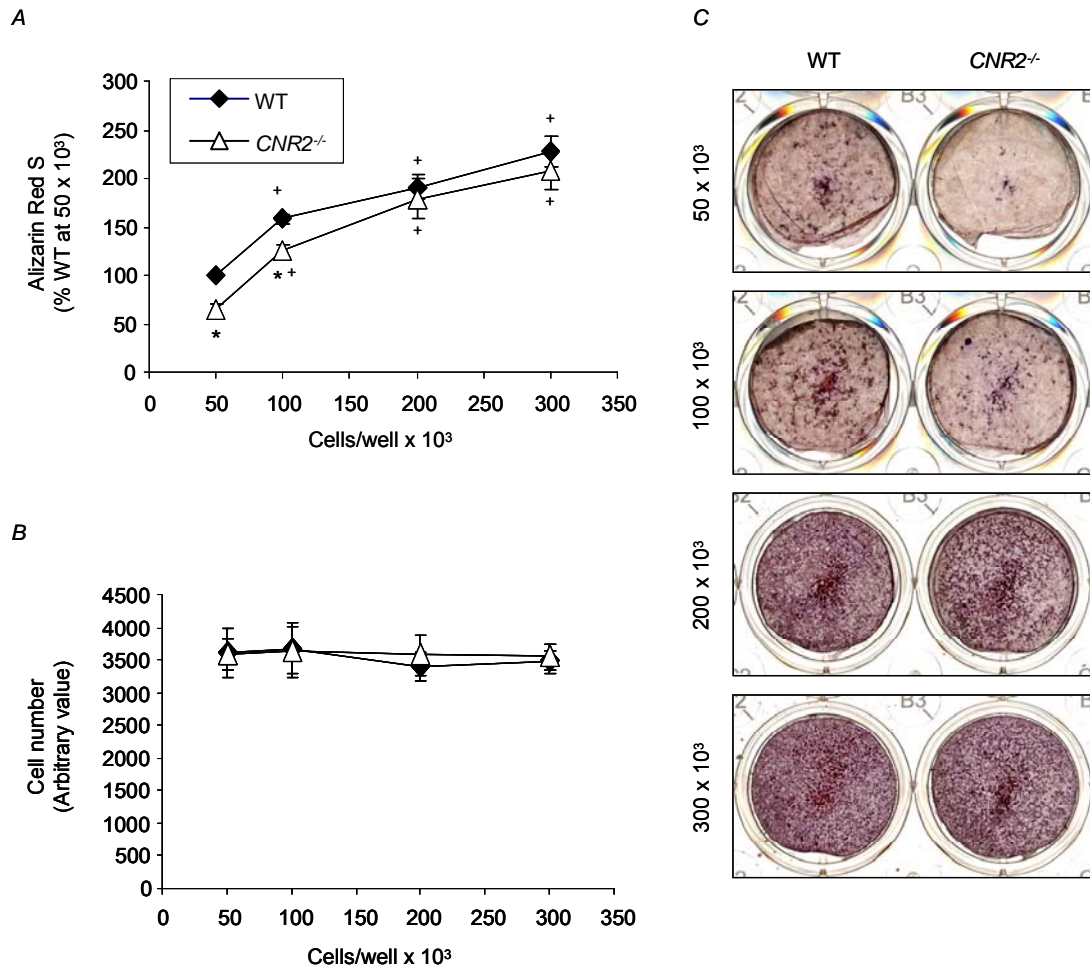
Figure 6.3: Calvarial osteoblasts from CNR2-deficient mice are defective in differentiation. *A*. Quantification of Alizarin Red staining concentration from bone nodules of calvarial osteoblasts from wild type and *CNR2*^{-/-} mouse neonates at different seeding densities (50, 100, 200 and 300 x 10^3 cells/well in 12-well plates), grown in osteogenic medium for 3 weeks. Changes in Alizarin Red staining concentration were expressed as a percent of values in wild type (WT) cultures at 50 x 10^3 cells/well seeding density. *B*. Number of calvarial osteoblasts in bone nodule cultures from wild type and *CNR2*^{-/-} mice at different seeding densities, assessed by Alamar Blue assay. *C*. Representative photomicrographs of cultures in *A*, stained with Alizarin Red. Values are means ± sem and were obtained from 3 independent experiments. *$p < 0.05$ from wild type cultures, [+]$p < 0.05$ from cultures at 50 x 10^3 cells/well seeding density of same the genotype.

191

6.3.4   Cannabinoid receptor ligands do not affect calvarial osteoblast differentiation or growth

To examine the effect of cannabinoid receptor ligands on osteoblast differentiation or growth, calvarial osteoblasts isolated from wild type neonates (c.f. section 2.2.5, page 77) were cultured for 72 hours and then exposed to the CNR2-selective agonists, HU308 and JWH133, the endocannabinoids, AEA and 2-AG, and the cannabinoid receptor antagonists/inverse agonists, AM251 and AM630, at concentrations varying from 0.5nM to 1μM, for 24 hours (c.f. section 2.2.5, page 77). Osteoblast differentiation and growth were investigated, using the Alkaline phosphatase (ALP) assay (c.f. section 2.2.9, page 81) and Alamar Blue assay (c.f. section 2.2.8, page 80), respectively.

As shown in Figure 6.4*A,B*, none of the cannabinoid receptor agonists, HU308, JWH133, AEA or 2-AG, had an effect on osteoblast ALP levels and hence differentiation, throughout the entire concentration range. The CNR2-selective antagonist/inverse agonist AM630, also did not affect the ALP activity (and hence differentiation) of osteoblasts at all concentrations tested (Figure 6.4*C*). Although nanomolar concentrations of AM251 also did not have an effect on osteoblast ALP levels, at 1μM, AM251 significantly reduced ALP activity and thus differentiation of calvarial osteoblasts as shown in Figure 6.4*C*. The significance of these results is still to be determined. Alamar Blue assay performed on the same cultures showed that the CNR2-selective agonists HU308 and JWH133, the endocannabinoids AEA and 2-AG, and the cannabinoid receptor antagonists/inverse agonists AM251 and AM630, did not have an effect on osteoblast number at any of the concentrations tested (Figure 6.5).

The cannabinoid receptor ligands HU308, JWH133, AEA and AM630, did not have an effect on differentiation or growth of calvarial osteoblasts from *CNR2*^{-/-} mice either, shown by the ALP assay and Alamar Blue assay performed simultaneously on calvarial osteoblasts from wild type and *CNR2*^{-/-} mice (Appendix 9, pages 281).
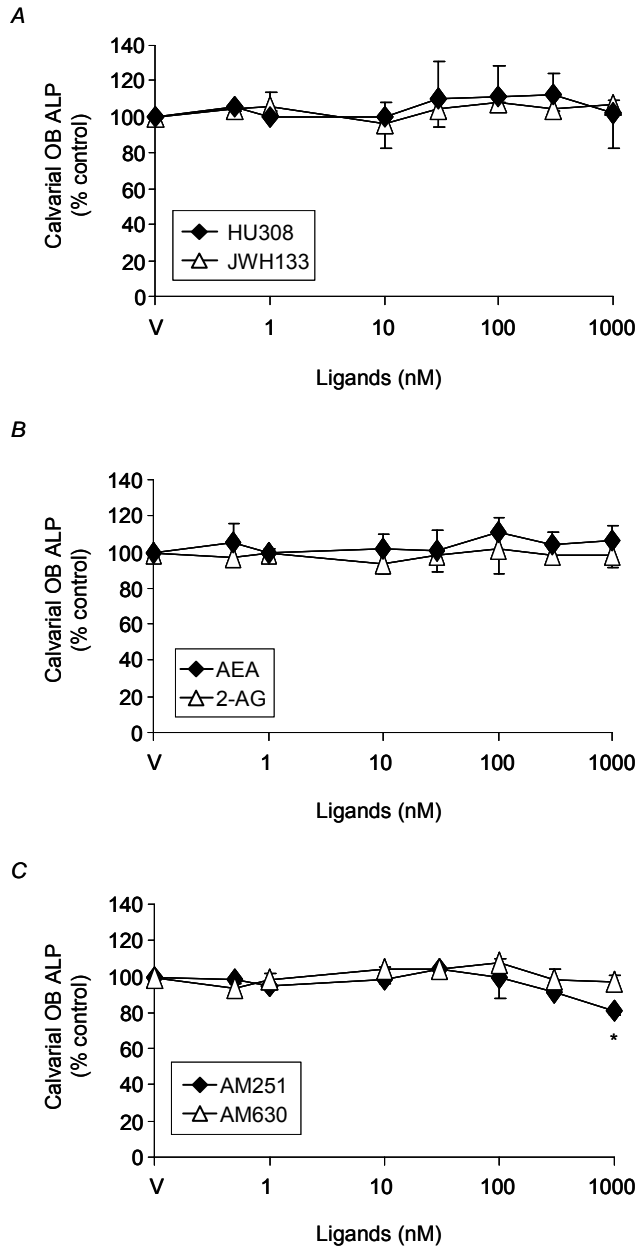
Figure 6.4: Effect of cannabinoid receptor ligands on ALP activity of calvarial osteoblasts. *A*. Osteoblast (OB) ALP activity in cultures exposed to vehicle (V), HU308 or JWH133, at the indicated concentrations for 24 hours. ALP levels were normalised to cell number and expressed as a percent of values in vehicle-treated cultures. Osteoblast ALP activity in cultures exposed to vehicle, AEA or 2-AG (*B*), or to vehicle, AM251 or AM630 (*C*), from similar experiments, expressed in the same way. Values are means ± sem and were obtained from 3 independent experiments. *p < 0.05 from vehicle-treated cultures.

193
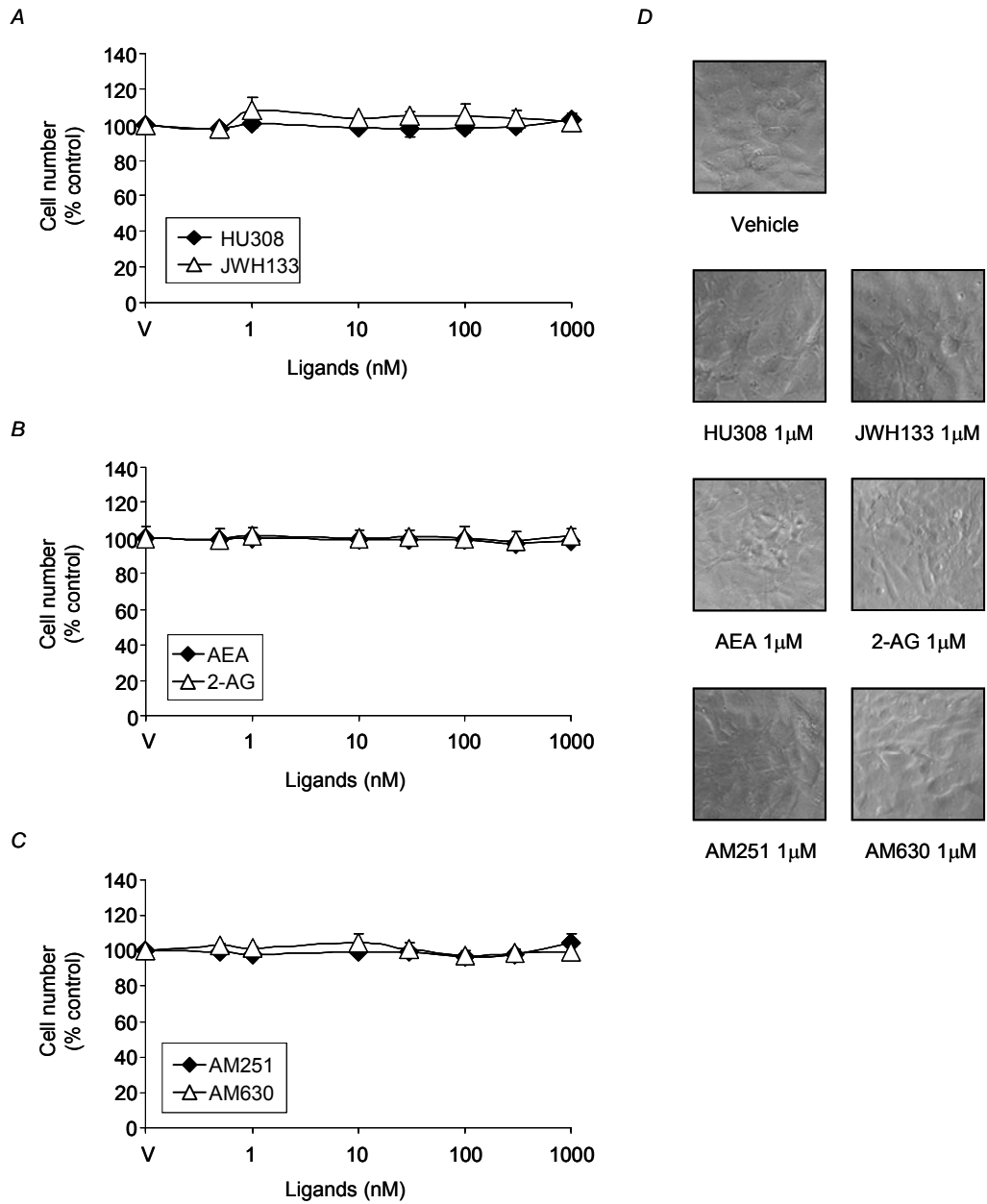
Figure 6.5: Effect of cannabinoid receptor ligands on calvarial osteoblast number. *A*. Osteoblast number in cultures exposed to vehicle (V), HU308 or JWH133, at the indicated concentrations for 24 hours. Changes in number were expressed as a percent of values in vehicle-treated cultures. Osteoblast number in cultures exposed to vehicle, AEA or 2-AG (*B*), or to vehicle, AM251 or AM630 (*C*), from similar experiments, expressed in the same way. *D*. Representative phase contrast photomicrographs from the cultures in *A*, *B*, and *C*. Values are means ± sem and were obtained from 3 independent experiments.

6.3.5 Cannabinoid receptor agonists stimulate nodule formation in calvarial osteoblast cultures

To investigate the effect of cannabinoid receptor agonists on osteoblast function, calvarial osteoblasts (100 x 10^3 cells/well in 12-well plates) were cultured in 50μg/ml Vitamin C and 3mM β-GP (osteogenic medium) and exposed to cannabinoid receptor ligands (10 - 100nM) for up to 3 weeks (c.f. section 2.2.5, page 77). As shown in Figure 6.6, treatment of calvarial osteoblasts with the endocannabinoid AEA, or the CNR2-selective agonists, HU308 and JWH133, at a concentration range of 10-100nM, stimulated bone nodule formation by 10-34% with AEA ($p<0.05$), 28-48% with HU308 ($p<0.05$) and 9-20% with JWH133 ($p<0.05$) (Figure 6.6*A*). In contrast, the CNR2-selective cannabinoid receptor antagonist/inverse agonist AM630, had no significant effect in nodule formation (Figure 6.6*A*). Alamar Blue assay showed that these cultures had equal number of osteoblasts (Figure 6.6*B*) indicating that the increase in nodule formation with cannabinoid receptor agonists was due to a stimulatory effect on osteoblast function, rather than cell number.
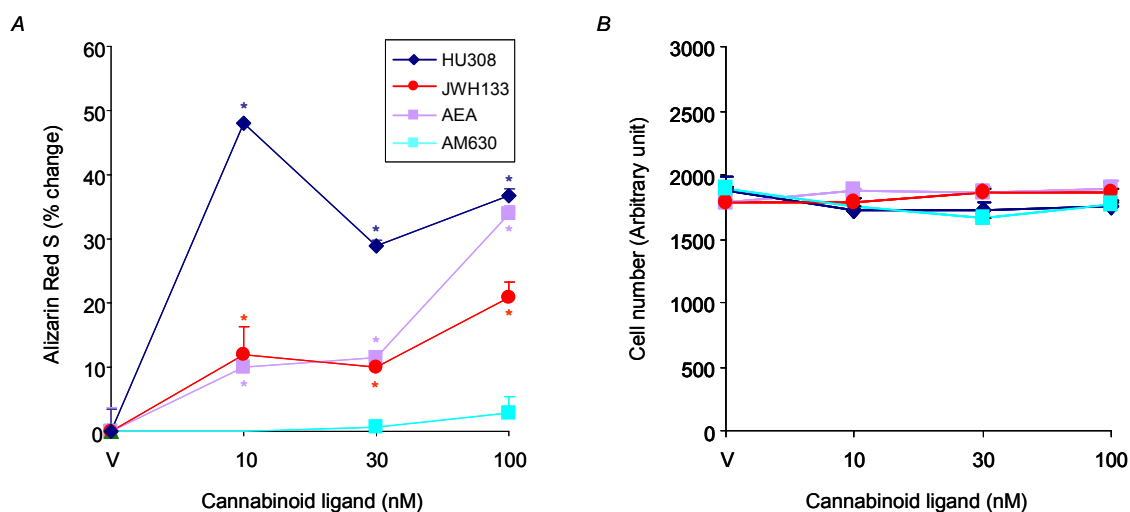
Figure 6.6: Effect of cannabinoid receptor ligands on bone nodule formation from calvarial osteoblasts. *A*. Quantification of Alizarin Red staining concentration of stained bone nodules from calvarial osteoblast cultures grown in osteogenic medium and exposed to vehicle (V), AEA, HU308, JWH133 and AM630 at the indicated concentrations for 3 weeks. Changes in concentration were expressed as percent changes from vehicle-treated cultures. *B*. Number of osteoblasts in cultures from *A*, assessed by Alamar Blue assay. This is only a representative experiment. Identical experiments were repeated 3 times. Values are means ± sd. *$p < 0.05$ from vehicle-treated cultures.

6.3.6 Effect of cannabinoid receptor agonists on bone nodule formation in calvarial osteoblast cultures from wild type and CNR2-deficient mice

To investigate whether the effects of cannabinoid receptor agonists on osteoblast function were mediated via the CNR2, bone nodule formation was assessed in cultures generated from wild type and $CNR2^{-/-}$ mouse neonates (c.f. section 2.2.5, page 77). These cultures were maintained in medium supplemented with 50μg/ml Vitamin C and 3mM β-GP (osteogenic medium) and exposed to cannabinoid receptor agonists (10 and 30nM) for up to 3 weeks (c.f. section 2.2.5, page 77).

The CNR2-selective agonists, HU308 and JWH133, stimulated nodule formation in wild type calvarial osteoblast cultures from concentrations as low as 10nM (Figure 6.7). The stimulatory effects of both CNR2-selective agonists on nodule formation at 10nM concentration, were blunted in osteoblast cultures from $CNR2^{-/-}$ mouse neonates (Figure 6.7A,B,E,F). These results suggest that the stimulatory effect of HU308 (10nM) and JWH133 (10nM) on nodule formation and hence osteoblast function were mediated via the CNR2. Treatment of $CNR2^{-/-}$ osteoblast cultures with HU308 at a concentration of 30nM, significantly increased bone nodule formation, yet to a lesser extent than in wild type cultures ($p < 0.05$) (Figure 6.7A). Alamar Blue assay confirmed that cell numbers of wild type and $CNR2^{-/-}$ osteoblast cultures were comparable at all times (Figure 6.7C,D).
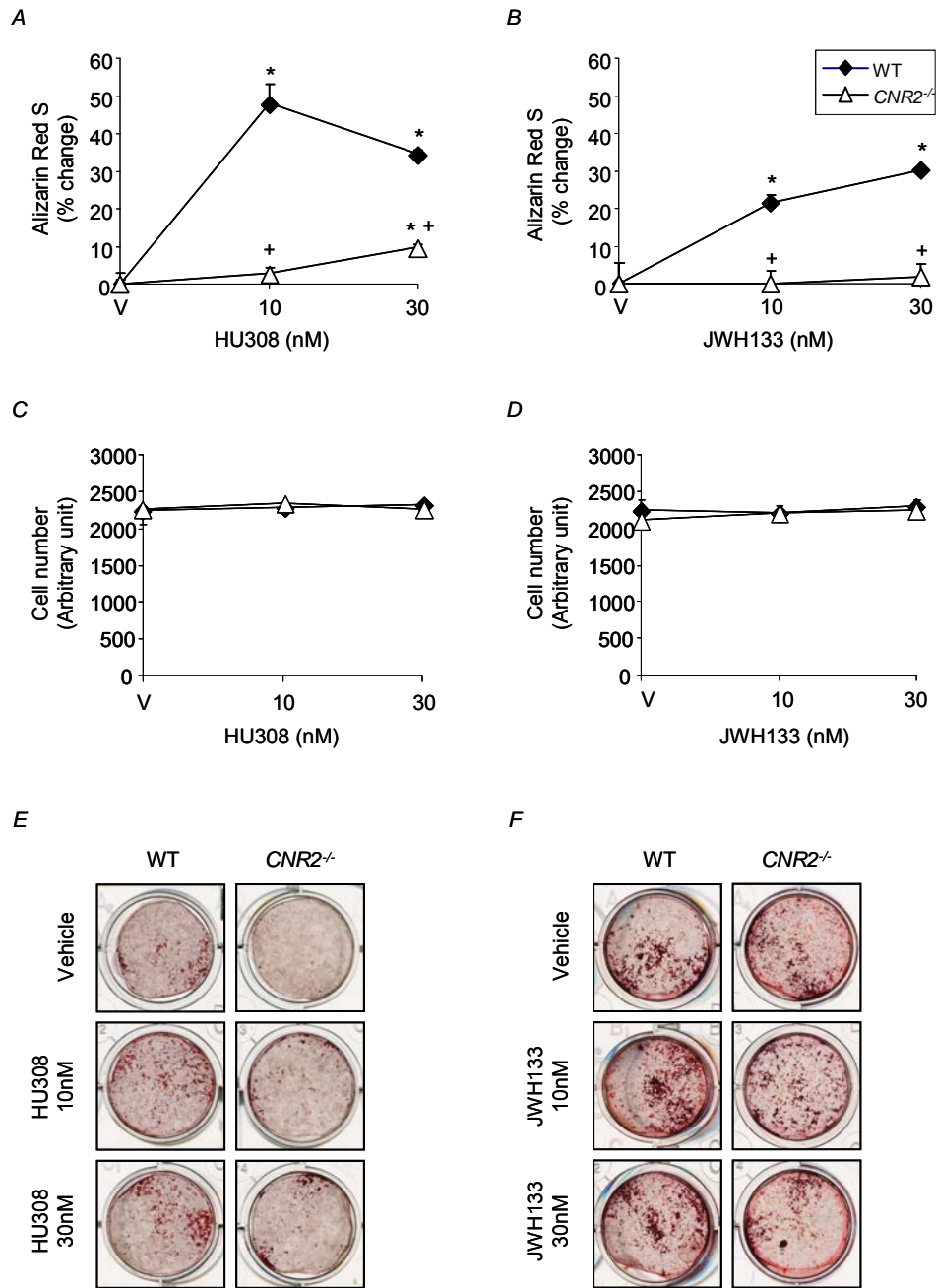
Figure 6.7: Effect of CNR2-selective agonists on nodule formation in calvarial osteoblast cultures from wild type and CNR2-deficient mice. *A,B*. Quantification of Alizarin Red staining concentration of bone nodules from wild type and *CNR2*^{-/-} calvarial osteoblast cultures grown in osteogenic medium and exposed to vehicle (V), HU308 (*A*) or JWH133 (*B*) at the indicated concentrations for 3 weeks. Changes in concentration were expressed as percent changes from vehicle-treated cultures. *C,D*. Number of osteoblasts in cultures from *A* and *B*, assessed by Alamar Blue assay. *E,F*. Representative photomicrographs of mineral staining with Alizarin Red from cultures in *A* and *B*. These are only representative experiments. Identical experiments were repeated 3 times. Values are means ± sd. *p < 0.05 from vehicle-treated cultures of same genotype, [+]p < 0.05 from wild type cultures with the same treatment.

Nodule-forming cultures were also treated with the endocannabinoid AEA. In contrast to HU308 and JWH133 that had an effect mainly on wild type osteoblasts, AEA stimulated bone nodule formation in both wild type and $CNR2^{-/-}$-derived calvarial osteoblast cultures (Figure 6.8*A,C*). This is probably due to the fact that AEA activates both cannabinoid receptors (Appendix 4, page 275), and is likely to enhance mineralisation via CNR1 and CNR2. These cultures had equal numbers of osteoblasts as shown by the Alamar Blue assay (Figure 6.8*B*) and therefore the increase in nodule formation was due to an effect on osteoblast function, rather than cell number.
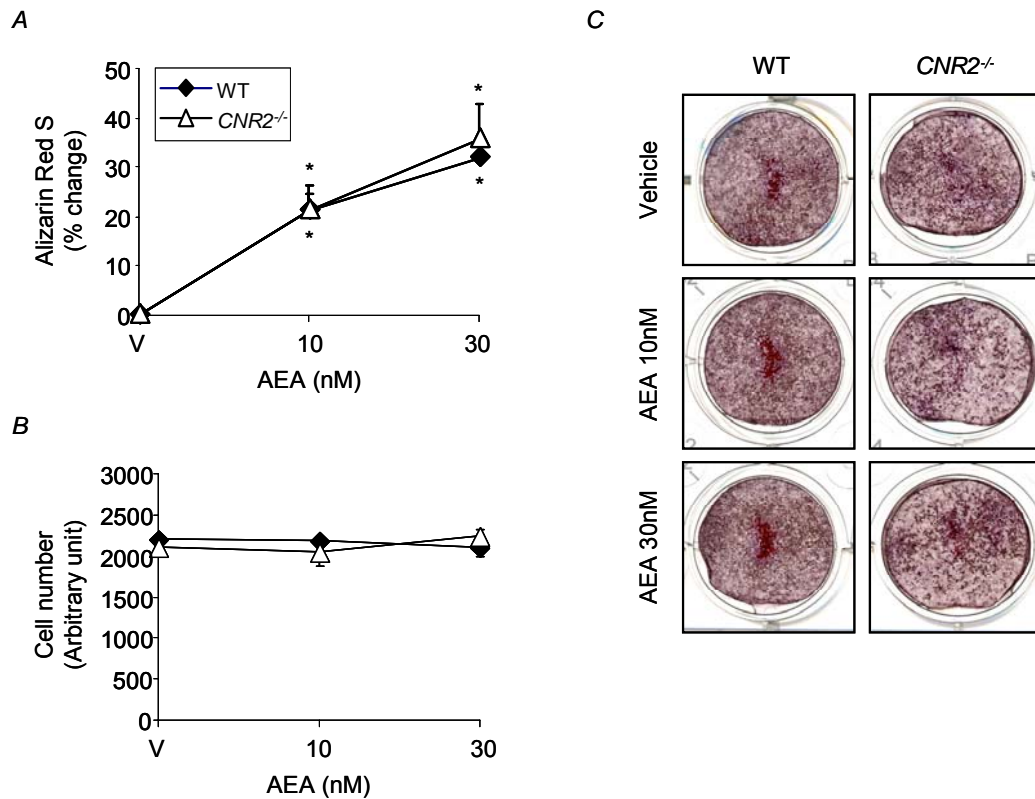
Figure 6.8: Effect of the endocannabinoid AEA on nodule formation in calvarial osteoblast cultures from wild type and CNR2-deficient mice. *A*. Quantification of Alizarin Red staining concentration of bone nodules from wild type and $CNR2^{-/-}$ calvarial osteoblast cultures grown in osteogenic medium and exposed to vehicle (V) and AEA at the indicated concentrations for 3 weeks. Changes in concentration were expressed as percent changes from vehicle-treated cultures. *B*. Number of osteoblasts in cultures from *A*, assessed by Alamar Blue assay. *C*. Representative photomicrographs of mineral staining with Alizarin Red from cultures in *A*. This is only a representative experiment. Identical experiments were repeated 3 times. Values are means ± sd. *$p < 0.05$ from vehicle-treated cultures of same genotype.

6.3.7   Effect of the CNR2-selective agonist HU308, on ovariectomy-induced bone loss

To investigate the role of CNR2 activation on osteoblast function and bone formation *in vivo*, 8-week old wild type and *CNR2*$^{-/-}$ female mice were subjected to ovariectomy (c.f. section 2.5.4, page 97), and then treated with the CNR2-selective agonist HU308 (intraperitoneal injections) at daily doses of 0.1 and 1.0mg/kg for 3 weeks (c.f. section 2.5.5, page 97). Mice received also two calcein injections 4 days apart towards the end of the treatment period (c.f. section 2.5.5, page 97). Mice were then sacrificed and μCT analysis was performed on isolated tibiae (c.f. section 2.5.8, page 99).

CNR2-selective agonist HU308, protects from ovariectomy-induced bone loss

As shown in Figure 6.9, treatment of wild type mice with the CNR2-selective agonist HU308, at a dose of 0.1 and 1.0mg/kg partially prevented ovariectomy induced bone loss in a dose-dependent manner. These mice lost 34% and 51% less (p < 0.05) trabecular bone volume than the vehicle-treated group, when treated with 0.1 and 1.0mg/kg of HU308 respectively (Figure 6.9*A*).

Conversely, *CNR2*$^{-/-}$ mice were resistant to the protective effects of HU308 at 0.1mg/kg, but responded moderately to the higher dose of HU308 at 1.0mg/kg. Although the maximal rescue of trabecular bone loss in these mice was about 50% when compared to the vehicle-treated group, such rescue did not achieve statistical significance, most likely due to high variability between samples (Figure 6.9*A*).
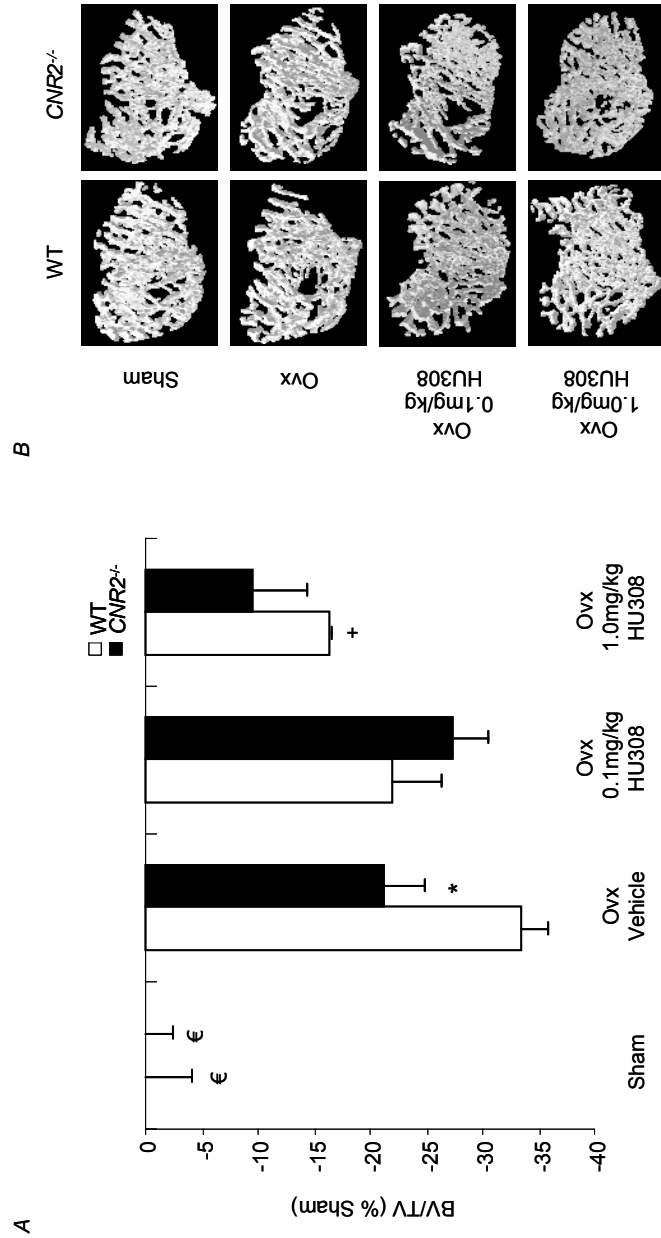
Figure 6.9: Effect of HU308 on ovariectomy-induced bone loss in wild type and CNR2-deficient mice. *A.* Trabecular bone volume (BV/TV) in wild type and *CNR2-/-* mice subjected to ovariectomy or sham operation and treated with vehicle or HU308 (0.1 and 1.0mg/kg) for 3 weeks, assessed by μCT analysis. Changes in trabecular bone volume were normalised to those in wild type sham-operated mice and expressed as percent change. *B.* Representative μCT images from the tibial metaphysis of wild type and *CNR2-/-* mice, from A. Values are means ± sem from 7-8 mice per group. *p < 0.05 from wild type mice, +p < 0.05 from ovariectomised, vehicle-treated mice of the same genotype, €p < 0.05 from all ovariectomised groups of the same genotype.

Further μCT analysis showed that the loss of trabecular thickness across all wild type ovariectomised groups did not significantly vary (Figure 6.10*A*). However, the loss of trabecular number among wild type groups was reduced with HU308 treatment, in a dose-dependant manner (Figure 6.10*B*). Accordingly, trabecular separation in wild type mice was also rescued in a similar manner. At 0.1mg/kg, HU308 reduced trabecular separation to levels that were no longer significantly different from sham-operated controls and at 1.0mg/kg of HU308 trabecular separation was significantly lower than in vehicle-treated mice (Figure 6.10*C*). Overall, HU308 significantly increased trabecular connectivity, indicated by the dose-dependant decrease in trabecular pattern factor (Figure 6.10*D*).

Treatment of *CNR2*$^{-/-}$ ovariectomised mice with HU308 had simply subtle effects on trabecular parameters. Although HU308 did not significantly rescue trabecular number compared to vehicle-treated controls, at high dose of 1.0mg/kg HU308 reserved trabecular number to levels that were not significantly different from sham-operated mice (Figure 6.10*B*). However, this was not accompanied by any changes in trabecular separation (Figure 6.10*C*). Although there was a trend towards reduced loss in trabecular thickness of *CNR2*$^{-/-}$ mice treated with 1.0mg/kg HU308, this was not statistically significant (Figure 6.10*A*). Finally, HU308 did not have an effect on trabecular pattern factor of *CNR2*$^{-/-}$ mice, which was already significantly lower than wild type vehicle-treated mice, indicating better trabecular connectivity (Figure 6.10*D*).

The actual values of all μCT parameters for the trabecular bone analysis of ovariectomised and sham-operated wild type and *CNR2*$^{-/-}$ female mice treated with the CNR2-selective agonist HU308 are shown in Appendix 10, page 282.
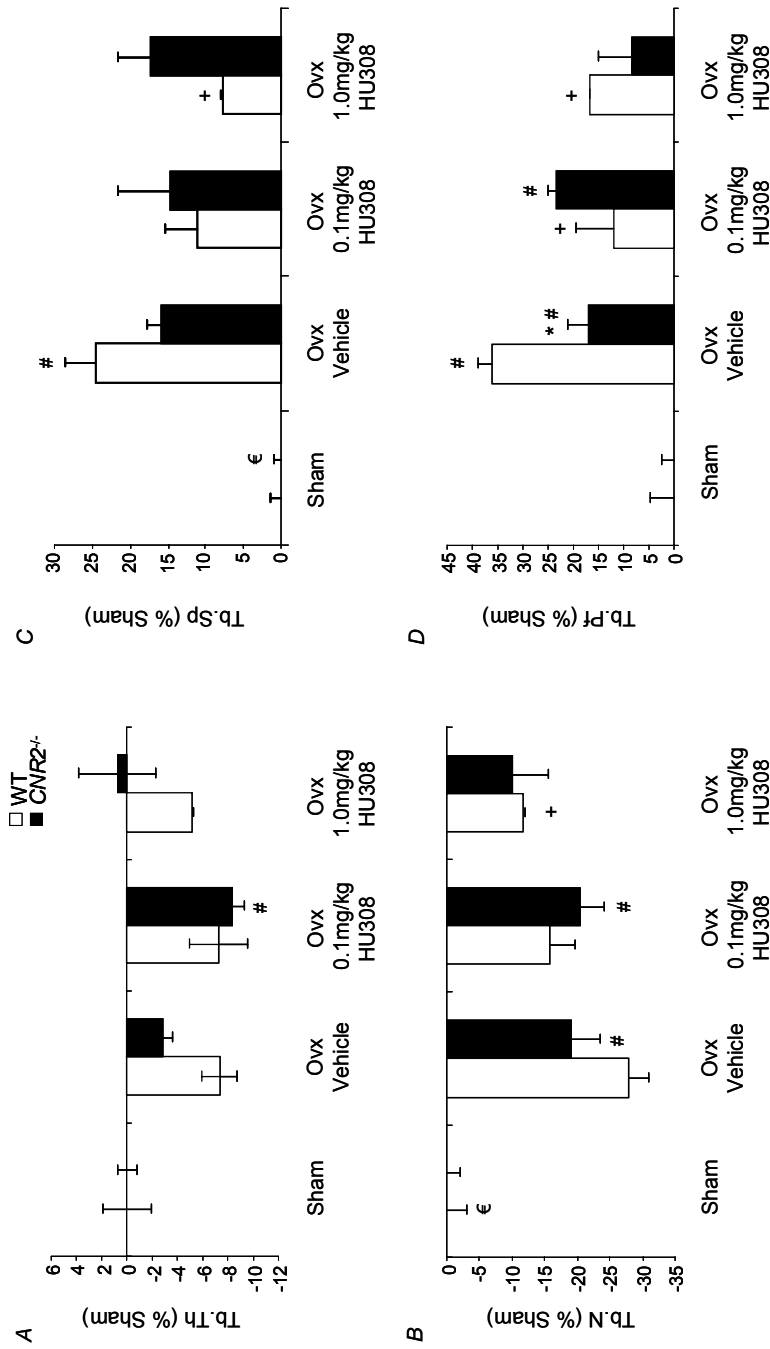
Figure 6.10: Effect of HU308 on other parameters of trabecular bone following ovariectomy in wild type and CNR2-deficient mice. *A*. Trabecular thickness (Tb.Th) in wild type and *CNR2⁻/⁻* littermates subjected to ovariectomy or sham operation and treated with vehicle or HU308 (0.1 and 1.0mg/kg) for 3 weeks, assessed by µCT analysis. Changes in trabecular thickness were normalised to those in sham-operated mice of the same genotype and expressed as percent change. Trabecular number (Tb.N) (*B*), trabecular separation (Tb.Sp) (*C*), and trabecular pattern factor (Tb.Pf) (*D*) of the same experiment, expressed in the same way. Values are means ± sem from 7-8 mice per group. *p < 0.05 from wild type mice, ⁺p < 0.05 from ovariectomised, vehicle-treated mice of the same genotype, #p < 0.05 from sham-operated mice of the same genotype, ᵋp < 0.05 from all ovariectomised groups of the same genotype.

CNR2-selective agonist HU308 does not have an effect on cortical bone of ovariectomised wild type and CNR2-deficient mice

To investigate the role of CNR2 activation on cortical bone, μCT analysis (c.f. section 2.5.8, page 99) was also performed at the proximal diaphysis of tibiae isolated from wild type and *CNR2*^{-/-} mice subjected to ovariectomy and treatment with the CNR2-selective agonist HU308 (0.1 and 1.0mg/kg) for 3 weeks.

μCT analysis showed that although there was a trend towards increased cortical bone volume (Ct.BV) in wild type mice treated with HU308 compared to vehicle-treated ovariectomised mice, this was not statistically significant (Figure 6.11*A*). However, HU308 at 0.1mg/kg increased cortical bone volume to levels that were significantly different from sham-operated controls (Figure 6.11*A*). Cortical bone volume in *CNR2*^{-/-} mice did not vary at all with HU308, but at 0.1mg/kg HU308 treatment cortical bone volume was significantly lower than in wild type mice (Figure 6.11*A*). Cortical thickness (Ct.Th) and medullary cavity diameter (Med.Cav.Dm) of wild type mice did not change with HU308 treatment, contrasting what was previously published (Ofek et al., 2006) (Figure 6.11*B,C*). Although there was a trend towards reduced cortical thickness and increased medullary cavity diameter in *CNR2*^{-/-} mice treated with 0.1mg/kg HU308 compared to vehicle-treated ovariectomised *CNR2*^{-/-} mice, this was not statistically significant (Figure 6.11*B,C*). However, the medullary cavity diameter of *CNR2*^{-/-} mice treated with 0.1mg/kg HU308 was significantly higher than in wild type mice (Figure 6.11*C*). Overall, cortical diameter did not change with HU308 treatment neither in wild type nor in *CNR2*^{-/-} mice (Figure 6.11*D*).

The actual values of all μCT parameters for cortical bone analysis of ovariectomised and sham-operated wild type and *CNR2*^{-/-} female mice treated with the CNR2-selective agonist HU308 are shown in Appendix 11, page 283.
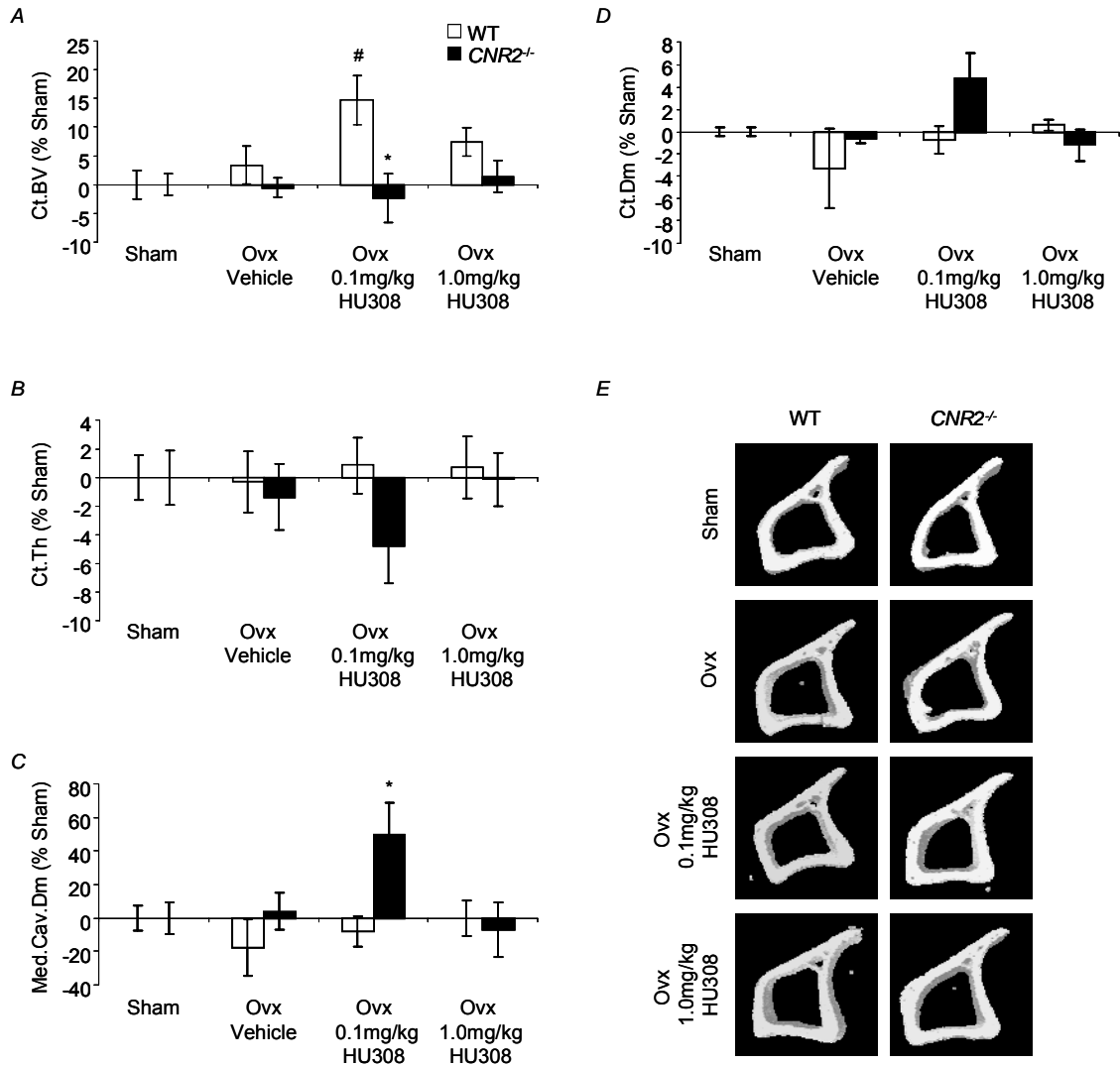
Figure 6.11: Effect of HU308 on cortical bone of wild type and CNR2-deficient mice following ovariectomy. *A*. Cortical bone volume at the proximal diaphysis in wild type and *CNR2^{-/-}* littermates subjected to ovariectomy or sham operation and treated with vehicle or HU308 (0.1 and 1.0mg/kg) for 3 weeks, assessed by μCT analysis. Changes in cortical bone volume were normalised to those in sham operated mice of the same genotype and expressed as percent change. Cortical thickness (Ct.Th) (*B*), medullary cavity diameter (Med.Cav.Dm) (*C*) and cortical diameter (Ct.Dm) (*D*) of the same experiment, expressed in the same way. *D*. Representative μCT images from the proximal diaphysis of wild type and *CNR2^{-/-}* mice of this experiment. Values are means ± sem from 7-8 mice per group. *p < 0.05 from wild type mice [#]p < 0.05 from sham-operated mice of the same genotype.

6.3.8 CNR2-selective agonist HU308 partially rescues ovariectomy-induced bone loss by increasing osteoblast numbers

Bone histomorphometric analysis (c.f. section 2.5.9, page 103) at the trabecular compartment of tibial metaphyses confirmed that HU308 rescued ovariectomy-induced bone loss only in wild type mice, whereas *CNR2*$^{-/-}$ mice were not responsive to its protective effects even at 1.0mg/kg HU308 (Table 6.1). Furthermore, histomorphometry showed that osteoblast numbers increased with HU308 treatment in wild type ovariectomised mice, while in *CNR2*$^{-/-}$ mice osteoblast numbers were not significantly different from vehicle-treated controls. Although osteoclast numbers and active resorption surfaces were slightly reduced in HU308-treated wild type groups, these changes were not significantly different from vehicle-treated controls (Table 6.1). Surprisingly, osteoclast numbers and active resorption surfaces were significantly increased in *CNR2*$^{-/-}$ mice treated with 1.0mg/kg HU308, but this is a non-CNR2 mediated effect (Table 6.1).

Dynamic histomorphometric analysis showed that although there was a trend towards increased mineral apposition rate (MAR) with 1.0mg/kg HU308 treatment in wild type mice, such increased did not achieve statistical significance. Nonetheless, there was a concentration-dependant increase in bone formation rate (BFR) with HU308 treatment in wild type mice but not in *CNR2*$^{-/-}$ mice, consistent with a CNR2-mediated effect (Table 6.1).

These data together suggest that HU308 partially protects from ovariectomy-induced bone loss, most likely by promoting osteoblast differentiation from precursors rather than stimulating osteoblast function.

		BV/TV (%)	Ob.N/BS (cells/mm)	Oc.N/BS (cells/mm)	Oc.S/BS (%)	MAR (µm/day)	BFR (µm²/µm/day)
WT	SHAM Vehicle	14.3 ± 2.8	16.5 ± 1.4	0.52 ± 0.14	1.4 ± 0.4	3.9 ± 0.3	2.1 ± 0.1
	OVX Vehicle	8.0 ± 0.5	21.9 ± 1.1[a]	0.82 ± 0.18	2.3 ± 0.5	4.6 ± 0.1	2.0 ± 0.05
	OVX HU308 0.1mg/kg	11.6 ± 18	33.9 ± 0.9[a,b]	0.71 ± 0.06	2.0 ± 0.2	4.4 ± 0.1	2.7 ± 0.2
	OVX HU308 1.0mg/kg	12.1 ± 0.8[b]	29.0 ± 0.9[a,b]	0.58 ± 0.09	1.5 ± 0.3	5.0 ± 0.3	2.9 ± 0.1[b]
CNR2−/−	SHAM Vehicle	15.4 ± 0.9	14.6 ± 1.0	0.43 ± 0.05	1.2 ± 0.1	4.3 ± 0.1	2.5 ± 0.04
	OVX Vehicle	9.0 ± 0.9[a]	25.8 ± 2.1[a]	0.60 ± 0.03	1.8 ± 0.2	4.3 ± 0.1	2.1 ± 0.1
	OVX HU308 0.1mg/kg	6.9 ± 1.4[a]	31.4 ± 2.4[a]	0.58 ± 0.12	1.6 ± 0.4	4.8 ± 0.2	2.1 ± 0.2
	OVX HU308 1.0mg/kg	13.1 ± 2.3	25.2 ± 1.3[a,c]	0.85 ± 0.08[a]	2.3 ± 0.3[a]	4.5 ± 0.3	2.4 ± 0.3

Table 6.1: Static and dynamic histomorphometry in wild type and CNR2-deficient mice following ovariectomy (OVX) and HU308 treatment (0.1 and 1.0mg/kg) for 3 weeks. BV/TV, trabecular bone volume (%); Ob.N/BS, osteoblast number/bone surface (cells/mm); Oc.N/BS, osteoclast number/bone surface (cells/mm); Oc.S/BS, osteoclast surface/bone surface (%); MAR, mineral apposition rate (µm/day); BFR, bone formation rate (µm²/µm/day). Values are expressed as means ± sem from 3-6 different samples. [a]$p < 0.05$ from sham-operated mice of the same genotype, [b]$p < 0.05$ from ovariectomised, vehicle-treated mice of the same genotype, [c]$p < 0.05$ from wild type mice undergone the same treatment.

206

CNR2-selective agonist HU308 does not affect body weight gain in ovariectomised mice

To establish whether pharmacological activation of CNR2 with the CNR2-selective agonist HU308, has an effect on body weight gain following ovariectomy, the weight of all mice used in this study was measured before the operation and 3 weeks after when mice were sacrificed. As shown in Figure 6.12, no significant difference in body weight gain was observed between wild type and *CNR2*^{-/-} mice subjected to the same type of operation and same drug treatment (Figure 6.12). However, all groups subjected to ovariectomy had at least a 2-fold increase in body weight gain than sham-operated mice (Figure 6.12).
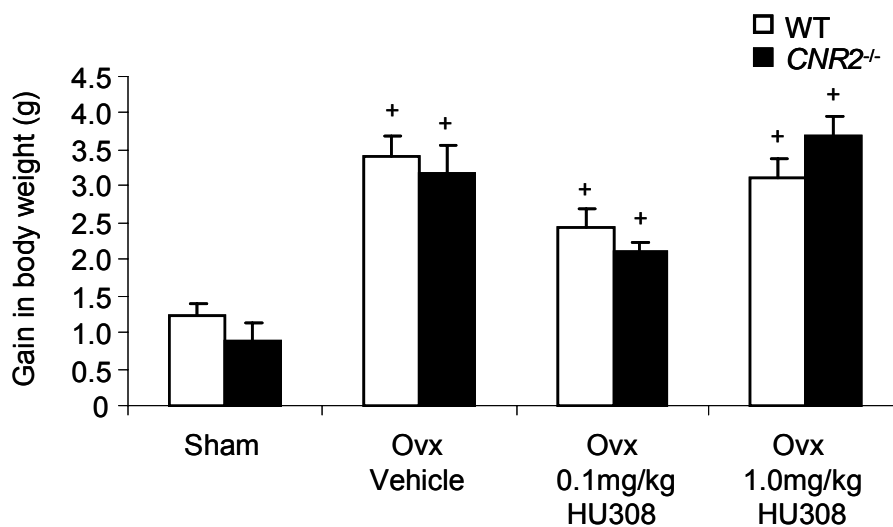
Figure 6.12: Effect of ovariectomy and HU308-treatment on body weight gain in wild type and CNR2-deficient mice. Actual gain in body weight of wild type and *CNR2*^{-/-} mice, treated with vehicle or HU308 (0.1 and 1.0mg/kg), following ovariectomy or sham operation. Values are means ± sem from 7-8 mice per group. [+]p < 0.05 from sham-operated mice of the same genotype.

CNR2-selective agonist HU308 does not affect uterine or spleen weights

The mean uterine weight from ovariectomised mice was reduced by about 75% regardless of genotype compared to the respective sham-operated mice, indicating that ovariectomy was carried out successfully (Figure 6.13*A*). Although operations were carried out without any infections and mice remained healthy throughout the treatment period, two groups of wild type ovariectomised mice had slightly heavier spleens than sham-operated wild type mice, possibly due to inflammation response after surgery (Figure 6.13*B*).
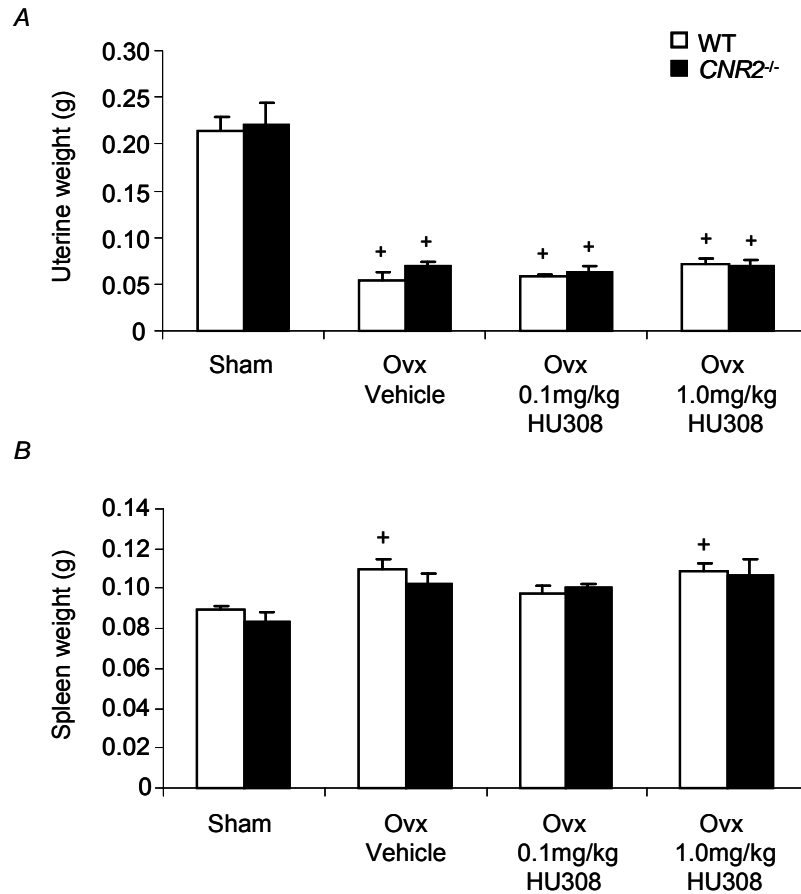
Figure 6.13: Effect of ovariectomy and HU308-treatment on uterine and spleen weights in wild type and CNR2-deficient mice. Weight of uterus (*A*) and spleen (*B*) isolated from wild type and *CNR2*$^{-/-}$ mice subjected to ovariectomy or sham operation and treated with HU308 (0.1 and 1.0mg/kg). Values are means ± sem from 7-8 mice per group. $^+$p < 0.05 from sham-operated mice of the same genotype.

6.4   DISCUSSION

Cannabinoid receptor agonists were previously shown to stimulate osteoclast formation (Idris et al., 2005; Ridge et al., 2007), whereas the CNR2-selective agonist HU308, was reported to inhibit bone resorption and stimulate endocortical bone formation *in vivo* (Ofek et al., 2006). In view of this, the aim of this chapter was to investigate further the role of CNR2 on osteoblast differentiation and function *in vitro* and ovariectomy-induced bone loss *in vivo*.

The study presented here showed that although primary osteoblast from *CNR2*$^{-/-}$ mice have normal growth, they are defective in differentiation. This was portrayed as reduced ALP activity from *CNR2*$^{-/-}$ bone marrow osteoblasts (early-stage differentiated osteoblasts) when cultures were exposed to PTH, and as defective nodule formation from *CNR2*$^{-/-}$ calvarial osteoblasts (mature osteoblasts) starting from low seeding densities. The fact that ALP activity of mature calvarial osteoblasts from *CNR2*$^{-/-}$ mice was no different from wild type osteoblasts (data shown in Appendix 12, page 284) and that *CNR2*$^{-/-}$ osteoblast cultures starting from fully confluent cell layers have normal nodule formation, suggested that CNR2 is involved in osteoblast differentiation. The PTH-resistance of bone marrow-derived osteoblasts from *CNR2*$^{-/-}$ mice compared to wild type osteoblasts, does not mean that PTH has a direct effect on CNR2, but that they may have a common mechanistic pathway. Bearing in mind that both PTH receptor 1 (PTH1R) and CNR2 are G-protein coupled receptors and regulate adenylate cyclase activity, might explain why genetic inactivation of CNR2 on bone marrow-derived osteoblasts, affect their response to PTH. In any case, further work is needed to investigate this.

Activation/inhibition of CNR2 with cannabinoid receptor agonists, such as HU308, JWH133, AEA and 2-AG, and the CNR2-selective antagonist/inverse agonist AM630, did not have a significant effect on osteoblast growth or differentiation. However, the

effect of CNR2-selective agonists on osteoblast proliferation should be assessed by BrdU incorporation assays in addition to Alamar Blue assay, and the effect of these cannabinoid ligands on differentiation should also be studied on early-stage differentiate osteoblasts from bone marrow, using ALP assay. Such experiments will be performed in the near future.

Pharmacological activation of type 2 cannabinoid receptors with the CNR2-selective agonists HU308 and JWH133 and the endocannabinoid AEA, stimulated nodule formation in calvarial osteoblast cultures at concentrations in the nanomolar range. To investigate whether the increase in nodule formation was a CNR2-mediated effect, further studies were performed on nodule-forming cultures from wild type and *CNR2*$^{-/-}$ calvarial osteoblasts. The stimulatory effect of the CNR2-selective ligands HU308 and JWH133 on nodule formation was clearly evident in wild type cultures, but was blunted in *CNR2*$^{-/-}$ calvarial osteoblast cultures. The CNR2-mediated effect of HU308 is consistent with previous work showing that osteoblast proliferation and nodule formation was increased with HU308 treatment only in calvarial osteoblasts cultures from wild type mice (Ofek et al., 2006). Conversely, both wild type and *CNR2*$^{-/-}$ calvarial osteoblast cultures responded to the stimulatory effects of AEA, because AEA behaves as a cannabinoid receptor agonist with affinity for CNR1 and CNR2 (Pertwee and Ross, 2002). It is also likely that the stimulatory effects of AEA on osteoblast function may have been mediated via other G-protein coupled receptors, such as GPR55 (Whyte et al., 2009). The attempt to examine the role of CNR2 receptors in nodule formation using bone marrow-derived osteoblasts isolated from C57BL/6 mice, was not successful since cell layers were too thick and before the end of the third week of treatment they would break or detach from the bottom of the well.

Chapter 5 reported that the CNR2-selective antagonist/inverse agonist AM630 had a protective effect on ovariectomy-induced bone loss due to an inhibitory effect on osteoclasts and bone resorption. Here, the pro-osteoblastic potential of the CNR2-

selective agonist HU308 seen *in vitro*, was also tested in ovariectomised mice to determine whether pharmacological activation of CNR2 can also prevent bone loss resulting from oestrogen deficiency. Administration of HU308 in ovariectomised wild type mice at a dose of 0.1 and 1.0mg/kg partially rescued ovariectomy-induced bone loss in a dose-dependent manner. Further μCT analysis showed that HU308 preserved bone volume, rescued trabecular number and increased trabecular connectivity, consistent with its anabolic effects *in vitro*. Analysis of bone histomorphometry showed that during the period of 3 weeks, HU308 treatment in wild type mice increased osteoblast numbers markedly, while it increased bone formation rate (BFR) slightly and did not significantly change mineral apposition rate (MAR). Considering that MAR reflects the rate at which new bone is deposited (Robling et al., 2001) (and hence osteoblast function), and that BFR depends on MAR and osteoblast surface area (Eklou-Kalonji et al., 1999) (and hence osteoblast number), these results together suggest that *in vivo* pharmacological activation of CNR2 with the agonist HU308, mainly promotes osteoblast differentiation from precursors rather than stimulates osteoblast function. Conversely, *CNR2*^{-/-} mice responded moderately to the protective effects of HU308 even after the high-dose treatment, consistent with a CNR2-mediate effect. These results were in agreement with the *in vitro* data showing that genetic inactivation of CNR2 caused a defective differentiation in *CNR2*^{-/-} bone marrow-osteoblast precursors and defective bone nodule formation from *CNR2*^{-/-} mature osteoblasts at sub-confluent densities.

Moreover, treatment of ovariectomised wild type mice with HU308 slightly reduced osteoclast numbers and bone resorption surfaces, but this effect did not exhibit statistical significance. In contrast, Ofek and colleagues reported that HU308 successfully attenuated trabecular bone loss following ovariectomy by reducing osteoclast-mediated bone resorption (Ofek et al., 2006). The differences observed between the two studies could be explained partly by the different dose of HU308 administered to mice, which in the study by Ofek and colleagues was 10-fold higher (Ofek et al., 2006) than in the study reported here. Taking into account that micromolar concentrations of HU308 may

inhibit osteoclast formation *in vitro* (Chapter 5), it is possible that *in vivo* accumulation of HU308 may display anti-osteoclast qualities, partly explaining the observations reported here and in the Ofek study. Furthermore, the fact that the study by Ofek et al. was performed on C3H mice (Ofek et al., 2006) whereas the mice used here were on a C57BL/6 genetic background, might also have contributed to the differences observed.

Analysis of cortical bone at the proximal diaphysis showed that cortical bone volume, cortical thickness and medullary cavity diameter of tibiae from wild type and *CNR2*^{-/-} mice were not significantly affected by HU308 treatment. This finding, contradicted previous published data by Ofek and colleagues, suggesting that HU308 stimulated endocortical bone formation in femoral diaphysis (Ofek et al., 2006). The fact that cortical analysis in the current study was performed on distinct skeletal sites than in the Ofek study [femurs (Ofek) *vs.* tibiae (current study)], could be the explanation of this discrepancy. In addition, the lack of cortical bone increase with HU308 treatment, opposed well-accepted effects observed with the intermitted treatment of PTH, the anabolic agent used for the management of osteoporosis [reviewed in (Compston, 2007)]. It is likely that continuous and intermitted treatment with HU308 has biphasic effects on bone, as previously exemplified by the case of PTH, where continuous treatment is catabolic while intermittent treatment is anabolic (Tam et al., 1982). Therefore, to investigate further the effects of CNR2-selective agonists on bone mass, ovariectomised mice should also be treated intermittently with HU308. Such treatment may exhibit greater evidence for the *in vivo* anabolic activity of HU308. Finally, in addition to the protective effects of HU308 in preventing bone loss after induced-oestrogen deficiency, the anabolic properties of this agent should be examined in the context of protecting from age-related bone loss. Such experiments will be performed in the near future.

In summary, the results reported in this chapter indicate that type 2 cannabinoid receptors regulate osteoblast differentiation and function *in vitro* and ovariectomy-

induced bone loss *in vivo*. CNR2-selective agonists show evidence of anabolic activity *in vitro* and *in vivo* by a CNR2 mediated pathway. These data suggest that such compounds might be of value as new treatments for osteoporosis.

CHAPTER SEVEN
DISCUSSION AND CONCLUSIONS

7   DISCUSSION AND CONCLUSIONS

Over recent years there has been increasing interest on the role of the endocannabinoid system in the regulation of bone metabolism. Previous studies from our group have shown that mice lacking the type 1 cannabinoid receptors (*CNR1*^{-/-}) had increased bone mass and were resistant to ovariectomy-induced bone loss (Idris et al., 2005). We have also shown that a CNR1-selective antagonist/inverse agonist caused osteoclast inhibition and prevented ovariectomy-induced bone loss in wild type mice (Idris et al., 2005). In contrast with these observations, other workers have reported that type 2 cannabinoid receptor knockout mice (*CNR2*^{-/-}) developed marked age-related osteoporosis, and that a CNR2-selective agonist inhibited osteoclast formation *in vitro* and rescued ovariectomy-induced bone loss *in vivo* (Ofek et al., 2006). In view of this, the aim of this PhD thesis was to investigate further the role of CNR2 in bone metabolism *in vitro* and *in vivo*, using genetic and pharmacological approaches.

Prior to beginning this study, the only indication about the existence of a skeletal endocannabinoid system was limited to findings of our group reporting the expression of type 1 and type 2 cannabinoid receptors in mouse osteoclasts (Idris et al., 2005). As the present CNR2 study was initiated, Ofek and colleagues reported that CNR2 is expressed in bone, in primary bone marrow-derived osteoblasts and osteoclasts as well as in MC3T3 E1 osteoblastic cells and in RAW 264.7 osteoclast-like cells (Ofek et al., 2006). Given that the presence of the cannabinoid receptors in bone microenvironment was well-established, the current CNR2 study was aiming to provide further evidence about the existence of more skeletal endocannabinoid machinery components, such as the enzymes involved in the metabolism of the endocannabinoids AEA and 2-AG. The data presented here demonstrate that apart from the mRNA and protein expression of CNR2 in bone marrow, macrophages, osteoclasts and calvarial osteoblasts, mRNA of enzymes involved in the synthesis (*NAPE-PLD* for AEA and *DAGLα/DAGLβ* for 2-AG) and degradation (*FAAH* for AEA and 2-AG, and *MGL* for 2-AG alone) of endocannabinoids

was also detected in the bone microenvironment at comparable levels to those found in the brain. These findings were in agreement with concurrent studies showing the expression of *DAGLα* and *DAGLβ* in bone, in MC3T3 E1 osteoblastic cells and in RAW 264.7 osteoclast-like cells (Tam et al., 2008), and the expression of *FAAH* and *NAPE-PLD* in cultured human osteoclasts (Rossi et al., 2009). Moreover, the detection of both endocannabinoids in cultured mouse osteoblasts and osteoclasts (Ridge et al., 2007), in bone and MC3T3 E1 osteoblasts (Tam et al., 2008) and in cultured human osteoclasts (Rossi et al., 2009), completed the picture of a skeletal endocannabinoid system.

In order to establish the role of CNR2 in bone development an *in vivo* mouse model of CNR2 deficiency was used. *CNR2$^{-/-}$* mice on a C57BL/6 genetic background were followed throughout their life and their skeletal development was studied using a variety of techniques. μCT analysis showed that *CNR2$^{-/-}$* mice have regular bone volume at 2-days of age and normal peak bone mass compared to wild type littermates. However, when female wild type and *CNR2$^{-/-}$* mice were subjected to ovariectomy-induced oestrogen deficiency, *CNR2$^{-/-}$* mice lost less bone than wild type controls because of a subtle defect in osteoclastic bone resorption. Likewise, the pharmacological blockade of CNR2 with the CNR2-selective antagonist/inverse agonist AM630, prevented ovariectomy-induced bone loss in wild type ovariectomised mice by blocking the increase in osteoclast numbers and bone resorption triggered by ovariectomy. Similar results were previously observed from studies in our group, with *CNR1$^{-/-}$* mice on an ABH genetic background. *CNR1$^{-/-}$* female mice were completely resistant to bone loss induced by ovariectomy, and pharmacological blockade of CNR1 with the CNR1-selective antagonist/inverse agonist AM251, prevented ovariectomy-induced bone loss in wild type mice, by inhibiting osteoclastic bone resorption (Idris et al., 2005). These results together indicate that CNR1 and CNR2 blockade in adult mice prevents ovariectomy-induced bone loss by inhibiting osteoclast formation and bone resorption. In keeping with this, *in vitro* experiments with bone marrow from wild type and *CNR2$^{-/-}$* mice showed that although there was normal growth of M-CSF-generated macrophages

in $CNR2^{-/-}$ cultures, in the presence of RANKL there was defective osteoclastogenesis with smaller number of osteoclast than in wild type cultures. Although a similar trend was also observed in the data published by Ofek and colleagues, no comments were made (Ofek et al., 2006). In agreement with the inhibitory effects of CNR2 genetic inactivation on osteoclast formation *in vitro*, pharmacological blockade of CNR2 with AM630 in bone marrow cultures also inhibited osteoclast formation in a concentration-dependent manner as previously described (Idris et al., 2005). While AM630 at high concentration (micromolar range) inhibited osteoclast formation in cultures generated from wild type and $CNR2^{-/-}$ mice, possibly as a result of non-specific binding to sites other than the CNR2 (i.e. CNR1), at low concentrations (nanomolar range), AM630 prevented osteoclast formation only in cultures generated from wild type mice consistent with a CNR2-mediated effect. These results together show that CNR1 and CNR2 play a role in regulating osteoclast function and bone loss resulting from oestrogen deficiency. Moreover, this data also suggests that cannabinoid receptor antagonists/inverse agonists may have potential value as anti-resorptive drugs for the treatment of bone diseases associated with enhanced osteoclastic bone resorption, such as osteoporosis.

Along with the fact that cannabinoid receptor antagonists/inverse agonists caused osteoclast inhibition, the endocannabinoids AEA and 2-AG, and the CNR2-selective agonists HU308 and JWH133, significantly increased osteoclast formation *in vitro* from concentrations at the nanomolar range. Although AEA, 2-AG and JWH133 had a stimulatory effect on osteoclast formation even at concentrations as high as 10μM, HU308 had stimulatory effects only up to 100-fold lower concentrations, i.e. at 100nM. Furthermore, unlike the endocannabinoids and JWH133, HU308 caused osteoclast inhibition at 10μM. Bearing in mind that this is 2000 times higher concentration than what is required for CNR2-mediated adenylyl cyclase inhibition (Hanus et al., 1999), it is likely that the inhibitory effects of HU308 at this concentration were mediated via pathways other than CNR2. Further studies conducted on bone marrow cultures from wild type and $CNR2^{-/-}$ mice showed that $CNR2^{-/-}$ osteoclasts were resistant to the

stimulatory effects of HU308 and JWH133 at nanomolar concentrations, indicating a CNR2-mediated effect. Nonetheless, the endocannabinoids AEA and 2-AG had a stimulatory effect on osteoclast formation in cultures from both wild type and *CNR2*$^{-/-}$ bone marrow, since they bind with high affinity to CNR1 as well (Pertwee and Ross, 2002). These results together indicate that CNR1 and CNR2 activation stimulates osteoclast formation. Although Ofek and colleagues showed that the effects of HU308 are indeed mediated via the CNR2, they reported that it inhibits osteoclast differentiation *in vitro* contradicting previous findings about the effect of cannabinoid agonists on osteoclast formation (Idris et al., 2005; Ridge et al., 2007).

To investigate the role of HU308 on bone mass *in vivo*, the ovariectomised mouse model was used. This study showed that HU308 inhibits ovariectomy-induced bone loss in a dose-dependent manner in agreement to previous work (Ofek et al., 2006). However, the protective effect of HU308 was blunted in *CNR2*$^{-/-}$ ovariectomised mice, consistent with a CNR2-mediated effect. Histomorphometric analysis showed that the protective effect of HU308 was attributable to the increase in osteoblast numbers and bone formation rate to levels higher than those measured in ovariectomised mice, without significantly affecting osteoclast numbers or resorption surfaces. In relation to this, the CNR2-selective agonists HU308 and JWH133 stimulated nodule formation in calvarial osteoblasts cultures from wild type mice. However, the stimulatory effect of CNR2-selective agonists was blunted in cultures from *CNR2*$^{-/-}$ mice, suggesting a CNR2-mediated effect. In contrast, calvarial osteoblast cultures from wild type and *CNR2*$^{-/-}$ mice were equally sensitive to the stimulatory effects of AEA on nodule formation, probably due to binding to CNR1 (Pertwee and Ross, 2002). Although the CNR2-selective antagonist/inverse agonist AM630 did not have an effect on bone nodule formation at concentrations at the nanomolar range, it inhibited nodule formation at concentrations at the micromolar range (Idris, A.I., personal communication). Along the same lines, primary osteoblast cultures from *CNR2*$^{-/-}$ mice had lower levels of ALP activity when treated with PTH and formed defective nodules, suggesting a role of

CNR2 signalling on osteoblast differentiation and function. These results together suggest that CNR2 may mediate anabolic effects on bone and that CNR2 agonists might be of value as new treatments for osteoporosis.

In disagreement with the results reported here, Ofek and colleagues proposed that HU308 treatment on ovariectomised mice rescued bone loss by reducing osteoclast-mediated bone resorption, supported by *in vitro* evidence mentioned above, and by stimulating endocortical bone formation (Ofek et al., 2006). The discrepancy between the two studies cannot be readily explained but it should be noted that differences such as: a) the strain of mice used (Ofek and colleagues curried out ovariectomy experiments on C3H mice unlike the present study which was done with C57BL/6 mice), b) the dosage of HU308 administered (Ofek et al. used 10-fold higher HU308 dose than the dose used in the current study) and c) the analysis on different skeletal sites (Ofek et al. analysed femoral bones whereas this study analysed tibial bones), might have contributed to the different outcomes observed.

Regardless of differences in pharmacological effects observed on ovariectomised mice after HU308 treatment, ageing experiments by both groups showed that 12-month old $CNR2^{-/-}$ mice developed profound osteoporosis, exceeding bone loss that C57BL/6 mice normally suffer from with age (Ferguson et al., 2003; Glatt et al., 2007). The present study described this as a result of decreased osteoblast numbers and defective bone formation, in line with our recent findings indicating that 12-month old $CNR1^{-/-}$ mice showed reduction in osteoblast numbers leading to age-related bone loss (Idris et al., 2008b). However, these observations differ from those of Ofek and colleagues, who suggested that the accelerated osteoporosis seen in $CNR2^{-/-}$ mice was the outcome of high bone turnover (Ofek et al., 2006). According to the data provided by Ofek and colleagues, it seems that their explanation of the severely osteoporotic $CNR2^{-/-}$ mice was based on detailed analysis performed on young mice only (Ofek et al., 2006). However, as it has been demonstrated by the present CNR2 study, it is possible that different

components of bone turnover cycle might appear to be defective at different ages. That is, defective osteoclasts were noticeable in young $CNR2^{-/-}$ mice, whereas defective osteoblasts became more obvious later with ageing.

In view of the fact that type 2 cannabinoid receptor protects against age-related osteoporosis, a CNR2-deficient mouse model should be studied on a background strain that does not undergo considerable bone loss with age, such as CD1 or C3H strain (Beamer et al., 1996). In contrast, the background strain of $CNR2^{-/-}$ mice, C57BL/6, has the lowest value for any given bone parameter (Beamer et al., 1996). For that reason $CNR2^{-/-}$ mice have been backcrossed to a CD1 strain and will be used to carry out further experiments in the near future. Moreover, due to the fact that pharmacological ligands currently available are not completely specific and can interact with both CNR1 and CNR2, additional experimentation will be conducted on a double knockout $CNR1^{-/-}$ $/CNR2^{-/-}$ mouse model on a CD1 genetic background to determine the effects of complete absence of cannabinoid receptor type 1 and type 2 on bone.

The results reported in this thesis clearly demonstrate that type 2 cannabinoid receptors contribute to the osteoclast and osteoblast differentiation *in vitro*, up-regulate bone remodelling in the ovariectomised mouse model *in vivo* and also protect from age-related bone loss by affecting both osteoclast and osteoblast function. Moreover, this thesis reports that CNR2-selective agonists have anabolic activities *in vivo*, whereas CNR2-selective antagonists/inverse agonists have potential value as anti-resorptive drugs. These findings together with evidence showing that the *CNR2* chromosomal region is implicated in osteoporosis (Devoto et al., 2005) and that there is strong association of *CNR2* polymorphisms with osteoporosis in human (Karsak et al., 2005; YAMADA et al., 2007), imply that CNR2 presents a molecular target for the diagnosis and treatment of osteoporosis and other bone diseases including rheumatoid arthritis, Paget's disease and bone metastases.

BIBLIOGRAPHY

Reference List

Aarden,E.M., Nijweide,P.J., van der,P.A., Alblas,M.J., Mackie,E.J., Horton,M.A., and Helfrich,M.H. (1996). Adhesive properties of isolated chick osteocytes in vitro. Bone *18*, 305-313.

Abe,E., Marians,R.C., Yu,W., Wu,X.B., Ando,T., Li,Y., Iqbal,J., Eldeiry,L., Rajendren,G., Blair,H.C., Davies,T.F., and Zaidi,M. (2003). TSH is a negative regulator of skeletal remodeling. Cell *115*, 151-162.

Ahdjoudj,S., Lasmoles,F., Holy,X., Zerath,E., and Marie,P.J. (2002). Transforming growth factor beta2 inhibits adipocyte differentiation induced by skeletal unloading in rat bone marrow stroma. J Bone Miner. Res. *17*, 668-677.

Ahluwalia,J., Urban,L., Bevan,S., and Nagy,I. (2003). Anandamide regulates neuropeptide release from capsaicin-sensitive primary sensory neurons by activating both the cannabinoid 1 receptor and the vanilloid receptor 1 in vitro. Eur. J Neurosci. *17*, 2611-2618.

Ahmed,S.A., Gogal,R.M., Jr., and Walsh,J.E. (1994). A new rapid and simple non-radioactive assay to monitor and determine the proliferation of lymphocytes: an alternative to [3H]thymidine incorporation assay. J Immunol. Methods *170*, 211-224.

Aitken,S.J., Landao-Bassonga,E., Ralston,S.H., and Idris,A.I. (2009). Beta2-adrenoreceptor ligands regulate osteoclast differentiation in vitro by direct and indirect mechanisms. Arch. Biochem. Biophys. *482*, 96-103.

Anderson,D.M., Maraskovsky,E., Billingsley,W.L., Dougall,W.C., Tometsko,M.E., Roux,E.R., Teepe,M.C., DuBose,R.F., Cosman,D., and Galibert,L. (1997). A homologue of the TNF receptor and its ligand enhance T-cell growth and dendritic-cell function. Nature *390*, 175-179.

Andersson,A.K., Li,C., and Brennan,F.M. (2008). Recent developments in the immunobiology of rheumatoid arthritis. Arthritis Res. Ther. *10*, 204.

Arai,F., Miyamoto,T., Ohneda,O., Inada,T., Sudo,T., Brasel,K., Miyata,T., Anderson,D.M., and Suda,T. (1999). Commitment and differentiation of osteoclast precursor cells by the sequential expression of c-Fms and receptor activator of nuclear factor kappaB (RANK) receptors. J Exp. Med. *190*, 1741-1754.

Asagiri,M. and Takayanagi,H. (2007). The molecular understanding of osteoclast differentiation. Bone *40*, 251-264.

Ashton,J.C., Friberg,D., Darlington,C.L., and Smith,P.F. (2006). Expression of the cannabinoid CB2 receptor in the rat cerebellum: an immunohistochemical study. Neurosci. Lett. *396*, 113-116.

Bab,I., Ofek,O., Tam,J., Rehnelt,J., and Zimmer,A. (2008). Endocannabinoids and the regulation of bone metabolism. J Neuroendocrinol. *20 Suppl 1*, 69-74.

Bab,I. and Zimmer,A. (2008). Cannabinoid receptors and the regulation of bone mass. Br. J Pharmacol *153*, 182-188.

Baldock,P.A., Allison,S.J., Lundberg,P., Lee,N.J., Slack,K., Lin,E.J., Enriquez,R.F., McDonald,M.M., Zhang,L., During,M.J., Little,D.G., Eisman,J.A., Gardiner,E.M., Yulyaningsih,E., Lin,S., Sainsbury,A., and Herzog,H. (2007). Novel role of Y1 receptors in the coordinated regulation of bone and energy homeostasis. J Biol. Chem. *282*, 19092-19102.

Baldock,P.A., Sainsbury,A., Couzens,M., Enriquez,R.F., Thomas,G.P., Gardiner,E.M., and Herzog,H. (2002). Hypothalamic Y2 receptors regulate bone formation. J Clin Invest *109*, 915-921.

Baldwin,G.C., Tashkin,D.P., Buckley,D.M., Park,A.N., Dubinett,S.M., and Roth,M.D. (1997). Marijuana and cocaine impair alveolar macrophage function and cytokine production. Am. J Respir. Crit Care Med. *156*, 1606-1613.

Bassett,J.H., O'Shea,P.J., Sriskantharajah,S., Rabier,B., Boyde,A., Howell,P.G., Weiss,R.E., Roux,J.P., Malaval,L., Clement-Lacroix,P., Samarut,J., Chassande,O., and Williams,G.R. (2007). Thyroid hormone excess rather than thyrotropin deficiency induces osteoporosis in hyperthyroidism. Mol. Endocrinol. *21*, 1095-1107.

Bassett,J.H., Williams,A.J., Murphy,E., Boyde,A., Howell,P.G., Swinhoe,R., Archanco,M., Flamant,F., Samarut,J., Costagliola,S., Vassart,G., Weiss,R.E., Refetoff,S., and Williams,G.R. (2008). A lack of thyroid hormones rather than excess thyrotropin causes abnormal skeletal development in hypothyroidism. Mol. Endocrinol. *22*, 501-512.

Bassett,J.H. and Williams,G.R. (2008). Critical role of the hypothalamic-pituitary-thyroid axis in bone. Bone *43*, 418-426.

Beamer,W.G., Donahue,L.R., Rosen,C.J., and Baylink,D.J. (1996). Genetic variability in adult bone density among inbred strains of mice. Bone *18*, 397-403.

Begg,M., Pacher,P., Batkai,S., Osei-Hyiaman,D., Offertaler,L., Mo,F.M., Liu,J., and Kunos,G. (2005). Evidence for novel cannabinoid receptors. Pharmacol Ther. *106*, 133-145.

Belanger,L.F., Choquette,L.P., and Cousineau,J.G. (1967). Osteolysis in reindeer antlers; sexual and seasonal variations. Calcif. Tissue Res. *1*, 37-43.

Benarroch,E.E. (2009). Neuropeptide Y: its multiple effects in the CNS and potential clinical significance. Neurology *72*, 1016-1020.

Besse,A., Trimoreau,F., Faucher,J.L., Praloran,V., and Denizot,Y. (1999). Prostaglandin E2 regulates macrophage colony stimulating factor secretion by human bone marrow stromal cells. Biochim. Biophys. Acta *1450*, 444-451.

Bi,W., Deng,J.M., Zhang,Z., Behringer,R.R., and de Crombrugghe,B. (1999). Sox9 is required for cartilage formation. Nat. Genet. *22*, 85-89.

Bifulco,M., Malfitano,A.M., Pisanti,S., and Laezza,C. (2008). Endocannabinoids in endocrine and related tumours. Endocr. Relat Cancer *15*, 391-408.

Black,D.M., Bilezikian,J.P., Ensrud,K.E., Greenspan,S.L., Palermo,L., Hue,T., Lang,T.F., McGowan,J.A., and Rosen,C.J. (2005). One year of alendronate after one year of parathyroid hormone (1-84) for osteoporosis. N. Engl. J Med. *353*, 555-565.

Black,L.J., Jones,C.D., and Falcone,J.F. (1983). Antagonism of estrogen action with a new benzothiophene derived antiestrogen. Life Sci. *32*, 1031-1036.

Blahos,J. (2007). Treatment and prevention of osteoporosis. Wien. Med. Wochenschr. *157*, 589-592.

Blair,H.C., Teitelbaum,S.L., Ghiselli,R., and Gluck,S. (1989). Osteoclastic bone resorption by a polarized vacuolar proton pump. Science *245*, 855-857.

Blair,H.C. and Zaidi,M. (2006). Osteoclastic differentiation and function regulated by old and new pathways. Rev. Endocr. Metab Disord. *7*, 23-32.

Blake,D.R., Robson,P., Ho,M., Jubb,R.W., and McCabe,C.S. (2006). Preliminary assessment of the efficacy, tolerability and safety of a cannabis-based medicine (Sativex) in the treatment of pain caused by rheumatoid arthritis. Rheumatology (Oxford) *45*, 50-52.

Bonewald,L.F. (2007). Osteocytes as dynamic multifunctional cells. Ann. N. Y. Acad. Sci. *1116*, 281-290.

Bonnick,S.L. (2006). Osteoporosis in men and women. Clin Cornerstone. *8*, 28-39.

Borgatti,P., Martelli,A.M., Bellacosa,A., Casto,R., Massari,L., Capitani,S., and Neri,L.M. (2000). Translocation of Akt/PKB to the nucleus of osteoblast-like MC3T3-E1 cells exposed to proliferative growth factors. FEBS Lett. *477*, 27-32.

Bouaboula,M., Perrachon,S., Milligan,L., Canat,X., Rinaldi-Carmona,M., Portier,M., Barth,F., Calandra,B., Pecceu,F., Lupker,J., Maffrand,J.P., Le Fur,G., and Casellas,P. (1997). A selective inverse agonist for central cannabinoid receptor inhibits mitogen-activated protein kinase activation stimulated by insulin or insulin-like growth factor 1. Evidence for a new model of receptor/ligand interactions. J Biol. Chem. *272*, 22330-22339.

Bouaboula,M., Rinaldi,M., Carayon,P., Carillon,C., Delpech,B., Shire,D., Le Fur,G., and Casellas,P. (1993). Cannabinoid-receptor expression in human leukocytes. Eur. J Biochem. *214*, 173-180.

Boyce,B.F. and Xing,L. (2008). Functions of RANKL/RANK/OPG in bone modeling and remodeling. Arch. Biochem. Biophys. *473*, 139-146.

Breen,E.C., van Wijnen,A.J., Lian,J.B., Stein,G.S., and Stein,J.L. (1994). In vivo occupancy of the vitamin D responsive element in the osteocalcin gene supports vitamin D-dependent transcriptional upregulation in intact cells. Proc. Natl. Acad. Sci. U. S. A *91*, 12902-12906.

Brown,A.J. (2007). Novel cannabinoid receptors. Br. J Pharmacol *152*, 567-575.

Buckley,N.E., McCoy,K.L., Mezey,E., Bonner,T., Zimmer,A., Felder,C.C., Glass,M., and Zimmer,A. (2000). Immunomodulation by cannabinoids is absent in mice deficient for the cannabinoid CB(2) receptor. Eur. J. Pharmacol. *396*, 141-149.

Burstein,S.H. and Hunter,S.A. (1995). Stimulation of anandamide biosynthesis in N-18TG2 neuroblastoma cells by delta 9-tetrahydrocannabinol (THC). Biochem. Pharmacol *49*, 855-858.

Burstein,S.H., Young,J.K., and Wright,G.E. (1995). Relationships between eicosanoids and cannabinoids. Are eicosanoids cannabimimetic agents? Biochem. Pharmacol *50*, 1735-1742.

Cabral,G.A., Raborn,E.S., Griffin,L., Dennis,J., and Marciano-Cabral,F. (2008). CB(2) receptors in the brain: role in central immune function. Br. J Pharmacol *153*, 240-251.

Calignano,A., La Rana,G., and Piomelli,D. (2001). Antinociceptive activity of the endogenous fatty acid amide, palmitylethanolamide. Eur. J. Pharmacol. *419*, 191-198.

Calvo,M.S., Eyre,D.R., and Gundberg,C.M. (1996). Molecular basis and clinical application of biological markers of bone turnover. Endocr. Rev. *17*, 333-368.

Canalis,E. (2005). Mechanisms of glucocorticoid action in bone. Curr. Osteoporos. Rep. *3*, 98-102.

Canalis,E., Giustina,A., and Bilezikian,J.P. (2007a). Mechanisms of anabolic therapies for osteoporosis. N. Engl. J Med. *357*, 905-916.

Canalis,E., Mazziotti,G., Giustina,A., and Bilezikian,J.P. (2007b). Glucocorticoid-induced osteoporosis: pathophysiology and therapy. Osteoporos. Int. *18*, 1319-1328.

Cardona,J.M. and Pastor,E. (1997). Calcitonin versus etidronate for the treatment of postmenopausal osteoporosis: a meta-analysis of published clinical trials. Osteoporos. Int. *7*, 165-174.

Caulfield,M.P. and Brown,D.A. (1992). Cannabinoid receptor agonists inhibit Ca current in NG108-15 neuroblastoma cells via a pertussis toxin-sensitive mechanism. Br. J Pharmacol *106*, 231-232.

Celil,A.B. and Campbell,P.G. (2005). BMP-2 and insulin-like growth factor-I mediate Osterix (Osx) expression in human mesenchymal stem cells via the MAPK and protein kinase D signaling pathways. J Biol. Chem. *280*, 31353-31359.

Cerretti,D.P., Wignall,J., Anderson,D., Tushinski,R.J., Gallis,B.M., Stya,M., Gillis,S., Urdal,D.L., and Cosman,D. (1988). Human macrophage-colony stimulating factor: alternative RNA and protein processing from a single gene. Mol. Immunol. *25*, 761-770.

Chabadel,A., Banon-Rodriguez,I., Cluet,D., Rudkin,B.B., Wehrle-Haller,B., Genot,E., Jurdic,P., Anton,I.M., and Saltel,F. (2007). CD44 and beta3 integrin organize two functionally distinct actin-based domains in osteoclasts. Mol. Biol. Cell *18*, 4899-4910.

Chang,Y.L., Stanford,C.M., and Keller,J.C. (2000). Calcium and phosphate supplementation promotes bone cell mineralization: implications for hydroxyapatite (HA)-enhanced bone formation. J Biomed. Mater. Res. *52*, 270-278.

Chenu,C., Pfeilschifter,J., Mundy,G.R., and Roodman,G.D. (1988). Transforming growth factor beta inhibits formation of osteoclast-like cells in long-term human marrow cultures. Proc. Natl. Acad. Sci. U. S. A *85*, 5683-5687.

Chenu,C., Serre,C.M., Raynal,C., Burt-Pichat,B., and Delmas,P.D. (1998). Glutamate receptors are expressed by bone cells and are involved in bone resorption. Bone *22*, 295-299.

Chowdhury,T.T., Salter,D.M., Bader,D.L., and Lee,D.A. (2008). Signal transduction pathways involving p38 MAPK, JNK, NFkappaB and AP-1 influences the response of chondrocytes cultured in agarose constructs to IL-1beta and dynamic compression. Inflamm. Res. *57*, 306-313.

Christakos,S., Dhawan,P., Liu,Y., Peng,X., and Porta,A. (2003). New insights into the mechanisms of vitamin D action. J Cell Biochem. *88*, 695-705.

Coelho,M.J., Cabral,A.T., and Fernande,M.H. (2000). Human bone cell cultures in biocompatibility testing. Part I: osteoblastic differentiation of serially passaged human bone marrow cells cultured in alpha-MEM and in DMEM. Biomaterials *21*, 1087-1094.

Coleman,R.E. (2006). Clinical features of metastatic bone disease and risk of skeletal morbidity. Clin Cancer Res. *12*, 6243s-6249s.

Coleman,R.E. (2008). Risks and benefits of bisphosphonates. Br. J Cancer *98*, 1736-1740.

Compston,J.E. (2007). Skeletal actions of intermittent parathyroid hormone: effects on bone remodelling and structure. Bone *40*, 1447-1452.

COPP,D.H. and CHENEY,B. (1962). Calcitonin-a hormone from the parathyroid which lowers the calcium-level of the blood. Nature *193*, 381-382.

Cravatt,B.F., Giang,D.K., Mayfield,S.P., Boger,D.L., Lerner,R.A., and Gilula,N.B. (1996). Molecular characterization of an enzyme that degrades neuromodulatory fatty-acid amides. Nature *384*, 83-87.

Cromer,B.A. (2008). Menstrual cycle and bone health in adolescents. Ann. N. Y. Acad. Sci. *1135*, 196-203.

Cundy,T., Hegde,M., Naot,D., Chong,B., King,A., Wallace,R., Mulley,J., Love,D.R., Seidel,J., Fawkner,M., Banovic,T., Callon,K.E., Grey,A.B., Reid,I.R., Middleton-Hardie,C.A., and Cornish,J. (2002). A mutation in the gene TNFRSF11B encoding osteoprotegerin causes an idiopathic hyperphosphatasia phenotype. Hum. Mol. Genet. *11*, 2119-2127.

Dai,X.M., Ryan,G.R., Hapel,A.J., Dominguez,M.G., Russell,R.G., Kapp,S., Sylvestre,V., and Stanley,E.R. (2002). Targeted disruption of the mouse colony-stimulating factor 1 receptor gene results in osteopetrosis, mononuclear phagocyte deficiency, increased primitive progenitor cell frequencies, and reproductive defects. Blood *99*, 111-120.

Daroszewska,A., Hocking,L.J., McGuigan,F.E., Langdahl,B., Stone,M.D., Cundy,T., Nicholson,G.C., Fraser,W.D., and Ralston,S.H. (2004). Susceptibility to Paget's disease of bone is influenced by a common polymorphic variant of osteoprotegerin. J Bone Miner. Res. *19*, 1506-1511.

De Petrocellis,L., Bisogno,T., Davis,J.B., Pertwee,R.G., and Di,M., V (2000). Overlap between the ligand recognition properties of the anandamide transporter and the VR1 vanilloid receptor: inhibitors of anandamide uptake with negligible capsaicin-like activity. FEBS Lett. *483*, 52-56.

De Petrocellis,L., Cascio,M.G., and Di,M., V (2004). The endocannabinoid system: a general view and latest additions. Br. J. Pharmacol. *141*, 765-774.

Deadwyler,S.A., Hampson,R.E., Bennett,B.A., Edwards,T.A., Mu,J., Pacheco,M.A., Ward,S.J., and Childers,S.R. (1993). Cannabinoids modulate potassium current in cultured hippocampal neurons. Receptors. Channels *1*, 121-134.

Deal,C., Omizo,M., Schwartz,E.N., Eriksen,E.F., Cantor,P., Wang,J., Glass,E.V., Myers,S.L., and Krege,J.H. (2005). Combination teriparatide and raloxifene therapy for postmenopausal osteoporosis: results from a 6-month double-blind placebo-controlled trial. J Bone Miner. Res. *20*, 1905-1911.

Delmas,P.D., Vergnaud,P., Arlot,M.E., Pastoureau,P., Meunier,P.J., and Nilssen,M.H. (1995). The anabolic effect of human PTH (1-34) on bone formation is blunted when bone resorption is inhibited by the bisphosphonate tiludronate--is activated resorption a prerequisite for the in vivo effect of PTH on formation in a remodeling system? Bone *16*, 603-610.

Dempster,D.W., Cosman,F., Kurland,E.S., Zhou,H., Nieves,J., Woelfert,L., Shane,E., Plavetic,K., Muller,R., Bilezikian,J., and Lindsay,R. (2001). Effects of daily treatment with parathyroid hormone on bone microarchitecture and turnover in patients with osteoporosis: a paired biopsy study. J Bone Miner. Res. *16*, 1846-1853.

Demuth,D.G. and Molleman,A. (2006). Cannabinoid signalling. Life Sci. *78*, 549-563.

Derocq,J.M., Jbilo,O., Bouaboula,M., Segui,M., Clere,C., and Casellas,P. (2000). Genomic and functional changes induced by the activation of the peripheral cannabinoid receptor CB2 in the promyelocytic cells HL-60. Possible involvement of the CB2 receptor in cell differentiation. J Biol. Chem. *275*, 15621-15628.

Devane,W.A., Hanus,L., Breuer,A., Pertwee,R.G., Stevenson,L.A., Griffin,G., Gibson,D., Mandelbaum,A., Etinger,A., and Mechoulam,R. (1992). Isolation and structure of a brain constituent that binds to the cannabinoid receptor. Science *258*, 1946-1949.

Devoto,M., Spotila,L.D., Stabley,D.L., Wharton,G.N., Rydbeck,H., Korkko,J., Kosich,R., Prockop,D., Tenenhouse,A., and Sol-Church,K. (2005). Univariate and bivariate variance component linkage analysis of a whole-genome scan for loci contributing to bone mineral density. Eur. J Hum. Genet. *13*, 781-788.

Dewey,W.L. (1986). Cannabinoid pharmacology. Pharmacol Rev. *38*, 151-178.

Di Munno,O. and Delle,S.A. (2008). Effects of glucocorticoid treatment on focal and systemic bone loss in rheumatoid arthritis. J Endocrinol. Invest *31*, 43-47.

Di,M., V, Bisogno,T., De Petrocellis,L., Melck,D., Orlando,P., Wagner,J.A., and Kunos,G. (1999). Biosynthesis and inactivation of the endocannabinoid 2-arachidonoylglycerol in circulating and tumoral macrophages. Eur. J Biochem. *264*, 258-267.

Di,M., V, Fontana,A., Cadas,H., Schinelli,S., Cimino,G., Schwartz,J.C., and Piomelli,D. (1994). Formation and inactivation of endogenous cannabinoid anandamide in central neurons. Nature *372*, 686-691.

Di,M., V, Goparaju,S.K., Wang,L., Liu,J., Batkai,S., Jarai,Z., Fezza,F., Miura,G.I., Palmiter,R.D., Sugiura,T., and Kunos,G. (2001). Leptin-regulated endocannabinoids are involved in maintaining food intake. Nature *410*, 822-825.

Di,M., V, Melck,D., Bisogno,T., and De Petrocellis,L. (1998). Endocannabinoids: endogenous cannabinoid receptor ligands with neuromodulatory action. Trends Neurosci. *21*, 521-528.

Diel,I.J., Bergner,R., and Grotz,K.A. (2007). Adverse effects of bisphosphonates: current issues. J Support Oncol. *5*, 475-482.

Doherty,M. (1999). Synovial inflammation and osteoarthritis progression: effects of nonsteroidal antiinflammatory drugs. Osteoarthritis. Cartilage. *7*, 319-320.

Dougall,W.C., Glaccum,M., Charrier,K., Rohrbach,K., Brasel,K., De Smedt,T., Daro,E., Smith,J., Tometsko,M.E., Maliszewski,C.R., Armstrong,A., Shen,V., Bain,S., Cosman,D., Anderson,D., Morrissey,P.J., Peschon,J.J., and Schuh,J. (1999). RANK is essential for osteoclast and lymph node development. Genes Dev. *13*, 2412-2424.

Douglas,D.L., Duckworth,T., Kanis,J.A., Jefferson,A.A., Martin,T.J., and Russell,R.G. (1981). Spinal cord dysfunction in Paget's disease of bone. Has medical treatment a vascular basis? J Bone Joint Surg. Br. *63B*, 495-503.

Ducy,P., Amling,M., Takeda,S., Priemel,M., Schilling,A.F., Beil,F.T., Shen,J., Vinson,C., Rueger,J.M., and Karsenty,G. (2000a). Leptin inhibits bone formation through a hypothalamic relay: a central control of bone mass. Cell *100*, 197-207.

Ducy,P., Schinke,T., and Karsenty,G. (2000b). The osteoblast: a sophisticated fibroblast under central surveillance. Science *289*, 1501-1504.

Duque,G., Macoritto,M., and Kremer,R. (2004). 1,25(OH)2D3 inhibits bone marrow adipogenesis in senescence accelerated mice (SAM-P/6) by decreasing the expression of peroxisome proliferator-activated receptor gamma 2 (PPARgamma2). Exp. Gerontol. *39*, 333-338.

Duque,G. and Rivas,D. (2007). Alendronate has an anabolic effect on bone through the differentiation of mesenchymal stem cells. J Bone Miner. Res. *22*, 1603-1611.

Duvernay,M.T., Filipeanu,C.M., and Wu,G. (2005). The regulatory mechanisms of export trafficking of G protein-coupled receptors. Cell Signal. *17*, 1457-1465.

Ebeling,P.R. (1998). Osteoporosis in men. New insights into aetiology, pathogenesis, prevention and management. Drugs Aging *13*, 421-434.

Edwards,C.M., Zhuang,J., and Mundy,G.R. (2008). The pathogenesis of the bone disease of multiple myeloma. Bone *42*, 1007-1013.

Egertova,M., Giang,D.K., Cravatt,B.F., and Elphick,M.R. (1998). A new perspective on cannabinoid signalling: complementary localization of fatty acid amide hydrolase and the CB1 receptor in rat brain. Proc. Biol. Sci. *265*, 2081-2085.

Eklou-Kalonji,E., Zerath,E., Colin,C., Lacroix,C., Holy,X., Denis,I., and Pointillart,A. (1999). Calcium-regulating hormones, bone mineral content, breaking load and trabecular remodeling are altered in growing pigs fed calcium-deficient diets. J Nutr. *129*, 188-193.

Elefteriou,F. (2008). Regulation of bone remodeling by the central and peripheral nervous system. Arch. Biochem. Biophys. *473*, 231-236.

Elefteriou,F., Ahn,J.D., Takeda,S., Starbuck,M., Yang,X., Liu,X., Kondo,H., Richards,W.G., Bannon,T.W., Noda,M., Clement,K., Vaisse,C., and Karsenty,G. (2005). Leptin regulation of bone resorption by the sympathetic nervous system and CART. Nature *434*, 514-520.

Ernst,M., Heath,J.K., and Rodan,G.A. (1989). Estradiol effects on proliferation, messenger ribonucleic acid for collagen and insulin-like growth factor-I, and parathyroid hormone-stimulated adenylate cyclase activity in osteoblastic cells from calvariae and long bones. Endocrinology *125*, 825-833.

Ettinger,B., San Martin,J., Crans,G., and Pavo,I. (2004). Differential effects of teriparatide on BMD after treatment with raloxifene or alendronate. J Bone Miner. Res. *19*, 745-751.

Faccio,R., Takeshita,S., Zallone,A., Ross,F.P., and Teitelbaum,S.L. (2003). c-Fms and the alphavbeta3 integrin collaborate during osteoclast differentiation. J Clin Invest *111*, 749-758.

Farrugia,A.N., Atkins,G.J., To,L.B., Pan,B., Horvath,N., Kostakis,P., Findlay,D.M., Bardy,P., and Zannettino,A.C. (2003). Receptor activator of nuclear factor-kappaB ligand expression by human myeloma cells mediates osteoclast formation in vitro and correlates with bone destruction in vivo. Cancer Res. *63*, 5438-5445.

Felicio,L.S., Nelson,J.F., and Finch,C.E. (1984). Longitudinal studies of estrous cyclicity in aging C57BL/6J mice: II. Cessation of cyclicity and the duration of persistent vaginal cornification. Biol. Reprod. *31*, 446-453.

Felson,D.T. and Lohmander,L.S. (2009). Whither osteoarthritis biomarkers? Osteoarthritis. Cartilage. *17*, 419-422.

Ferguson,V.L., Ayers,R.A., Bateman,T.A., and Simske,S.J. (2003). Bone development and age-related bone loss in male C57BL/6J mice. Bone *33*, 387-398.

Filppula,S., Yaddanapudi,S., Mercier,R., Xu,W., Pavlopoulos,S., and Makriyannis,A. (2004). Purification and mass spectroscopic analysis of human CB2 cannabinoid receptor expressed in the baculovirus system. J Pept. Res. *64*, 225-236.

Fink,H.A., Ewing,S.K., Ensrud,K.E., Barrett-Connor,E., Taylor,B.C., Cauley,J.A., and Orwoll,E.S. (2006). Association of testosterone and estradiol deficiency with osteoporosis and rapid bone loss in older men. J Clin Endocrinol. Metab *91*, 3908-3915.

Finkelstein,J.S., Hayes,A., Hunzelman,J.L., Wyland,J.J., Lee,H., and Neer,R.M. (2003). The effects of parathyroid hormone, alendronate, or both in men with osteoporosis. N. Engl. J Med. *349*, 1216-1226.

Firestein,G.S. (2003). Evolving concepts of rheumatoid arthritis. Nature *423*, 356-361.

Firestein,G.S., Alvaro-Gracia,J.M., and Maki,R. (1990). Quantitative analysis of cytokine gene expression in rheumatoid arthritis. J Immunol. *144*, 3347-3353.

Franzoso,G., Carlson,L., Xing,L., Poljak,L., Shores,E.W., Brown,K.D., Leonardi,A., Tran,T., Boyce,B.F., and Siebenlist,U. (1997). Requirement for NF-kappaB in osteoclast and B-cell development. Genes Dev. *11*, 3482-3496.

Friedman,P.A. (2000). Mechanisms of renal calcium transport. Exp. Nephrol. *8*, 343-350.

Fuchs,R.K., Allen,M.R., Condon,K.W., Reinwald,S., Miller,L.M., McClenathan,D., Keck,B., Phipps,R.J., and Burr,D.B. (2008). Strontium ranelate does not stimulate bone formation in ovariectomized rats. Osteoporos. Int. *19*, 1331-1341.

Fuller,K. and Chambers,T.J. (1989). Effect of arachidonic acid metabolites on bone resorption by isolated rat osteoclasts. J Bone Miner. Res. *4*, 209-215.

Galiegue,S., Mary,S., Marchand,J., Dussossoy,D., Carriere,D., Carayon,P., Bouaboula,M., Shire,D., Le Fur,G., and Casellas,P. (1995). Expression of central and peripheral cannabinoid receptors in human immune tissues and leukocyte subpopulations. Eur. J Biochem. *232*, 54-61.

Gao,J., Tiwari-Pandey,R., Samadfam,R., Yang,Y., Miao,D., Karaplis,A.C., Sairam,M.R., and Goltzman,D. (2007). Altered ovarian function affects skeletal homeostasis independent of the action of follicle-stimulating hormone. Endocrinology *148*, 2613-2621.

George,K.L., Saltman,L.H., Stein,G.S., Lian,J.B., and Zurier,R.B. (2008). Ajulemic acid, a nonpsychoactive cannabinoid acid, suppresses osteoclastogenesis in mononuclear precursor cells and induces apoptosis in mature osteoclast-like cells. J Cell Physiol *214*, 714-720.

Girasole,G., Jilka,R.L., Passeri,G., Boswell,S., Boder,G., Williams,D.C., and Manolagas,S.C. (1992). 17 beta-estradiol inhibits interleukin-6 production by bone marrow-derived stromal cells and osteoblasts in vitro: a potential mechanism for the antiosteoporotic effect of estrogens. J Clin Invest *89*, 883-891.

Girotra,M., Rubin,M.R., and Bilezikian,J.P. (2006). The use of parathyroid hormone in the treatment of osteoporosis. Rev. Endocr. Metab Disord. *7*, 113-121.

Giuliani,N., Pedrazzoni,M., Negri,G., Passeri,G., Impicciatore,M., and Girasole,G. (1998). Bisphosphonates stimulate formation of osteoblast precursors and mineralized nodules in murine and human bone marrow cultures in vitro and promote early osteoblastogenesis in young and aged mice in vivo. Bone *22*, 455-461.

Glatt,V., Canalis,E., Stadmeyer,L., and Bouxsein,M.L. (2007). Age-related changes in trabecular architecture differ in female and male C57BL/6J mice. J Bone Miner. Res. *22*, 1197-1207.

Goltzman,D. (2008). Studies on the mechanisms of the skeletal anabolic action of endogenous and exogenous parathyroid hormone. Arch. Biochem. Biophys. *473*, 218-224.

Gomez,d.P., Velasco,G., and Guzman,M. (2000). The CB1 cannabinoid receptor is coupled to the activation of protein kinase B/Akt. Biochem. J *347*, 369-373.

Gonsiorek,W., Lunn,C., Fan,X., Narula,S., Lundell,D., and Hipkin,R.W. (2000). Endocannabinoid 2-arachidonyl glycerol is a full agonist through human type 2 cannabinoid receptor: antagonism by anandamide. Mol. Pharmacol *57*, 1045-1050.

Gonzalez,D., Ghiringhelli,G., and Mautalen,C. (1986). Acute antiosteoclastic effect of salmon calcitonin in osteoporotic women. Calcif. Tissue Int. *38*, 71-75.

Gonzalez,S., Manzanares,J., Berrendero,F., Wenger,T., Corchero,J., Bisogno,T., Romero,J., Fuentes,J.A., Di,M., V, Ramos,J.A., and Fernandez-Ruiz,J. (1999). Identification of endocannabinoids and cannabinoid CB(1) receptor mRNA in the pituitary gland. Neuroendocrinology *70*, 137-145.

Goutopoulos,A. and Makriyannis,A. (2002). From cannabis to cannabinergics: new therapeutic opportunities. Pharmacol. Ther. *95*, 103-117.

Gowen,M., Lazner,F., Dodds,R., Kapadia,R., Feild,J., Tavaria,M., Bertoncello,I., Drake,F., Zavarselk,S., Tellis,I., Hertzog,P., Debouck,C., and Kola,I. (1999). Cathepsin K knockout mice develop osteopetrosis due to a deficit in matrix degradation but not demineralization. J Bone Miner. Res. *14*, 1654-1663.

Griffin,G., Atkinson,P.J., Showalter,V.M., Martin,B.R., and Abood,M.E. (1998). Evaluation of cannabinoid receptor agonists and antagonists using the guanosine-5'-O-(3-[35S]thio)-triphosphate binding assay in rat cerebellar membranes. J Pharmacol Exp. Ther. *285*, 553-560.

Griffin,G., Tao,Q., and Abood,M.E. (2000). Cloning and pharmacological characterization of the rat CB(2) cannabinoid receptor. J. Pharmacol. Exp. Ther. *292*, 886-894.

Grodstein,F., Manson,J.E., Colditz,G.A., Willett,W.C., Speizer,F.E., and Stampfer,M.J. (2000). A prospective, observational study of postmenopausal hormone therapy and primary prevention of cardiovascular disease. Ann. Intern. Med. *133*, 933-941.

Guzman,M. (2003). Cannabinoids: potential anticancer agents. Nat. Rev. Cancer *3*, 745-755.

Hadjidakis,D.J. and Androulakis,I.I. (2006). Bone remodeling. Ann. N. Y. Acad. Sci. *1092*, 385-396.

Hanus,L., Abu-Lafi,S., Fride,E., Breuer,A., Vogel,Z., Shalev,D.E., Kustanovich,I., and Mechoulam,R. (2001). 2-arachidonyl glyceryl ether, an endogenous agonist of the cannabinoid CB1 receptor. Proc. Natl. Acad. Sci. U. S. A *98*, 3662-3665.

Hanus,L., Breuer,A., Tchilibon,S., Shiloah,S., Goldenberg,D., Horowitz,M., Pertwee,R.G., Ross,R.A., Mechoulam,R., and Fride,E. (1999). HU-308: a specific agonist for CB(2), a peripheral cannabinoid receptor. Proc. Natl. Acad. Sci. U. S. A *96*, 14228-14233.

Hart,S., Fischer,O.M., and Ullrich,A. (2004). Cannabinoids induce cancer cell proliferation via tumor necrosis factor alpha-converting enzyme (TACE/ADAM17)-mediated transactivation of the epidermal growth factor receptor. Cancer Res. *64*, 1943-1950.

Hawse,J.R., Subramaniam,M., Ingle,J.N., Oursler,M.J., Rajamannan,N.M., and Spelsberg,T.C. (2008). Estrogen-TGFbeta cross-talk in bone and other cell types: role of TIEG, Runx2, and other transcription factors. J Cell Biochem. *103*, 383-392.

Hayman,A.R. and Cox,T.M. (2003). Tartrate-resistant acid phosphatase knockout mice. J Bone Miner. Res. *18*, 1905-1907.

Hayman,A.R., Macary,P., Lehner,P.J., and Cox,T.M. (2001). Tartrate-resistant acid phosphatase (Acp 5): identification in diverse human tissues and dendritic cells. J Histochem. Cytochem. *49*, 675-684.

Heath,D.J., Chantry,A.D., Buckle,C.H., Coulton,L., Shaughnessy,J.D., Jr., Evans,H.R., Snowden,J.A., Stover,D.R., Vanderkerken,K., and Croucher,P.I. (2009). Inhibiting Dickkopf-1 (Dkk1) removes suppression of bone formation and prevents the development of osteolytic bone disease in multiple myeloma. J Bone Miner. Res. *24*, 425-436.

Heino,T.J., Hentunen,T.A., and Vaananen,H.K. (2002). Osteocytes inhibit osteoclastic bone resorption through transforming growth factor-beta: enhancement by estrogen. J Cell Biochem. *85*, 185-197.

Hermann,H., De Petrocellis,L., Bisogno,T., Schiano,M.A., Lutz,B., and Di,M., V (2003). Dual effect of cannabinoid CB1 receptor stimulation on a vanilloid VR1 receptor-mediated response. Cell Mol. Life Sci. *60*, 607-616.

Hill,P.A. (1998). Bone remodelling. Br. J Orthod. *25*, 101-107.

Hillard,C.J., Manna,S., Greenberg,M.J., DiCamelli,R., Ross,R.A., Stevenson,L.A., Murphy,V., Pertwee,R.G., and Campbell,W.B. (1999). Synthesis and characterization of

potent and selective agonists of the neuronal cannabinoid receptor (CB1). J Pharmacol Exp. Ther. *289*, 1427-1433.

Hinoi,E., Bialek,P., Chen,Y.T., Rached,M.T., Groner,Y., Behringer,R.R., Ornitz,D.M., and Karsenty,G. (2006). Runx2 inhibits chondrocyte proliferation and hypertrophy through its expression in the perichondrium. Genes Dev. *20*, 2937-2942.

Ho,B.Y., Uezono,Y., Takada,S., Takase,I., and Izumi,F. (1999). Coupling of the expressed cannabinoid CB1 and CB2 receptors to phospholipase C and G protein-coupled inwardly rectifying K+ channels. Receptors. Channels *6*, 363-374.

Hocking,L.J., Lucas,G.J., Daroszewska,A., Mangion,J., Olavesen,M., Cundy,T., Nicholson,G.C., Ward,L., Bennett,S.T., Wuyts,W., Van Hul,W., and Ralston,S.H. (2002). Domain-specific mutations in sequestosome 1 (SQSTM1) cause familial and sporadic Paget's disease. Hum. Mol. Genet. *11*, 2735-2739.

Hofbauer,L.C., Gori,F., Riggs,B.L., Lacey,D.L., Dunstan,C.R., Spelsberg,T.C., and Khosla,S. (1999a). Stimulation of osteoprotegerin ligand and inhibition of osteoprotegerin production by glucocorticoids in human osteoblastic lineage cells: potential paracrine mechanisms of glucocorticoid-induced osteoporosis. Endocrinology *140*, 4382-4389.

Hofbauer,L.C., Khosla,S., Dunstan,C.R., Lacey,D.L., Spelsberg,T.C., and Riggs,B.L. (1999b). Estrogen stimulates gene expression and protein production of osteoprotegerin in human osteoblastic cells. Endocrinology *140*, 4367-4370.

Hofbauer,L.C. and Schoppet,M. (2004). Clinical implications of the osteoprotegerin/RANKL/RANK system for bone and vascular diseases. JAMA *292*, 490-495.

Hoff,A.O., Catala-Lehnen,P., Thomas,P.M., Priemel,M., Rueger,J.M., Nasonkin,I., Bradley,A., Hughes,M.R., Ordonez,N., Cote,G.J., Amling,M., and Gagel,R.F. (2002). Increased bone mass is an unexpected phenotype associated with deletion of the calcitonin gene. J Clin Invest *110*, 1849-1857.

Hoff,J. (2000). Methods of blood collection in the mouse. Lab Anim (NY) *29*, 47-53.

Horowitz,M.C., Xi,Y., Wilson,K., and Kacena,M.A. (2001). Control of osteoclastogenesis and bone resorption by members of the TNF family of receptors and ligands. Cytokine Growth Factor Rev. *12*, 9-18.

Hou,Y.C., Janczuk,A., and Wang,P.G. (1999). Current trends in the development of nitric oxide donors. Curr. Pharm. Des *5*, 417-441.

Howlett,A.C. (1984). Inhibition of neuroblastoma adenylate cyclase by cannabinoid and nantradol compounds. Life Sci. *35*, 1803-1810.

Howlett,A.C. (1985). Cannabinoid inhibition of adenylate cyclase. Biochemistry of the response in neuroblastoma cell membranes. Mol. Pharmacol *27*, 429-436.

Howlett,A.C. (2002). The cannabinoid receptors. Prostaglandins Other Lipid Mediat. *68-69*, 619-631.

Howlett,A.C., Champion-Dorow,T.M., McMahon,L.L., and Westlake,T.M. (1991). The cannabinoid receptor: biochemical and cellular properties in neuroblastoma cells. Pharmacol Biochem. Behav. *40*, 565-569.

Howlett,A.C., Qualy,J.M., and Khachatrian,L.L. (1986). Involvement of Gi in the inhibition of adenylate cyclase by cannabimimetic drugs. Mol. Pharmacol *29*, 307-313.

Hsu,H., Lacey,D.L., Dunstan,C.R., Solovyev,I., Colombero,A., Timms,E., Tan,H.L., Elliott,G., Kelley,M.J., Sarosi,I., Wang,L., Xia,X.Z., Elliott,R., Chiu,L., Black,T., Scully,S., Capparelli,C., Morony,S., Shimamoto,G., Bass,M.B., and Boyle,W.J. (1999). Tumor necrosis factor receptor family member RANK mediates osteoclast differentiation and activation induced by osteoprotegerin ligand. Proc. Natl. Acad. Sci. U. S. A *96*, 3540-3545.

Huebner,A.K., Keller,J., Catala-Lehnen,P., Perkovic,S., Streichert,T., Emeson,R.B., Amling,M., and Schinke,T. (2008). The role of calcitonin and alpha-calcitonin gene-related peptide in bone formation. Arch. Biochem. Biophys. *473*, 210-217.

Huebner,A.K., Schinke,T., Priemel,M., Schilling,S., Schilling,A.F., Emeson,R.B., Rueger,J.M., and Amling,M. (2006). Calcitonin deficiency in mice progressively results in high bone turnover. J Bone Miner. Res. *21*, 1924-1934.

Huffman,J.W., Liddle,J., Yu,S., Aung,M.M., Abood,M.E., Wiley,J.L., and Martin,B.R. (1999). 3-(1',1'-Dimethylbutyl)-1-deoxy-delta8-THC and related compounds: synthesis of selective ligands for the CB2 receptor. Bioorg. Med. Chem. *7*, 2905-2914.

Hughes,A.E., Ralston,S.H., Marken,J., Bell,C., MacPherson,H., Wallace,R.G., Van Hul,W., Whyte,M.P., Nakatsuka,K., Hovy,L., and Anderson,D.M. (2000). Mutations in TNFRSF11A, affecting the signal peptide of RANK, cause familial expansile osteolysis. Nat. Genet. *24*, 45-48.

Hughes,D.E., Dai,A., Tiffee,J.C., Li,H.H., Mundy,G.R., and Boyce,B.F. (1996). Estrogen promotes apoptosis of murine osteoclasts mediated by TGF-beta. Nat. Med. *2*, 1132-1136.

Idris,A.I., van't Hof,R.J., Greig,I.R., Ridge,S.A., Baker,D., Ross,R.A., and Ralston,S.H. (2005). Regulation of bone mass, bone loss and osteoclast activity by cannabinoid receptors. Nat. Med. *11*, 774-779.

Idris,A.I. (2008). Role of cannabinoid receptors in bone disorders: alternatives for treatment. Drug News Perspect. *21*, 533-540.

Idris,A.I., Rojas,J., Greig,I.R., van't Hof,R.J., and Ralston,S.H. (2008a). Aminobisphosphonates cause osteoblast apoptosis and inhibit bone nodule formation in vitro. Calcif. Tissue Int. *82*, 191-201.

Idris, A. I., Sophocleous, A., Landao-Bassonga, E., van't Hof, R. J., and Ralston, S. H. Bidirectional regulation of peak bone mass and age-related bone loss by the type 1 cannabinoid receptor. Calcif.Tissue Int. 82[Suppl 1], S57. 2008b.
Ref Type: Abstract

Idris,A.I., Sophocleous,A., Landao-Bassonga,E., van't Hof,R.J., and Ralston,S.H. (2008c). Regulation of bone mass, osteoclast function, and ovariectomy-induced bone loss by the type 2 cannabinoid receptor. Endocrinology *149*, 5619-5626.

Idris,A.I., Greig,I.R., Bassonga-Landao,E., Ralston,S.H., and van't Hof,R.J. (2009). Identification of novel biphenyl carboxylic acid derivatives as novel antiresorptive agents that do not impair parathyroid hormone-induced bone formation. Endocrinology *150*, 5-13.

Ikeda,K., Mangin,M., Dreyer,B.E., Webb,A.C., Posillico,J.T., Stewart,A.F., Bander,N.H., Weir,E.C., Insogna,K.L., and Broadus,A.E. (1988). Identification of transcripts encoding a parathyroid hormone-like peptide in messenger RNAs from a variety of human and animal tumors associated with humoral hypercalcemia of malignancy. J Clin Invest *81*, 2010-2014.

Inzerillo,A.M., Zaidi,M., and Huang,C.L. (2002). Calcitonin: the other thyroid hormone. Thyroid *12*, 791-798.

Iotsova,V., Caamano,J., Loy,J., Yang,Y., Lewin,A., and Bravo,R. (1997). Osteopetrosis in mice lacking NF-kappaB1 and NF-kappaB2. Nat. Med. *3*, 1285-1289.

Izzo,A.A., Mascolo,N., and Capasso,F. (2001). The gastrointestinal pharmacology of cannabinoids. Curr. Opin. Pharmacol *1*, 597-603.

Jilka,R.L. (1998). Cytokines, bone remodeling, and estrogen deficiency: a 1998 update. Bone *23*, 75-81.

Jilka,R.L., Weinstein,R.S., Bellido,T., Parfitt,A.M., and Manolagas,S.C. (1998). Osteoblast programmed cell death (apoptosis): modulation by growth factors and cytokines. J Bone Miner. Res. *13*, 793-802.

Jones,D.H., Kong,Y.Y., and Penninger,J.M. (2002). Role of RANKL and RANK in bone loss and arthritis. Ann. Rheum. Dis. *61 Suppl 2*, ii32-ii39.

Jordan,V.C. (2003). Tamoxifen: a most unlikely pioneering medicine. Nat. Rev. Drug Discov. *2*, 205-213.

Jordan,V.C. and Morrow,M. (1994). Should clinicians be concerned about the carcinogenic potential of tamoxifen? Eur. J Cancer *30A*, 1714-1721.

Jung,A., Bisaz,S., and Fleisch,H. (1973). The binding of pyrophosphate and two diphosphonates by hydroxyapatite crystals. Calcif. Tissue Res. *11*, 269-280.

Kalu,D.N. (1991). The ovariectomized rat model of postmenopausal bone loss. Bone Miner. *15*, 175-191.

Kanematsu,M., Sato,T., Takai,H., Watanabe,K., Ikeda,K., and YAMADA,Y. (2000). Prostaglandin E2 induces expression of receptor activator of nuclear factor-kappa B ligand/osteoprotegrin ligand on pre-B cells: implications for accelerated osteoclastogenesis in estrogen deficiency. J Bone Miner. Res. *15*, 1321-1329.

Kapur,R.P., Yao,Z., Iida,M.H., Clarke,C.M., Doggett,B., Xing,L., and Boyce,B.F. (2004). Malignant autosomal recessive osteopetrosis caused by spontaneous mutation of murine Rank. J Bone Miner. Res. *19*, 1689-1697.

Karasik,D. (2008). Osteoporosis: an evolutionary perspective. Hum. Genet. *124*, 349-356.

Karlsson,M., Contreras,J.A., Hellman,U., Tornqvist,H., and Holm,C. (1997). cDNA cloning, tissue distribution, and identification of the catalytic triad of monoglyceride lipase. Evolutionary relationship to esterases, lysophospholipases, and haloperoxidases. J Biol. Chem. *272*, 27218-27223.

Karsak,M., Cohen-Solal,M., Freudenberg,J., Ostertag,A., Morieux,C., Kornak,U., Essig,J., Erxlebe,E., Bab,I., Kubisch,C., de Vernejoul,M.C., and Zimmer,A. (2005). Cannabinoid receptor type 2 gene is associated with human osteoporosis. Hum. Mol. Genet. *14*, 3389-3396.

Karsenty,G. (2008). Transcriptional control of skeletogenesis. Annu. Rev. Genomics Hum. Genet. *9*, 183-196.

Karsenty,G. and Wagner,E.F. (2002). Reaching a genetic and molecular understanding of skeletal development. Dev. Cell *2*, 389-406.

Katagiri,T. and Takahashi,N. (2002). Regulatory mechanisms of osteoblast and osteoclast differentiation. Oral Dis. *8*, 147-159.

Kawano,M., Hirano,T., Matsuda,T., Taga,T., Horii,Y., Iwato,K., Asaoku,H., Tang,B., Tanabe,O., Tanaka,H., and . (1988). Autocrine generation and requirement of BSF-2/IL-6 for human multiple myelomas. Nature *332*, 83-85.

Keller,E.T. and Brown,J. (2004). Prostate cancer bone metastases promote both osteolytic and osteoblastic activity. J Cell Biochem. *91*, 718-729.

Keller,H. and Kneissel,M. (2005). SOST is a target gene for PTH in bone. Bone *37*, 148-158.

Kemp,B.E., Moseley,J.M., Rodda,C.P., Ebeling,P.R., Wettenhall,R.E., Stapleton,D., Diefenbach-Jagger,H., Ure,F., Michelangeli,V.P., Simmons,H.A., and . (1987). Parathyroid hormone-related protein of malignancy: active synthetic fragments. Science *238*, 1568-1570.

Khosla,S. (2001). Minireview: the OPG/RANKL/RANK system. Endocrinology *142*, 5050-5055.

Kishimoto,S., Kobayashi,Y., Oka,S., Gokoh,M., Waku,K., and Sugiura,T. (2004). 2-Arachidonoylglycerol, an endogenous cannabinoid receptor ligand, induces accelerated production of chemokines in HL-60 cells. J Biochem. *135*, 517-524.

Klein,T.W. (2005). Cannabinoid-based drugs as anti-inflammatory therapeutics. Nat. Rev. Immunol. *5*, 400-411.

Klein,T.W., Newton,C., and Friedman,H. (1998). Cannabinoid receptors and immunity. Immunol. Today *19*, 373-381.

Klein,T.W., Newton,C., Larsen,K., Lu,L., Perkins,I., Nong,L., and Friedman,H. (2003). The cannabinoid system and immune modulation. J Leukoc. Biol. *74*, 486-496.

Komori,T., Yagi,H., Nomura,S., Yamaguchi,A., Sasaki,K., Deguchi,K., Shimizu,Y., Bronson,R.T., Gao,Y.H., Inada,M., Sato,M., Okamoto,R., Kitamura,Y., Yoshiki,S., and Kishimoto,T. (1997). Targeted disruption of Cbfa1 results in a complete lack of bone formation owing to maturational arrest of osteoblasts. Cell *89*, 755-764.

Kong,Y.Y., Yoshida,H., Sarosi,I., Tan,H.L., Timms,E., Capparelli,C., Morony,S., Oliveira-dos-Santos,A.J., Van,G., Itie,A., Khoo,W., Wakeham,A., Dunstan,C.R.,

Lacey,D.L., Mak,T.W., Boyle,W.J., and Penninger,J.M. (1999). OPGL is a key regulator of osteoclastogenesis, lymphocyte development and lymph-node organogenesis. Nature *397*, 315-323.

Kornak,U., Kasper,D., Bosl,M.R., Kaiser,E., Schweizer,M., Schulz,A., Friedrich,W., Delling,G., and Jentsch,T.J. (2001). Loss of the ClC-7 chloride channel leads to osteopetrosis in mice and man. Cell *104*, 205-215.

Kornak,U., Schulz,A., Friedrich,W., Uhlhaas,S., Kremens,B., Voit,T., Hasan,C., Bode,U., Jentsch,T.J., and Kubisch,C. (2000). Mutations in the a3 subunit of the vacuolar H(+)-ATPase cause infantile malignant osteopetrosis. Hum. Mol. Genet. *9*, 2059-2063.

Kousteni,S., Bellido,T., Plotkin,L.I., O'Brien,C.A., Bodenner,D.L., Han,L., Han,K., DiGregorio,G.B., Katzenellenbogen,J.A., Katzenellenbogen,B.S., Roberson,P.K., Weinstein,R.S., Jilka,R.L., and Manolagas,S.C. (2001). Nongenotropic, sex-nonspecific signaling through the estrogen or androgen receptors: dissociation from transcriptional activity. Cell *104*, 719-730.

Krishnan,V., Moore,T.L., Ma,Y.L., Helvering,L.M., Frolik,C.A., Valasek,K.M., Ducy,P., and Geiser,A.G. (2003). Parathyroid hormone bone anabolic action requires Cbfa1/Runx2-dependent signaling. Mol. Endocrinol. *17*, 423-435.

Kunos,G., Batkai,S., Offertaler,L., Mo,F., Liu,J., Karcher,J., and Harvey-White,J. (2002). The quest for a vascular endothelial cannabinoid receptor. Chem. Phys. Lipids *121*, 45-56.

Lacey,D.L., Erdmann,J.M., Teitelbaum,S.L., Tan,H.L., Ohara,J., and Shioi,A. (1995). Interleukin 4, interferon-gamma, and prostaglandin E impact the osteoclastic cell-forming potential of murine bone marrow macrophages. Endocrinology *136*, 2367-2376.

Lacey,D.L., Timms,E., Tan,H.L., Kelley,M.J., Dunstan,C.R., Burgess,T., Elliott,R., Colombero,A., Elliott,G., Scully,S., Hsu,H., Sullivan,J., Hawkins,N., Davy,E., Capparelli,C., Eli,A., Qian,Y.X., Kaufman,S., Sarosi,I., Shalhoub,V., Senaldi,G., Guo,J., Delaney,J., and Boyle,W.J. (1998). Osteoprotegerin ligand is a cytokine that regulates osteoclast differentiation and activation. Cell *93*, 165-176.

Laketic-Ljubojevic,I., Suva,L.J., Maathuis,F.J., Sanders,D., and Skerry,T.M. (1999). Functional characterization of N-methyl-D-aspartic acid-gated channels in bone cells. Bone *25*, 631-637.

Lakkakorpi,P.T., Horton,M.A., Helfrich,M.H., Karhukorpi,E.K., and Vaananen,H.K. (1991). Vitronectin receptor has a role in bone resorption but does not mediate tight sealing zone attachment of osteoclasts to the bone surface. J Cell Biol. *115*, 1179-1186.

Laurin,N., Brown,J.P., Morissette,J., and Raymond,V. (2002). Recurrent mutation of the gene encoding sequestosome 1 (SQSTM1/p62) in Paget disease of bone. Am. J Hum. Genet. *70*, 1582-1588.

Le Moullec,J.M., Jullienne,A., Chenais,J., Lasmoles,F., Guliana,J.M., Milhaud,G., and Moukhtar,M.S. (1984). The complete sequence of human preprocalcitonin. FEBS Lett. *167*, 93-97.

Lecka-Czernik,B., Gubrij,I., Moerman,E.J., Kajkenova,O., Lipschitz,D.A., Manolagas,S.C., and Jilka,R.L. (1999). Inhibition of Osf2/Cbfa1 expression and terminal osteoblast differentiation by PPARgamma2. J Cell Biochem. *74*, 357-371.

Ledent,C., Valverde,O., Cossu,G., Petitet,F., Aubert,J.F., Beslot,F., Bohme,G.A., Imperato,A., Pedrazzini,T., Roques,B.P., Vassart,G., Fratta,W., and Parmentier,M. (1999). Unresponsiveness to cannabinoids and reduced addictive effects of opiates in CB1 receptor knockout mice. Science *283*, 401-404.

Lee,J.W., Chung,H.Y., Ehrlich,L.A., Jelinek,D.F., Callander,N.S., Roodman,G.D., and Choi,S.J. (2004). IL-3 expression by myeloma cells increases both osteoclast formation and growth of myeloma cells. Blood *103*, 2308-2315.

Lee,K.S., Kim,H.J., Li,Q.L., Chi,X.Z., Ueta,C., Komori,T., Wozney,J.M., Kim,E.G., Choi,J.Y., Ryoo,H.M., and Bae,S.C. (2000). Runx2 is a common target of transforming growth factor beta1 and bone morphogenetic protein 2, and cooperation between Runx2 and Smad5 induces osteoblast-specific gene expression in the pluripotent mesenchymal precursor cell line C2C12. Mol. Cell Biol. *20*, 8783-8792.

Lee,M.H., Kim,Y.J., Kim,H.J., Park,H.D., Kang,A.R., Kyung,H.M., Sung,J.H., Wozney,J.M., Kim,H.J., and Ryoo,H.M. (2003a). BMP-2-induced Runx2 expression is mediated by Dlx5, and TGF-beta 1 opposes the BMP-2-induced osteoblast differentiation by suppression of Dlx5 expression. J Biol. Chem. *278*, 34387-34394.

Lee,M.H., Kwon,T.G., Park,H.S., Wozney,J.M., and Ryoo,H.M. (2003b). BMP-2-induced Osterix expression is mediated by Dlx5 but is independent of Runx2. Biochem. Biophys. Res. Commun. *309*, 689-694.

Lee,S.K., Kalinowski,J., Jastrzebski,S., and Lorenzo,J.A. (2002). 1,25(OH)2 vitamin D3-stimulated osteoclast formation in spleen-osteoblast cocultures is mediated in part by enhanced IL-1 alpha and receptor activator of NF-kappa B ligand production in osteoblasts. J Immunol. *169*, 2374-2380.

Lefebvre,V., Li,P., and de Crombrugghe,B. (1998). A new long form of Sox5 (L-Sox5), Sox6 and Sox9 are coexpressed in chondrogenesis and cooperatively activate the type II collagen gene. EMBO J *17*, 5718-5733.

Lerner,U.H. (2006). Bone remodeling in post-menopausal osteoporosis. J Dent. Res. *85*, 584-595.

Lewis,S.E., Erickson,R.P., Barnett,L.B., Venta,P.J., and Tashian,R.E. (1988). N-ethyl-N-nitrosourea-induced null mutation at the mouse Car-2 locus: an animal model for human carbonic anhydrase II deficiency syndrome. Proc. Natl. Acad. Sci. U. S. A *85*, 1962-1966.

Li,Y.P., Chen,W., Liang,Y., Li,E., and Stashenko,P. (1999). Atp6i-deficient mice exhibit severe osteopetrosis due to loss of osteoclast-mediated extracellular acidification. Nat. Genet. *23*, 447-451.

Lian,J.B., Javed,A., Zaidi,S.K., Lengner,C., Montecino,M., van Wijnen,A.J., Stein,J.L., and Stein,G.S. (2004). Regulatory controls for osteoblast growth and differentiation: role of Runx/Cbfa/AML factors. Crit Rev. Eukaryot. Gene Expr. *14*, 1-41.

Lichtenstein,A., Berenson,J., Norman,D., Chang,M.P., and Carlile,A. (1989). Production of cytokines by bone marrow cells obtained from patients with multiple myeloma. Blood *74*, 1266-1273.

Lin,H.Y., Harris,T.L., Flannery,M.S., Aruffo,A., Kaji,E.H., Gorn,A., Kolakowski,L.F., Jr., Lodish,H.F., and Goldring,S.R. (1991). Expression cloning of an adenylate cyclase-coupled calcitonin receptor. Science *254*, 1022-1024.

Lin,R., Amizuka,N., Sasaki,T., Aarts,M.M., Ozawa,H., Goltzman,D., Henderson,J.E., and White,J.H. (2002). 1Alpha,25-dihydroxyvitamin D3 promotes vascularization of the chondro-osseous junction by stimulating expression of vascular endothelial growth factor and matrix metalloproteinase 9. J Bone Miner. Res. *17*, 1604-1612.

Logothetis,C.J. and Lin,S.H. (2005). Osteoblasts in prostate cancer metastasis to bone. Nat. Rev. Cancer *5*, 21-28.

Lomaga,M.A., Yeh,W.C., Sarosi,I., Duncan,G.S., Furlonger,C., Ho,A., Morony,S., Capparelli,C., Van,G., Kaufman,S., van der,H.A., Itie,A., Wakeham,A., Khoo,W., Sasaki,T., Cao,Z., Penninger,J.M., Paige,C.J., Lacey,D.L., Dunstan,C.R., Boyle,W.J., Goeddel,D.V., and Mak,T.W. (1999). TRAF6 deficiency results in osteopetrosis and defective interleukin-1, CD40, and LPS signaling. Genes Dev. *13*, 1015-1024.

Lucas,G.J., Mehta,S.G., Hocking,L.J., Stewart,T.L., Cundy,T., Nicholson,G.C., Walsh,J.P., Fraser,W.D., Watts,G.D., Ralston,S.H., and Kimonis,V.E. (2006). Evaluation of the role of Valosin-containing protein in the pathogenesis of familial and sporadic Paget's disease of bone. Bone *38*, 280-285.

Lundberg,P., Allison,S.J., Lee,N.J., Baldock,P.A., Brouard,N., Rost,S., Enriquez,R.F., Sainsbury,A., Lamghari,M., Simmons,P., Eisman,J.A., Gardiner,E.M., and Herzog,H. (2007). Greater bone formation of Y2 knockout mice is associated with increased osteoprogenitor numbers and altered Y1 receptor expression. J Biol. Chem. *282*, 19082-19091.

Lunn,C.A., Reich,E.P., Fine,J.S., Lavey,B., Kozlowski,J.A., Hipkin,R.W., Lundell,D.J., and Bober,L. (2008). Biology and therapeutic potential of cannabinoid CB(2) receptor inverse agonists. Br. J Pharmacol *153*, 226-239.

Luppen,C.A., Smith,E., Spevak,L., Boskey,A.L., and Frenkel,B. (2003). Bone morphogenetic protein-2 restores mineralization in glucocorticoid-inhibited MC3T3-E1 osteoblast cultures. J Bone Miner. Res. *18*, 1186-1197.

Lutz,B. (2002). Molecular biology of cannabinoid receptors. Prostaglandins Leukot. Essent. Fatty Acids *66*, 123-142.

Maccarrone,M., Bari,M., Lorenzon,T., Bisogno,T., Di,M., V, and Finazzi-Agro,A. (2000). Anandamide uptake by human endothelial cells and its regulation by nitric oxide. J Biol. Chem. *275*, 13484-13492.

Mach,D.B., Rogers,S.D., Sabino,M.C., Luger,N.M., Schwei,M.J., Pomonis,J.D., Keyser,C.P., Clohisy,D.R., Adams,D.J., O'Leary,P., and Mantyh,P.W. (2002). Origins of skeletal pain: sensory and sympathetic innervation of the mouse femur. Neuroscience *113*, 155-166.

Mackie,E.J. (2003). Osteoblasts: novel roles in orchestration of skeletal architecture. Int. J Biochem. Cell Biol. *35*, 1301-1305.

Mackie,K. and Hille,B. (1992). Cannabinoids inhibit N-type calcium channels in neuroblastoma-glioma cells. Proc. Natl. Acad. Sci. U. S. A *89*, 3825-3829.

Mackie,K., Lai,Y., Westenbroek,R., and Mitchell,R. (1995). Cannabinoids activate an inwardly rectifying potassium conductance and inhibit Q-type calcium currents in AtT20 cells transfected with rat brain cannabinoid receptor. J Neurosci. *15*, 6552-6561.

Maier,C.S., Yan,X., Harder,M.E., Schimerlik,M.I., Deinzer,M.L., Pasa-Tolic,L., and Smith,R.D. (2000). Electrospray ionization Fourier transform ion cyclotron resonance mass spectrometric analysis of the recombinant human macrophage colony stimulating factor beta and derivatives. J Am. Soc. Mass Spectrom. *11*, 237-243.

Majumdar,M.K., Thiede,M.A., Mosca,J.D., Moorman,M., and Gerson,S.L. (1998). Phenotypic and functional comparison of cultures of marrow-derived mesenchymal stem cells (MSCs) and stromal cells. J Cell Physiol *176*, 57-66.

Makin,G., Lohnes,D., Byford,V., Ray,R., and Jones,G. (1989). Target cell metabolism of 1,25-dihydroxyvitamin D3 to calcitroic acid. Evidence for a pathway in kidney and bone involving 24-oxidation. Biochem. J *262*, 173-180.

Malfait,A.M., Gallily,R., Sumariwalla,P.F., Malik,A.S., Andreakos,E., Mechoulam,R., and Feldmann,M. (2000). The nonpsychoactive cannabis constituent cannabidiol is an oral anti-arthritic therapeutic in murine collagen-induced arthritis. Proc. Natl. Acad. Sci. U. S. A *97*, 9561-9566.

Mannstadt,M., Juppner,H., and Gardella,T.J. (1999). Receptors for PTH and PTHrP: their biological importance and functional properties. Am. J Physiol *277*, F665-F675.

Manolagas,S.C. (2000). Birth and death of bone cells: basic regulatory mechanisms and implications for the pathogenesis and treatment of osteoporosis. Endocr. Rev. *21*, 115-137.

Manolagas,S.C., Kousteni,S., and Jilka,R.L. (2002). Sex steroids and bone. Recent Prog. Horm. Res. *57*, 385-409.

Marie,P.J. (2006). Strontium ranelate: a physiological approach for optimizing bone formation and resorption. Bone *38*, S10-S14.

Marie,P.J. (2008). Transcription factors controlling osteoblastogenesis. Arch. Biochem. Biophys. *473*, 98-105.

Marotti,G. (1996). The structure of bone tissues and the cellular control of their deposition. Ital. J Anat. Embryol. *101*, 25-79.

Martin,B.R. (1986). Cellular effects of cannabinoids. Pharmacol Rev. *38*, 45-74.

Martin,B.R., Mechoulam,R., and Razdan,R.K. (1999). Discovery and characterization of endogenous cannabinoids. Life Sci. *65*, 573-595.

Masuyama,R., Stockmans,I., Torrekens,S., Van Looveren,R., Maes,C., Carmeliet,P., Bouillon,R., and Carmeliet,G. (2006). Vitamin D receptor in chondrocytes promotes osteoclastogenesis and regulates FGF23 production in osteoblasts. J Clin Invest *116*, 3150-3159.

Matias,I., Pochard,P., Orlando,P., Salzet,M., Pestel,J., and Di,M., V (2002). Presence and regulation of the endocannabinoid system in human dendritic cells. Eur. J Biochem. *269*, 3771-3778.

Matsuda,L.A., Lolait,S.J., Brownstein,M.J., Young,A.C., and Bonner,T.I. (1990). Structure of a cannabinoid receptor and functional expression of the cloned cDNA. Nature *346*, 561-564.

Mayer,M.L. and Westbrook,G.L. (1987). The physiology of excitatory amino acids in the vertebrate central nervous system. Prog. Neurobiol. *28*, 197-276.

Mazziotti,G., Angeli,A., Bilezikian,J.P., Canalis,E., and Giustina,A. (2006). Glucocorticoid-induced osteoporosis: an update. Trends Endocrinol. Metab *17*, 144-149.

McCarthy,T.L., Chang,W.Z., Liu,Y., and Centrella,M. (2003). Runx2 integrates estrogen activity in osteoblasts. J Biol. Chem. *278*, 43121-43129.

McGill,G.G., Horstmann,M., Widlund,H.R., Du,J., Motyckova,G., Nishimura,E.K., Lin,Y.L., Ramaswamy,S., Avery,W., Ding,H.F., Jordan,S.A., Jackson,I.J., Korsmeyer,S.J., Golub,T.R., and Fisher,D.E. (2002). Bcl2 regulation by the melanocyte master regulator Mitf modulates lineage survival and melanoma cell viability. Cell *109*, 707-718.

McHugh,K.P., Hodivala-Dilke,K., Zheng,M.H., Namba,N., Lam,J., Novack,D., Feng,X., Ross,F.P., Hynes,R.O., and Teitelbaum,S.L. (2000). Mice lacking beta3 integrins are osteosclerotic because of dysfunctional osteoclasts. J Clin Invest *105*, 433-440.

McKallip,R.J., Nagarkatti,M., and Nagarkatti,P.S. (2005). Delta-9-tetrahydrocannabinol enhances breast cancer growth and metastasis by suppression of the antitumor immune response. J Immunol. *174*, 3281-3289.

Mechoulam,R., Ben Shabat,S., Hanus,L., Ligumsky,M., Kaminski,N.E., Schatz,A.R., Gopher,A., Almog,S., Martin,B.R., Compton,D.R., and . (1995). Identification of an endogenous 2-monoglyceride, present in canine gut, that binds to cannabinoid receptors. Biochem. Pharmacol *50*, 83-90.

Mechoulam,R., Hanus,L., and Fride,E. (1998). Towards cannabinoid drugs--revisited. Prog. Med. Chem. *35*, 199-243.

Meier,C.A. (1998). Role of novel antiresorptive agents for the prevention and treatment of osteoporosis. Eur. J Endocrinol. *139*, 18-19.

Meikle,M.C., Bord,S., Hembry,R.M., Compston,J., Croucher,P.I., and Reynolds,J.J. (1992). Human osteoblasts in culture synthesize collagenase and other matrix metalloproteinases in response to osteotropic hormones and cytokines. J Cell Sci. *103 (Pt 4)*, 1093-1099.

Merle,B., Itzstein,C., Delmas,P.D., and Chenu,C. (2003). NMDA glutamate receptors are expressed by osteoclast precursors and involved in the regulation of osteoclastogenesis. J Cell Biochem. *90*, 424-436.

Meunier,P.J., Roux,C., Seeman,E., Ortolani,S., Badurski,J.E., Spector,T.D., Cannata,J., Balogh,A., Lemmel,E.M., Pors-Nielsen,S., Rizzoli,R., Genant,H.K., and Reginster,J.Y. (2004). The effects of strontium ranelate on the risk of vertebral fracture in women with postmenopausal osteoporosis. N. Engl. J Med. *350*, 459-468.

Miller,J., Chan,B.K., and Nelson,H.D. (2002). Postmenopausal estrogen replacement and risk for venous thromboembolism: a systematic review and meta-analysis for the U.S. Preventive Services Task Force. Ann. Intern. Med. *136*, 680-690.

Milne,G.M., Jr. and Johnson,M.R. (1981). Levonantradol: a role for central prostanoid mechanisms? J Clin Pharmacol *21*, 367S-374S.

Mizuno,A., Amizuka,N., Irie,K., Murakami,A., Fujise,N., Kanno,T., Sato,Y., Nakagawa,N., Yasuda,H., Mochizuki,S., Gomibuchi,T., Yano,K., Shima,N., Washida,N., Tsuda,E., Morinaga,T., Higashio,K., and Ozawa,H. (1998). Severe osteoporosis in mice lacking osteoclastogenesis inhibitory factor/osteoprotegerin. Biochem. Biophys. Res. Commun. *247*, 610-615.

Monroe,D.G., Secreto,F.J., Subramaniam,M., Getz,B.J., Khosla,S., and Spelsberg,T.C. (2005). Estrogen receptor alpha and beta heterodimers exert unique effects on estrogen- and tamoxifen-dependent gene expression in human U2OS osteosarcoma cells. Mol. Endocrinol. *19*, 1555-1568.

Monteleone,P., Matias,I., Martiadis,V., De Petrocellis,L., Maj,M., and Di,M., V (2005). Blood levels of the endocannabinoid anandamide are increased in anorexia nervosa and in binge-eating disorder, but not in bulimia nervosa. Neuropsychopharmacology *30*, 1216-1221.

Moonga,B.S., Alam,A.S., Bevis,P.J., Avaldi,F., Soncini,R., Huang,C.L., and Zaidi,M. (1992). Regulation of cytosolic free calcium in isolated rat osteoclasts by calcitonin. J Endocrinol. *132*, 241-249.

Morohashi,T., Sano,T., and Yamada,S. (1994). Effects of strontium on calcium metabolism in rats. I. A distinction between the pharmacological and toxic doses. Jpn. J Pharmacol *64*, 155-162.

Mulari,M.T., Zhao,H., Lakkakorpi,P.T., and Vaananen,H.K. (2003). Osteoclast ruffled border has distinct subdomains for secretion and degraded matrix uptake. Traffic. *4*, 113-125.

Mullender,M.G., van der Meer,D.D., Huiskes,R., and Lips,P. (1996). Osteocyte density changes in aging and osteoporosis. Bone *18*, 109-113.

Mundy,G.R., Rodan,S.B., Majeska,R.J., DeMartino,S., Trimmier,C., Martin,T.J., and Rodan,G.A. (1982). Unidirectional migration of osteosarcoma cells with osteoblast characteristics in response to products of bone resorption. Calcif. Tissue Int. *34*, 542-546.

Munro,S., Thomas,K.L., and Abu-Shaar,M. (1993). Molecular characterization of a peripheral receptor for cannabinoids. Nature *365*, 61-65.

Munson,A.E., Harris,L.S., Friedman,M.A., Dewey,W.L., and Carchman,R.A. (1975). Antineoplastic activity of cannabinoids. J Natl. Cancer Inst. *55*, 597-602.

Murray J.Favus [Editor]. Primer on the Metabolic Bone Diseases and Disorders of Mineral Metabolism (Fifth Edition). 2006. The American Society for Bone and Mineral Research.
Ref Type: Generic

Navarro,M., Carrera,M.R., Fratta,W., Valverde,O., Cossu,G., Fattore,L., Chowen,J.A., Gomez,R., del,A., I, Villanua,M.A., Maldonado,R., Koob,G.F., and Rodriguez,d.F. (2001). Functional interaction between opioid and cannabinoid receptors in drug self-administration. J Neurosci. *21*, 5344-5350.

Neer,R.M., Arnaud,C.D., Zanchetta,J.R., Prince,R., Gaich,G.A., Reginster,J.Y., Hodsman,A.B., Eriksen,E.F., Ish-Shalom,S., Genant,H.K., Wang,O., and Mitlak,B.H. (2001). Effect of parathyroid hormone (1-34) on fractures and bone mineral density in postmenopausal women with osteoporosis. N. Engl. J Med. *344*, 1434-1441.

Nelson,J.F. and Felicio,L.S. (1990). Hormonal influences on reproductive aging in mice. Ann. N. Y. Acad. Sci. *592*, 8-12.

Nelson,J.F., Felicio,L.S., Osterburg,H.H., and Finch,C.E. (1981). Altered profiles of estradiol and progesterone associated with prolonged estrous cycles and persistent vaginal cornification in aging C57BL/6J mice. Biol. Reprod. *24*, 784-794.

Ng,L.J., Wheatley,S., Muscat,G.E., Conway-Campbell,J., Bowles,J., Wright,E., Bell,D.M., Tam,P.P., Cheah,K.S., and Koopman,P. (1997). SOX9 binds DNA, activates transcription, and coexpresses with type II collagen during chondrogenesis in the mouse. Dev. Biol. *183*, 108-121.

Nicholson,G.C., Moseley,J.M., Sexton,P.M., Mendelsohn,F.A., and Martin,T.J. (1986). Abundant calcitonin receptors in isolated rat osteoclasts. Biochemical and autoradiographic characterization. J Clin Invest *78*, 355-360.

Nishida,S., Yamaguchi,A., Tanizawa,T., Endo,N., Mashiba,T., Uchiyama,Y., Suda,T., Yoshiki,S., and Takahashi,H.E. (1994). Increased bone formation by intermittent parathyroid hormone administration is due to the stimulation of proliferation and differentiation of osteoprogenitor cells in bone marrow. Bone *15*, 717-723.

Noble,B.S. (2008). The osteocyte lineage. Arch. Biochem. Biophys. *473*, 106-111.

Noble,B.S., Peet,N., Stevens,H.Y., Brabbs,A., Mosley,J.R., Reilly,G.C., Reeve,J., Skerry,T.M., and Lanyon,L.E. (2003). Mechanical loading: biphasic osteocyte survival and targeting of osteoclasts for bone destruction in rat cortical bone. Am. J Physiol Cell Physiol *284*, C934-C943.

Nunez,E., Benito,C., Pazos,M.R., Barbachano,A., Fajardo,O., Gonzalez,S., Tolon,R.M., and Romero,J. (2004). Cannabinoid CB2 receptors are expressed by perivascular microglial cells in the human brain: an immunohistochemical study. Synapse *53*, 208-213.

Ofek,O., Karsak,M., Leclerc,N., Fogel,M., Frenkel,B., Wright,K., Tam,J., Attar-Namdar,M., Kram,V., Shohami,E., Mechoulam,R., Zimmer,A., and Bab,I. (2006). Peripheral cannabinoid receptor, CB2, regulates bone mass. Proc. Natl. Acad. Sci. U. S. A *103*, 696-701.

Ohno-Shosaku,T., Maejima,T., and Kano,M. (2001). Endogenous cannabinoids mediate retrograde signals from depolarized postsynaptic neurons to presynaptic terminals. Neuron *29*, 729-738.

Olsen,B.R., Reginato,A.M., and Wang,W. (2000). Bone development. Annu. Rev. Cell Dev. Biol. *16*, 191-220.

Olson,J.M., Kennedy,S.J., and Cabral,G.A. (2003). Expression of the murine CB2 cannabinoid receptor using a recombinant Semliki Forest virus. Biochem. Pharmacol *65*, 1931-1942.

Orriss,I.R., Key,M.L., Colston,K.W., and Arnett,T.R. (2009). Inhibition of osteoblast function in vitro by aminobisphosphonates. J Cell Biochem. *106*, 109-118.

Oseni,T., Patel,R., Pyle,J., and Jordan,V.C. (2008). Selective estrogen receptor modulators and phytoestrogens. Planta Med. *74*, 1656-1665.

Otto,F., Thornell,A.P., Crompton,T., Denzel,A., Gilmour,K.C., Rosewell,I.R., Stamp,G.W., Beddington,R.S., Mundlos,S., Olsen,B.R., Selby,P.B., and Owen,M.J. (1997). Cbfa1, a candidate gene for cleidocranial dysplasia syndrome, is essential for osteoblast differentiation and bone development. Cell *89*, 765-771.

Oursler,M.J., Cortese,C., Keeting,P., Anderson,M.A., Bonde,S.K., Riggs,B.L., and Spelsberg,T.C. (1991). Modulation of transforming growth factor-beta production in normal human osteoblast-like cells by 17 beta-estradiol and parathyroid hormone. Endocrinology *129*, 3313-3320.

Owen,T.A., Aronow,M.S., Barone,L.M., Bettencourt,B., Stein,G.S., and Lian,J.B. (1991). Pleiotropic effects of vitamin D on osteoblast gene expression are related to the proliferative and differentiated state of the bone cell phenotype: dependency upon basal levels of gene expression, duration of exposure, and bone matrix competency in normal rat osteoblast cultures. Endocrinology *128*, 1496-1504.

Oyajobi,B.O., Lomri,A., Hott,M., and Marie,P.J. (1999). Isolation and characterization of human clonogenic osteoblast progenitors immunoselected from fetal bone marrow stroma using STRO-1 monoclonal antibody. J Bone Miner. Res. *14*, 351-361.

Ozgur,S., Sumer,H., and Kocoglu,G. (1996). Rickets and soil strontium. Arch. Dis. Child *75*, 524-526.

Pacifici,R. (1999). Aging and cytokine production. Calcif. Tissue Int. *65*, 345-351.

Palumbo,C., Palazzini,S., and Marotti,G. (1990). Morphological study of intercellular junctions during osteocyte differentiation. Bone *11*, 401-406.

Papapoulos,S. and Makras,P. (2008). Selection of antiresorptive or anabolic treatments for postmenopausal osteoporosis. Nat. Clin Pract. Endocrinol. Metab *4*, 514-523.

Paredes,R., Arriagada,G., Cruzat,F., Olate,J., Van Wijnen,A., Lian,J., Stein,G., Stein,J., and Montecino,M. (2004). The Runx2 transcription factor plays a key role in the 1alpha,25-dihydroxy Vitamin D3-dependent upregulation of the rat osteocalcin (OC) gene expression in osteoblastic cells. J Steroid Biochem. Mol. Biol. *89-90*, 269-271.

Parfitt,A.M., Drezner,M.K., Glorieux,F.H., Kanis,J.A., Malluche,H., Meunier,P.J., Ott,S.M., and Recker,R.R. (1987). Bone histomorphometry: standardization of nomenclature, symbols, and units. Report of the ASBMR Histomorphometry Nomenclature Committee. J Bone Miner. Res. *2*, 595-610.

Parikka,V., Lehenkari,P., Sassi,M.L., Halleen,J., Risteli,J., Harkonen,P., and Vaananen,H.K. (2001). Estrogen reduces the depth of resorption pits by disturbing the organic bone matrix degradation activity of mature osteoclasts. Endocrinology *142*, 5371-5378.

Patel,M.S. and Elefteriou,F. (2007). The new field of neuroskeletal biology. Calcif. Tissue Int. *80*, 337-347.

Pearse,R.N., Sordillo,E.M., Yaccoby,S., Wong,B.R., Liau,D.F., Colman,N., Michaeli,J., Epstein,J., and Choi,Y. (2001). Multiple myeloma disrupts the TRANCE/ osteoprotegerin cytokine axis to trigger bone destruction and promote tumor progression. Proc. Natl. Acad. Sci. U. S. A *98*, 11581-11586.

Pertwee,R.G. (1997). Pharmacology of cannabinoid CB1 and CB2 receptors. Pharmacol Ther. *74*, 129-180.

Pertwee,R.G. (1999). Pharmacology of cannabinoid receptor ligands. Curr. Med. Chem. *6*, 635-664.

Pertwee,R.G. (2001). Cannabinoid receptors and pain. Prog. Neurobiol. *63*, 569-611.

Pertwee,R.G. and Ross,R.A. (2002). Cannabinoid receptors and their ligands. Prostaglandins Leukot. Essent. Fatty Acids *66*, 101-121.

Petzel,M. (2007). Action of leptin on bone and its relationship to menopause. Biomed. Pap. Med. Fac. Univ Palacky. Olomouc. Czech. Repub. *151*, 195-199.

Pfeilschifter,J., Chenu,C., Bird,A., Mundy,G.R., and Roodman,G.D. (1989). Interleukin-1 and tumor necrosis factor stimulate the formation of human osteoclastlike cells in vitro. J Bone Miner. Res. *4*, 113-118.

Pingle,S.C., Matta,J.A., and Ahern,G.P. (2007). Capsaicin receptor: TRPV1 a promiscuous TRP channel. Handb. Exp. Pharmacol 155-171.

Politou,M.C., Heath,D.J., Rahemtulla,A., Szydlo,R., Anagnostopoulos,A., Dimopoulos,M.A., Croucher,P.I., and Terpos,E. (2006). Serum concentrations of Dickkopf-1 protein are increased in patients with multiple myeloma and reduced after autologous stem cell transplantation. Int. J Cancer *119*, 1728-1731.

Raisz,L.G. (1999). Physiology and pathophysiology of bone remodeling. Clin Chem. *45*, 1353-1358.

Ralston,S.H. (2008). Pathogenesis of Paget's disease of bone. Bone *43*, 819-825.

Ralston,S.H., Langston,A.L., and Reid,I.R. (2008). Pathogenesis and management of Paget's disease of bone. Lancet *372*, 155-163.

Rebel,A., Malkani,K., Basle,M., Bregeon,C., Patezour,A., and Filmon,R. (1974). Ultrastructural characteristics of osteoclasts in Paget's disease. Rev. Rhum. Mal Osteoartic. *41*, 767-771.

Reddy,S.V., Kurihara,N., Menaa,C., and Roodman,G.D. (2001). Paget's disease of bone: a disease of the osteoclast. Rev. Endocr. Metab Disord. *2*, 195-201.

Redzepovic,J., Weinmann,G., Ott,I., and Gust,R. (2008). Current trends in multiple myeloma management. J Int. Med. Res. *36*, 371-386.

Reginster,J.Y. and Lecart,M.P. (1995). Efficacy and safety of drugs for Paget's disease of bone. Bone *17*, 485S-488S.

Reginster,J.Y., Seeman,E., de Vernejoul,M.C., Adami,S., Compston,J., Phenekos,C., Devogelaer,J.P., Curiel,M.D., Sawicki,A., Goemaere,S., Sorensen,O.H., Felsenberg,D., and Meunier,P.J. (2005). Strontium ranelate reduces the risk of nonvertebral fractures in postmenopausal women with osteoporosis: Treatment of Peripheral Osteoporosis (TROPOS) study. J Clin Endocrinol. Metab *90*, 2816-2822.

Reichman,M., Nen,W., and Hokin,L.E. (1991). Delta 9-tetrahydrocannabinol inhibits arachidonic acid acylation of phospholipids and triacylglycerols in guinea pig cerebral cortex slices. Mol. Pharmacol *40*, 547-555.

Ridge, S. A., Ford, L, Cameron, GA, Ross, RA, and Rogers, M. J. Endocannabinoids are produced by bone cells and stimulate bone resorption in vitro. Bone 40[Suppl 2], S120. 2007.
Ref Type: Abstract

Riggs,B.L., Khosla,S., and Melton,L.J., III (2002). Sex steroids and the construction and conservation of the adult skeleton. Endocr. Rev. *23*, 279-302.

Riggs,B.L. and Melton,L.J., III (1986). Involutional osteoporosis. N. Engl. J Med. *314*, 1676-1686.

Riggs,B.L., Melton,L.J., Robb,R.A., Camp,J.J., Atkinson,E.J., McDaniel,L., Amin,S., Rouleau,P.A., and Khosla,S. (2008). A population-based assessment of rates of bone loss at multiple skeletal sites: evidence for substantial trabecular bone loss in young adult women and men. J Bone Miner. Res. *23*, 205-214.

Robling,A.G., Bellido,T., and Turner,C.H. (2006). Mechanical stimulation in vivo reduces osteocyte expression of sclerostin. J Musculoskelet. Neuronal. Interact. *6*, 354.

Robling,A.G., Burr,D.B., and Turner,C.H. (2001). Recovery periods restore mechanosensitivity to dynamically loaded bone. J Exp. Biol. *204*, 3389-3399.

Rodan,G.A. and Fleisch,H.A. (1996). Bisphosphonates: mechanisms of action. J Clin Invest *97*, 2692-2696.

Rodan,G.A. and Martin,T.J. (2000). Therapeutic approaches to bone diseases. Science *289*, 1508-1514.

Rodriguez,d.F., del,A., I, Bermudez-Silva,F.J., Bilbao,A., Cippitelli,A., and Navarro,M. (2005). The endocannabinoid system: physiology and pharmacology. Alcohol Alcohol *40*, 2-14.

Roelofs,A.J., Thompson,K., Gordon,S., and Rogers,M.J. (2006). Molecular mechanisms of action of bisphosphonates: current status. Clin Cancer Res. *12*, 6222s-6230s.

Rogers,M.J. (2003). New insights into the molecular mechanisms of action of bisphosphonates. Curr. Pharm. Des *9*, 2643-2658.

Roodman,G.D. (1996). Advances in bone biology: the osteoclast. Endocr. Rev. *17*, 308-332.

Roodman,G.D. (2004). Mechanisms of bone metastasis. N. Engl. J Med. *350*, 1655-1664.

Rose,A.A. and Siegel,P.M. (2006). Breast cancer-derived factors facilitate osteolytic bone metastasis. Bull. Cancer *93*, 931-943.

Rosen,E.D. and MacDougald,O.A. (2006). Adipocyte differentiation from the inside out. Nat. Rev. Mol. Cell Biol. *7*, 885-896.

Ross,F.P. (2006). M-CSF, c-Fms, and signaling in osteoclasts and their precursors. Ann. N. Y. Acad. Sci. *1068*, 110-116.

Rossi,F., Siniscalco,D., Luongo,L., De Petrocellis,L., Bellini,G., Petrosino,S., Torella,M., Santoro,C., Nobili,B., Perrotta,S., Di,M., V, and Maione,S. (2009). The endovanilloid/endocannabinoid system in human osteoclasts: possible involvement in bone formation and resorption. Bone *44*, 476-484.

Roth,B.L., Beinfeld,M.C., and Howlett,A.C. (1984). Secretin receptors on neuroblastoma cell membranes: characterization of 125I-labeled secretin binding and association with adenylate cyclase. J Neurochem. *42*, 1145-1152.

Rozenberg,S., Kroll,M., Pastijn,A., and Vandromme,J. (1995). Osteoporosis prevention and treatment with sex hormone replacement therapy. Clin Rheumatol. *14 Suppl 3*, 14-17.

Rubin,M.R. and Bilezikian,J.P. (2003). The anabolic effects of parathyroid hormone therapy. Clin Geriatr. Med. *19*, 415-432.

Rueda,D., Galve-Roperh,I., Haro,A., and Guzman,M. (2000). The CB(1) cannabinoid receptor is coupled to the activation of c-Jun N-terminal kinase. Mol. Pharmacol *58*, 814-820.

Ruggiero,R.J. and Likis,F.E. (2002). Estrogen: physiology, pharmacology, and formulations for replacement therapy. J Midwifery Womens Health *47*, 130-138.

Ruocco,M.G., Maeda,S., Park,J.M., Lawrence,T., Hsu,L.C., Cao,Y., Schett,G., Wagner,E.F., and Karin,M. (2005). I{kappa}B kinase (IKK){beta}, but not IKK{alpha}, is a critical mediator of osteoclast survival and is required for inflammation-induced bone loss. J Exp. Med. *201*, 1677-1687.

Ryberg,E., Larsson,N., Sjogren,S., Hjorth,S., Hermansson,N.O., Leonova,J., Elebring,T., Nilsson,K., Drmota,T., and Greasley,P.J. (2007). The orphan receptor GPR55 is a novel cannabinoid receptor. Br. J Pharmacol *152*, 1092-1101.

Safran,J.B., Butler,W.T., and Farach-Carson,M.C. (1998). Modulation of osteopontin post-translational state by 1, 25-(OH)2-vitamin D3. Dependence on Ca2+ influx. J Biol. Chem. *273*, 29935-29941.

Salazar,M., Carracedo,A., Salanueva,I.J., Hernandez-Tiedra,S., Lorente,M., Egia,A., Vazquez,P., Blazquez,C., Torres,S., Garcia,S., Nowak,J., Fimia,G.M., Piacentini,M., Cecconi,F., Pandolfi,P.P., Gonzalez-Feria,L., Iovanna,J.L., Guzman,M., Boya,P., and Velasco,G. (2009). Cannabinoid action induces autophagymediated cell death through stimulation of ER stress in human glioma cells. J Clin Invest *119*, 1359-1372.

Salo,J., Lehenkari,P., Mulari,M., Metsikko,K., and Vaananen,H.K. (1997). Removal of osteoclast bone resorption products by transcytosis. Science *276*, 270-273.

Salo,J., Metsikko,K., Palokangas,H., Lehenkari,P., and Vaananen,H.K. (1996). Bone-resorbing osteoclasts reveal a dynamic division of basal plasma membrane into two different domains. J. Cell Sci. *109 (Pt 2)*, 301-307.

Samadfam,R., Xia,Q., and Goltzman,D. (2007). Co-treatment of PTH with osteoprotegerin or alendronate increases its anabolic effect on the skeleton of oophorectomized mice. J Bone Miner. Res. *22*, 55-63.

Samuels,J., Krasnokutsky,S., and Abramson,S.B. (2008). Osteoarthritis: a tale of three tissues. Bull. NYU. Hosp. Jt. Dis. *66*, 244-250.

Sarfaraz,S., Adhami,V.M., Syed,D.N., Afaq,F., and Mukhtar,H. (2008). Cannabinoids for cancer treatment: progress and promise. Cancer Res. *68*, 339-342.

Savinainen,J.R., Jarvinen,T., Laine,K., and Laitinen,J.T. (2001). Despite substantial degradation, 2-arachidonoylglycerol is a potent full efficacy agonist mediating CB(1) receptor-dependent G-protein activation in rat cerebellar membranes. Br. J Pharmacol *134*, 664-672.

Sawzdargo,M., George,S.R., Nguyen,T., Xu,S., Kolakowski,L.F., and O'Dowd,B.F. (1997). A cluster of four novel human G protein-coupled receptor genes occurring in close proximity to CD22 gene on chromosome 19q13.1. Biochem. Biophys. Res. Commun. *239*, 543-547.

Schaller,S., Henriksen,K., Sorensen,M.G., and Karsdal,M.A. (2005). The role of chloride channels in osteoclasts: ClC-7 as a target for osteoporosis treatment. Drug News Perspect. *18*, 489-495.

Schatz,A.R., Lee,M., Condie,R.B., Pulaski,J.T., and Kaminski,N.E. (1997). Cannabinoid receptors CB1 and CB2: a characterization of expression and adenylate cyclase modulation within the immune system. Toxicol. Appl. Pharmacol. *142*, 278-287.

Schmid,P.C., Krebsbach,R.J., Perry,S.R., Dettmer,T.M., Maasson,J.L., and Schmid,H.H. (1995). Occurrence and postmortem generation of anandamide and other long-chain N-acylethanolamines in mammalian brain. FEBS Lett. *375*, 117-120.

Schmid,P.C., Paria,B.C., Krebsbach,R.J., Schmid,H.H., and Dey,S.K. (1997). Changes in anandamide levels in mouse uterus are associated with uterine receptivity for embryo implantation. Proc. Natl. Acad. Sci. U. S. A *94*, 4188-4192.

Seibel,M.J., Dunstan,C.R., Zhou,H., Allan,C.M., and Handelsman,D.J. (2006). Sex steroids, not FSH, influence bone mass. Cell *127*, 1079-1.

Serre,C.M., Farlay,D., Delmas,P.D., and Chenu,C. (1999). Evidence for a dense and intimate innervation of the bone tissue, including glutamate-containing fibers. Bone *25*, 623-629.

Shi,Y., Yadav,V.K., Suda,N., Liu,X.S., Guo,X.E., Myers,M.G., Jr., and Karsenty,G. (2008). Dissociation of the neuronal regulation of bone mass and energy metabolism by leptin in vivo. Proc. Natl. Acad. Sci. U. S. A *105*, 20529-20533.

Shimoyama,A., Wada,M., Ikeda,F., Hata,K., Matsubara,T., Nifuji,A., Noda,M., Amano,K., Yamaguchi,A., Nishimura,R., and Yoneda,T. (2007). Ihh/Gli2 signaling promotes osteoblast differentiation by regulating Runx2 expression and function. Mol. Biol. Cell *18*, 2411-2418.

Shire,D., Carillon,C., Kaghad,M., Calandra,B., Rinaldi-Carmona,M., Le Fur,G., Caput,D., and Ferrara,P. (1995). An amino-terminal variant of the central cannabinoid receptor resulting from alternative splicing. J Biol. Chem. *270*, 3726-3731.

Simonet,W.S., Lacey,D.L., Dunstan,C.R., Kelley,M., Chang,M.S., Luthy,R., Nguyen,H.Q., Wooden,S., Bennett,L., Boone,T., Shimamoto,G., DeRose,M., Elliott,R., Colombero,A., Tan,H.L., Trail,G., Sullivan,J., Davy,E., Bucay,N., Renshaw-Gegg,L.,

Hughes,T.M., Hill,D., Pattison,W., Campbell,P., Sander,S., Van,G., Tarpley,J., Derby,P., Lee,R., and Boyle,W.J. (1997). Osteoprotegerin: a novel secreted protein involved in the regulation of bone density. Cell *89*, 309-319.

Sims,N.A., Dupont,S., Krust,A., Clement-Lacroix,P., Minet,D., Resche-Rigon,M., Gaillard-Kelly,M., and Baron,R. (2002). Deletion of estrogen receptors reveals a regulatory role for estrogen receptors-beta in bone remodeling in females but not in males. Bone *30*, 18-25.

Skaper,S.D., Buriani,A., Dal Toso,R., Petrelli,L., Romanello,S., Facci,L., and Leon,A. (1996). The ALIAmide palmitoylethanolamide and cannabinoids, but not anandamide, are protective in a delayed postglutamate paradigm of excitotoxic death in cerebellar granule neurons. Proc. Natl. Acad. Sci. U. S. A *93*, 3984-3989.

Smart,D., Gunthorpe,M.J., Jerman,J.C., Nasir,S., Gray,J., Muir,A.I., Chambers,J.K., Randall,A.D., and Davis,J.B. (2000). The endogenous lipid anandamide is a full agonist at the human vanilloid receptor (hVR1). Br. J Pharmacol *129*, 227-230.

Smith,E. and Frenkel,B. (2005). Glucocorticoids inhibit the transcriptional activity of LEF/TCF in differentiating osteoblasts in a glycogen synthase kinase-3beta-dependent and -independent manner. J Biol. Chem. *280*, 2388-2394.

Smith,S.R., Terminelli,C., and Denhardt,G. (2000). Effects of cannabinoid receptor agonist and antagonist ligands on production of inflammatory cytokines and anti-inflammatory interleukin-10 in endotoxemic mice. J Pharmacol Exp. Ther. *293*, 136-150.

Sobacchi,C., Frattini,A., Guerrini,M.M., Abinun,M., Pangrazio,A., Susani,L., Bredius,R., Mancini,G., Cant,A., Bishop,N., Grabowski,P., Del Fattore,A., Messina,C., Errigo,G., Coxon,F.P., Scott,D.I., Teti,A., Rogers,M.J., Vezzoni,P., Villa,A., and Helfrich,M.H. (2007). Osteoclast-poor human osteopetrosis due to mutations in the gene encoding RANKL. Nat. Genet. *39*, 960-962.

Song,Y., Peng,X., Porta,A., Takanaga,H., Peng,J.B., Hediger,M.A., Fleet,J.C., and Christakos,S. (2003). Calcium transporter 1 and epithelial calcium channel messenger ribonucleic acid are differentially regulated by 1,25 dihydroxyvitamin D3 in the intestine and kidney of mice. Endocrinology *144*, 3885-3894.

Soysa,N.S. and Alles,N. (2009). NF-kappaB functions in osteoclasts. Biochem. Biophys. Res. Commun. *378*, 1-5.

Srivastava,S., Weitzmann,M.N., Cenci,S., Ross,F.P., Adler,S., and Pacifici,R. (1999). Estrogen decreases TNF gene expression by blocking JNK activity and the resulting production of c-Jun and JunD. J Clin Invest *104*, 503-513.

Srivastava,S., Weitzmann,M.N., Kimble,R.B., Rizzo,M., Zahner,M., Milbrandt,J., Ross,F.P., and Pacifici,R. (1998). Estrogen blocks M-CSF gene expression and osteoclast formation by regulating phosphorylation of Egr-1 and its interaction with Sp-1. J Clin Invest *102*, 1850-1859.

Stanley,E.R., Guilbert,L.J., Tushinski,R.J., and Bartelmez,S.H. (1983). CSF-1--a mononuclear phagocyte lineage-specific hemopoietic growth factor. J Cell Biochem. *21*, 151-159.

Stossi,F., Barnett,D.H., Frasor,J., Komm,B., Lyttle,C.R., and Katzenellenbogen,B.S. (2004). Transcriptional profiling of estrogen-regulated gene expression via estrogen receptor (ER) alpha or ERbeta in human osteosarcoma cells: distinct and common target genes for these receptors. Endocrinology *145*, 3473-3486.

Strobel,A., Issad,T., Camoin,L., Ozata,M., and Strosberg,A.D. (1998). A leptin missense mutation associated with hypogonadism and morbid obesity. Nat. Genet. *18*, 213-215.

Strom,T.M. and Juppner,H. (2008). PHEX, FGF23, DMP1 and beyond. Curr. Opin. Nephrol. Hypertens. *17*, 357-362.

Studd,J.W., Holland,E.F., Leather,A.T., and Smith,R.N. (1994). The dose-response of percutaneous oestradiol implants on the skeletons of postmenopausal women. Br. J Obstet. Gynaecol. *101*, 787-791.

Su,M., Jiang,H., Zhang,P., Liu,Y., Wang,E., Hsu,A., and Yokota,H. (2006). Knee-loading modality drives molecular transport in mouse femur. Ann. Biomed. Eng *34*, 1600-1606.

Suda,T., Nakamura,I., Jimi,E., and Takahashi,N. (1997). Regulation of osteoclast function. J. Bone Miner. Res. *12*, 869-879.

SUGAHARA,K., UEMURA,A., AKAMATSU,N., TSURUDA,A., HASEGAWA,H., YANAGIHARA,K., YAMADA,Y., and KAMIHIRA,S. (2006). A Relevant Reference Gene and Normalization for mRNA Real-Time PCR Quantification in Specimens with Distinct Cell Types and Variant Integrity. Acta Medica Nagasakiensia *51*, 57-63.

Sugiura,T., Kobayashi,Y., Oka,S., and Waku,K. (2002). Biosynthesis and degradation of anandamide and 2-arachidonoylglycerol and their possible physiological significance. Prostaglandins Leukot. Essent. Fatty Acids *66*, 173-192.

Sugiura,T., Kodaka,T., Kondo,S., Nakane,S., Kondo,H., Waku,K., Ishima,Y., Watanabe,K., and Yamamoto,I. (1997). Is the cannabinoid CB1 receptor a 2-arachidonoylglycerol receptor? Structural requirements for triggering a Ca2+ transient in NG108-15 cells. J Biochem. *122*, 890-895.

Sugiura,T., Kondo,S., Sukagawa,A., Nakane,S., Shinoda,A., Itoh,K., Yamashita,A., and Waku,K. (1995). 2-Arachidonoylglycerol: a possible endogenous cannabinoid receptor ligand in brain. Biochem. Biophys. Res. Commun. *215*, 89-97.

Sugiura,T., Kondo,S., Sukagawa,A., Tonegawa,T., Nakane,S., Yamashita,A., Ishima,Y., and Waku,K. (1996). Transacylase-mediated and phosphodiesterase-mediated synthesis of N-arachidonoylethanolamine, an endogenous cannabinoid-receptor ligand, in rat brain microsomes. Comparison with synthesis from free arachidonic acid and ethanolamine. Eur. J Biochem. *240*, 53-62.

Sun,L., Peng,Y., Sharrow,A.C., Iqbal,J., Zhang,Z., Papachristou,D.J., Zaidi,S., Zhu,L.L., Yaroslavskiy,B.B., Zhou,H., Zallone,A., Sairam,M.R., Kumar,T.R., Bo,W., Braun,J., Cardoso-Landa,L., Schaffler,M.B., Moonga,B.S., Blair,H.C., and Zaidi,M. (2006). FSH directly regulates bone mass. Cell *125*, 247-260.

Sundquist,K.T., Leppilampi,M., Jarvelin,K., Kumpulainen,T., and Vaananen,H.K. (1987). Carbonic anhydrase isoenzymes in isolated rat peripheral monocytes, tissue macrophages, and osteoclasts. Bone *8*, 33-38.

Sutherland,M.K., Geoghegan,J.C., Yu,C., Turcott,E., Skonier,J.E., Winkler,D.G., and Latham,J.A. (2004). Sclerostin promotes the apoptosis of human osteoblastic cells: a novel regulation of bone formation. Bone *35*, 828-835.

Takayanagi,H. (2005). Mechanistic insight into osteoclast differentiation in osteoimmunology. J. Mol. Med. *83*, 170-179.

Takayanagi,H., Kim,S., Koga,T., Nishina,H., Isshiki,M., Yoshida,H., Saiura,A., Isobe,M., Yokochi,T., Inoue,J., Wagner,E.F., Mak,T.W., Kodama,T., and Taniguchi,T. (2002). Induction and activation of the transcription factor NFATc1 (NFAT2) integrate RANKL signaling in terminal differentiation of osteoclasts. Dev. Cell *3*, 889-901.

Takeda,S., Elefteriou,F., Levasseur,R., Liu,X., Zhao,L., Parker,K.L., Armstrong,D., Ducy,P., and Karsenty,G. (2002). Leptin regulates bone formation via the sympathetic nervous system. Cell *111*, 305-317.

Takeda,S. and Karsenty,G. (2008). Molecular bases of the sympathetic regulation of bone mass. Bone *42*, 837-840.

Tam,C.S., Heersche,J.N., Murray,T.M., and Parsons,J.A. (1982). Parathyroid hormone stimulates the bone apposition rate independently of its resorptive action: differential effects of intermittent and continuous administration. Endocrinology *110*, 506-512.

Tam,J., Ofek,O., Fride,E., Ledent,C., Gabet,Y., Muller,R., Zimmer,A., Mackie,K., Mechoulam,R., Shohami,E., and Bab,I. (2006). Involvement of neuronal cannabinoid

receptor CB1 in regulation of bone mass and bone remodeling. Mol. Pharmacol. *70*, 786-792.

Tam,J., Trembovler,V., Di,M., V, Petrosino,S., Leo,G., Alexandrovich,A., Regev,E., Casap,N., Shteyer,A., Ledent,C., Karsak,M., Zimmer,A., Mechoulam,R., Yirmiya,R., Shohami,E., and Bab,I. (2008). The cannabinoid CB1 receptor regulates bone formation by modulating adrenergic signaling. FASEB J *22*, 285-294.

Tamori,Y., Masugi,J., Nishino,N., and Kasuga,M. (2002). Role of peroxisome proliferator-activated receptor-gamma in maintenance of the characteristics of mature 3T3-L1 adipocytes. Diabetes *51*, 2045-2055.

Tatsumi,S., Ishii,K., Amizuka,N., Li,M., Kobayashi,T., Kohno,K., Ito,M., Takeshita,S., and Ikeda,K. (2007). Targeted ablation of osteocytes induces osteoporosis with defective mechanotransduction. Cell Metab *5*, 464-475.

Taylor,A.F. (2002). Osteoblastic glutamate receptor function regulates bone formation and resorption. J Musculoskelet. Neuronal. Interact. *2*, 285-290.

Teitelbaum,S.L. (2000). Bone resorption by osteoclasts. Science *289*, 1504-1508.

Terpos,E., Sezer,O., Croucher,P., and Dimopoulos,M.A. (2007). Myeloma bone disease and proteasome inhibition therapies. Blood *110*, 1098-1104.

Teti,A., Blair,H.C., Teitelbaum,S.L., Kahn,A.J., Koziol,C., Konsek,J., Zambonin-Zallone,A., and Schlesinger,P.H. (1989). Cytoplasmic pH regulation and chloride/bicarbonate exchange in avian osteoclasts. J Clin Invest *83*, 227-233.

Tian,E., Zhan,F., Walker,R., Rasmussen,E., Ma,Y., Barlogie,B., and Shaughnessy,J.D., Jr. (2003). The role of the Wnt-signaling antagonist DKK1 in the development of osteolytic lesions in multiple myeloma. N. Engl. J Med. *349*, 2483-2494.

Tobias,J.H., Chow,J.W., and Chambers,T.J. (1993a). 3-Amino-1-hydroxypropylidine-1-bisphosphonate (AHPrBP) suppresses not only the induction of new, but also the persistence of existing bone-forming surfaces in rat cancellous bone. Bone *14*, 619-623.

Tobias,J.H., Gallagher,A., and Chambers,T.J. (1993b). Prolonged intermittent but not continuous administration of oestradiol-17 beta increases bone volume in the rat. J Endocrinol. *139*, 267-273.

Tobimatsu,T., Kaji,H., Sowa,H., Naito,J., Canaff,L., Hendy,G.N., Sugimoto,T., and Chihara,K. (2006). Parathyroid hormone increases beta-catenin levels through Smad3 in mouse osteoblastic cells. Endocrinology *147*, 2583-2590.

Tsuji,K., Bandyopadhyay,A., Harfe,B.D., Cox,K., Kakar,S., Gerstenfeld,L., Einhorn,T., Tabin,C.J., and Rosen,V. (2006). BMP2 activity, although dispensable for bone formation, is required for the initiation of fracture healing. Nat. Genet. *38*, 1424-1429.

Turner,R.T. (1999). Mice, estrogen, and postmenopausal osteoporosis. J Bone Miner. Res. *14*, 187-191.

Turner,R.T., Riggs,B.L., and Spelsberg,T.C. (1994). Skeletal effects of estrogen. Endocr. Rev. *15*, 275-300.

Umeda,S., Takahashi,K., Naito,M., Shultz,L.D., and Takagi,K. (1996). Neonatal changes of osteoclasts in osteopetrosis (op/op) mice defective in production of functional macrophage colony-stimulating factor (M-CSF) protein and effects of M-CSF on osteoclast development and differentiation. J Submicrosc. Cytol. Pathol. *28*, 13-26.

Usuda,H., Naito,M., Umeda,S., Takahashi,K., and Shultz,L.D. (1994). Ultrastructure of macrophages and dendritic cells in osteopetrosis (op) mutant mice lacking macrophage colony-stimulating factor (M-CSF/CSF-1) activity. J Submicrosc. Cytol. Pathol. *26*, 111-119.

Vaananen,H.K., Karhukorpi,E.K., Sundquist,K., Wallmark,B., Roininen,I., Hentunen,T., Tuukkanen,J., and Lakkakorpi,P. (1990). Evidence for the presence of a proton pump of the vacuolar H(+)-ATPase type in the ruffled borders of osteoclasts. J Cell Biol. *111*, 1305-1311.

Vaananen,H.K. and Laitala-Leinonen,T. (2008). Osteoclast lineage and function. Arch. Biochem. Biophys. *473*, 132-138.

van Abel,M., Hoenderop,J.G., van der Kemp,A.W., Friedlaender,M.M., van Leeuwen,J.P., and Bindels,R.J. (2005). Coordinated control of renal Ca(2+) transport proteins by parathyroid hormone. Kidney Int. *68*, 1708-1721.

Van Campenhout,A. and Golledge,J. (2008). Osteoprotegerin, vascular calcification and atherosclerosis. Atherosclerosis.

van der Eerden,B.C., Hoenderop,J.G., de Vries,T.J., Schoenmaker,T., Buurman,C.J., Uitterlinden,A.G., Pols,H.A., Bindels,R.J., and van Leeuwen,J.P. (2005). The epithelial Ca2+ channel TRPV5 is essential for proper osteoclastic bone resorption. Proc. Natl. Acad. Sci. U. S. A *102*, 17507-17512.

Van Sickle,M.D., Duncan,M., Kingsley,P.J., Mouihate,A., Urbani,P., Mackie,K., Stella,N., Makriyannis,A., Piomelli,D., Davison,J.S., Marnett,L.J., Di,M., V, Pittman,Q.J., Patel,K.D., and Sharkey,K.A. (2005). Identification and functional characterization of brainstem cannabinoid CB2 receptors. Science *310*, 329-332.

van Staa,T.P., Selby,P., Leufkens,H.G., Lyles,K., Sprafka,J.M., and Cooper,C. (2002). Incidence and natural history of Paget's disease of bone in England and Wales. J Bone Miner. Res. *17*, 465-471.

van't Hof,R.J., Macphee,J., Libouban,H., Helfrich,M.H., and Ralston,S.H. (2004). Regulation of bone mass and bone turnover by neuronal nitric oxide synthase. Endocrinology *145*, 5068-5074.

van't Hof,R.J. and Ralston,S.H. (2001). Nitric oxide and bone. Immunology *103*, 255-261.

van't Hof,R.J., Tuinenburg-Bol Raap,A.C., and Nijweide,P.J. (1995). Induction of osteoclast characteristics in cultured avian blood monocytes; modulation by osteoblasts and 1,25-(OH)2 vitamin D3. Int. J Exp. Pathol. *76*, 205-214.

Votta,B.J., Levy,M.A., Badger,A., Bradbeer,J., Dodds,R.A., James,I.E., Thompson,S., Bossard,M.J., Carr,T., Connor,J.R., Tomaszek,T.A., Szewczuk,L., Drake,F.H., Veber,D.F., and Gowen,M. (1997). Peptide aldehyde inhibitors of cathepsin K inhibit bone resorption both in vitro and in vivo. J Bone Miner. Res. *12*, 1396-1406.

Vu,T.H., Shipley,J.M., Bergers,G., Berger,J.E., Helms,J.A., Hanahan,D., Shapiro,S.D., Senior,R.M., and Werb,Z. (1998). MMP-9/gelatinase B is a key regulator of growth plate angiogenesis and apoptosis of hypertrophic chondrocytes. Cell *93*, 411-422.

Wada,T., Nakashima,T., Hiroshi,N., and Penninger,J.M. (2006). RANKL-RANK signaling in osteoclastogenesis and bone disease. Trends Mol. Med. *12*, 17-25.

Wang,B.L., Dai,C.L., Quan,J.X., Zhu,Z.F., Zheng,F., Zhang,H.X., Guo,S.Y., Guo,G., Zhang,J.Y., and Qiu,M.C. (2006). Parathyroid hormone regulates osterix and Runx2 mRNA expression predominantly through protein kinase A signaling in osteoblast-like cells. J Endocrinol. Invest *29*, 101-108.

Washimi,Y., Ito,M., Morishima,Y., Taguma,K., Ojima,Y., Uzawa,T., and Hori,M. (2007). Effect of combined humanPTH(1-34) and calcitonin treatment in ovariectomized rats. Bone *41*, 786-793.

Waters,K.M., Rickard,D.J., Riggs,B.L., Khosla,S., Katzenellenbogen,J.A., Katzenellenbogen,B.S., Moore,J., and Spelsberg,T.C. (2001). Estrogen regulation of human osteoblast function is determined by the stage of differentiation and the estrogen receptor isoform. J Cell Biochem. *83*, 448-462.

Watts,G.D., Wymer,J., Kovach,M.J., Mehta,S.G., Mumm,S., Darvish,D., Pestronk,A., Whyte,M.P., and Kimonis,V.E. (2004). Inclusion body myopathy associated with Paget

disease of bone and frontotemporal dementia is caused by mutant valosin-containing protein. Nat. Genet. *36*, 377-381.

Weir,E.C., Horowitz,M.C., Baron,R., Centrella,M., Kacinski,B.M., and Insogna,K.L. (1993). Macrophage colony-stimulating factor release and receptor expression in bone cells. J. Bone Miner. Res. *8*, 1507-1518.

Whitfield,J.F. (2001). Leptin: brains and bones. Expert. Opin. Investig. Drugs *10*, 1617-1622.

Whyte, L., Ryberg, E., Sims, N. A., Ridge, S., Mackie, K., Greasley, P., Ross, R. A., and Rogers, M. J. GPR55: A novel cannabinoid receptor involved in the regulation of osteoclast function and bone mass. Bone 44[Suppl 1], S138. 2009.
Ref Type: Abstract

Whyte,M.P. and Hughes,A.E. (2002). Expansile skeletal hyperphosphatasia is caused by a 15-base pair tandem duplication in TNFRSF11A encoding RANK and is allelic to familial expansile osteolysis. J Bone Miner. Res. *17*, 26-29.

Wilson,R.I. and Nicoll,R.A. (2001). Endogenous cannabinoids mediate retrograde signalling at hippocampal synapses. Nature *410*, 588-592.

Wong,B.R., Rho,J., Arron,J., Robinson,E., Orlinick,J., Chao,M., Kalachikov,S., Cayani,E., Bartlett,F.S., III, Frankel,W.N., Lee,S.Y., and Choi,Y. (1997). TRANCE is a novel ligand of the tumor necrosis factor receptor family that activates c-Jun N-terminal kinase in T cells. J Biol. Chem. *272*, 25190-25194.

Wuyts,W., Van Wesenbeeck,L., Morales-Piga,A., Ralston,S., Hocking,L., Vanhoenacker,F., Westhovens,R., Verbruggen,L., Anderson,D., Hughes,A., and Van Hul,W. (2001). Evaluation of the role of RANK and OPG genes in Paget's disease of bone. Bone *28*, 104-107.

Xie,W.F., Zhang,X., Sakano,S., Lefebvre,V., and Sandell,L.J. (1999). Trans-activation of the mouse cartilage-derived retinoic acid-sensitive protein gene by Sox9. J Bone Miner. Res. *14*, 757-763.

YAMADA,Y., Ando,F., and Shimokata,H. (2007). Association of candidate gene polymorphisms with bone mineral density in community-dwelling Japanese women and men. Int. J Mol. Med. *19*, 791-801.

Yao,G.Q., Sun,B.H., Weir,E.C., and Insogna,K.L. (2002). A role for cell-surface CSF-1 in osteoblast-mediated osteoclastogenesis. Calcif. Tissue Int. *70*, 339-346.

Yasuda,H., Shima,N., Nakagawa,N., Mochizuki,S.I., Yano,K., Fujise,N., Sato,Y., Goto,M., Yamaguchi,K., Kuriyama,M., Kanno,T., Murakami,A., Tsuda,E., Morinaga,T., and Higashio,K. (1998a). Identity of osteoclastogenesis inhibitory factor (OCIF) and osteoprotegerin (OPG): a mechanism by which OPG/OCIF inhibits osteoclastogenesis in vitro. Endocrinology *139*, 1329-1337.

Yasuda,H., Shima,N., Nakagawa,N., Yamaguchi,K., Kinosaki,M., Mochizuki,S., Tomoyasu,A., Yano,K., Goto,M., Murakami,A., Tsuda,E., Morinaga,T., Higashio,K., Udagawa,N., Takahashi,N., and Suda,T. (1998b). Osteoclast differentiation factor is a ligand for osteoprotegerin/osteoclastogenesis-inhibitory factor and is identical to TRANCE/RANKL. Proc. Natl. Acad. Sci. U. S. A *95*, 3597-3602.

Yoshida,C.A., Yamamoto,H., Fujita,T., Furuichi,T., Ito,K., Inoue,K., Yamana,K., Zanma,A., Takada,K., Ito,Y., and Komori,T. (2004). Runx2 and Runx3 are essential for chondrocyte maturation, and Runx2 regulates limb growth through induction of Indian hedgehog. Genes Dev. *18*, 952-963.

Yoshida,H., Hayashi,S., Kunisada,T., Ogawa,M., Nishikawa,S., Okamura,H., Sudo,T., Shultz,L.D., and Nishikawa,S. (1990). The murine mutation osteopetrosis is in the coding region of the macrophage colony stimulating factor gene. Nature *345*, 442-444.

Zaidi,M., Inzerillo,A.M., Moonga,B.S., Bevis,P.J., and Huang,C.L. (2002). Forty years of calcitonin--where are we now? A tribute to the work of Iain Macintyre, FRS. Bone *30*, 655-663.

Zhang,J., Dai,J., Qi,Y., Lin,D.L., Smith,P., Strayhorn,C., Mizokami,A., Fu,Z., Westman,J., and Keller,E.T. (2001). Osteoprotegerin inhibits prostate cancer-induced osteoclastogenesis and prevents prostate tumor growth in the bone. J Clin Invest *107*, 1235-1244.

Zhang,Y., Proenca,R., Maffei,M., Barone,M., Leopold,L., and Friedman,J.M. (1994). Positional cloning of the mouse obese gene and its human homologue. Nature *372*, 425-432.

Zhao,S., Zhang,Y.K., Harris,S., Ahuja,S.S., and Bonewald,L.F. (2002). MLO-Y4 osteocyte-like cells support osteoclast formation and activation. J Bone Miner. Res. *17*, 2068-2079.

Zoratti,C., Kipmen-Korgun,D., Osibow,K., Malli,R., and Graier,W.F. (2003). Anandamide initiates Ca(2+) signaling via CB2 receptor linked to phospholipase C in calf pulmonary endothelial cells. Br. J Pharmacol *140*, 1351-1362.

APPENDICES

APPENDIX 1. MATERIALS, REAGENTS, APPARATUS and SOFTWARE

All **materials** and **reagents** used in this study are listed in the table below in alphabetical order.

Materials and reagents	Supplier
1.5ml eppendorf tubes with cap	Greiner Bio-One Inc, Gloucestershire, UK
10mM dMTP Mix	Invitrogen, Paisley, UK
1ml pasteur pipette	Fisher Scientific, Leicestershire, UK
2-AG	Tocris Biosciences, Bristol, UK
2-methoxyethyl acetate (MEA)	Sigma Aldrich, Dorset, UK
2-Propanol	Sigma Aldrich, Dorset, UK
5X first-strand buffer	Invitrogen, Paisley, UK
99.7-100% AnalaR Ethanol	VWR International LTD, Leicestershire, UK
Acetic Acid Glacial	Sigma Aldrich, Dorset, UK
AEA	Tocris Biosciences, Bristol, UK
alamarBlue^{TM} reagent	Invitrogen, Paisley, UK
Alizarin Red S	Sigma Aldrich, Dorset, UK
AM251	Tocris Biosciences, Bristol, UK
AM630	Tocris Biosciences, Bristol, UK
Amersham Hybond^{TM}-P	GE Healthcare Life Sciences, Buckinghamshire, UK
Basic fuchsin	Sigma Aldrich, Dorset, UK
Bicinchoninic acid (BCA) protein assay	Sigma Aldrich, Dorset, UK
Borax	Taab Lab, Berkshire, UK
Boric Acid	Taab Lab, Berkshire, UK
Bovine serum albumin	Sigma Aldrich, Dorset, UK
Bromophenol Blue	BDH Laboratory Supplies, Poole, Dorset, UK
Calcein	Sigma Aldrich, Dorset, UK
CB2 receptor (CNR2) polyclonal antibody	Cayman Chemical (Europe), Tallinn, Estonia
Centrifuge tubes (15 and 50ml)	Fisher Scientific, Leicestershire, UK
Cetyl pyridinium chloride monohydrate	Sigma Aldrich, Dorset, UK
Chloroform	Sigma Aldrich, Dorset, UK
Collagenase (type 1A)	Sigma Aldrich, Dorset, UK
Copper (II)-sulfate	Sigma Aldrich, Dorset, UK
Cover slips	Scientific Laboratory supplies Ltd, Hessle, UK
Criterion^{TM} XT pre-cast gels (12% Bis-Tris)	Bio-Rad Laboratories, Hertfordshire, UK
CTX serum assay (RatLaps^{TM} EIA)	Immunodiagnostic Systems Ltd. (IDS), Boldon Colliery, UK

DEPC Treated Water	Invitrogen, Paisley, UK
Dibenzoylperoxide	Leica Microsystems, Milton Keynes, UK
Dibutyl Phthalate	Sigma Aldrich, Dorset, UK
Diethanolamin	Sigma Aldrich, Dorset, UK
DL-Dithiothreitol (DTT)	Sigma Aldrich, Dorset, UK
DMSO	Sigma Aldrich, Dorset, UK
DNA Ladder 1kb	New England Biolabs, Hitchin, Hertfordshire, UK
dNTPs	Promega, Southampton, UK
DPX mounting medium	Sigma Aldrich, Dorset, UK
DTT	Invitrogen, Paisley, UK
EDTA	Sigma Aldrich, Dorset, UK
Electronic Pipette	Starlab, Milton Keynes, UK
Electrophoresis power supply	Anachem, Bedfordshire, UK
Embedding baskets	Leica Microsystems, Milton Keynes, UK
Embedding molds	Custom-made by the University workshop
Embedding rings	Leica Microsystems, Milton Keynes, UK
Ethanol Absolute	Fisher Scientific, Leicestershire, UK
EU One-piece, non-skirted thin wall plate natural	Genetic Research Instrumentation Ltd (GRI), Essex, UK
EU One-piece,sub-skirted Thin wall plate white	Genetic Research Instrumentation Ltd (GRI), Essex, UK
EU OP flat cap thin wall 8-cap strip	Genetic Research Instrumentation Ltd (GRI), Essex, UK
Extra thick blot papers	Bio-Rad Laboratories, Hertfordshire, UK
Fetal calf serum (FCS)	Fisher Scientific, Leicestershire, UK
Filter Paper	Fisher Scientific, Leicestershire, UK
Filter Tips Axygen	Thistle Scientific, Glasgow, UK
Forceps watchmaker's	Fisher Scientific, Leicestershire, UK
Fuchsin Acid	Taab Lab, Berkshire, UK
Gelatin	Sigma Aldrich, Dorset, UK
Glycerol 2 phosphate	Sigma Aldrich, Dorset, UK
Glycine	BDH Laboratory Supplies, Poole, Dorset, UK
Hanks buffer (HBSS)	Sigma Aldrich, Dorset, UK
HistoResin Mounting Medium (solution and powder)	Leica Microsystems, Milton Keynes, UK
HU308	Gift from Dr. Roel J. Arends (Organon)
Human recombinant RANKL	Gift from Dr. Patrick Mollat (Proskelia SASU)
Hydrochloric acid	BDH Laboratory Supplies, Poole, Dorset, UK
Hydroquinone	Taab Lab, Berkshire, UK

Invisorb® Spin Tissue Mini Kit	Thistle Scientific, Glasgow, UK
Isopropanol	Sigma Aldrich, Dorset, UK
Jackson ImmunoResearch Anti-rabbit secondary ab	Stratech Scientific Unit, Newmarket Suffolk, UK
JWH133	Tocris Biosciences, Bristol, UK
Kaleidoscope	Bio-Rad Laboratories, Hertfordshire, UK
Kisol foil	Taab Lab, Berkshire, UK
Knife 16cm long tungsten carbide tipped profile D	Leica Microsystems, Milton Keynes, UK
Knife Holder NZ	Leica Microsystems, Milton Keynes, UK
L-Glutamine	Invitrogen, Paisley, UK
Low molecular weight DNA ladder	New England Biolabs, Hitchin, Hertfordshire, UK
Magic Marker	Invitrogen, Paisley, UK
Magnesium chloride	Sigma Aldrich, Dorset, UK
Mannitol	BDH Laboratory Supplies, Poole, Dorset, UK
M-CSF mouse recombinant	R & D Systems, Abingdon, UK
Medium density linkage panel	Illumina Inc., California, US
Methanol	Fisher Scientific, Leicestershire, UK
Methyl Methacrylate	Sigma Aldrich, Dorset, UK
Mettler Toledo Titrator	Fisher Scientific, Leicestershire, UK
Microtubes (0.5, 1.5, 2ml)	Sarstedt Ltd, Leicester, UK
N,N-Dimethylformamide	Fisher Scientific, Leicestershire, UK
N,N-dimethyl-p-toluidine	Leica Microsystems, Milton Keynes, UK
Napthol-AS-BI-phosphate	Sigma Aldrich, Dorset, UK
Needles (19, 21 and 25G)	Fisher Scientific, Leicestershire, UK
Neubauer Haemocytometer	Hawksley, Lancing, UK
Nitrile gloves	Fisher Scientific, Leicestershire, UK
Novoscave or Scavenger	Novochem, Nieuwegein, The Netherlands
Oligo(dt)20 Primer	Invitrogen, Paisley, UK
Orange G loading dye	Sigma Aldrich, Dorset, UK
Paraformaldehyde	Taab Lab, Berkshire, UK
Pararosanilin	Sigma Aldrich, Dorset, UK
PBS tablets	Invitrogen, Paisley, UK
PCR lid strip	Fisher Scientific, Leicestershire, UK
PCR microplate 96 well and lids	Fisher Scientific, Leicestershire, UK
PCR primers	Invitrogen, Paisley, UK
PCR microtubes	Fisher Scientific, Leicestershire, UK
Penicillin/Streptomycin	Invitrogen, Paisley, UK

Perkadox 16	Akzo Nobel Polymer Chemicals, Amersfoort The Netherlands
Petri Dishes	Becton Dickinson, Berkshire, UK
Pierce SuperSignal® West Dura Extended Duration Substrate	Fisher Scientific, Leicestershire, UK
PINP serum assay (Rat/Mouse PINP EIA)	Immunodiagnostic Systems Ltd. (IDS), Boldon Colliery, UK
Pipette tips (all sizes)	Starlab, Milton Keynes, UK
p-Nitrophenol	Sigma Aldrich, Dorset, UK
p-Nitrophenol-phosphate	Sigma Aldrich, Dorset, UK
Polysciences Silane coated microscope slides	Park Scientific Ltd., Northampton, UK
PTH	Sigma Aldrich, Dorset, UK
QIAquick PCR Purification Kit	Qiagen (UK), West Sussex, UK
Quant-iT^{TM} PicoGreen® assay	Invitrogen, Paisley, UK
Rabbit Anti-Actin (AA20-33) IgG	Sigma Aldrich, Dorset, UK
RiboGreen RNA Quantitation Kit	Invitrogen, Paisley, UK
RNase-free water	Invitrogen, Paisley, UK
RnaseOut Recombinant Rnase Inhibitor	Invitrogen, Paisley, UK
Scalpel, disposable	VWR International LTD, Leicestershire, UK
Scissors (fine points and spring bow handles)	S Murray & Co Ltd, Surrey, UK
SensiMix(dT) Taq polymerase	GC Biotech, Alphen aan den Rijn, The Netherlands
Silver nitrate	Sigma Aldrich, Dorset, UK
Slide press cover slips	Taab Lab, Berkshire, UK
Sodium acetate unhydrous	Sigma Aldrich, Dorset, UK
Sodium barbiturate	BDH Laboratory Supplies, Poole, Dorset, UK
Sodium chloride	Sigma Aldrich, Dorset, UK
Sodium dodecyl sulphate (SDS)	Bio-Rad Laboratories, Hertfordshire, UK
Sodium hydroxide	VWR International LTD, Leicestershire, UK
Sodium phosphate	Sigma Aldrich, Dorset, UK
Sodium tartrate dibasic ehydrate	Sigma Aldrich, Dorset, UK
Sodium tetraborate	BDH Laboratory Supplies, Poole, Dorset, UK
Steel Knife 16cm "c"	Leica Microsystems, Milton Keynes, UK
Sterile filter (0.45μm)	Sartorius Mechatronics UK Ltd., Epsom Surrey, UK
Stripettes (5, 10, 25 and 50ml)	Sarstedt Ltd, Leicester, UK
SuperScript III Reverse Transcriptase	Invitrogen, Paisley, UK
SYBR Safe DNA gel stain	Invitrogen, Paisley, UK
SYBR Safe	Invitrogen, Paisley, UK
Syngene BIO imaging system	Fisher Scientific, Leicestershire, UK

Syringes (all sizes)	Becton Dickinson, Berkshire, UK
Taq DNA Polymerase	Invitrogen, Paisley, UK
TaqMan® Gene Expression Assay Mix for 18S rRNA	Applied Biosystems, Cheshire, UK
TBE buffer 10X	Invitrogen, Paisley, UK
Tissue culture 75cm^2 flasks	Fisher Scientific, Leicestershire, UK
Tissue culture microplates (6, 12, 24, 48 and 96-well plates)	Fisher Scientific, Leicestershire, UK
Toluidine Blue	Sigma Aldrich, Dorset, UK
Tris	Bio-Rad Laboratories, Hertfordshire, UK
Tris-EDTA buffer	Sigma Aldrich, Dorset, UK
Triton X-100^{TM}	Sigma Aldrich, Dorset, UK
Trizol reagent	Invitrogen, Paisley, UK
Trizol® Reagent	Invitrogen, Paisley, UK
Trypsin/EDTA	Sigma Aldrich, Dorset, UK
Tween-20	Bio-Rad Laboratories, Hertfordshire, UK
Ultraclear Xylene	Taab Lab, Berkshire, UK
UPL probes	Roche Diagnostics Ltd., East Sussex, UK
UV 96 well plates for plate reader	Fisher Scientific, Leicestershire, UK
Vacuum desiccator	Fisher Scientific, Leicestershire, UK
Vitamin C (Ascorbic acid)	BDH Laboratory Supplies, Poole, Dorset, UK
XT-MOPS	Bio-Rad Laboratories, Hertfordshire, UK
Xylene	Sigma Aldrich, Dorset, UK
α–Minimum Essential Medium (αMEM)	Sigma Aldrich, Dorset, UK
β-glycerophosphate disodium	Sigma Aldrich, Dorset, UK

All **apparatus** used in this study are listed in the table below in alphabetical order.

Apparatus	Supplier
AA Hoefer® protein transfer apparatus	Fisher Scientific, Leicestershire, UK
Astec Bioquell Monair 5 fume cabinet	Jencons PLS, East Grinstead, UK
Automatic tissue processor	Leica Microsystems, Milton Keynes, UK
AxioImager A1 upright research microscope	Carl Zeiss Ltd., Hertfordshire, UK
Axiovert 200 inverted research Microcope	Carl Zeiss Ltd., Hertfordshire, UK
Axiovert 40 CFL inverted microscope	Carl Zeiss Ltd., Hertfordshire, UK
Balancer Fisherbrand	Fisher Scientific, Leicestershire, UK
Bench-top centrifuge	SciQuip, Shropshire, UK
Bench-top Eppendorf centrifuge	Fisher Scientific, Leicestershire, UK
Bio-Tek Synergy HT plate reader	Fisher Scientific, Leicestershire, UK
Envair Bio2 safety cabinets	H&V Commissioning Services Ltd., Ayrshire, UK
Grant OLS 200 water bath	Thistle Scientific, Glasgow, UK
Horizontal electrophoresis tanks	Fisher Scientific, Leicestershire, UK
Hotplate/stirrer	Thistle Scientific, Glasgow, UK
Ika Vortex	Thistle Scientific, Glasgow, UK
MJ Research Chromo 4 Real Time PCR thermocycler	Genetic Research Instrumentation Ltd (GRI), Essex, UK
MJ Research Tetrad Thermal cycler	Genetic Research Instrumentation Ltd (GRI), Essex, UK
Nichiryo America Inc. Pipettes (2, 10, 100, 200 and 1000μl)	Thistle Scientific, Glasgow, UK
NoAir Class II Biological safety cabinet	TripleRed Ltd., Buckinghamshire, UK
Origo PSU-400/200 power supply for electrophoresis	Anachem, Bedfordshire, UK
PowerPac basic™	Bio-Rad Laboratories, Hertfordshire, UK
QImaging Retiga 4000R CCD camera	Media Cybernetics UK, Berkshire, UK
Rotary Microtome	Leica Microsystems, Milton Keynes, UK
Rotary tool	Dremel UK, Uxbridge, UK
SkyScan 1172 X-ray Microtomography system	SKYSCAN, Kontich, Belgium
Syngene GeneGenius Gel Bio-Imaging system	Fisher Scientific, Leicestershire, UK
SynSyngene GeneGnome Bio-Imaging system for chemiluminescence	Fisher Scientific, Leicestershire, UK
Vertical Criterion™ gel tanks	Bio-Rad Laboratories, Hertfordshire, UK

All **software** used in this study are listed in the table below in alphabetical order.

Software	Supplier
Aphelion Image Analysis tool kit	ADCIS, Hérouville-Saint-Clair, France
Bio-Tek Gen5^{TM} plate reader software	Fisher Scientific, Leicestershire, UK
GraphPad Prism (version 4)	GraphPad Software Inc., California, US
Opticon Monitor analysis software version 3	Genetic Research Instrumentation Ltd (GRI), Essex, UK
QCapture Pro software	Media Cybernetics UK, Berkshire, UK
Skyscan 1172 MicroCT software	SKYSCAN, Kontich, Belgium
Skyscan CTAn analysis software	SKYSCAN, Kontich, Belgium
Skyscan CTVol software	SKYSCAN, Kontich, Belgium
Skyscan NRecon reconstruction system	SKYSCAN, Kontich, Belgium
SPSS version 13	SPSS Ltd. UK, Surrey, UK
Syngene GeneSnap software	Fisher Scientific, Leicestershire, UK
Syngene GeneTool software	Fisher Scientific, Leicestershire, UK

APPENDIX 2. SOLUTIONS

Appendix 2.1 Solutions for TRAcP staining

Naphthol-AS-BI-phosphate
10mg/ml Naphthol-AS-BI-phosphate in Dimethylformamide

Veronal buffer
1.17g sodium acetate anhydrous and 2.94g sodium barbiturate both dissolved in 100ml of dH_2O

Acetate buffer
0.82g sodium acetate anhydrous dissolved in 100ml of dH_2O and pH adjusted to 5.2 with 0.6ml glacial acetic acid made up to 100ml with dH_2O

Pararosanilin
1g Pararosanilin dissolved in 20ml of dH_2O and 5ml of 5M HCl added to it
The solution was heated carefully whilst stirring and filtered after cooling.

TRAcP Staining Solution
The TRAcP staining solution was freshly prepared by mixing solution A and B as outlined below.

Solution A
150ml of Napthol-AS-BI-phosphate
750ml of Veronal buffer
900ml Acetate buffer
900ml Acetate buffer with 100mM Sodium Tartate

Solution B
120ml of Pararosanilin
120ml of Sodium Nitrate (4% w/v)

Appendix 2.2 Solutions for ALP assay

Diethanolamine (DEA)/MgCl₂ buffer

1M DEA and 1M $MgCl_2$ made up in 100ml dH_2O and pH adjusted to 9.8. Left at room temperature for 24 hours

ALP Lysis buffer

0.05% Triton X-100 added to DEA/MgCl₂ buffer

p-Nitrophenol standard solution

p-Nitrophenol standards (1.25 – 30nM) prepared in lysis buffer

Substrate solution

20mM p-nitrophenol-phopshate made up in DEA/MgCl₂ buffer and pH adjusted to 9.8

Appendix 2.3 Solution for cell Lysis

RIPA Lysis buffer

1% Triton 100X, 0.5% (w/v) Sodium Deoxycholate, 0.1% (w/v) Sodium Dodecyl Sulphate (SDS), 50mM Tris-HCl (pH 7.4) and 150nM Sodium Chloride were dissolved in dH_2O.

Appendix 2.4 Solutions for PAGE and western blot

Electrophoresis running buffer

50ml of XT-MOPS (20X) in 1000ml of dH2O

Samples loading protein buffer (5X stock)

5.2ml of 1M Tris-HCl pH adjusted to 6.8, 1g of DL-Dithiothreitol (DTT), 3g SDS, 6.5ml glycerol and 130μl of 10% (w/v) Bromophenol Blue. Stored at -20°C.

Transfer buffer
3.63g of Tris, 14.4g of Glycine, 200ml of Methanol and 3.75ml of 10% (w/v) SDS made up to 1000ml with dH$_2$O. Stored at room temperature.

TBS
1M of Tris and 1M Tris-HCl. pH adjusted to 7.9 prior to addition of 3M Sodium Chloride. Stored at room temperature.

TBST
0.1% (v/v) Tween-20 in TBS. Stored at room temperature.

Stripping buffer
1mM DTT, 2% (w/v) SDS and 62.5mM Tris-HCl (pH 6.7). Stored at room temperature.

Appendix 2.5 Solutions for Histology

Infiltrating solution
89g MMA, 10g Dibutyl phthalate, 1g Perkadox 16, and 0.01g Novoscave for 100g of infiltration solution

Embedding solution
Same as infiltration solution but 1 week old

Paragon staining solution
0.625g basic fuchsin and 1.875g toluidine blue in 250ml 30% (v/v) ethanol

Borax buffer
6g boric acid and 2g sodium tetraborate in 500ml dH$_2$O

APPENDIX 3. The chemical structures of endocannabinoids, cannabinoid receptor agonists and antagonists/inverse agonists
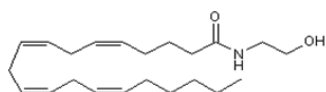
AEA
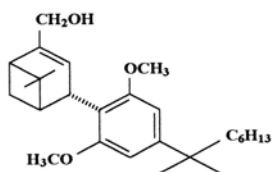
HU308
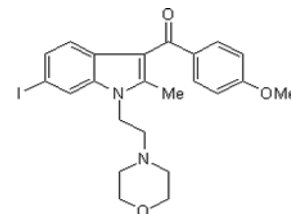
AM630
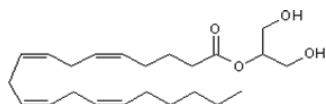
2-AG
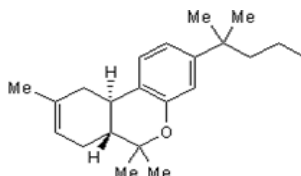
JWH133
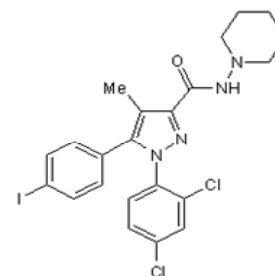
AM251
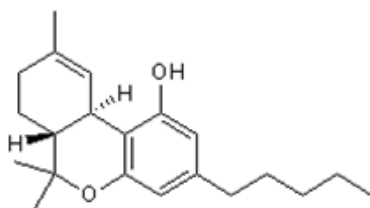
Δ9-Tetrahydrocannabinol (THC)
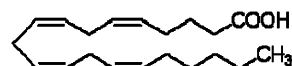
Arachidonic acid

APPENDIX 4. Ki values of endocannabinoids, CNR1- and CNR2-selective ligands. Adjusted from Pertwee, R.G. (Tocris Bioscience review series).

Compound	Chemical Name	CNR1 Ki value (nM)	CNR2 Ki value (nM)
Endocannabinoids			
AEA	N-(2-Hydroxyethyl)-5Z,8Z,11Z,14Z-eicosatetraenamide	89	371
2-AG	(5Z,8Z,11Z,14Z)-5,8,11,14-Eicosatetraenoic acid, 2-hydroxy-1-(hydroxymethyl)ethyl ester	472	1400
CNR2-selective agonists			
HU308	4-[4-(1,1-diemethylheptyl)-2,6-dimethoxyphenyl]-6,6-dimethylbicyclo[3.1.1]hept-2-ene-2-methanol	>10000	22.7
JWH133	(6aR,10aR)-3-(1,1-Dimethylbutyl)-6a,7,10,10a-tetrahydro -6,6,9-trimethyl-6H-dibenzo[b,d]pyran	677	3.4
CNR2-selective antagonist/inverse agonist			
AM630	6-Iodo-2-methyl-1-[2-(4-morpholinyl)ethyl]-1H-indol-3-y l](4-methoxyphenyl)methanone	5152	31.2
CNR1-selective antagonist/inverse agonist			
AM251	N-(Piperidin-1-yl)-5-(4-iodophenyl)-1-(2,4-dichlorophen yl)-4-methyl-1H-pyrazole-3-carboxamide	7.49	2290

APPENDIX 5. Comparison of wild type and CNR2-deficient mice of this study to 'pure' C57BL/6 mice

SNP ID	SNP	Pure C57BL/6 (Reference)	WT mice			CNR2$^{-/-}$ mice		
			1	2	3	1	2	3
rs3695988	[T/G]	AA	AA	AA	AA	AA	--	AA
rs6191076	[T/G]	AA	--	--	--	--	--	--
rs3723062	[T/C]	BB	BB	--	--	BB	BB	BB
rs13476003	[G/C]	AA	AA	AA	AA	AA	--	AA
rs3685919	[T/C]	BB	BB	--	--	BB	BB	BB
rs13466711	[A/G]	AA	--	--	--	--	--	--
rs13477019	[A/T]	BB	AA	AA	AA	AA	AA	AA
rs6301139	[T/A]	NN	--	--	--	--	--	--
rs13477439	[A/G]	BB	BB	--	--	BB	BB	BB
rs13477448	[T/A]	BB	--	BB	--	BB	BB	BB
rs6355837	[A/C]	AA	AA	AA	AA	BB	BB	BB
UT_4_132.137715	[T/G]	AA	AA	AA	AA	BB	BB	BB
rs3663950	[T/C]	AA	AA	AA	AA	BB	BB	BB
rs4224864	[A/G]	BB	--	--	--	--	--	--
rs3700706	[T/G]	AA	AB	AB	AA	AB	AA	AB
rs6215373	[T/C]	BB	AB	AB	AB	AA	AA	AA
rs13478223	[T/G]	BB	AB	AB	AB	AA	AA	AA
rs3659933	[T/G]	BB	--	--	--	--	--	--
CEL-5_45872918	[C/G]	BB	AB	AB	AB	AA	AA	AA
rs6192958	[T/C]	AA	AB	AB	AB	BB	BB	BB
rs3664008	[A/G]	AA	AB	AB	AB	BB	BB	BB
mCV23125912	[A/G]	BB	AB	AB	AB	AA	AA	AA
CEL-5_56167948	[T/C]	AA	BB	BB	BB	BB	BB	BB
rs3090667	[T/C]	BB	AA	AA	AA	AA	AA	AA
rs6340166	[T/C]	BB	AB	AB	AB	AB	AB	--
rs13478617	[A/C]	AA	AA	AA	AA	AA	AA	--
rs13478783	[A/G]	AA	BB	BB	BB	BB	BB	BB
rs13478971	[C/G]	BB	BB	AB	AA	AA	AA	AA
rs6401637	[T/C]	AA	AA	AB	BB	BB	BB	BB
mCV23042866	[T/G]	AA	AA	AB	BB	BB	BB	BB
rs3695724	[T/A]	AA	BB	BB	BB	BB	BB	BB
gnf06.122.747	[A/G]	BB	BB	BB	--	BB	BB	BB
rs13479522	[A/G]	AA	BB	BB	BB	BB	BB	BB
rs3711570	[T/G]	AA	AA	AA	AA	--	--	AA
rs3719401	[A/G]	BB	AB	AA	AB	AB	AA	AB
CEL-8_51607005	[T/C]	BB	BB	AB	BB	AB	AA	AB
rs13479776	[G/C]	AA	AA	AB	AA	AB	BB	AB
rs3725286	[T/C]	BB	BB	AB	BB	AB	AA	AB
rs3706149	[A/C]	BB	BB	BB	AB	BB	BB	BB
rs3669235	[A/G]	AA	AA	AA	AB	AA	AA	AA
rs13479956	[T/C]	BB	BB	BB	AB	BB	BB	BB

gnf08.108.032	[A/G]	AA	AA	AA	AB	AA	AA	AA
rs3662808	[A/G]	AA	AA	AA	AB	AA	AA	AA
rs6237645	[A/G]	AA	AA	AA	AB	AA	AA	AA
rs13479995	[A/C]	AA	AB	AA	BB	AA	AA	AA
rs3705725	[T/C]	AA	AA	AA	AA	--	--	--
rs13480122	[A/G]	AA	BB	BB	BB	BB	BB	BB
rs6174757	[T/G]	BB	BB	--	--	BB	BB	BB
rs3721056	[A/G]	BB	BB	--	--	BB	BB	BB
rs13480619	[A/G]	AA	BB	BB	BB	BB	BB	BB
CEL-10_58149652	[T/C]	BB	AA	AA	AA	AA	AA	AA
rs13480759	[T/C]	BB	AA	AA	AA	AA	AA	AA
rs3676330	[T/A]	BB	--	--	--	--	--	--
rs3654344	[T/G]	AA	AA	AB	AA	AB	AA	AB
rs13481009	[C/G]	BB	AB	AB	BB	AB	BB	AB
rs13481014	[T/C]	AA	BB	BB	BB	BB	BB	BB
rs6199956	[A/C]	AA	AB	AB	AA	AB	AB	AB
rs13481033	[A/G]	AA	AA	AA	AA	AA	--	AA
rs4228731	[A/G]	AA	AB	AB	AA	AB	AB	AB
rs3684076	[A/G]	BB	AB	AB	BB	AB	AB	AB
rs13481297	[A/G]	AA	--	--	--	--	--	--
rs13481445	[A/G]	AA	AA	AA	AA	AA	--	AA
rs13481588	[T/C]	BB	--	--	--	BB	BB	BB
rs13481734	[A/G]	AA	BB	BB	BB	BB	BB	BB
CEL-14_116404928	[T/C]	BB	AA	AA	AA	AA	AA	AA
CEL-15_4222769	[A/G]	BB	BB	BB	--	BB	BB	BB
rs13482661	[A/G]	BB	--	--	--	--	--	--
rs6276391	[A/C]	AA	--	--	--	--	--	--
rs13482744	[A/G]	BB	BB	BB	BB	BB	--	BB
rs4165065	[T/C]	AA	BB	BB	BB	AA	AB	AB
rs4165279	[A/G]	AA	AA	AA	AA	--	--	AA
rs3680665	[G/C]	BB	BB	--	BB	BB	BB	BB
rs13483055	[T/C]	AA	AA	AA	AA	AB	BB	AA
CEL-18_60214752	[T/C]	BB	BB	BB	--	BB	BB	BB
CEL-X_59515625	[T/G]	AA	AA	AA	AA	--	--	AA
CEL-X_66015326	[T/C]	AA	--	--	--	--	--	--
rs13483921	[A/G]	BB	BB	BB	--	BB	BB	BB
CEL-X_117683749	[T/C]	BB	BB	--	BB	--	--	BB
No. of different SNPs/1449 SNPs			40/1449	52/1449	53/1449	64/1449	55/1449	49/1449

Appendix 5: A display of SNP sites where wild type (in yellow) or *CNR2$^{-/-}$* mice (in blue) have different genotypes from pure C57BL/6 mice (reference genotypes provide by Illumina Inc.), across 1449 SNP loci.

APPENDIX 6. CNR2-deficient mice have normal body weight throughout their lives.
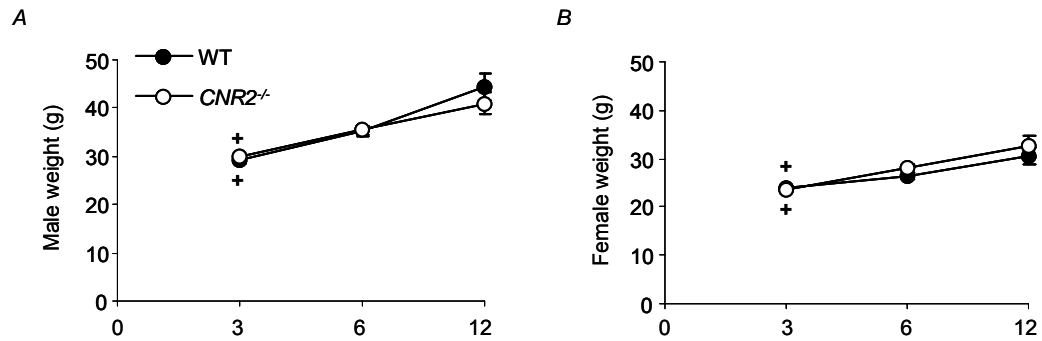
Appendix 6: Body weight of wild type (WT) and $CNR2^{-/-}$ male (*A*) and female (*B*) mice at age 3 months, 6 months and 12 months. Values are means ± sem from 7-8 mice per group. [+]p < 0.05 from 6 and 12-month old mice of same genotype.

APPENDIX 7. Table with actual values of µCT analysis of trabecular bone from wild type (WT) and CNR2-deficient mice following ovariectomy (OVX) or sham operation.

		BV/TV (%)	Tb.Th (µm)	Tb.N (1/mm)	Tb.Sp (µm)	Tb.Pf (1/mm)
WT	**SHAM**	11.4 ± 0.7	46.2 ± 0.3	2.46 ± 0.2	233.3 ± 9.4	23.7 ± 1.1
	OVX	7.9 ± 0.4	44.3 ± 0.6	1.79 ± 0.1	298.6 ± 21.2	31.6 ± 0.8
CNR2$^{-/-}$	**SHAM**	10.9 ± 0.2	47.4 ± 0.7	2.29 ± 0.1	262.6 ± 7.12	23.9 ± 0.3
	OVX	8.7 ± 0.2	48.3 ± 1.0	1.80 ± 0.1	282.6 ± 7.12	28.3 ± 0.6

Appendix 7: BV/TV, trabecular bone volume (%); Tb.Th, trabecular thickness (µm); Tb.N, trabecular number (1/mm); Tb.Sp, trabecular separation (µm); Tb.Pf, trabecular pattern factor (1/mm). Values are expressed as means ± sem from 7-8 mice per group.

APPENDIX 8. Actual values of μCT analysis of trabecular bone from wild type (WT) and CNR2-deficient mice following ovariectomy (OVX) and AM630 treatment.

		BV/TV (%)	Tb.Th (μm)	Tb.N (1/mm)	Tb.Sp (μm)	Tb.Pf (1/mm)
WT	SHAM Vehicle	12.9 ± 0.5	46.4 ± 0.9	2.78 ± 0.08	211.6 ± 3.2	21.9 ± 1.0
	OVX Vehicle	8.6 ± 0.3	43.0 ± 0.6	2.01 ± 0.08	253.2 ± 9.3	23.3 ± 0.6
	OVX AM630 0.1mg/kg	11.5 ± 0.4	46.6 ± 1.2	2.48 ± 0.08	239.0 ± 4.8	24.9 ± 0.9
	OVX AM630 1.0mg/kg	11.3 ± 0.4	46.3 ± 0.7	2.43 ± 0.05	241.8 ± 7.1	25.9 ± 0.7
CNR2-/-	SHAM Vehicle	12.2 ± 0.3	48.3 ± 0.4	2.52 ± 0.05	227.7 ± 2.4	23.0 ± 0.5
	OVX Vehicle	9.6 ± 0.5	47.0 ± 0.8	2.04 ± 0.09	277.9 ± 9.8	26.9 ± 1.0
	OVX AM630 0.1mg/kg	8.8 ± 0.4	48.8 ± 1.7	1.82 ± 0.11	311.2 ± 17.0	27.7 ± 0.7
	OVX AM630 1.0mg/kg	11.0 ± 0.7	49.4 ± 1.4	2.22 ± 0.08	255.2 ± 11.2	26.0 ± 0.9

Appendix 8: BV/TV, trabecular bone volume (%); Tb.Th, trabecular thickness (μm); Tb.N, trabecular number (1/mm); Tb.Sp, trabecular separation (μm); Tb.Pf, trabecular pattern factor (1/mm). Values are expressed as means ± sem from 7-8 mice per group.

APPENDIX 9. Effect of cannabinoid receptor ligands on calvarial osteoblast growth and differentiation from wild type and CNR2-deficient mouse neonates.
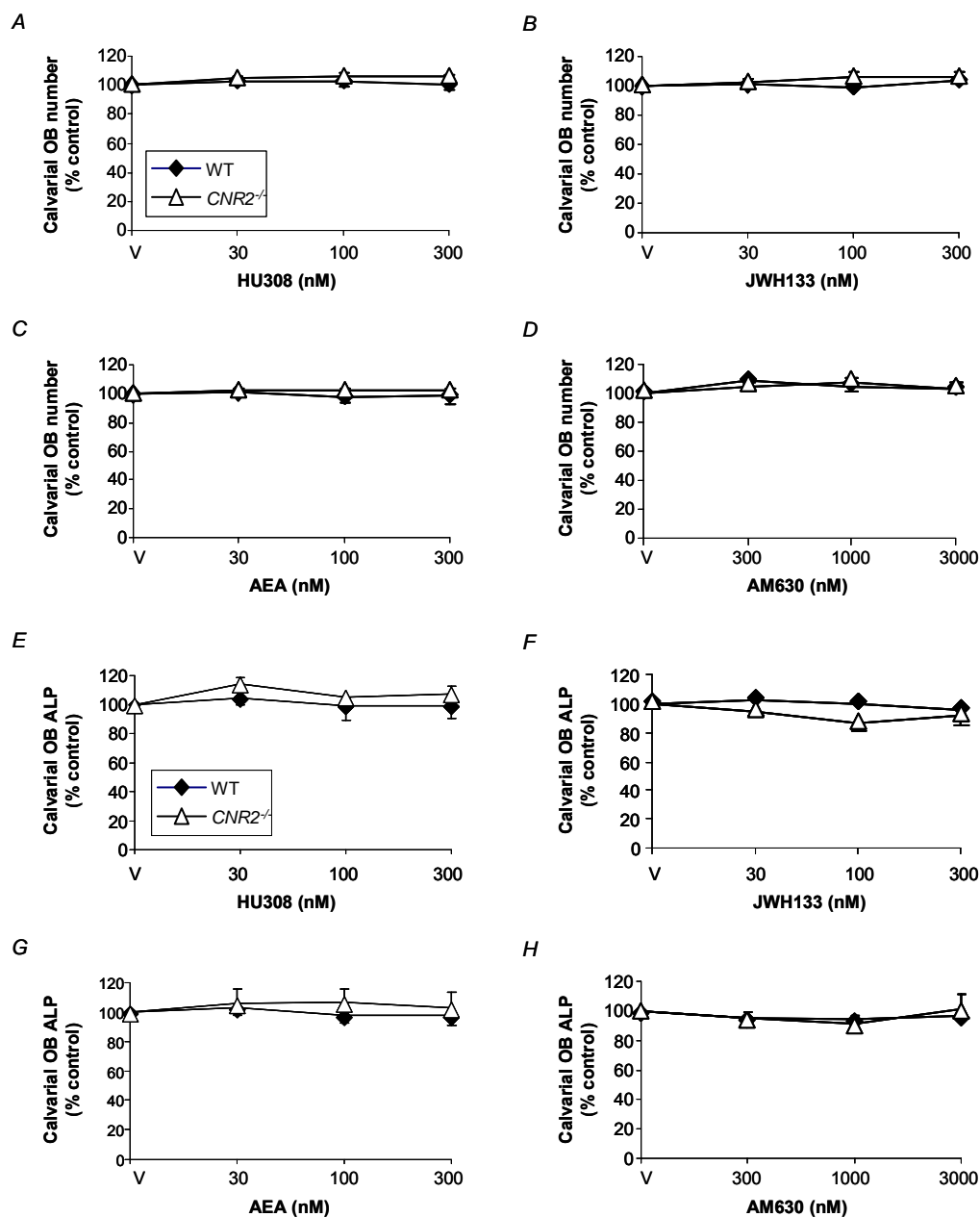
Appendix 9: *A-D.* Number of calvarial osteoblasts (OB) in cultures from wild type and *CNR2^{-/-}* mice, exposed to vehicle (V), HU308 (*A*), JWH133 (*B*), AEA (*C*) and AM630 (*D*) at the indicated concentrations for 24 hours, assessed by Alamar Blue assay. Changes in osteoblast number were expressed as a percent of values in vehicle-treated cultures. *E-H.* ALP activity of calvarial osteoblasts in cultures from wild type and *CNR2^{-/-}* mice, exposed to vehicle (V), HU308 (*E*), JWH133 (*F*), AEA (*G*) and AM630 (*H*) at the indicated concentrations for 24 hours, assessed by ALP assay. ALP levels were normalised to cell number and expressed as a percent of values in wild type vehicle-treated cultures. Values are means ± sem and were obtained from 3 independent experiments.

APPENDIX 10. Actual values of μCT analysis of trabecular bone from wild type (WT) and CNR2-deficient mice following ovariectomy (OVX) and treatment with HU308.

		BV/TV (%)	Tb.Th (μm)	Tb.N (1/mm)	Tb.Sp (μm)	Tb.Pf (1/mm)
WT	SHAM Vehicle	12.9 ± 0.5	46.4 ± 0.9	2.78 ± 0.08	211.6 ± 3.2	21.9 ± 1.0
	OVX Vehicle	8.6 ± 0.3	43.0 ± 0.6	2.01 ± 0.08	253.2 ± 9.3	29.8 ± 0.6
	OVX HU308 0.1mg/kg	10.1 ± 0.5	43.0 ± 1.0	2.34 ± 0.10	235.2 ± 8.3	24.5 ± 1.5
	OVX HU308 1.0mg/kg	10.8 ± 0.4	44.0 ± 1.0	2.46 ± 0.12	228.0 ± 7.3	25.5 ± 0.7
CNR2⁻/⁻	SHAM Vehicle	12.2 ± 0.3	48.3 ± 0.4	2.52 ± 0.05	227.7 ± 2.4	23.0 ± 0.5
	OVX Vehicle	9.6 ± 0.4	47.0 ± 0.8	2.04 ± 0.09	277.9 ± 9.8	26.9 ± 1.0
	OVX HU308 0.1mg/kg	8.9 ± 0.4	44.3 ± 0.5	2.01 ± 0.10	282.0 ± 18.3	28.4 ± 0.4
	OVX HU308 1.0mg/kg	11.0 ± 0.6	48.7 ± 1.2	2.27 ± 0.12	267.0 ± 7.3	24.9 ± 1.3

Appendix 10: BV/TV, trabecular bone volume (%); Tb.Th, trabecular thickness (μm); Tb.N, trabecular number (1/mm); Tb.Sp, trabecular separation (μm); Tb.Pf, trabecular pattern factor (1/mm). Values are expressed as means ± sem from 7-8 mice per group.

APPENDIX 11. Actual values of µCT analysis of cortical bone from wild type (WT) and CNR2-deficient mice following ovariectomy (OVX) and treatment with HU308.

		Ct.BV (mm^3)	Ct.Th (µm)	Ct.Dm (µm)	Med.Cav.Dm (µm)
WT	SHAM Vehicle	0.43 ± 0.01	187.9 ± 3.0	455.7 ± 1.9	79.9 ± 6.0
	OVX Vehicle	0.44± 0.01	187.3 ± 3.6	440.6 ± 16.5	66.0 ± 13.5
	OVX HU308 0.1mg/kg	0.49 ± 0.01	189.5 ± 3.7	452.6 ± 5.6	73.7 ± 7.2
	OVX HU308 1.0mg/kg	046 ± 0.01	189.2 ± 4.1	458.4 ± 2.2	79.9± 8.5
CNR2$^{-/-}$	SHAM Vehicle	0.47 ± 0.01	192.3 ± 3.7	457.3 ± 1.9	72.5 ± 7.4
	OVX Vehicle	0.47 ± 0.01	189.7 ± 4.5	454.7 ± 2.1	75.3 ± 8.0
	OVX HU308 0.1mg/kg	0.46 ± 0.01	183.1 ± 5.0	479.0 ± 1.3	108.5 ± 15.1
	OVX HU308 1.0mg/kg	0.48 ± 0.01	192.1 ± 3.6	451.7 ± 6.2	67.6 ± 11.7

Appendix 11: Ct.BV, cortical bone volume (mm^3); Ct.Th, cortical thickness (µm); Ct.Dm, cortical diameter (µm); Med.Cav.Dm, medullary cavity diameter (µm). Values are expressed as means ± sem from 7-8 mice per group.

APPENDIX 12. Growth and alkaline phosphatase activity of calvarial osteoblasts from wild type and CNR2-deficient mice.

Alkaline phosphatase (ALP) assay (c.f. section 2.2.9, page 81) demonstrated that $CNR2^{-/-}$ calvarial osteoblasts, unlike $CNR2^{-/-}$ bone marrow-derived osteoblasts (section 6.3.1, page 187), responded to PTH treatment (25-100nM) in a similar manner to that seen in wild type cultures, and showed increased ALP activity compared to vehicle-treated cultures (Figure below). Alamar Blue assay (c.f. section 2.2.8, page 80), showed that wild type and $CNR2^{-/-}$ calvarial osteoblasts demonstrated a comparable growth, which was not significantly affected following PTH treatment, regardless of genotype (Figure below, panel B).
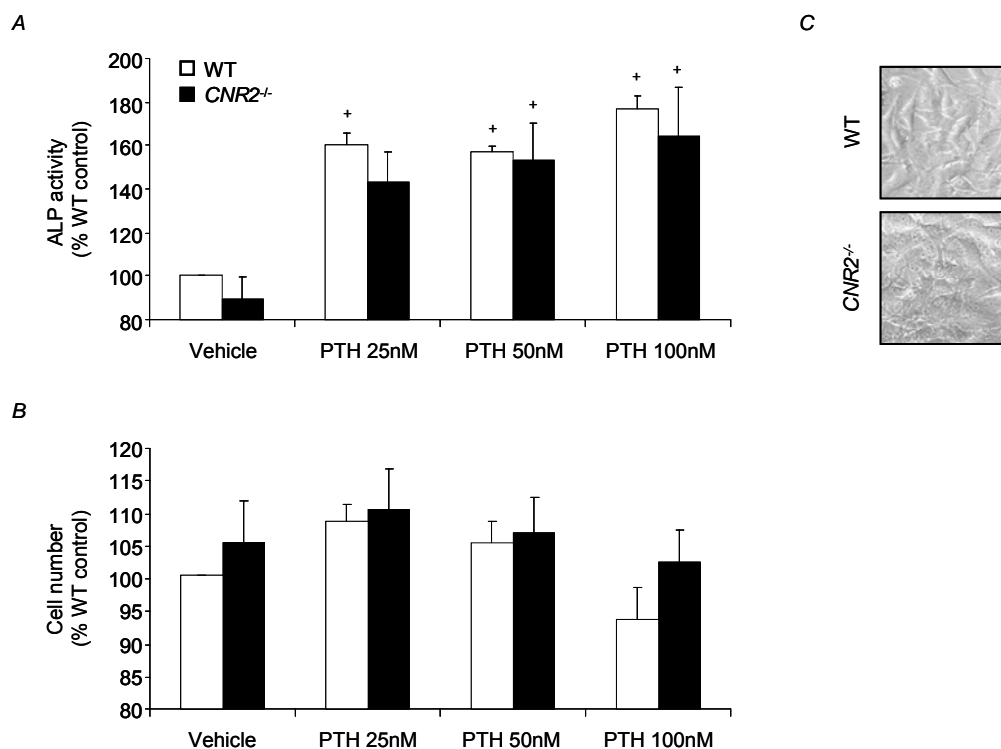
Appendix 12: ALP activity and growth of calvarial osteoblasts from wild type and CNR2-deficient mice. *A*. Alkaline phosphatase (ALP) activity of calvarial osteoblasts from wild type and $CNR2^{-/-}$ mouse neonates exposed to PTH (25-100nM) for 24 hours, assessed by ALP assay. ALP levels were normalised to cell number and expressed as a percent of values in wild type vehicle-treated cultures. *B*. Number of calvarial osteoblasts from cultures in *A*, assessed by Alamar Blue assay. Changes in osteoblast number were expressed as a percent of values in wild type vehicle-treated cultures. *C*. Representative phase contrast photomicrographs of wild type and $CNR2^{-/-}$ calvarial osteoblasts. Values are means ± sem and were obtained from 3 independent experiments. $^+$p < 0.05 from vehicle-treated cultures of same genotype.

APPENDIX 13. Published papers

Idris, A.I., **Sophocleous, A.**, Landao-Bassonga, E., van't Hof, R.J. & Ralston, S.H. (2008). Regulation of bone mass, osteoclast function, and ovariectomy-induced bone loss by the type 2 cannabinoid receptor. *Endocrinology*. **149**, 5619-5626.

Idris, A.I., **Sophocleous, A.**, Landao-Bassonga, E., Canals, M., Milligan, G.I., Baker, D., van't Hof, R.J. & Ralston, S.H. Cannabinoid receptor type 1 protects against age-related bone loss by regulating osteoblast and adipocyte differentiation in marrow stromal cells. *Cell metabolism.***10**, 139-147.